NOTTINGHAM TRENT UNIVERSITY

A Study of Rainfall Infiltration on Slope Stability using Sand Piles to Reinforce Slopes

Sohaib Naseer

A thesis submitted in partial fulfillment of the requirements of Nottingham Trent University for the degree of Doctor of Philosophy

December 2023

DEDICATIONS

Dedicated to my beloved Family.

DECLARATION

The thesis is being submitted to Nottingham Trent University (NTU) in pursuit of a PhD degree. The work presented in this thesis adheres to the regulations of NTU and is original, except as explicitly referenced in the text. I affirm that none of the content in the thesis has been previously submitted to fulfil the requirements of another degree or qualification, either at this educational institution or any other institution in the United Kingdom or abroad. The ideas expressed in the thesis only reflect the author's perspective and do not represent the views of the University.

Signed:..... ..... (Candidate), Date: .....24/07/2024.....

.

ACKNOWLEDGEMENTS

Praise to Allah Almighty

First and foremost, I attribute praise and prestige to the almighty Allah for giving me the strength and determination to prevail over obstacles, as well as for showering my life with overflowing mercy and blessings.

I would like to express my sincere gratitude to my Director of Studies, Dr. Robert Evans, for his expert guidance, assistance, and unwavering support throughout my Ph.D. journey. My heartfelt thanks also extend to my second supervisor, Professor Anton Ianakiev, for his valuable support. Special appreciation is reserved for my independent assessor, Dr. Zakwan Arab, whose excellent assessments and insightful comments significantly contributed to the successful completion of my thesis.

I extend my eternal gratitude to my colleague, Dr. Bubaker H. Shakmak, for his invaluable help and support throughout the thesis process.

A special acknowledgment goes to my friend, Engr Israr ul Haq, who not only encouraged me to embark on my Ph.D. journey but also supported me in achieving this significant milestone in my life.

I am truly thankful to the technical team of NTU workshop, particularly Mr. Alan Chambers and Stephen Chamberlain, for their assistance in fabricating the experimental setup for laboratory testing.

I dedicate this thesis to my beloved father and mother, whose encouragement and unwavering support have been instrumental throughout my Ph.D. journey. Their firm belief in my abilities has been a constant source of inspiration, guiding me through the challenges and triumphs of this academic endeavor. Their words of wisdom, kindness, and love have been the pillars that strengthened my resolve to pursue and complete my Ph.D. I am profoundly grateful for the sacrifices they have made and the unwavering faith they have placed in my aspirations. This dedication is a tribute to their immeasurable contributions to my academic success and personal growth.

ABSTRACT

Slope instability, predominantly manifested as landslides, stands as one of the most formidable natural hazards, posing significant challenges to sustainability. Prolonged rainfall events are a vital trigger for landslides, with global variations in rainfall patterns primarily attributed to climate change. For instance, on October 3, 2020, the UK experienced its wettest day since 1891, with an average of 31.7 mm of rainfall, illustrating this climatic change.

This research aims to investigate the mechanisms of soil slope failure under varying rainfall conditions by combining finite element modeling with physical modeling. The primary objective is to understand the complexities of soil slope failure under different rainfall intensities and durations and to evaluate the effectiveness of sand piles in mitigating failure and reducing damages.

The study begins with a numerical analysis using finite element methods, examining various soil slopes with different inclination angles subjected to varying rainfall conditions. A coupled flow-deformation analysis is conducted to unravel the behavior of slopes during rainfall infiltration. Sand piles' length, diameter, spacing, and stiffness are optimized for effectiveness.

Next, the optimized parameters from the numerical analysis guide the design and testing of a laboratory-based physical model. This dual approach reveals how slope geometry significantly influences rainfall-induced instability. Gravity forces increase with slope height and inclination, while gentler slopes with longer ponding times, experience more significant rainfall impact. This prolonged infiltration reduces matric suction, diminishing soil shear strength and destabilizing the slope. Conversely, steeper slopes, with shorter ponding times, see more water as surface runoff.

The efficacy of sand piles in stabilizing fine soil slopes is highlighted. Sand piles function as both drainage and reinforcement mechanisms, providing effective drainage paths and facilitating the transfer of infiltrated water to the surface as runoff. This reduces pore water pressure and increases matric suction, thereby enhancing soil shear strength and slope stability. The slope was monitored, and soil displacements were measured using a novel approach called the Automated Sensory and Signal Processing System (ASPS). Images captured during the experimental program were processed in MATLAB, applying mathematical equations to extract useful features and categorize slopes based on displacement levels. Low displacement

indicated stable conditions, while high displacement signaled potential instability and the need for further intervention.

To validate the findings, a case study was conducted on the Azad Pattan Road in Kashmir, Pakistan. This site, consisting of fine silty soil similar to the soil type used in the finite element and lab modeling, provided a real-world application of sand piles. The geology of the slope mirrored the conditions studied in the numerical and physical models, allowing for the practical application of optimized sand pile parameters.

In conclusion, this research significantly contributes to understanding slope stability under varying rainfall conditions. By integrating numerical analysis, physical modeling, and the application of sand piles, the study offers a comprehensive view of the factors influencing slope failures and effective stabilization techniques. The case study on Azad Pattan Road in Kashmir further validates these findings, demonstrating practical implications for mitigating landslides in areas prone to slope instability. These insights are invaluable for fortifying resilience against climate change-induced natural hazards.

Table of Contents

List of Tables

List of Figures

CHAPTER 1: INTRODUCTION

1.1 Background

Landslides or slope failures pose a significant challenge to the sustainable development of infrastructure. Among the common issues encountered in geotechnical engineering, problems related to slope stability are prominent. Given the practical importance of slope stability, evaluating the stability of both natural and man-made slopes has garnered widespread attention within the geotechnical community over many decades. A fundamental query arises: why does a previously stable natural slope undergo sudden failure after an extended period of stability? The influence of rainfall emerges as a critical factor in addressing this question. The occurrence of slope failure is intricately linked to rainfall, prompting numerous studies to delve into the climatic and geomorphic processes that serve as triggers for slope failures. Various researchers have examined the physical characteristics of the slopes that have failed, the impact of the slope angle, changes in moisture content and pore water pressure, the mechanism behind the movement of debris avalanches, and the features of the resulting deposits (Fisher 1971; Hutchinson and Bhandari, 1971; Scott 1981; Williams and Guy 1973; Swanston 1974; Campbell 1975a; Hollingsworth and Kovacs, 1981; Istok and Harward, 1982).

Landslides induced by rainfall occur when rainwater infiltrates the soil mass, moving downward as a wetting front. This process creates a saturated zone between the wetting front and the soil surface, with its dimensions and properties influenced by factors such as precipitation intensity, total amount of rainfall, and soil hydraulic characteristics. The saturation of soil pores results in elevated pore water pressures and a subsequent decrease in effective stresses within the soil mass. Consequently, shear strength is significantly diminished, posing a potential risk to stability and the onset of failure (see Figure 1.1).

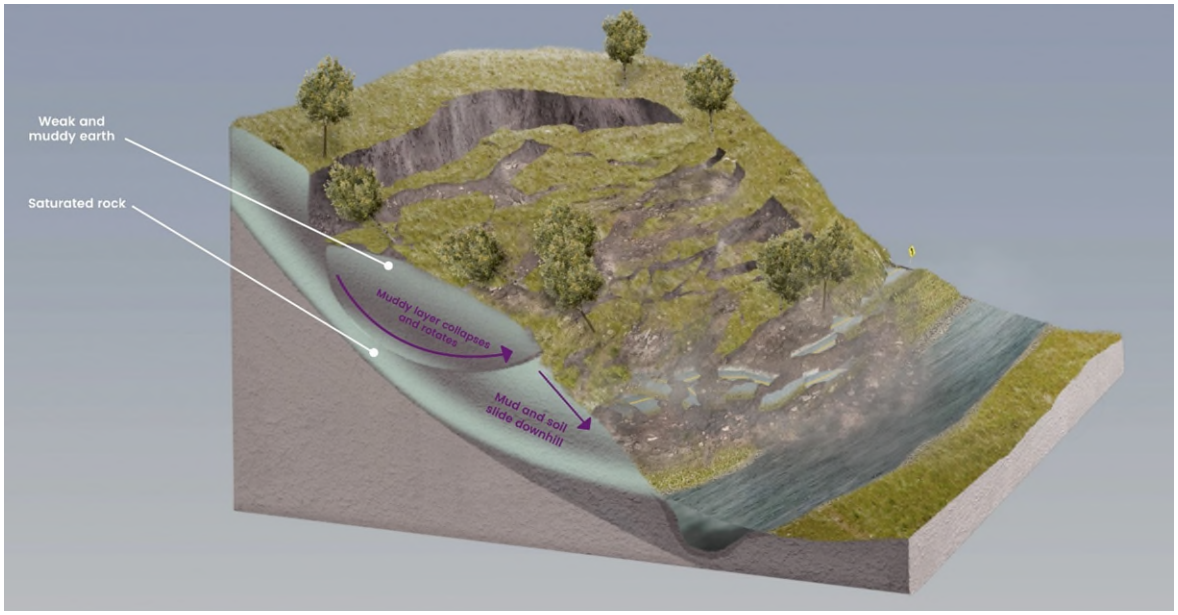

Figure 1.1: Slope failure rainfall infiltration and gravitational loading (Shaw-Shong 2004).

Rainfall and soil properties are widely acknowledged as primary factors controlling rainfall-induced slope movement, mostly in tropical regions characterized by high-intensity rainfall and humid conditions, as indicated by studies such as those by Brand (1984) and Rahardjo et al. (2016). Rainfall can also trigger extensive and substantial chemical erosion of slopes, resulting in the removal of minerals from soils located close to the surface. This process can result in exposed soil structures near the surface of the slope, which are frequently characterized by elevated void ratios. The hydraulic characteristics of soil, which are closely connected to the void ratio, determine the quantity of rain that can penetrate the slope, potentially leading to slope failures.

Rainfall events, characterized by factors such as intensity, duration, antecedent conditions, resolution, and pattern, exert a crucial influence on rainfall-induced slope failures, as indicated by various researchers (Brand 1984; Fourie et al. 1999; Gasmo et al. 2000; Rahardjo et al. 2001; Hearman and Hinz, 2007; Rahimi et al. 2011; Muntohar et al. 2013a). The triggering role of intense rainfall in slope failures worldwide has been documented by several studies (Fuchu et al. 1999; Guzzetti et al. 2008; Huat et al. 2006; Olivares and Picarelli, 2003; Shaw-Shong 2004; Van Asch et al. 1999). Prolonged rainfall has also been associated with numerous slope failures (Massey et al. 2013). Antecedent rainfall is recognized as a significant factor in the failures of low-conductivity slopes, while its impact is considered less significant in high-conductivity slopes (Rahardjo et al. 2005).

The precision of rainfall data is crucial in predicting the quantity of precipitation infiltration that can cause slope failures, considering the typical variations in rainfall intensity. Accordingly, the utilization of high-resolution rainfall data, such as hourly instead of daily data, in the analysis of rainfall-induced slope failures is recommended by Hearman and Hinz (2007). Furthermore, rainfall patterns that exhibit initial high intensities followed by a continuous decrease have been associated with the most severe slope instability, the lowest minimum factor of safety, and the shortest time required to achieve the minimum factor of safety (Rahimi et al. 2011; Muntohar et al. 2013b). In Shaziba Town, Mazhe County, Hubei Province, China, continuous rainfall from June to August 2020 triggered a massive landslide on July 21, 2020. Figure 1.2 shows the landslide and landslide dam formed as a result of slow movement. The landslide, with an estimated volume of 2.8 million cubic meters, severely damaged over 60 houses and caused extensive cracking on the ground and structures, including a 700-meter stretch on the Tunyu Highway. Approximately 250,000 cubic meters of soil slid into the Qingjiang River, creating a landslide dam that was overtopped and breached 4.25 hours later, resulting in a peak flood flow of about 200 cubic meters per second. This flood deposited significant sediment downstream, flattening the riverbed (Tengfei et al. 2012).

The relationship between rainfall events and soil hydraulic properties is pivotal in determining the volume of rainwater infiltration needed to diminish the suction of the surface soil, potentially triggering a slope failure. Theoretically, when the intensity of rainfall closely aligns with the magnitude of soil hydraulic conductivity, the entire incident rainfall can be fully absorbed by the soil. In such cases, the infiltrated rainwater is likely to reduce the suction of the surface soil to a critical condition. Rainfall with very low intensity can completely permeate the surface soil, yet it might be inadequate to reduce the soil's suction. Conversely, high-intensity rainfall may result in partial runoff, rendering rainwater infiltration insufficient to diminish the soil's suction, particularly as intense rainfall tends to be of shorter duration.

In recent decades, our understanding of the mechanics behind shallow slope collapses caused by rainfall has undergone a transformation. Traditionally, the elevation of groundwater levels in soils with high hydraulic conductivity and the generation of artesian uplift pressure in surface soils were commonly associated with underlying failure mechanisms without considering the influence of matric suction above the water table. A pivotal change in perspective occurred after the investigation of slope failures in Hong Kong's residual soils from 1950 to 1973 by Lumb (1975). The study identified rainwater infiltration as the primary cause of slope failures,

contrasting with the earlier assumption of failures being triggered by seepage from below. This observation is supported by the stability of many residual soil slopes with deep groundwater tables and inclination angles greater than the repose angle during dry seasons, only to experience failure when subjected to prolonged and intense rainfall. In such cases, the contribution of matric suction to shear strength becomes significant, as highlighted by Rahardjo and Fredlund (1993). Although matric suction enhances the strength of unsaturated soils, this strength undergoes a substantial decrease as rainwater infiltrates the surface soil of the slope.

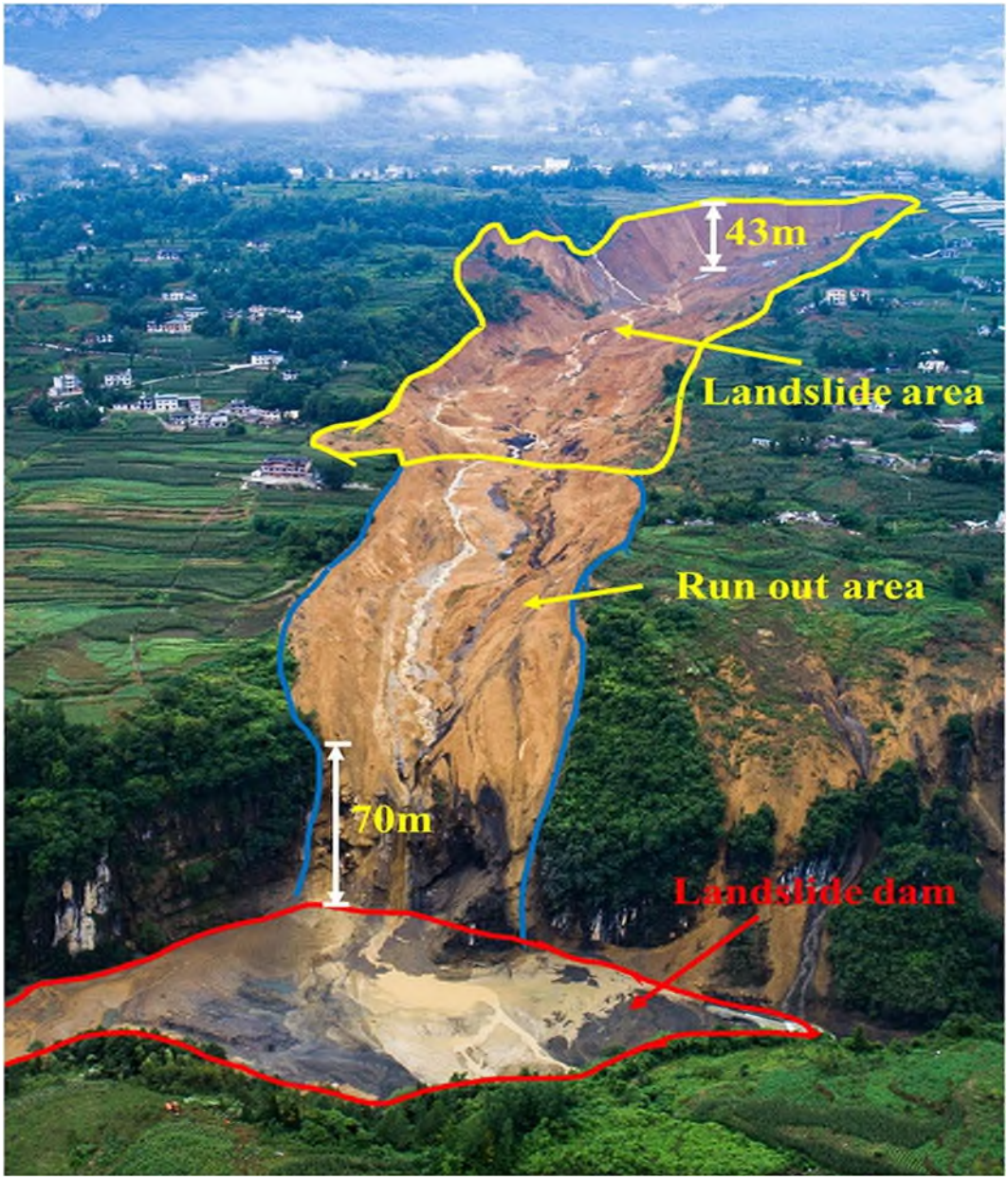

Figure 1.2: Shaziba Town Landslide and formation of landslide Dam (Tengfei et al. 2012)

Several investigations have demonstrated that matric suction is a crucial factor in the occurrence of shallow slope failures (Pradel and Raad, 1993; Gasmo et al. 2000; Au 1998; Fourie et al.). As rainfall seeps into the slope, the matric suction reduces, and the wetting front descends. Eventually, it reaches a critical depth where the slope's shear strength is unable to sustain stability (Fourie et al. 1999). Failures of these kinds are more likely to happen in slopes with lower hydraulic conductivity than slopes with higher hydraulic conductivity, such as those composed of clean sand (Pradel and Raad, 1993).

It is commonly understood that shallow slope failure processes are triggered by the penetration of rainfall into surface soils, as previously described. The utilisation of this mechanism has been employed to create an approximation technique for forecasting the likelihood of landslides by utilizing statistical rainfall data and soil characteristics, as demonstrated by studies conducted by Pradel and Raad (1993) and Fourie et al. (1999). However, it's important to note that this approximate method tends to yield conservative results due to inherent simplifications in the modelling process.

1.2 Research Motivation

Slope failures have emerged as the most frequent natural hazard globally, surpassing other common occurrences such as storms, volcanoes, earthquakes, floods, and tsunamis (Shaw-Shong, 2004). Between 1998 and 2017, landslides affected an estimated 4.8 million people worldwide and caused over 18,000 deaths (Azeze, 2020). The Global Landslide Catalog (GLC), compiled by NASA, identified over 11,000 reported rainfall-triggered landslides from 2007 to 2019 (Emberson et al. 2020). In 2010 alone, there were 494 slope failures triggered by rainfall, resulting in a staggering 6,211 recorded deaths (Suradi 2015).

In numerous territories, slope failures are a recurring occurrence, resulting in substantial losses. A notable example is the Nepal Himalaya region, where rainfall-induced slope failures during the monsoon season have inflicted significant harm to lives, property, infrastructure, and the environment (Dahal 2012). The Nepal Himalayan region stands out as one of the most vulnerable areas globally to landslides, contributing approximately 30% to the world's total landslide-related damage value. This region has witnessed a series of landslides with severe consequences, such as the loss of 50 lives during the half-monsoon period from June 10 to August 15, 2009 (Li 1990).

In 1988, a massive landslide at Darbang, approximately 200 km west of Kathmandu, Nepal, claimed the lives of 109 people and temporarily blocked the Myagdi River. Furthermore, sixty-two years prior to this incident, Darbang had experienced another landslide that buried the area, resulting in the death of 500 people (Yagi et al. 1990). This incident remains the worst landslide disaster in the history of Himalayan landslides. Another tragic landslide occurred at Malpa in Uttarakhand, India, on August 18, 1998, causing the death of 380 people as a massive landslide washed away the entire village. Beyond these major landslides, many small-scale incidents go unreported when they occur in remote areas of the Himalayas (Loo et al. 2015).

Furthermore, the loss of productive lands in the hills due to landslides and associated mass erosion phenomena during rainy seasons, often unreported unless involving loss of life, appears to be substantial. If quantified, the economic loss would likely rival that of other major natural hazards. National infrastructure, including roads, bridges, dams, hydropower stations, canals, and buildings, continually faces damage from landslides and floods. Additionally, the rapid population growth over the Himalayan hills in the past three decades has contributed to continuous losses of lives, property, and significant damage to the crucial economic systems of nations in the Himalayan Region.

China faces significant geological disasters, including landslides triggered by rainfall, contributing to substantial economic losses. Annually, direct economic losses from geological disasters make up over 20% of the total losses incurred by all natural disasters in the country. The combined direct and indirect economic losses related to landslides exceed 2 billion EUR every year nationwide (Bai et al. 2011; Hu and Tang, 2005). Data from the China Institute of Geo-Environment Monitoring reveals the magnitude of the issue, with a total of 102,804 geological disasters reported across the country in 2006, of which 86% were landslides. In 2007, there were 25,364 recorded entries, with landslides accounting for 61%. The year 2008 saw 14,350 landslides among a total of 26,580 geological disasters, constituting 54% of the reported incidents. Comparing losses from landslides with those resulting from other natural hazards, such as flooding, is challenging. According to the Association of British Insurers, losses from flooding amount to approximately £500 million per year (Dailey et al. 2009). Similarly, losses from geological hazards, specifically 'subsidence,' are of a comparable magnitude, around £350 million per year (Culshaw and Harrison, 2010).

The US Geological Survey (USGS) reported that landslides caused thousands of deaths and up to 2 billion USD in property damage annually (Highland 2006). The UK Met Office publishes

rainfall data on a monthly basis and reported that due to climate change, the UK is experiencing extreme rainfall events. UK rainfall-induced landslide statistics are presented in Figure 1.3, which shows a significant increase in rainfall frequency and landslide events.

However, this overall figure does not distinguish the contribution from land sliding alone. Further research is necessary to more accurately determine the true cost of land sliding in the UK. Without this information, it remains challenging to assess whether the current government expenditure on landslide mitigation is appropriate.

1.3 Aim and Objectives

This aim of this study was to investigate the major controlling factors of rainfall-triggered soil movement and the efficiency of sand piles when used as a stabilisation technique for slopes with fine soils, through the use of both labroratory-based small scale slopes and also finite element modelling. In particular, the effect of the intensity and duration of rainfall on the slope failure is taken into consideration. To conduct this study, a series of small-scale laboratory-based slopes with artificial rainfall setups were tested with various inflow and rainfall durations, with full scale models of similar slopes analysed by finite element modelling. To achieve the overall aim, the study had the following objectives:

i. Review existing literature on slope stability analysis and procedures and compare methods developed for slope stability analysis;
ii. Analyse the failure behaviour of natural slopes with different slope angles and varying rainfall patterns using Finite Element Modelling (FEM);
iii. Investigate the failure behaviour of natural slopes subjected to varying rainfall patterns using small-scale laboratory testing;
iv. Compare the results of small-scale laboratory testing with FEM analysis results for slope stability;
v. Conduct a case study of a real-life slope failure to validate the results obtained from small-scale laboratory testing and FEM analysis;
vi. Stabilize the same slopes as used above (in both the laboratory testing and FEM), using sand piles, and investigate the effectiveness of sand piles for slope stability;
vii. Evaluate and analyse the overall effectiveness of the implemented sand pile stabilization method in the context of real-life slope stability.

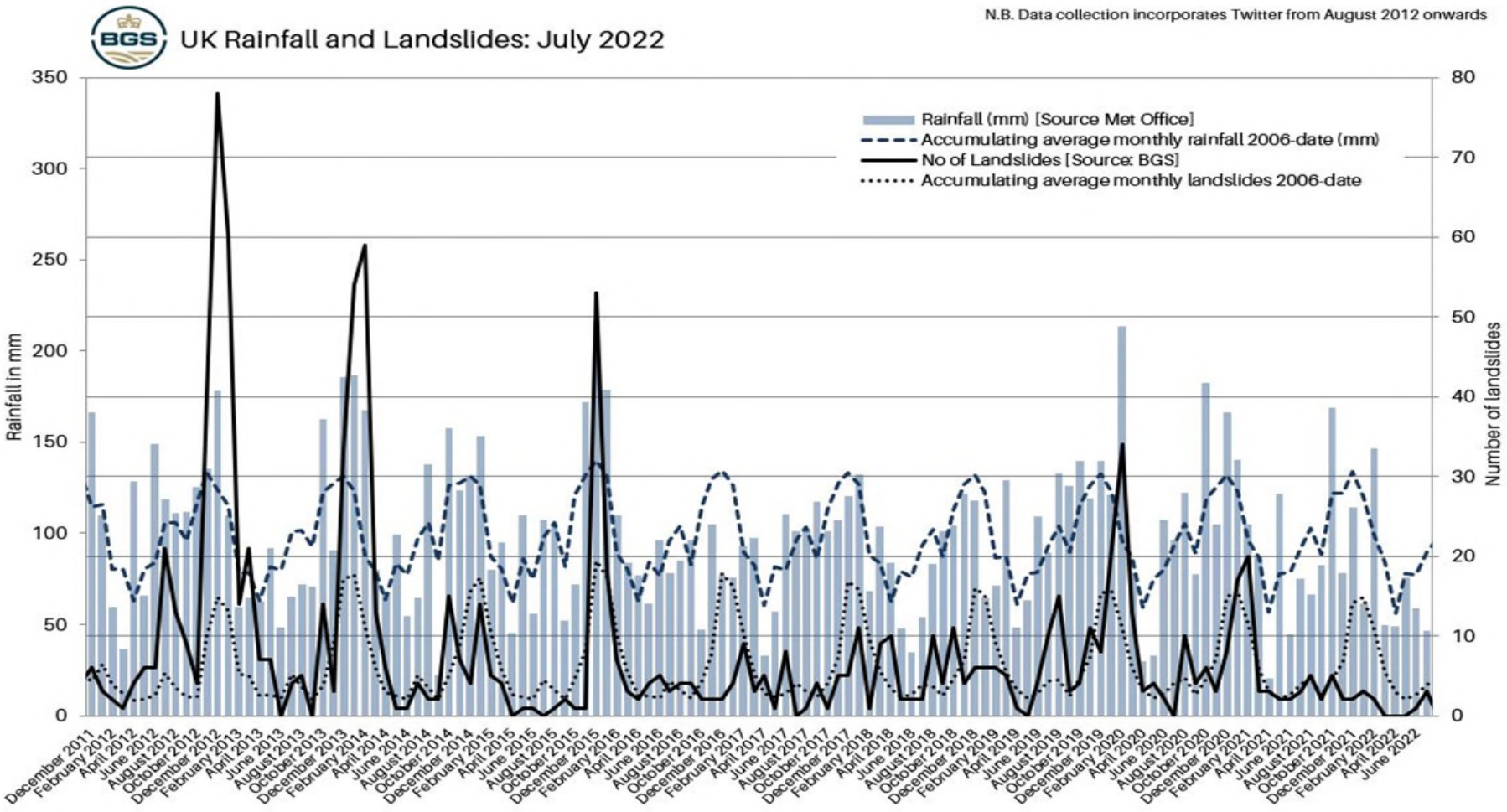

Figure 1.3: Statistics for amount of rainfall and number of Landslides occurring in the UK between 2011 to 2022 (Source: British Geological Survey)

1.4 Thesis Outline

The structure of the thesis is divided into various chapters. The current chapter presents a brief background of rainfall-induced slope failures, research motivation, overall aim and objectives of this research and thesis outline.

In Chapter 2, a detailed review of existing knowledge and research was carried out. The chapter starts with a background study on the failure mechanism of slopes triggered by rainfall stability analysis methods developed by different researchers. Further, a brief description of the infiltration process, including factors affecting infiltration, is included. Also, the difference between saturated and unsaturated soil properties and their shear strength characteristics are reviewed. Additionally, shallow depth slope failure, wetting band theory and soil water characteristics curve (SWCC) subject was studied. Furthermore, Capter 2 provides an extensive overview of the latest advancements in slope stabilization techniques, encompassing a wide range of methodologies devised by dedicated researchers. This chapter delves into the realm of slope failure mitigation, examining various cutting-edge approaches, including physical, chemical, and biological methods. The data collected from laboratory experiments was in image form and it was interpreted and analyzed using Particle Image Velocimetry (PIV) technique. Therefore, the last part of Chapter 2 presents a detailed description of PIV, the principles, and the application of this technique for various engineering applications, civil engineering, and, more specifically, geotechnical engineering. The chapter commences by offering an in-depth explanation of the fundamental principles underlying PIV.

In Chapter 3, detailed methods and procedures are presented, including details of the equipment, devices used and preparation of the model slope. In addition, this chapter also discusses the methodology, procedure, and apparatus specification for this experimental work. Also, details of different laboratory experiments were provided to determine the basic classification and strength properties of the soil used for this research study. Furthermore, slope model test preparation procedures are explained, including the compaction process and data recording. Additionally, the details of finite element modelling and analysis using PLAXIS 2D are presented in this chapter.

Chapter 4 focuses on the finite element modelling and analysis conducted as part of the research study. This chapter presents the analysis and results obtained from the finite element simulations conducted on un-stabilized slopes and slopes stabilized with micro-piles.

Chapter 5 provides the results and findings as well as discussions on laboratory testing conducted as part of the research study, including the physical and strength characteristics of soil used in this study, findings of tests conducted on model slopes, un-stabilized and after stabilization with micro-piles.

Chapter 6 presents the case study conducted during this research: A case of an active landslide in the Punjab province of Pakistan was selected, a numerical simulation was conducted, and the results are presented in this chapter.

Finally, Chapter 7 concludes the discussion and recommendations based on this research study. The potential of sand piles for the stabilisation of soil slopes is briefly presented in this chapter.

CHAPTER 2: LITERATURE REVIEW

2.1 Overview

The evaluation of slope stability is an interesting, important, and challenging factor in the field of Civil Engineering. During the past 80 years, in-depth investigations on slope stability have been conducted based on the principles of engineering geology, geotechnical engineering, and soil/rock mechanics. Several methods can be used to improve slope stability, including adding a surface cover to a slope to improve stability, altering the slope's geometry by excavation, strengthening the slope with support structures, or controlling the draining of groundwater in the slope.

Slopes can be either natural or man-made. A stable slope can withstand its own weight and external forces without experiencing any movement or displacement. When a slope failure takes place (also known as a landslide), it can be caused by slow or rapid movement. Earthquakes, rainfall (increasing the pore water pressure), or decline of the mechanical potentials of the ground are common trigger events for landslides. Every year, several fatalities are caused by slope failures, in addition to damage to infrastructure (Yagi et al. 1990; Bai et al. 2011; Hu and Tang, 2005; Dahal 2012).

The research is structured into three major sections. The first stage focuses on evaluating slope stability, discussing different analysis methods, and identifying factors affecting slope stability. The second stage examines various stabilization techniques used to mitigate landslide risks. In the final stage, the focus shifts to image processing techniques, specifically particle image velocimetry, used for measuring slope deformations. In this study, slope measurements and deformations were determined using image processing techniques. Therefore, a detailed overview of these techniques will be provided. This will include an explanation of how image processing contributes to accurate monitoring and assessment of slope stability and deformation, enhancing our understanding of landslide dynamics and improving stabilization strategies.

2.2 Types of Landslides and Factors Affecting their Stability

A landslide refers to a range of mechanisms that cause materials such as rock, soil, or artificial fill to move downhill and outward on slopes. It's possible for the materials to move via toppling, sliding, spreading, or flowing. In regions with minimal elevation changes, landslides can occur

in various ways. These include the collapse of piles of waste material from mining activities, particularly in areas where coal is extracted. Other forms of landslides in such areas include the erosion of riverbanks, incidents where excavated areas for roads and buildings collapse, the lateral spreading of landslides, and slope failures related to open-pit mines and quarries. In the following sections, a detail discussion about the types of landslides and factors controlling their stability is presented.

2.2.1 Types of Land Sliding Movement

Landslides can be classified according to the materials involved and their movement patterns. A classification system that utilizes these criteria is illustrated in Figure 2.1 and each type is further described in the following sections. This classification was initially presented by Varnes (1978).

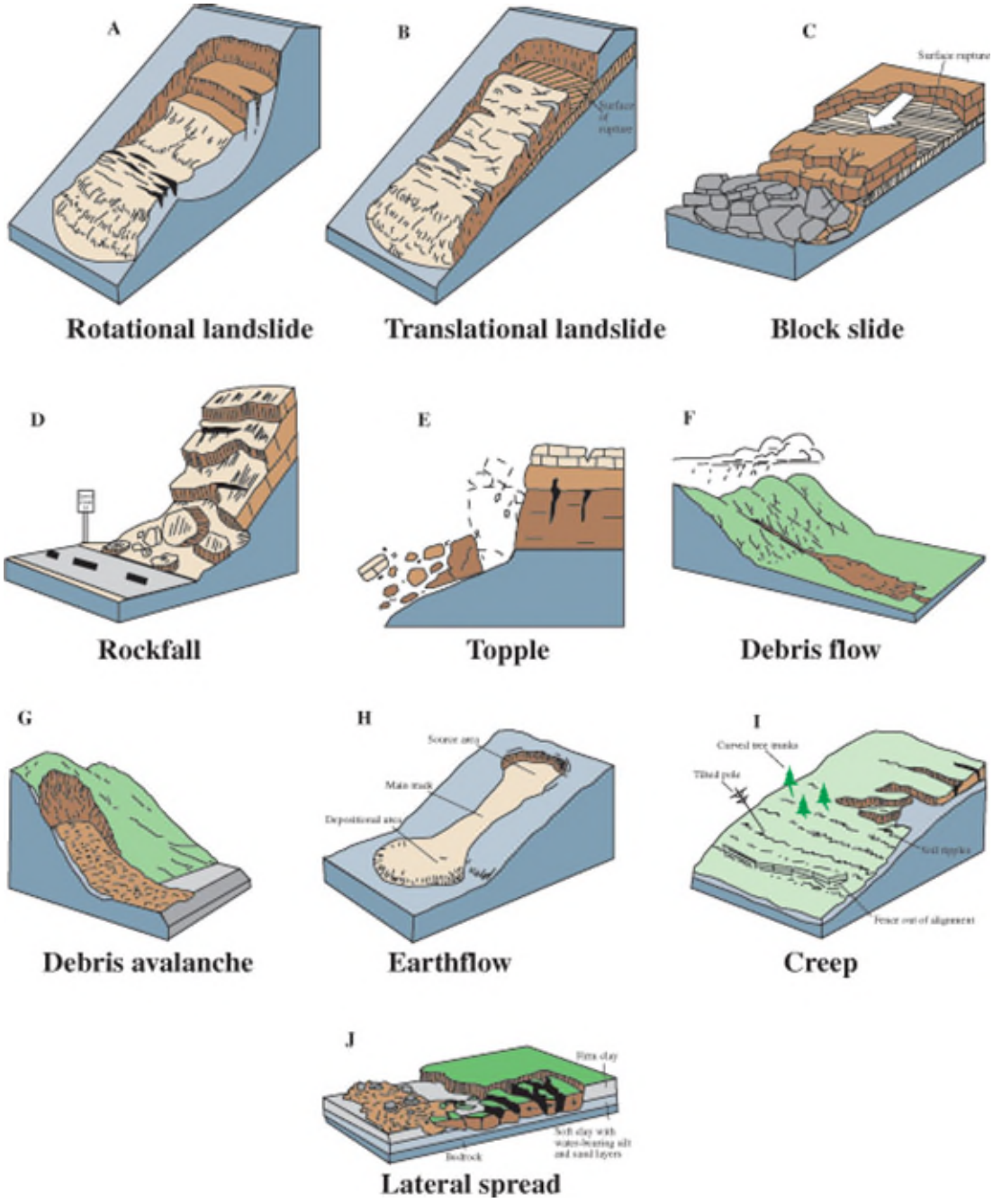

Figure 2.1: Type of Landslides (USGS 2004)

2.2.1.1 Surface Landslides

A slide is the downward movement of material that occurs along a characteristic sliding or damaged surface. Surface landslides tend to be deeper in terms of the amount of material they displace compared to other types of landslides and are structurally uncontrolled. There are two main types of surface slides: rotational slides and translational slides. The detailed explanation of these types is explained as follows:

Rotational slides: A slide-type landslide is characterized by the downward flow of debris along a clearly defined rupture or circular slip surface. In contrast to other forms of landslides, the slip surface in this scenario is not limited by structural constraints and often occurs at a higher depth. This form of landslip is distinguished by a convex upward-curving rupture surface and exhibits rotational movement along an axis that is parallel to the ground and perpendicular to the direction of the slide (see Figure 2.1a).

Translational slides: With this type of slide, there is little rotation or reverse tilt as the landslide mass slides down along a relatively flat surface. A block slide is a translational slide in which the mass moving down the slope consists of only one unit or a small group of closely connected units (see Figure 2.1b).

2.2.1.2 Land Falls

Falls are the sudden movements of geologic material masses from overhangs or steep slopes, where the movement involves falling freely, bouncing, and rolling, and separation happens along discontinuities like bedding planes, fractures, and joints. Falls are notably influenced by the presence of interstitial water, mechanical weathering, and the force of gravity. Falls occur quite swiftly and don't require any lubrication from water (see Figure 2.1d).

2.2.1.3 Topples

A topple landslide is a type of landslide that happens when a mass of rock or soil rotates forward and downward over a curved surface, much like a falling domino. The rock or soil block loses its stability and flips over in this type of landslide due to a variety of factors, such as gravity, erosion, or changes in the underlying topography. Topples are widespread in regions with layers of rock or soil that are resistant to erosion to varied degrees (see Figure 2.1e).

2.2.1.4 Flows

Flows, which are a kind of landslides, occur when substances having characteristics similar to fluids move downward over a slope. After the movement of the landslip material stops, the flows often leave behind a unique deposit that is characterized by an inverted funnel form. There are five basic categories of flows, each characterized by distinct features that differentiate them from one another.

2.2.1.5 Debris flow

A debris flow is the consequence of the amalgamation of loose soil, organic matter, rock, air, and water, resulting in the formation of a slurry that moves downhill. Roughly half of the debris flows are composed of tiny particles. These occurrences are often initiated by vigorous surface-water flow caused by substantial rainfall or quick snowmelt, which erodes and carries away loose soil or rock on steep inclines. Debris-flow deposits are easily identified by the presence of debris fans located at the mouths of gullies. These deposits are often found in steep gullies near their source locations (see Figure 2.1f).

2.2.1.6 Debris avalanche

A debris avalanche is a quick and unpredictable mass movement down a slope containing a mixture of rock, soil, plants, and other debris. Debris avalanches are among the most dangerous types of landslides, capable of causing major damage and covering wide areas with rubble. They can travel at extremely high speeds and have the potential to cause widespread devastation to the landscape and infrastructure. Debris avalanches are common in mountainous places or areas with steep slopes, and they are usually caused by a combination of variables such as severe rainfall, quick snowmelt, earthquakes, volcanic activity, or human activities that damage the slope's stability (see Figure 2.3g).

2.2.1.7 Earthflow

An earthflow is defined as a kind of flow that is driven by gravity and moves downhill. It consists of materials that are fine-grained and saturated with water, resulting in a viscous flow. Earthflows are a kind of mass-wasting event that exhibit characteristics similar to both mudflows and downhill creep. Earthflows are likely to occur in materials such as clay, fine sand, silt, and fine-grained pyroclastic debris. Earth flows have a distinct "hourglass" shape. The slope's head is formed by a bowl-shaped dip or runout from the slope material. It typically occurs on moderate slopes and in saturated conditions in fine-grained or clay-containing rocks, although granular material flows can occur dry. Slope material can move downslope at various speeds ranging from 1 millimetre per day to meters per day. Intermittent activity can last for years as long as the earthflow periodically settles and stabilizes. The velocity of the flow is controlled by the water content; the higher the water content, the higher the flow (see Figure 2.1h).

2.2.1.8 Creep

The gradual, relatively slow, steady descent of soil or rock downslope is known as creep. Shear stress is not sufficient to produce shear collapse but is substantial enough to cause permanent deformation, which causes movement (see Figure 2.1i).

2.2.1.9 Lateral spreads

Lateral spreads typically occur on relatively flat terrain or gentle slopes. With shear or tensile fractures, lateral extension is the predominant mechanism of movement. Liquefaction is the cause of this type of failure, typically where saturated, loose, cohesion-free sediments (often sands and silts) are created from a previously more stable condition. It is typically brought on by sudden ground motion, such as that present during an earthquake (see Figure 2.1j).

2.2.2 Factors Affecting the Stability of Slopes

Varnes (1978) classifies the factors that affect the stability of slopes into two major categories: internal and external factors. Internal factors are related to the shear strength of soil, whilst external factors include the increase in applied shear stress. The major factor influencing the shear strength is pore water pressure. Higher pore water pressure cases a reduction in effective stress and, thus, a reduction in shear strength, which then leads to slope failure. The external factors include all kinds of loadings, e.g. construction activities at the top of the slope, unloading or excavation at the toe of the slope, increase of soil weight due to increased water content with the soil body or stress resulting from earthquakes. When ground water is kept from rising within the slide mass, stability is increased. This can be done by:

- Directing surface water away from the landslide;
- Reducing the potential for a rise in groundwater levels by draining groundwater away from the landslide;
- Using an impermeable membrane to cover the landslide;
- Reducing surface irrigation.

To improve slope stability, one may enhance it by adding weight or installing retaining structures at the base of the landslip. Alternatively, stability may be enhanced by reducing the mass (weight) near the top of the slope. The following factors affect slope stability:

- Rainfall intensity and duration;

- Geometry of the slope and its characteristics;
- Presence of Groundwater;
- Dynamic forces, e.g. earthquakes, moving vehicles, and any other vibration loads.

2.2.2.1 Rainfall Intensity and duration

During the wet seasons, precipitation is considered an important issue for slope stability. Different studies have been carried out to investigate the failure mechanism of the slope under the rainfall infiltration (Campbell 1975b; Crosta and Frattini, 2008; Van Asch et al. 1999; Rahardjo et al. 2005; Muntohar et al. 2013b). Studies proved that soil properties significantly affect the stability of slopes, and most commonly, the hydraulic characteristics of soils have a major impact. A study by Brand et al. (1984) determined that the duration and intensity of precipitation have a great impact on the failure of slopes. Rahimi et al. (2010) describe that the slopes in sandy soils fail under short-term but heavy rainfall events, whilst slopes in clayey and silty soils fail under low-intensity prolonged rainfall events. The hydraulic properties of sandy soils showed a quick response against rainfall events because of their high hydraulic conductivity and less water retention capacity. On the other hand, the Clayey Sand silty soils showed a slow response to low-intensity (but prolonged rainfall) events due to their lower hydraulic conductivity and high water storage capacity. Therefore, it is important to consider the relationship between soil hydraulic characteristics and rainfall duration/intensity in the stability analysis of slopes. Hearman and Hinz (2007) state that as rainwater seeps into the slope, it creates pore-water pressure, which may eventually cause the slope to break. Hence, it is important to include both the magnitude and duration of precipitation while doing stability analysis. Nevertheless, it is important to acknowledge that a fraction of the precipitation that descends on the incline may be redirected as runoff rather than fully permeating the slope, introducing an extra level of intricacy to the relationship between rainfall and soil stability.

When a slope receives rainfall that has a similar intensity to its hydraulic conductivity, the rainwater might potentially fully infiltrate the slope, resulting in slope collapse. According to the author, a rainfall intensity between 0.2 and 0.6 times the soil hydraulic conductivity (0.2k - 0.6k) has a significant impact on infiltration and represents a key threshold for possible slope destabilization. Precipitation with a very low intensity (I = 0.2k) can completely penetrate the soil, but it may not be enough to saturate it. On the other hand, when the intensity of rainfall is high (I > 0.6k), some of the precipitation may cause runoff since the ground is unable to absorb it all. Therefore, the resolution of rainfall, which determines the timing of rainfall intensity, is

expected to have a significant impact on the amount of water that seeps into a slope. In the past, Hearma and Hinz (2007) researchers employed daily rainfall data in their analysis of slope stability; however, hourly rainfall data have been used on occasion due to the availability of hourly data from weather bureaus. The author claims that using daily data may underestimate the infiltration surplus and exaggerate the amount of infiltration. They also propose that when considering infiltration projections in the tropics where high-intensity precipitation is more likely, better resolution rainfall data, such as hourly rainfall data, becomes more crucial. In reality, there are large variations in the typical distribution measure of precipitation intensity over a given time period. Because it represents rainfall data that is more indicative of actual weather conditions, high-resolution rainfall should be taken into account in slope stability evaluations. Results would be more precise as a result (Ng et al. 2001). In addition, in order to analyse and optimise the effect of different levels of rainfall intensity on the stability of slopes, particularly in sensitivity studies, slope stability evaluations often assume that precipitation intensities remain constant during a given time of observation. However, this method is in direct opposition to the usual, highly fluctuating, and sporadic pattern of rainfall intensity. The typical distribution of rainfall intensity may have a major impact on changes in pore water pressure, which is an important issue to consider when doing a thorough investigation of slope stability.

It is generally acknowledged that precipitation, especially persistent precipitation, is the main factor contributing to slope failure during the rainy season. On the other hand, the interaction between rainfall and soil affects how a slope responds to rainfall in terms of failure. Slope failure is mostly determined by how much rainfall water infiltrates the slope. Therefore, a key factor in precipitation-induced slope collapse is the nature of the slope's soil hydraulic conductivity in proportion to the severity of the precipitation. Furthermore, it is important to take into account the prior event, duration, resolution, and pattern when considering rainfall occurrences as a trigger for slope failure. A seepage analysis that takes into account all of these factors would produce input parameters for the investigation of precipitation-induced slope instability.

2.2.2.2 Geometry of Slopes

The geometry of a slope plays a vital role in determining its stability. The essential geometric components of a slope, such as height, overall slope angle, and the size of the failure surface, are crucial factors in determining its stability. Significantly, as the height of a slope grows,

there is a gradual reduction in slope stability, highlighting the importance of geometric elements in evaluating and comprehending slope behaviour. In order to prevent any ground deformation in the mine's vicinity, it is important to consider the possibility of failure occurring beyond the crest as the total slope angle increases. In general, slope height, slope angle, and slope profile are the three main parameters in any slope design or geometric modification of natural slopes. Cut and embankment slopes can be created using single-slope, multi-slope, and bench-slope profiles. These profiles function differently in terms of slope stability, though, depending on the nature of the slope material, its height, and the hydrological circumstances. To adequately resist failure with a constrained elevation, a single slope profile is used in the cut and embankments of dense soils. Shear stress on the probable rupture plane will increase as height (h) and slope angle both increase. In cuts where the soil stratigraphy consists of two or more strata with different strengths, multi-sloped profiles are possible. In the stiffer and weaker layers of the slope section, the approach permits the use of both steep and gradual slopes. A bench slope is a technique for breaking up a large hill into numerous smaller slopes. Lowering the slope weight lessens the pushing forces above the failure surface. Bench slope performance is primarily affected by bench slope, bench height, and bench breadth. Figure 2.2 illustrates the various components of a slope, including the bench, bench angle, toe, and crest.

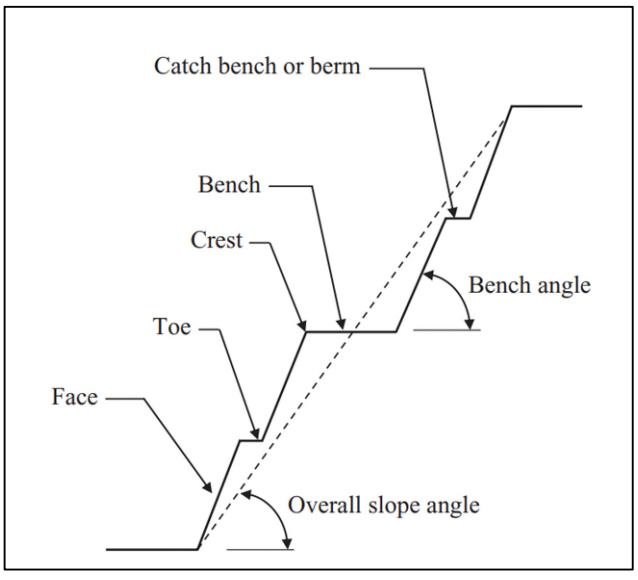

Figure 2.2: Schematic diagram showing bench and slope angles in slopes (Chaulya and Prasad, 2016)

2.2.2.3 Groundwater

Groundwater may cause changes in soil characteristics, resulting in variations to both cohesion and friction soil strength metrics. Moreover, the influence of groundwater entails a decrease in

the effective tension inside the soil. These modifications highlight the interactive connection between groundwater and soil behaviour, emphasizing the need to take hydrogeological parameters into account when assessing and forecasting changes in soil attributes. Groundwater thus has a negative impact on the stability of slopes and can also increase upthrust and driving forces. Further, water inside rock joints can affect the friction and cohesiveness of a discontinuity surface physically as well as chemically. By providing elevation on the joints and lowering the frictional resistance, the physical effect lowers the shearing resistance along a plane of failure and, as a result, the effective normal stress.

2.2.2.4 Dynamic forces

The blasting creates a vibration that increases shear stress and maximizes material dynamic acceleration, both of which lead to instability in the sloping plane. Bench face angles rise as a result of the blasting process, and bench instability can also be caused by improper blasting techniques. These parameters, such as the bench face angle and blasting vibrations, also affect the failure in the rock mass as a result of blast damage and back break (Chaulya and Prasad, 2016; Sari et al. 2014). Many smooth blasting techniques have been used on small-size slopes to mitigate these effects. Blasting has fewer negative effects on greater slopes due to blast damage and back breaks to benches on the steady overall slope angle. The high-frequency waves created by the blasting process cause less damage to the greater slopes than the low-frequency waves, but they cause more back breaks and hence prevent huge rock masses from being displaced. For large-scale slopes, blast-induced failures are thus a minor issue. In mountain regions, seismic occurrences, or low-frequency vibrations, are more likely to cause large-scale slope failures (Ghasemi 2017; Chang et al. 2023; Djordjevic et al. 1999; Sari et al. 2014).

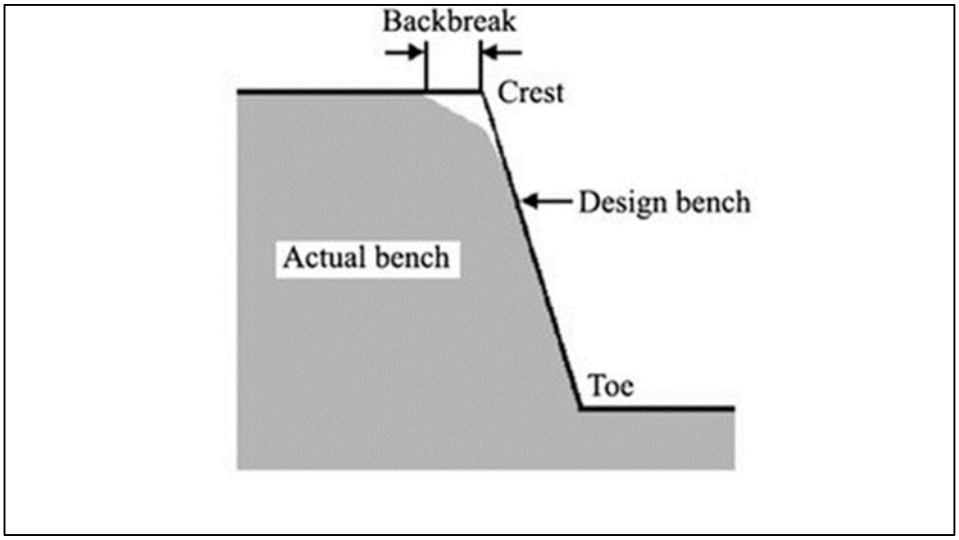

Figure 2.3: Illustration of back break in bench blasting (Sari et al. 2014)

2.2.3 Rainfall Infiltration Parameters Affecting Slope Stability

During rainfall-induced landslides, the process of rainwater infiltration occurs in a sequential manner. At first, rainwater seeps into the upper layers of the slope, gradually moving into deeper levels as the downpour persists. In the end, any surplus water that is not soaked up by the soil helps to replenish the groundwater. The process of rainfall infiltration is significantly affected by the intensity, type, and length of the rainfall event. In order to have a deeper comprehension of the dynamics, the seepage process may be divided into three distinct phases, which can be identified by analysing the force and motion attributes of water:

- Imbibition stage
- Leakage stage
- Osmotic stage

2.2.3.1 Imbibition stage

The focus at this stage is molecular force. After being absorbed by soil particles, infiltration water changes into pellicular water (suspended water above the ground water table). In dry soil, this stage is particularly obvious as water enters the soil and is trapped in air voids; hence does not join the ground water table. This stage eventually vanishes as the soil moisture content exceeds the maximum molecular moisture.

2.2.3.2 Leakage stage

Capillary force and gravity action define this stage. When water infiltrates soil pores, it does so in an irregular downward flow that gradually fills the pores with water until they are fully saturated. The two stages can typically be referred to as leakage stages.

2.2.3.3 Osmotic stage

When the soil pores are completely saturated with water, the water begins to flow steadily downward due to gravity. Unsaturated water moves through seepage, whereas saturated water moves through infiltration.

There is no distinct boundary between these phases in the actual penetration of water. The infiltration rate of a landslip governs the amount of rainwater that penetrates a certain surface area. The rate in question is the precise measurement of the volume of water that flows into a certain unit area of a surface during a specific time period. It is often denoted as I or qi. When the intensity of rainfall is below the minimum infiltration rate of the topsoil, the infiltration rate matches the rainfall intensity. Given these circumstances and assuming a consistent intensity of rainfall, the rate at which water infiltrates the ground stays constant.

The topsoil moisture content gradually increases until it reaches a constant amount when there is continuous precipitation. Some precipitation produces runoff or seepage when rainfall intensity exceeds the capacity of unsaturated topsoil to absorb water, while other precipitation seeps underground. A portion of the water that seeps into the ground is retained in soil pores above the water table, while the remainder that exceeds the soil's capacity for water retention simply recharges the groundwater. The primary elements impacting a slope's ability to absorb rain are as follows:

- Slope features;
- Precipitation;
- Evaporation.

According to the slope perspective, the slope's main features are:

- Slope seepage properties;
- Slope gradient, vegetation coverage on the slope surface;
- Fissure distribution;

- Soil capillary water.

Rainfall types, duration, and intensities are the three basic elements of precipitation. The primary determinants of evaporation are the length and intensity of surface evaporation. The duration and intensities of surface evaporation are the main determinants of evaporation. External forces like precipitation and evaporation have an impact on slope stability by primarily altering the water distribution in the slope. Internal variables are the characteristics of the slope itself, and rock and soil permeability are crucial. The main way that external factors like precipitation and evaporation affect slope stability is by changing the water distribution on the slope. The slope's internal features, including the permeability of the rock and soil, are key internal variables.

Infiltration refers to the process where water moves from the surface into the subsurface, permeating the soil. This process is significant in both soil science and hydrology as it affects soil moisture levels and groundwater replenishment. The rate at which water enters the soil is known as the infiltration rate. Understanding the infiltration rate is crucial for assessing soil health and structure. A high rate indicates well-aggregated soil with a good crumb structure. The maximum rate at which soil can absorb water, known as infiltration capacity, is usually measured in meters per day. It is always higher than or equal to the infiltration rate and decreases as the soil becomes more saturated. Factors influencing infiltration capacity include soil grain size and vegetation cover.

2.2.3.4 Factors Affecting Infiltration

The following are the key influencing factors:

2.2.3.5 Porosity

When estimating infiltration capacity, soil porosity is crucial. Smaller pore sizes, like those found in clay, result in lower infiltration capacities and slower infiltration rates (e.g., for clay 1 to 5 mm/hr, clay loam 5 to 10 mm/hr, loam 20 to 20mm/hr) than larger pore sizes, like those found in sands (e.g., sandy loam 20 to 30mm/hr, sand 30 to 40mm/hr). When clay is in a dry condition, this rule is an exception because, in this scenario, the soil may experience significant cracking, which would increase infiltration capacity.

2.2.3.6 Geometry of Slope

Infiltration rates are significantly affected by the slope of the land. On steeper slopes, water tends to run off quickly, resulting in less infiltration. The rapid runoff reduces the time water has to permeate the soil, leading to lower infiltration rates. In contrast, locations with gentle slopes or plain terrain experience higher infiltration rates (Shiferaw 2021a). The slower movement of water in these areas allows more time for it to be absorbed by the soil. Additionally, the flatter terrain minimizes runoff, promoting more extensive infiltration and better groundwater recharge. Therefore, understanding the relationship between land slope and infiltration is crucial for effective water management and soil conservation strategies.

2.2.3.7 Texture of Soil

The rate at which water infiltrates the soil is influenced by its texture. For coarse-grained soil, the infiltration rate is considerable (e.g., sandy loam 20 to 30mm/hr, sand 30 to 40mm/hr). For fine-grained soil, the rate of water infiltration is relatively low (e.g., for clay 1 to 5 mm/hr, clay loam 5 to 10 mm/hr, loam 20 to 20mm/hr) (Gasmo et al. 2000; Gavin and Xue, 2008).

2.2.3.8 Groundwater Table

Where the groundwater table is relatively close to the surface, it slows down the pace of water infiltration because of less space available for infiltration. Further, shallow groundwater causes capillary rise increases soil saturation and promotes surface runoff (Gavin and Xue, 2008; Gasmo et al. 2000).

2.2.3.9 Rainfall Intensity

When there is high-intensity rainfall, the mechanical compaction caused by the water's impact slows the pace of infiltration, while low-intensity rainfall increases the infiltration rate because of the less compaction energy being transferred to the soil layers (Gasmo et al. 2000; Gavin and Xue, 2008).

2.2.3.10 Temperature

The soil mass becomes impermeable when the saturated soil temperature is very low, which results in a low infiltration rate because, at low temperatures, water within the soil freezes and prevents further infiltration into the soil and therefore makes it impermeable (Gasmo et al. 2000; Gavin and Xue, 2008).

2.2.3.11 Seepage

One of the main influences on slope stability is seepage flow. According to research findings, rainfall infiltration and water level variations can significantly affect soil shear strength and, thus, the slope's stability (Kim et al. 1992; Dahal 2012; Zhang et al. 2007; Crosta and Frattini, 2008; Rahimi et al. 2011; Wu et al. 2017; Kim et al. 2004; Olivares and Picarelli, 2003). A slope's rock mass typically contains a significant quantity of groundwater and is further affected by seasonal rainfall. Recent changes in the global climate, such as excessive rainfall, may be causing more frequent occurrences of different geological disasters on slopes (Dehn et al. 2000; Davies 2011; Kolathayar et al. 2021; Bračko et al. 2022). Varying types of rainfall have different effects on a slope's ability to seep water; brief periods of rain can create a temporary saturation zone in the shallow layer of a slope, and long periods of rain can raise the groundwater level. The physical composition, sedimentary features, and intricate geological processes on the rock and soil mass differ significantly due to rainfall infiltration, which is a constant and dynamic process. The impact of rainfall infiltration on the stability of the rock slope and the seepage field must be thoroughly examined while considering its inherent spatial variability.

2.2.4 Effect of Climate Change on Slopes Instabilities

The acknowledgement of ongoing climate change is now widespread, and it is recognized that this phenomenon will impact the processes and parameters influencing slope stability. Nevertheless, there persists a considerable degree of uncertainty when it comes to accurately forecasting these changes over the long term. The intricate nature of climate dynamics introduces challenges in predicting the specific alterations in factors that contribute to slope stability, underscoring the need for ongoing research and improved modelling techniques to better understand and anticipate the implications of climate change on slope behaviour. Climate change has profound effects on various aspects of our planet, including rainfall patterns and slope failures. The driving force behind these changes is primarily attributed to the escalating levels of greenhouse gases, such as carbon dioxide, in the atmosphere. Human activities, notably the burning of FOSsil fuels and deforestation, contribute significantly to the increased concentration of these gases, amplifying the impact of climate change on various environmental processes, including those influencing slope stability. The interplay of human-induced factors with natural systems underscores the complex and interconnected nature of the challenges posed by climate change. Various studies on the effect of climate change reported

that climate change can lead to alterations in rainfall patterns, which can result in more frequent and intense extreme weather events like droughts, heavy rainfall, and storms (Ciabatta et al. 2016; Corominas 2000; Gariano and Guzzetti, 2016; Dailey et al. 2009; Merat et al. 2017; Bračko et al. 2022). This occurs due to several interconnected mechanisms:

Increased Evaporation: Rising global temperatures cause increased evaporation from land, oceans, and vegetation. This leads to higher moisture levels in the atmosphere.

Intensified Water Cycle: A warmer atmosphere can hold more moisture. As a result, when rainfall does occur, it can be more intense, resulting in heavy downpours and potentially causing flooding.

Shifts in Rainfall Patterns: Climate change can cause shifts in the distribution of rainfall, leading to changes in the timing, duration, and location of rainy seasons. This can impact ecosystems, agriculture, water availability, and overall water management.

Climate change can increase the occurrence of slope failures, such as landslides and mudslides, through a combination of factors that directly or indirectly affect the stability of slopes. Climate change contributes to an increased risk of slope failures by:

Increased Precipitation Intensity: Climate change is associated with more frequent and intense rainfall events. Heavy rainfall can saturate the soil, reducing its stability and causing increased pore water pressure. This weakens the friction between soil particles and can trigger landslides.

Erosion and Soil Degradation: Intense rainfall can lead to soil erosion, removing the protective top layer of soil that helps bind the slope together. This erosion weakens the slope's stability and increases the likelihood of slope failures.

Thawing Permafrost: In cold regions, climate change can cause permafrost (frozen ground) to thaw. Thawing permafrost can lead to a loss of ground stability, as the frozen ground becomes unstable and prone to sliding, especially on steep slopes.

Increased Groundwater Levels: Elevated rainfall due to climate change can lead to higher groundwater levels. Excess water in the soil can reduce the soil's shear strength, making it more susceptible to sliding.

Deforestation and Land Use Changes: Human activities, often intensified by climate change impacts like shifting agricultural practices or rapid urbanization, can result in deforestation and changes in land use. Removing vegetation reduces the stabilizing effects of roots that bind the soil, making slopes more vulnerable to failure.

Increased Temperature Extremes: Climate change can lead to temperature fluctuations. Rapid freeze-thaw cycles can weaken the rock and soil in slopes, making them more susceptible to sliding.

In summary, climate change significantly impacts rainfall patterns and slope failures. The alteration of rainfall distribution and intensity, coupled with changes in soil stability, can lead to increased occurrences of landslides and other slope failures. These changes have implications for human communities, ecosystems, infrastructure, and overall environmental resilience (Vardon 2015; Agency 2017; Stoffel and Huggel, 2012; Gariano and Guzzetti, 2016; Stoffel et al. 2014).

2.2.5 Rainfall Infiltration and Shallow Landslides

Around the world, landslides are common and pose serious risks to both economics and safety. The most common trigger, especially in tropical regions, is rainfall. In areas with heavy precipitation and humid climates, residual soils, which are typically found in unsaturated environments, are common. Water that seeps through unsaturated soil surfaces may result in reduced matric suction and decreased soil shear strength, which raises the risk of slope failure. Although runoff has typically received less attention than infiltration and groundwater, they are nonetheless major contributors to shallow landslides. In regions where slopes contain high permeability soils on top of low permeability soils, shallow landslides frequently occur (Olivares and Picarelli, 2003; Guzzetti et al. 2008; Matsushi et al. 2006). High water pressures are created when water is trapped in shallower soil due to low soil permeability, and the topsoil might become unstable and slip downslope when it becomes saturated with water.

A shallow landslide is one that has its sliding surface beneath the soil mantle or eroded bedrock, often at a depth of a few decimeters to several meters. Landslides that are deeply seated or well below the maximum rooting depth of trees, for example, are ones in which the sliding surface is predominantly deeply located. They frequently contain major slope collapses linked to translational, rotational, or complicated movements and deep regolith, weathered rock, and/or bedrock (Caruden and Varnes, 1996; Varnes 1978). Concave scarps at the top and steep

sections at the toe help visually identify them. In addition to altering landscapes across geological eras, deep-seated landslides can release silt that significantly changes the path of fluvial streams.

2.2.6 Uncertainties in Slope Stability under Rainfall Conditions

A slope's susceptibility to land sliding and the frequency with which it occurs are elements of hazard. The hazard and the effects of land sliding are both parts of the risk. The risk can be described in terms of both the potential for human life to be lost as well as economic loss (including property damage and destruction). Traditional geotechnical analysis methods, whether deterministic or probabilistic, fall short of providing a reliable way to assess the risk and hazard of land sliding (Oh and Lu, 2015a; Ali et al. 2014; Crosta and Frattini, 2008; Chen et al. 2004). The likelihood must be reflected in hazard in both a spatial and a temporal sense. Therefore, historical information derived from field observation is required for its evaluation. Observation, deduction, and subjective judgement are also needed for the identification of vulnerable elements and the assessment of their susceptibility. The basic objectives of urban landslide control can be summed up as follows for places where rainfall is the primary triggering agent for landslides:

- Identifying the connection between rain and land slipping;
- Predicting the likelihood of land sliding in various locations;
- Putting slopes at the top of the list for prevention and repair;
- Construction of early warning systems;
- Creating methods for hazard and risk assessment in real-time during downpours.

2.2.7 Infiltration in Unsaturated Soil Slopes

Rainfall has been blamed for many slope failures and landslides that happened in regions with high seasonal rainfall (Loo et al. 2015; Crosta and Frattini, 2008; Rahimi et al. 2011; Matziaris 2019; Travis et al. 2010; Gofar and Rahardjo, 2017). The analysis of infiltration's influence on slope stability is often based on imperfect correlations with rainfall and runoff since direct field data is typically lacking. Several variables, including rainfall duration and intensity, surface type, saturation level, slope angle, permeability ratios, and the existence of perched water tables, present considerable difficulties in accurately assessing slope stability. The significance of water infiltration is often disregarded or insufficiently considered in several evaluations of slope stability. This highlights the need for more comprehensive approaches that include the

complex interaction of these different elements when assessing and controlling slope stability (Gofar and Rahardjo, 2017; Gallipoli et al. 2003; Haxaire et al. 2011; Ng et al. 2003).

Matric suction is a fundamental stress variable in the theory of unsaturated soils. The presence of matric suction contributes to an increase in the soil's strength and robustness. A deep groundwater table is typical of hilly tropical countries, and in this case, controlling the soil shear strength (which will be greatly influenced by the soil matrix suction, which causes negative pore water pressure) is essential for maintaining the stability of many steep slopes. Shallow landslides frequently occur on steep slopes with leftover soil after protracted and heavy rainfall. As water infiltration into the soil advances toward saturation, the matric suction, particularly close to the ground surface, will gradually decline and eventually vanish.

It is commonly known that a significant drop in matric suction, which causes an increase in pore water pressure, leads to a fall in soil shear strength. This loss in shear strength is a major factor contributing to the occurrence of shallow landslides. The field has relied heavily on hydrological research, where water infiltration plays a vital role in connecting surface and subsurface hydrology. Precise measurement and subtraction of infiltrated water from surface runoff is crucial in flood prediction studies and surface water management. Many researchers have acknowledged the importance of infiltration in studying the stability of residual soils on slopes (Othman 1989; Anderson 1991; Abdullah and Ali, 1994; Suhaimi 1997; Ali and Rahardjo, 2004). They have included this aspect in their evaluations, so enhancing our overall understanding of the many components that affect slope behaviour. Most slope stability analyses assume that the slope's infiltration rate of water into the soil is constant. Except in certain layered bedding problems, the soil is also assumed to be homogeneous.

2.2.8 Mechanisms of Rainfall-Triggered Landslides

Numerous landslides have been caused by storms that have caused significant rainfall for as little as a few hours or more extreme rainfall for a few days (Crosta and Frattini, 2008; Brand 1984; Hutchinson 1988; Van Asch et al. 1999; Sassa et al. 2007). During the most severe stages of a storm, small landslides often happen on steep slopes in soils and worn rock formations. The presence of these landslides often requires precise criteria regarding the combined intensity and length of the storm. This suggests that certain circumstances, marked by a crucial combination of intensity and duration, must be fulfilled in order for shallow landslides to occur during intense storm events on steep ground. Campbell (1975) conducted research which found that when rainfall exceeded a certain threshold of 6.35 mm/hr, it caused shallow landslides in

the Santa Monica Mountains of southern California. These landslides then resulted in disastrous debris flows. In 1982, a significant event took place in the San Francisco Bay area of California. During a period of about 32 hours, there was heavy rainfall, which resulted in over 18,000 landslides. These landslides were mostly composed of soil and worn rock, and they were generally shallow in nature. The broad occurrence of landslides led to the obstruction of many main and subsidiary highways, highlighting the substantial influence of protracted and strong rainfall events on the stability of slopes in the area.

It is generally accepted that the process by which most shallow landslides are formed during storms is the quick penetration of rainfall, which results in soil saturation and a brief increase in pore-water pressures. Transiently increased pore pressures have been detected in hillside soils and shallow bedrock during rainstorms linked to a lot of shallow lands sliding thanks to advancements in instrumentation and electronic monitoring systems (Lu and Godt, 2013; Philip 1991; Matsushita et al. 2006).

Wildfires can create a layer of hydrophobic (water-repellent) soil beneath and parallel to the burned surface, which, along with the removal of vegetation, encourages the ravelling of loose, coarse soil grains and fragments at the surface. Small debris flows are then caused by development and heightened overland movement. Major storms produce high sediment content in streams (hyper-concentrated flows) or significant debris flows on the lower portions of hill slopes and In-Stream Channels.

2.2.9 Methods of Slopes Stability Analysis

Slope stability analysis can be carried out using manifold methods. Figure 2.4 presents the various methods commonly used for slope stability analysis presented by (Duncan et al. 2014). Boundary Element Method (BEM), Finite Element Method (FEM), Limit Equilibrium Method (LEM), and Finite Volume Method (VEM) and many more are used to evaluate the analysis of slope stability. Various different types of software are currently available for slope stability analysis, including packages such as PLAXIS, GEO5 Rock Stability, Stereonet, Dips, SV Slope, Rock Plane, Slide2/ Slide3, Wedge/ SWedge, and others. The site characteristics/geoengineering features influence which program is used and the type of software and behavioural model chosen must be influenced by the geomechanical conditions (geo-materials) of the site, not by assumptions. Additionally, another factor influencing the choice of software is the type or results of the analysis that is required. Slide, Phase2 (FEM), FLAC (FDM), and PLAXIS (FEM) are good options if only a single safety factor in a static

scenario is required. Software that uses FEM or FDM is required if displacements as well as the safety factor are required (e.g., FLAC, Plaxis, Phase2). Such software also provides the feature of dynamic analysis, whilst Slide2/Slide3 can only perform pseudo-static analysis.

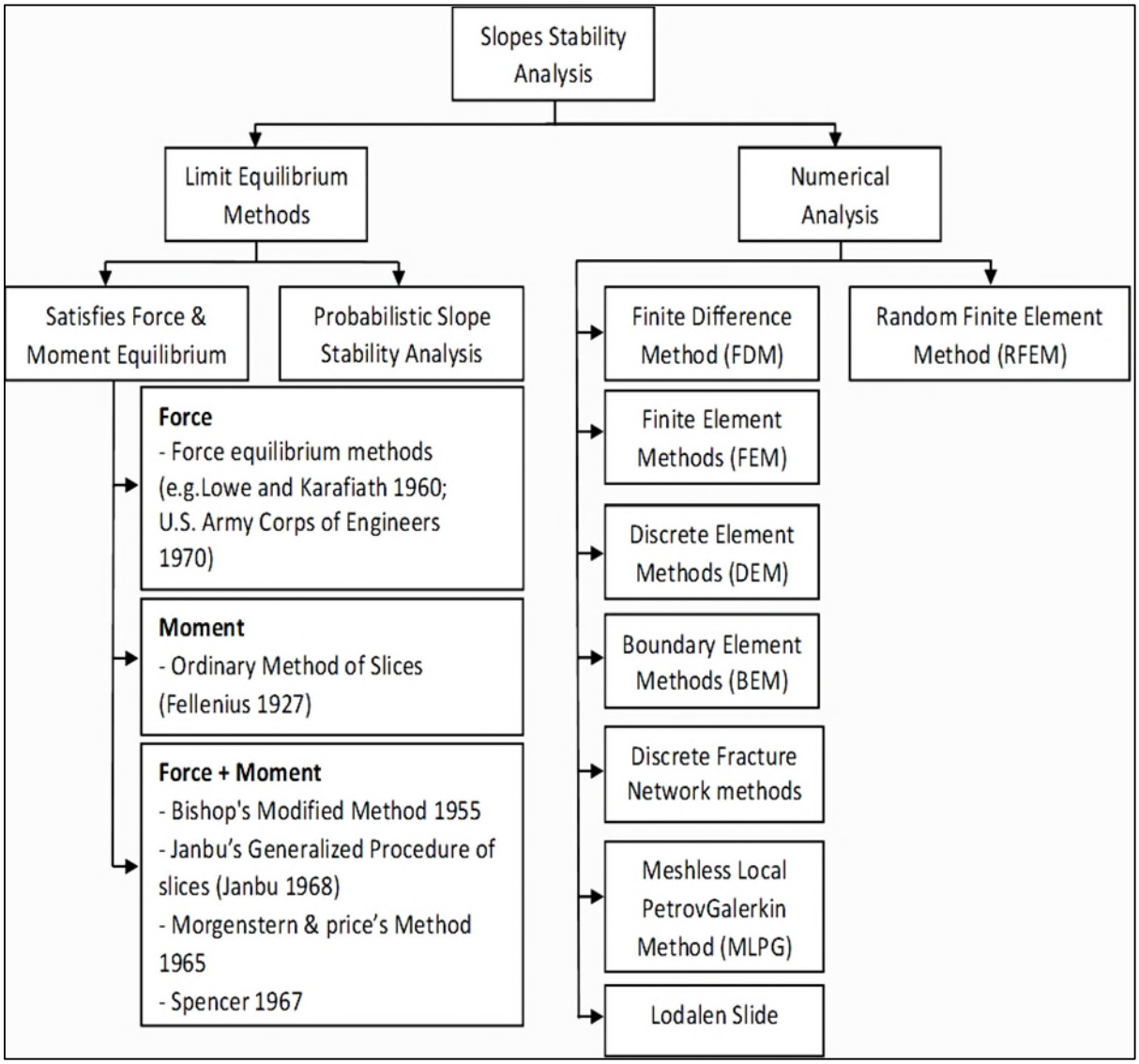

Figure 2.4: Methods for Slope Stability Analysis (Duncan et al. 2014)

2.2.9.1 Limit Equilibrium Method (LEM)

The Limit Equilibrium Method (LEM) comprises a range of procedures that require dividing the soil or rock mass into slices. In LEM, it is essential to have a continuous surface that goes through the soil mass. This is because initial assumptions need to be made before doing slope stability calculations. In this approach, it is necessary to artificially assume the presence of lateral forces and their respective directions in order to build an equation of equilibrium. Other slope stability analysis approaches, such as the Ordinary Method, Force Equilibrium Method,

Morgenstern and Price's Method, Janbu's Method, Bishop's Modified Method, and Spencer's Method, often use similar assumptions. The Limit Equilibrium Method is still a very popular technique for assessing the stability of slopes in both two and three dimensions (Hammah 2005; Yamin and Liang, 2010a; Kanjanakul and Chub-uptaken, 2013; Namdar 2010; Lu et al. 2013; Liu et al. 2015). This approach is used to evaluate probable failure mechanisms and safety implications in certain geotechnical circumstances. This procedure employs a range of stability analysis techniques, such as basic equations to determine the factor of safety for planar failures, stability charts, the method of slices for two-dimensional analysis, three-dimensional analysis methods, and considerations for ensuring the dependability of slope design. These approaches, categorised as limit equilibrium techniques, ascertain the shear strength along the sliding surface by using the Mohr-Coulomb formula. The shear strength of soil refers to the highest level of resistance to shear forces that might occur at a probable failure surface inside the soil. The shear strength of the soil is determined by its type and the effective normal stress, whereas the shear stress that is exerted relies on the external forces applied to the soil mass. Engineers and geotechnical specialists may get vital insights into the safety and stability issues of a specific geological setting by using these stability analysis methodologies.

Depending on the soil type, the loading circumstances, and the amount of time following loading, there are two different approaches to considering soil strength. The *total stress* strength is used in clayey soils for consideration of short-term behaviour (i.e., relatively soon after loading). The *effective stress* strength is used in any type of soil for long-term conditions and can be determined when pore water pressure is known. Multiple vertical slice techniques have considerably enhanced gradient analysis utilizing the limit equilibrium (LEM) method. Most commonly used are the usual or Fellenius (1936), Bishop (1955), Janbu (1954), Spencer (1967), and Morgenstern and Price (1965). The limit equilibrium approach is used to compute the safety factor. The limit equilibrium (LE) approach employs the Mohr-Coulomb failure criterion to calculate shear strength along the slip plane.

A LE exists when the recruited shear stress is specified as a percentage of the shear strength. Sliding masses are stratified for LE analysis, shear and normal forces between strata are calculated, and force and/or moment balance equations required for static equilibrium conditions are satisfied. Fellenius (1936) presented the first LE approach for rounded slip surfaces. Bishop (1955) later improved the method of smoothness analysis. On the other hand, Janbu (1954) showed how to create a non-circular fracture surface by separating the sliding

mass into several vertical slices. Subsequently, Morgenstern and Price (1965), Spencer 1967), Sarma (1973) and others developed approaches to improve various inter-slice force hypotheses. These approaches are widely used due to their relatively high accuracy in determining FOS (Lin and Cao, 2012; Cheng et al. 2007; Ugai and Leshchinsky, 1995; Deng et al. 2017).

2.2.9.2 Finite Element Method (FEM)

In past decades, the FEM has increasingly been used for the analysis of slope stability (Wu et al. 2017; Zienkiewicz et al. 1975; Zheng et al. 2006; Zheng et al. 2009; Zhang et al. 2018a; Griffiths and Lane, 1999; Griffiths and Marquez, 2007; Le 2014; Hu et al. 2017; Xu et al. 2017). The FEM is more recommended because, in the analysis of slope stability, there is no need for assumptions such as the failure surface shape and location. There is no need to assume the side forces and their direction because the FEM works on complex slope configurations. In the FEM, 2D/3D elements and different types of material could be inserted for the analysis. The FEM accurate and fast procedure can evaluate the equilibrium of stress, strains, shear strength, and displacement in soil or rock mass. FEM can also evaluate the deformation at terrain surfaces and monitor the progressive failure, which includes the overall shear failure with it. The finite element approach is a technique for methodically approximating continuous functions as discrete models. The domain is discretized into a finite number of points and subdomains. The points, also known as nodes, are where the values of the supplied function are stored. In order to store piecewise and local approximations of the function that are uniquely defined in terms of the values held at their nodes, non-overlapping subdomains, referred to as finite elements, are connected at nodes on their boundaries. The meshing method is used to create the mesh, which is made up of discretized components and nodes. The use of numerical modelling in geotechnical analysis has become popular and is considered the most effective way to solve complex technical problems (Peng and Zhang, 2012; Liu et al. 2015; Su and Xu et al. 2017; Zhang et al. 2018b). The Finite Element Method and the Finite Differential Method are the two most common forms of numerical methods. FE for modelling slope stability in this study uses the stress-strain behaviour of the soil. A major advantage of finite element analysis is that it does not require assumptions about the shape of inclined or slip surfaces. The model is split into fragments or mesh elements using the FE approach. The material laws of the slope stability model are used to determine stresses and strains. Natural failure occurs when the soil has an insufficient capacity to withstand the shear loads induced. Also it is also possible to obtain the finite element reduction factor (RF) using the "c-reduction" approach. This technique

requires a gradual reduction in the strength parameter of the soil to destroy it. The FE method can calculate the FOS of a slope using a shear strength reduction methodology.

2.2.10 Application of Limit Equilibrium and Finite Element Methods in Slope Stability Analysis

Malla and Dahal (2021) studied the failure of slopes in Nepal caused by rain, which is considered a geotechnical hazard that occurs all around the world. The process of infiltration of rainwater into the soil lowers the matric suction and increases pore water pressure, which in turn lowers shear strength, which causes failure in slopes. For study and research purposes, the natural slope of the Paima area, which is in the Bajura district, was selected by the authors (Malla and Dahal, 2021). GeoStudio software was used for numerical modelling to check and analyze the stability of the slope and seepage. The software (GeoStudio) was used for the analysis of slope stability, which was performed by the limit equilibrium methods using the Morgenstern-Price formula. Infiltration of rainwater in soil results in the reduction of a factor of safety, whereas when the intensity of rainfall increases, the rate of reduction also increases. By studying the parameters, it is concluded that slopes with high-permeability soil become critical in a short time, while slopes with low permeability remain stable for a relatively long duration.

Goh et al. (2020) conducted research work on the analysis of residual soil slope stability using numerical modelling, comparing the finite element method (FEM) against the limit equilibrium method (LEM). Engineers and designers have become more interested in simulation methods for the prediction of soil behaviour because of the developments in numerical simulation with computer modelling software. Modelling or performing calculations to assess slope stability is an extremely complex process, and, as a result, computer modelling software is used for modern evaluations of natural slope stability. The analysis by FEM and PLAXIS-2D software was used by authors Goh et al. (2020) to implement the soil slope model assessments. The parameters of the soil layers that were used in these slope models were determined by laboratory testing. Then, using SLOPE/W software and the LEM, the resultant (FOS) values were compared to earlier findings for slope models of a similar nature. The assessed results showed that the computed FOS could be significantly impacted by a change in slope geometry. Additionally, the safety factor determined by the FEM approach was nearly identical to but marginally greater than the outcomes determined by using LEM. However, both approaches were successful in identifying the optimal phenomena behind the failures of slope behaviour.

However, the use of FEM provides a compelling alternative to conventional methods for the issue, particularly for LEM.

Gholamzade and Khalkhali (2021) researched pore water pressure and internal stability in the landslide area of Zarm-Rood Dam, Iran. GeoStudio's program SLOPE/W was utilized to evaluate pore water pressure and internal stability of selected landslide areas. Based on this analysis, it was concluded that when the range of porewater pressure is between 0.2 and 0.4, the factor of safety decreased by 10%. Whereas when the range of porewater pressure is between 0.4 and 0.6, the factor of safety decreased by 17%. This research analysis results in the successful utilization of the GeoStudio program SLOPE/W for analysis of slope stability in mega projects, i.e., dam construction.

Waseem et al. (2021) conducted a research study in Qalandarabad, Khyber Pakhtunkhwa, Pakistan, aimed to examine slope failure and calculate the safety factor for slope stabilisation analysis. The Limit Equilibrium Method (LEM) was used with GeoStudio Software to compute the factor of safety (FOS) for slope stability. The SLOPE/W programme used many techniques, such as Bishop, Morgenstern-Price, Janbu, and the usual method of slices, to analyse slope stability. The analysis took into account both dry and completely saturated field drainage conditions. The Factor of Safety (FOS) values for the Gravity Loading condition varied from 0.344 to 0.383, suggesting an unstable slope. Under Seismic Loading circumstances, the Factor of Safety (FOS) ranged from 0.287 to 0.332, indicating the slopes' pronounced instability. The FOS values indicate an unstable slope condition, which is likely responsible for the numerous occurrences of slope failures in Qalandarabad. To mitigate these stability problems, a retaining wall was constructed to bolster the slope. After this adjustment, the Factor of Safety (FOS) under Gravity Loading circumstances rose from 1.531 to 1.690, suggesting enhanced stability. Similarly, under seismic loading circumstances, the factor of safety (FOS) saw an increase from 1.293 to 1.482 after the slope was reinforced. The increased Factor of Safety (FOS) values observed after the construction of the retaining wall indicate a significant improvement in the stability of the slope. This highlights the effectiveness of engineering interventions in reducing the likelihood of slope collapses.

Malik (2020) evaluated seepage and slope stability at Haditha Dam in Iraq. They used the Geo-Studio Software for their investigation. The modelling method for Haditha Dam used the SLOPE/W and SEEP/W sub-programs inside GeoStudio. The research examined three water level scenarios: the highest water level, the average water level, and the lowest water level.

Bishop's (1995) technique was used to determine the maximum water level on the upstream side, while the ordinary method of slices (OMS) was used on the downstream side. The Morgenstern-Price technique was used on the upstream side, and OMS was used on the downstream side at the Normal water level. Ultimately, when the water level reached its lowest point, the Bishop technique was implemented on the side of the river that was closer to the source, while the Janbu approach was implemented on the side of the river that was further away from the source. Applying these methodologies in the modelling effort resulted in the determination that the dams are regarded safe in regard to seepage and slope collapse. The research indicated that the design and stability of Haditha Dam are resilient against possible problems associated with seepage and slope stability under different water level circumstances.

Meng et al. (2020) carried out research work on quantitative analysis of slope stability during reservoir water level fluctuations using a combined FEM-LEM method. The safety of hydroelectric plants is seriously threatened by the steep slopes along the banks of the reservoirs. An important factor in slope stability is the change in the water level of the reservoir. However, the application of the unsaturated soil resistance hypothesis will not be able to measure the parameters that characterize the relationship between water content, matrix attraction and soil resistance. A simple combined FEM-LEM scheme is described to determine the factor of safety, considering pore pressure, osmotic force and weakening of the resistance. A numerical analysis was performed on how changes in reservoir water levels affect the stability of the glaciofluvial deposits. The slope stability of glacial alluvial deposits to changes in water levels was estimated using two general configurations. The results show that in rapid drawdown conditions, the overall failure safety factor is reduced. Rapid draining conditions lead to a reduction in the factor of safety. The most critical sliding surface has a safety factor of 1.073, resulting in small redundancy when the lake level fluctuates between 2230 and 2265 meters above sea level. The final recommendation is to set up monitoring tools and more extensive on-site tests before launching projects. Considering the alternating pore pressure, seepage force and the change of resistance parameters, the proposed FEM-LEM combined technique can describe the mechanism of influence of water level on slope stability. This paper has suggested a simple tool (combination of the FEM-LEM method) that will be useful for irrigation engineering projects in Southwest China to analyse slope stability under reservoir water level fluctuations.

El-Hazek et al. (2020) analyzed the slope and seepage stability of an earth-fill dam using finite element modelling via GeoStudio software. Several programs were used for the stability analysis of the dam. The SEEP/W program was used for the analysis of seepage, whereas SLOPE/W was implemented in GeoStudio for the analysis of slope stability for earth-fill dam stability. Numerical and experimental modelling was performed by introducing four types of sandy soil (different particle sizes and hydraulic conductivities) to check the behaviour of the earth-fill dam. Multiple upstream slope ratios (i.e., 1:2, 1:2.5, 1:3, and 1:3.5) were simulated in software for the stability analysis of the dam (whereas the downstream slope was kept constant at 1.2). An earth-fill experimental model was also constructed in a hydraulics laboratory. Analysis showed that when the upstream slope and hydraulic conductivity increased for every kind of soil, the FOS and seepage also increased. Moreover, decreases occur in seepage when both upstream slope and hydraulic conductivity decrease at the same time.

Azeze (2020) states that the analysis of slope stability could be done using various programs. However, all the various computer programs allow for the input of data such as pore water conditions, soil parameters, different types of soil failure, and manifold methods for the stability analysis. The methodology includes the measurement of slope (width, length, depth) and geotechnical soil investigation to further carry out the parameters such as unit weight, φ, and c. The soil sample was selected on the base of 3 slope sections, and a laboratory test was performed on it to determine the unit weight, φ, and c of the soil. The determined parameters were used in numerical modelling for slope stability analysis. The SLOPE/W program was used to calculate the factor of safety using different general limit equilibrium methods. In the first slope section, the FOS was less than one under dry and wet slope conditions. In the second and third sections of the slope, FOS was greater than one under wet and dry slope conditions. By laboratory tests and numerical modelling, it was concluded that when the moisture content and slope gradient increase, the Factor of Safety decreases.

Hazari et al. (2020) conducted an experimental and numerical study on a reinforced soil slope. In laboratory modelling, several tests were performed on a shaking table for modelled slopes, which were reinforced with different quantities of geogrid (polyethene) and geotextile (polypropylene). A numerical analysis was also performed by PLAXIS 2D using parameters obtained from laboratory investigations. Model slopes are constructed using c-ϕ soil. Results reveal that when the water content increases, the acceleration amplification and horizontal deformations of the slope decrease. The result shows that the geogrid reinforced slope is better

at reducing deformations compared to the geotextile reinforced slope. The experimental results of laboratory modelling have also been verified through the two-dimensional finite element method.

The research by Saftner et al. (2017) focuses on analyzing the stability of Minnesota slopes, chosen due to its comprehensive investigation and significance for future generations. The study aims to address the recurring maintenance needs of locally maintained Minnesota slopes to prevent natural disasters like slope failures, which disrupt nature, damage infrastructure, and pose safety risks. The research involved site investigations, analysis of various slope stabilization methods, laboratory testing for soil strength properties, including Atterberg limit and Sieve analysis and direct shear test for shear strength parameters φ and c. GeoStudio software was employed for modelling, using SLOPE/W to calculate FOS for each slope and the bishop method to assess slope stability. The findings highlighted that incorporating drainage features in the lower part of slopes enhances slope stability.

Sazzad et al. (2016) emphasise the potential vulnerability of waterfront infrastructure, such as embankments, dams, and naturally existing riverside slopes, to instability caused by fluctuations in water levels. The variability in water levels presents a potential hazard when water seeps into the tiny spaces within the soil, diminishing the force exerted on it and so compromising its structural integrity. The decrease in soil strength may have catastrophic implications for the stability of land slopes. The study uses both the Limit Equilibrium Method (LEM) and Finite Element Method (FEM) to evaluate the influence of altering water levels on slope stability. The LEM analysis utilises many approaches, including Fellenius, Bishop, Janbu, Morgenstern Price, and Spencer. Conversely, the FEM analysis uses the Mohr-Coulomb material model. This multi-faceted approach enables a complete assessment of the influence of fluctuating water levels on slope stability. It incorporates many approaches to get a comprehensive knowledge of the possible consequences on both waterfront constructions and natural slopes. LEM and FEM base investigations were prepared using a numerical model, and for the FEM-based numerical analysis, the model's geometric bounds are kept fixed at the bottom and confined horizontally on the left and right sides. GEO5, a tool for studying slope stability issues based on both LEM and FEM, incorporates the geometric model. GEO5 was used to assign material attributes and do numerical analysis. The numerical outcomes were computed while the water level was changed. According to the study, the variable water level has an impact on the slopes' safety factor. With an increase in the groundwater table, the safety

factor is reduced. The study also showed that, compared to FEM, LEM produces a slightly greater result for the safety factor.

2.3 SLOPE STABILIZATION

2.3.1 Introduction

Slope instabilities and failures constitute major environmental hazards. Various factors contribute to these failures, such as earthquakes, rainfall, excavation at the toe of slopes, and loading at the top of the slope. Slope failures triggered by rainfall are particularly prevalent in high tropical regions. These events significantly impact society, with extensive landslide occurrences posing threats to life, infrastructure, and local communities. The resultant damage often impedes economic development in affected areas.

The initial phase in the identification, mitigation, and management of the risk associated with landslides involves assessing the risks across various scales, ranging from regional to site-specific. Conducting such assessments necessitates acquiring data on the topographic, geotechnical, and hydrological characteristics of the slope. These factors can exhibit considerable variability over time and space, rendering them inherently unreliable.

The assessment of slope stability typically incorporates the application of a factor of safety (FOS), a quantitative measure representing the ratio between observed shear strength and the required shear strength for achieving equilibrium along a designated potential failure surface at a specific location. The enhancement of slope stability involves a series of procedural steps, starting with the identification of the most significant regulating process influencing slope stability. Subsequently, the appropriate technique must be selected and applied effectively to mitigate the influence of that specific process.

To be effective, slope stabilization efforts should be tailored to the unique conditions of the slope under consideration. For instance, implementing drainage pipes on a slope with minimal groundwater may prove futile. Such efforts can take place either during the construction phase or in response to unforeseen stability issues post-construction. An exhaustive examination of the soil's characteristics and a comprehensive understanding of the underlying soil and rock mechanics are imperative prerequisites for most slope engineering procedures. This comprehensive approach ensures that the chosen mitigation strategy is well-suited to address the specific conditions of the slope in question, promoting effective and sustainable slope stability.

2.3.2 Considerations for Estimating Slope Stability

2.3.2.1 Ground Investigations

Before conducting a detailed analysis of an existing slope or a designated site for slope building, it is crucial to carry out a thorough ground investigation. This procedure entails collecting vital data on the site, including information about the composition of the ground and layers, the amount of wetness, the presence of standing water, and the existence of any preexisting shear planes. In addition, the use of piezometer tubes inserted into the soil may aid in the surveillance of fluctuations in water levels over a period of time. Engineers and geotechnical specialists may make well-informed judgements on the design, construction, and stability of slopes by collecting crucial ground investigation data. By using a proactive strategy, the aim is to identify and address possible hazards related to ground conditions, hence enhancing the safety and dependability of slope structures. Other ground investigation information can include:

- In-situ and laboratory tests;
- Geological maps to determine expected soil conditions;
- Observing and visiting the slope;
- Aerial photographs.

2.3.2.2 Most Critical Surface Failures

The event of slope failure may occur on several possible surfaces inside the slope, which adds complexity to the study of slope stability. Identifying the most crucial failure surfaces, which are highly susceptible to failure, is a fundamental element of this study. Deep-seated shear failure surfaces in homogenous soils, unaffected by faults or beds, often display a circular, rotating pattern. Contemporary computer programs for slope stability sometimes use limit equilibrium analysis to assess the inclination of a soil mass to slide downwards due to the force of gravity. The predominant approach for doing limit equilibrium analysis is the "method of slices," which involves dividing the slope into several vertical segments. The stability of the slope is evaluated by doing calculations on each segment, taking into account the soil parameters and the forces operating inside the slice. These calculations are done along a selected rotational failure surface.

A proficient method for analysing slope stability entails using "trial circles" to ascertain the most crucial surface. This involves analysing a set of slip circles that have different radii but

have a common centre of rotation. The safety factor for each circle is then graphed against the radius in order to identify the lowest Factor of Safety (FOS). This procedure is iterated for many circles, each symbolising various probable failure surfaces, investigated from separate rotating centres. Through a systematic analysis of trial circles, engineers may identify the most crucial failure surfaces and optimise strategies to enhance slope stability appropriately. An efficient approach to determining the most crucial failure surface in slope stability analysis is constructing a grid of rectangular centres. Every centre on this grid is linked to a minimal FOS, and the centre with the lowest FOS out of all the centres indicates the FOS for the whole slope. This approach presupposes a thorough examination, taking into account a multitude of circles with a diverse range of radii and includes a complete grid of centres. Engineers may use this grid-based technique to systematically investigate probable failure surfaces, allowing them to identify the most susceptible locations and optimise slope stability solutions appropriately.

2.3.2.3 Tension Cracks

A tension crack at the top of a slope signals impending instability. Tension cracks are used in slope stability calculations on occasion, and they are occasionally considered to be filled with water. Hydrostatic forces contributing to soil movement will emerge if this is the case.

2.3.2.4 Submerged Slopes

The application of an external water load to a slope, especially on the upstream side of a reservoir or dam, generates a stabilising pressure that acts on the slope. In the study of slopes exposed to water forces, it is necessary to include both the vertical and horizontal forces produced by the water. In order to account for these external water pressures, engineers must use submerged densities while doing slope analysis. Concurrently, the study should exclude the influence of external water, guaranteeing a thorough evaluation of the stabilising consequences of water pressure on the slope. This technique is critical for appropriately analysing the stability of slopes modified by external water loads.

2.3.2.5 Factor of Safety

The FOS is calculated as a ratio of the obtainable shear strength to the required shear strength to keep the slope stable, as suggested by Sadzevicius et al. (2019), presented in Table 2-1.

Table 2-1: Values of Minimal Factor of Safety (Sadzevicius et al. 2019)

Factor of safety	Details of slope
<1.0	Predicted to fail
1.0 1.25	Edge of Failure point
1.25 - 1.4	Acceptable for routine cuts and fills Unsafe for dams or where failure would be catastrophic
>1.4	Acceptable for dams

Even for dams, the safety factor can be as low as 1.2 to 1.25 for highly unlikely loading conditions. For example, situations involving seismic effects or rapid drawdown of a reservoir's water level (Sadzevicius et al. 2019).

2.3.2.6 Progressive Failures

Progressive failure is a term that describes a condition in which different parts of the failure plane reach failure at different times. This commonly happens when a potential fracture surface is either already fractured or intersects with a joint or base material that already has a fractured surface. The shear strength peaks are reached before other locations due to the large strain values at these crack-initiated locations.

2.3.3 Types of Stabilizing Techniques

Slope stabilization techniques play a crucial role in preventing and mitigating slope failures, ensuring the safety of infrastructure, and minimizing environmental risks. Several methods have been developed and utilized to address slope instability concerns. Figure 2.5 presents an overview of various commonly used techniques for the stabilization of slopes. Each stabilization method has its advantages, limitations, and suitability depending on the specific slope conditions, geological characteristics, and project requirements. A comprehensive assessment of the slope, including geotechnical investigations, is crucial to selecting the most appropriate stabilization method to ensure long-term slope stability and safety. These techniques are further explained in more detail in the following sections.

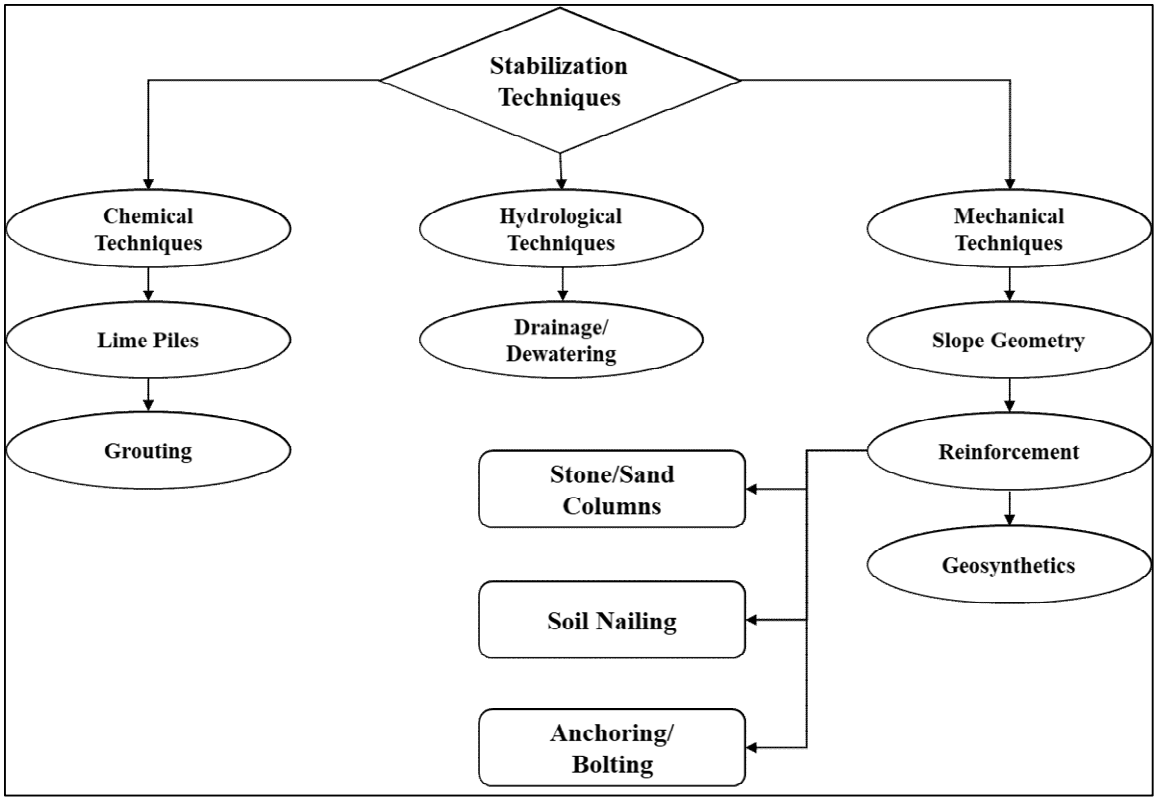

Figure 2.5: Various techniques used for slope stabilization.

2.3.3.1 Chemical Techniques for Slope Stabilisation

2.3.3.1.1 Lime Treated Methods

The treatment of poor soils with lime has been utilized extensively and successfully all over the world as a mix-in-place method. Lime-based novel approaches are currently being explored. Utilizing lime piles to stabilize shallow slopes is one such method. The chemical processes involved in the stabilization of lime piles have been studied recently (Kitsugi, 1982; Rogers and Glendinning, 1996; Anon 1963; Rogers and Glendinning, 1997d; Rogers and Glendinning, 1993; Wang 1989; Rogers and Glendinning, 1997a).

The fundamental concept behind slope stabilisation is the migration of lime from piles into the surrounding soil, where it then reacts with the in-situ clay to enhance the clay's strength. This process relies on the migration or transit of calcium ions (Ca2+) and hydroxyl ions (OH-) from the lime heaps to the nearby soil. Hydroxyl ions are necessary for the formation of strongly alkaline conditions, which are crucial for the start and advancement of the stabilisation processes. Essentially, the combination of lime migration and the creation of alkaline conditions allows for the improvement of the soil's durability, adding to the overall stability of

the slope. Various authors have discussed the utilization of lime piles in slope stabilization, including (Anon 1963; Handy and Williams, 1966; Lutenegger and Dickson, 1984; Rogers and Glendinning, 1997b, 1997d)

Handy and Williams (1966) demonstrated the usefulness of quicklime piles in stabilising an unstable fill slope. This approach was successful in a scenario where traditional treatments had previously been ineffectual. Figure 2.6 illustrates the detailed procedure of application of lime piles for slope stabilization. In this particular instance, piles of 150mm in diameter were carefully built at intervals of 1.5m, deliberately breaching the shear zone located inside a perched water table. The building method included the insertion of drilled holes, into which quicklime was introduced and moistened. The clay deposit in the specified region consisted mostly of calcium montmorillonite minerals. The clay inside the active slippage zone was found to have a cohesiveness (c') of 4 kPa, an internal friction angle (φ) of 17°, and a water content of 27.2%. Following a three-month duration, samples were collected (although the exact sites of sampling were not specified), uncovering a 4% decrease in water content. At the end of one year, the unconfined compressive strength had grown by almost 55% in comparison to the strength measured at the three-month point. This case study highlights the efficacy of quicklime piles as a stabilising solution for fill slopes, especially in difficult situations where conventional treatments have proven unsuccessful.

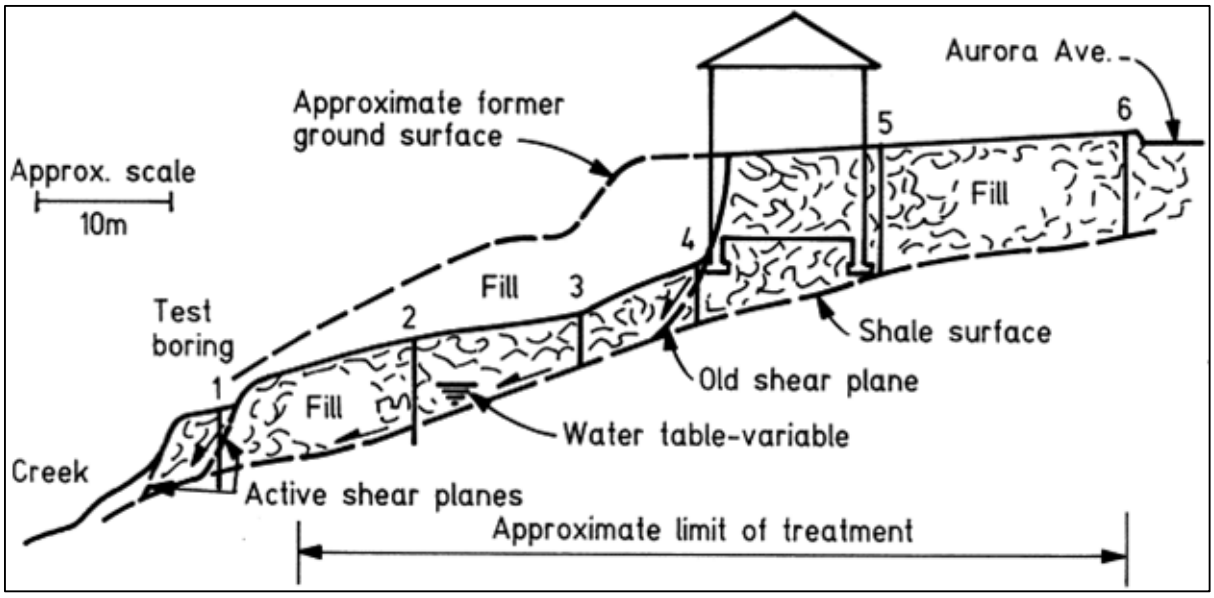

Figure 2.6: Application of lime piles in slope stabilization in Iowa (Handy and Williams, 1966)

Figure 2.7 (Ingles and Metcalf, 1972) depicts one method of building lime piles in which quicklime is pushed into a hollow tube that has been inserted into the soil to the necessary depth and then pulled out of the ground. The tube's end is forced open by the pressure, allowing lime to fill the space below. The tube's end is closed after each meter has been filled, and the lime that forms the pile is compacted using it. A different technique for stabilising self-supporting soil is drilling holes to the necessary depth, injecting quicklime, and then compressing the soil in layers, either directly or via a central stem. The selection of a stabilisation mechanism may impact the choice between hydrated lime or lime slurry, with the latter being more often used. The lime slurry may be introduced into the augured holes based on the particular requirements of the application. This method enables the deliberate incorporation of lime-based stabilisers into the soil, hence enhancing soil characteristics and overall stability. The process of augering and incorporating lime-based materials provides a flexible alternative for improving the engineering properties of self-supporting soils in different construction and stabilisation applications.

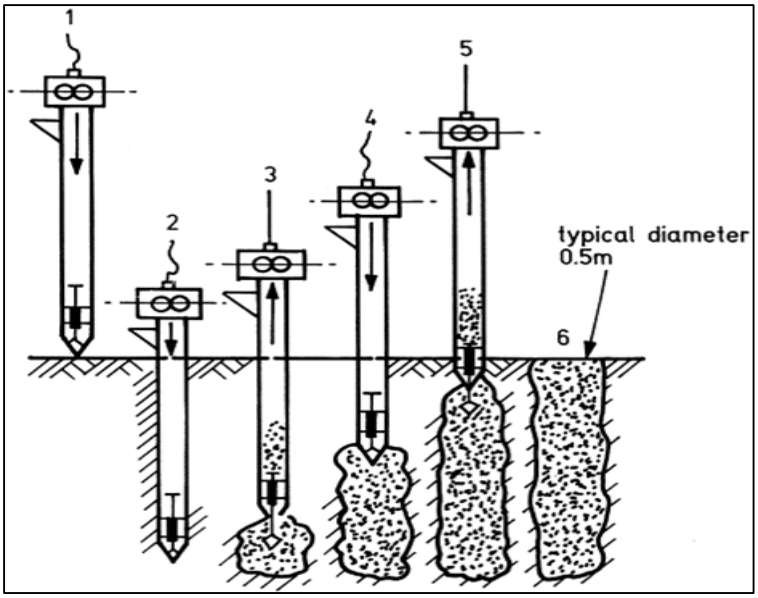

Figure 2.7: Process of Installation of lime piles in soft soils (Ingles and Metcalf, 1972)

2.3.3.1.2 Clay–lime reaction

It has been extensively observed that lime migrates from the piles and reacts with the nearby (clayey) soil, stabilizing it in the process (Kitsugi 1982; Rogers and Glendinning, 1997c). During the slope stabilization process with lime treatment, the passage of both calcium and hydroxyl ions through the clay is crucial for its effectiveness. In order to enhance cation exchange on the exchange sites of clay minerals that are easily accessible, it is necessary to fully saturate the system with calcium ions. The formation of calcium silicate hydrate and

calcium aluminate hydrate gels, which promote stabilization, need the breakdown of silica and alumina at very alkaline conditions (pH > 12.4). In order for these reactions to take place, it is essential that the migration lengths of calcium and hydroxyl ions remain relatively short inside undisturbed clay. The effectiveness of the stabilization process depends on fully saturating the system with calcium ions, which helps facilitate the exchange of cations on clay minerals and creates the alkaline conditions required for the development of stabilizing gels (Rogers and Glendinning, 1996).

2.3.3.1.3 Reduction in Pore Water Pressure (PWP)

When quicklime is added to soil, the pore water pressures become negative, attracting water to the piles where it can react. This suction will be high only in the immediate region of the pile and for a brief time in soft, damp, and generally permeable soils. However, in low permeability, drier clays, the suctions will be stronger and continue longer, increasing the mean normal effective stress and making the soil more robust and stable. If only some time were needed or additional stabilization mechanisms to kick in, this could be quite advantageous for failing slopes (Rogers and Glendinning, 1997a; Tsytovich et al. 1971; Rogers and Glendinning, 1993). Additionally, these suctions will cause consolidation of the shear zone.

2.3.3.1.4 Consolidation of the shear zone

If negative pore water pressures continue for a long time, they may cause the consolidation of clay in the remoulded shear zone of a failed slope by increasing the average normal effective stress. Consolidation is the process of decreasing the empty spaces inside the clay by releasing excessive pressure from the water-filled pores. This dissipation causes a rise in the effective stress within the soil, resulting in heightened soil strength and greater stability. The occurrence highlights the intricate relationship between the pressure of water inside the pores of soil and the process of soil consolidation, which together affect the behaviour of slopes, particularly those that have undergone failure, as discussed in detail by (Rogers and Glendinning, 1993). The key stabilizing processes advocated in this work are lateral consolidation brought on by pile expansion and drying, both of which are considered to "increase cohesiveness" in the soil. By measuring the change in void ratio brought on by the expansion and multiplying the lower water content by the specific gravity, this improvement is computed.

The void ratio-effective normal stress relationship is utilized to determine the increase in stress, which is then multiplied by a "strengthening factor" to determine the change in "cohesion." By

taking into account the fact that lateral consolidation takes up some of the soil's settlement capacity, the reduction in vertical settlement is estimated. Calculating the length of the piles needed is made possible by equations that quantify these concepts. The expansion of the lime appears to be the sole cause of the lateral movements. The hypothesis is supported by evidence from piles in the field that have a markedly higher capacity than the casings that were used. During pile building, the diameter of the pile may increase due to the absorption of water from the surrounding soil. Even if there is no noticeable change in volume, the diameter of the pile still expands to some extent. The increase in diameter may be ascribed to many sources. Firstly, the act of driving the casing causes horizontal soil displacement, which in turn contributes to the total expansion. Moreover, when the lime is poured with force and then compressed, it causes the hole in the earth to grow even more, particularly in soil that is less firm. The simultaneous impact of these parameters demonstrates the intricate nature of pile building and its influence on the expansion and diameter of the produced piles. As a result, the construction process results in physical displacement rather than lime pile growth from hydration.

2.3.3.2 Plantation or Bioengineering

Slope stabilisation may be accomplished by purposely planting or encouraging the growth of indigenous plants. The use of vegetation has shown its efficacy in reducing landslides, particularly as a result of the combined mechanical and hydrological impacts it exerts. Physically, the roots of plants interlock the soil particles, increasing soil cohesion and providing structural reinforcement to the slope. This fortification serves to mitigate soil erosion and reduces the likelihood of slope collapse. The root systems serve as a natural means of fortification, enhancing the overall stability of the slope. From a hydrological perspective, vegetation is essential for effectively controlling water infiltration and runoff. Vegetation has a crucial role in mitigating the erosive impact of rainfall on slopes by absorbing and decelerating the water. The root systems further contribute to the formation of preferred flow channels for water, facilitating improved drainage and decreasing the probability of saturated conditions that may initiate landslides. Vegetation's combined mechanical and hydrological impacts provide it with a viable and environmentally benign method for stabilizing slopes. Moreover, the visual and environmental advantages of green landscapes enhance the overall health of the ecosystem and neighbouring communities (Norris et al. 2008). The plant hydrological effect has occasionally been measured and reported in the scientific literature despite being recognized (Simon and Collison, 2002; Stokes et al. 2014). On the other hand, a

lot of research has been done on the mechanical impact of plants on slope stabilization (Wu et al. 1979; Mickovski et al. 2009; Bordoni et al. 2016).

It is crucial to understand how vegetation responds hydrologically to reduce the chance of slope instability and the risks linked with it (Duan et al. 2016; McVicar et al. 2010). This knowledge could be very helpful in choosing plant species that are both efficient and sustainable (Lu and Godt, 2013; Fell and Lacasse, 2015). The hydrological effect of vegetation is the result of numerous systems interacting along the continuum of soil, plants, and atmosphere (Rodríguez-Iturbe and Porporato, 2007). These can be divided into two categories: soaking and drying. During a rainstorm, vegetation may be able to influence how much water reaches the soil (wetting). The aerial elements (such as a tree canopy), according to Lloren and Domingo (2007), may intercept some of the precipitation, creating an "umbrella effect" that may lessen the quantity of rain that can permeate the soil. However, some of the rainwater will seep into the ground and down the stem. Stemflow may be detrimental to the stability of the slope when the water jets into the soil through the root channels and funnels around the tree base. Bypass flow may alter the state of soil stress or encourage the formation of perched water levels at depth (Lu and Godt, 2013).

Drying often decreases the moisture content of the soil after a rainstorm event. Bioengineering is the deliberate use of vegetation, including both living and dead plants, as well as plant-based materials like jute and coir, together with engineered constructions, to improve the stability of slopes. This comprehensive strategy encompasses a range of measures, such as vegetation and horticulture practices, coir/jute netting, geotextiles, asphalt mulch solution, retards, wattling, and other techniques, in addition to slope modification and enhanced agronomic methods.

Ensuring the stability of slopes and avoiding the erosion of soil are crucial components of bioengineering, in which the presence of vegetation is essential. The capacity of plants to conserve topsoil becomes most apparent during periods of heightened precipitation, which coincide with the monsoon season. The quick growth of vegetation contributes to the mitigation of surface erosion. It is important to understand that heavy rainfall may increase the danger of mass loss by saturating the subsoil with moisture. This emphasizes the complex relationship between vegetation, rainfall, and soil stability in bioengineering activities (Galay, 1987).

Vegetation cover significantly enhances the shear strength of soil by means of its root network, providing mechanical reinforcement, anchoring, and compaction. The presence of plant roots

plays a crucial role in soil stabilization, thereby minimizing the likelihood of slope collapses. Furthermore, vegetation has a desiccating influence on the soil by absorbing groundwater and aiding in the removal of water via processes like evapotranspiration. Nevertheless, the capacity of vegetation to maintain slope stability depends on the extent to which roots may enter the soil. When a landslip goes beyond a certain depth, the ability of vegetation to offer sufficient support decreases. In such cases, the vegetation may lack the capacity to adequately sustain the slope, necessitating the implementation of supplementary measures, such as engineering solutions or a blend of bioengineering approaches, to effectively tackle underlying instability problems. The degree to which vegetation can contribute to long-term slope stabilization is limited by the depth of root penetration.

Through the various mechanisms mentioned above (such as rainfall interception, streamflow, and water intake), vegetation influences the water flow conditions and, consequently, the soil matric suction. However, combining data from the field and the UES, this effect has never been examined on soils with woody plants. The UES was designed exclusively for soil, but plant roots and soil combine to produce a composite substance (Thorne 1990). Given that the root systems will alter the soil's pore size and distribution (Scanlan and Hinz, 2010), water retention dynamics (Carminati et al. 2010; Scholl et al. 2014), and permeability, this substance is likely to behave hydromechanically differently from a fallow soil (Gonzalez-Ollauri and Mickovski, 2017; Vergani and Graf, 2016).

Figure 2.8: Schematic and photograph of a gabion wall along a highway. (Photograph of gabions located in the Pocono Mountains, Pennsylvania, USA, by Lynn Highland, U.S. Geological Survey.)(Highland and Bobrowsky, 2008)

2.3.3.3 Drainage

Drainage systems have been widely used for years to stabilize landslides, especially groundwater-influenced landslides (Lau and Kenney, 1984; McKay 2006; Pohll et al. 2013; Ismail et al. 2017; Rahardjo et al. 2003). Due to their affordability and ease of installation, horizontal drains are one of the most commonly used drainage techniques in engineering (Rahimi et al. 2011). Numerical simulations are often used to optimize the design of horizontal drainage channels because they can account for different formations and handle different boundary conditions. An important aspect of these numerical (finite element) models is how the discharge is simulated. Four main approaches are commonly used. In the first method, the drain is considered a hole in the finite element grid. This method requires the use of very small elements near the drain to achieve accurate flow rates. This method significantly increases mesh density and computation time. A second method ignores the size effect of the drainage borehole and treats the borehole as a point or line sink with no pore pressure (Gureghian and Youngs 1975). Although horizontal culvert designs are becoming more rational and reliable, the long-term effectiveness of horizontal culverts is still an issue in embankment construction. The siphon drainage approach, first described by Gillarduzzi (2008), is an effective strategy to improve flow velocity and drainage efficiency (Tohari et al. 2021; Sun et al. 2019a; Yu et al. 2019). A vacuum inside a siphon tube increases the water flow rate. In addition, siphon dewatering can be automatically started when there is a water pressure difference between both ends of the siphon pipe. Siphon height limitations in early siphon dewatering processes required the siphon tube to pass through a vertical borehole, requiring the use of an electric water pump to pump water below 10m (approximately 10m) below the surface. However, electricity is not always available at landslide sites. Instead of using vertical wells, Land sliding in hilly places has been successfully stabilized by using this upgraded siphon drainage technique (Cai et al. 2014; Sun et al. 2019b; Sun et al. 2019; Yuequan et al. 2015; Zheng et al. 2021).

Yu et al. (2021) conducted a numerical study using GeoStudio software to investigate the efficiency of siphon drainage for slope stabilization. They concluded that embankments with horizontal drainage had lower FOS than embankments with extended siphonic drainage. Lowering the relative hydraulic conductivity simulates the effects of clogging in horizontal drainage systems. The results show that the horizontal drainage method previously demonstrated in engineering practice is less effective in the long term than the modified siphon drainage method.

2.3.3.4 Controlling Groundwater drainage

The presence of groundwater in the soil is a common cause of slope failure. Water reduces the soil's ability to withstand shearing, resulting in slope failure. A drop in effective stress is caused by an increase in pore pressure (due to groundwater). The presence of water reduces soil shear strength because effective stress controls soil strength and deformation characteristics. Controlling groundwater in the slope region is a key component of increasing shear resistance. The amount of water in the slope material is reduced because of drainage. Water can be controlled via drainage wells, trenches, surface drains, and horizontal drains. The quantity of infiltration soil encounters is limited by surface drains. After infiltration, water can be diverted using trenches, drains, and wells, whose construction differs depending on the project type. There are numerous drainage designs and installation techniques to consider. The size, spacing, and arrangement of drainage features are frequently determined by site conditions and contractor experience. A typical recommendation is to locate drains close to the failure zone and close to the slope's steepest angle. The location near the toe of gravity-controlled horizontal drains typically yields the greatest advantage. Most of the time, local factors determine which strategy is used. Drainage pipes all have the same objective, which is to remove water that has already gotten into the region and can slide, although they differ greatly in material, size, and installation technique (H. Sun et al. 2019a; Yu et al. 2019).

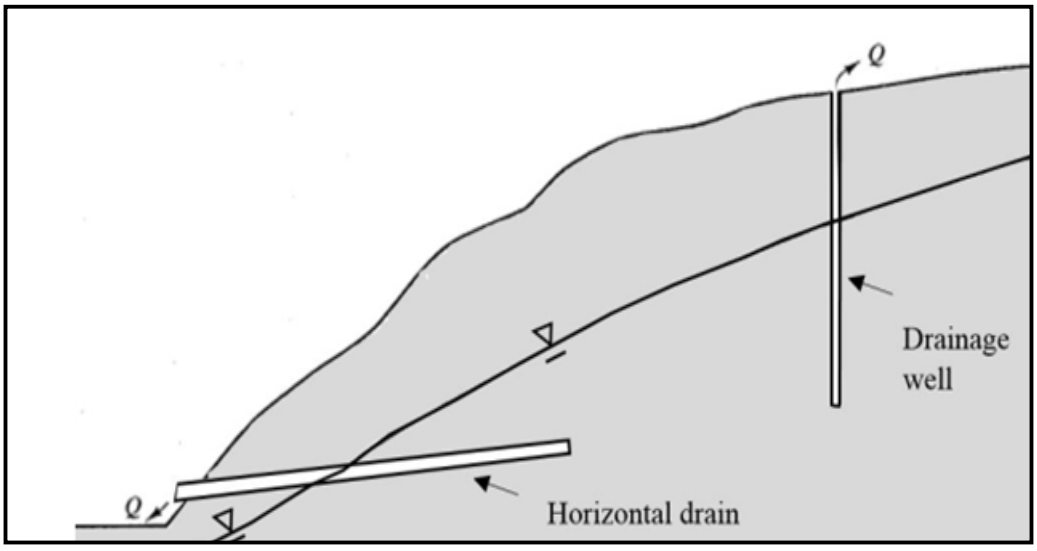

Figure 2.9 Example of Common drainage features including horizontal drain and drainage well (Pohll et al. 2013)

The main advantage of drainage is that it lessens the impact of pore pressure on shear strength. Dewatering is normally done with a pump system and effectively lowers the groundwater table,

but it can be time-consuming and expensive. Drainage channels and de-watering pumps can improve shear strength and reduce related slope stability issues caused by water if excavation below the groundwater table is necessary.

2.3.3.5 Surface Cover

Covering the surface of the slope is another approach for stabilizing slopes and preventing failure. Appropriate soil cover can improve slope stability by redirecting water, reducing erosion, and supplying stabilizing forces to the slope's upper layer. Ground cover techniques include rip-rap, vegetative cover, replacement fill, and buttressing. The use of vegetation as a ground cover is frequent and simple. Slopes are protected from erosion by a vegetative cover, which has both aesthetic and environmental benefits. Rainwater and surface runoff can be protected from the slope material by grass and other vegetative cover.

The plant roots' effects on the shear strength of soil were presented by (Operstein and Frydman, 2000). The study examined the mechanical characteristics of plant roots. Each form of vegetated soil has a shear strength that is higher than the soil's initial strength. Roots of plants drain the soil of water, reducing the pore pressure's impact on the material of the slope. At the surface, roots also act as mechanical reinforcement. In general, slopes with vegetation are more stable than those with no vegetation on slopes of the same soil type.

The simplicity of installation is another benefit of vegetative cover. No specialized tools are needed. Material is easily accessible, grass seeding is simple, and labour costs are minimal. After a slope stabilization project, it's usual to install surface vegetation. Although rip-rap placement requires more labour and typically costs more than earthwork buttressing, it can prevent erosion. Another choice with comparable cover benefits is to use high-flow concrete (shotcrete). Many cover techniques focus largely on preventing erosion; however, depending on the material and site design, adding cover material might make a slope heavier and reduce overall stability.

Figure 2.10: A Vetiver grass system is being used in the Democratic Republic of the Congo for gully control in urban areas and for highway stabilization. These gullies are a major problem in this area and other West African countries (top); the same slope now has improved drainage, and the slope has been planted in Vetiver grass (middle); this planting of Vetiver grass is about three months old (bottom) (Highland and Bobrowsky, 2008)

2.3.3.6 Excavating and Decreasing Load

Changing the slope's geometry can reduce the forces that lead to failure. Reducing the slope and inclination angle is a possibility if boundaries around the job site and the right-of-way do not pose a problem. The removal of any load or surcharge from the slope, so restricting additional weight, is another method of reducing driving forces. For instance, a case study of the slopes surrounding the Pelton Dam in central Oregon is provided by Cornforth (2005). Repair crews addressed slopes with a reduced angle of inclination, leading to a significant decrease in slope failures.

Lower driving (or applied forces) pressures and slope weight can be achieved by using light fill. According to Abramson et al. (2001a), polystyrene foam, shredded tyres, encapsulated sawdust, seashells, and expanded shale are some examples of lightweight fillers. The choice of material is heavily influenced by local availability and shipping expenses. Lightweight fill is a material choice for slope rehabilitation and a design consideration when building a new slope.

The features of free-draining compacted fill make it perfect for use as a slope material. Slope soil replacement using engineered fill, which can include clean sand or tested borrow material, reduces ground conditions uncertainty and eliminates elements that contribute to slope instability. The design team can additionally manage the slope geometry by removing in situ dirt and filling it in. This strategy, however, may be impractical due to space and economic constraints. Proper fill selection enhances in situ strength and drainage qualities in circumstances where the remove-and-replace option is appropriate.

This technique lessens the driving force, which enhances stability. Only cuts into deep soil where rotational landslides may occur are appropriate for this strategy. It is ineffectual for landslides of the flow type as well as translational failures on long, homogeneous, or planar slopes. Lowering the slope's height by lessening the weight of the soil mass or lowering the height of a cut bank reduces the driving force on the failure plane. Figure 2.11 and Figure 2.12 illustrates the soil removal from the toe and top of the slope, respectively.

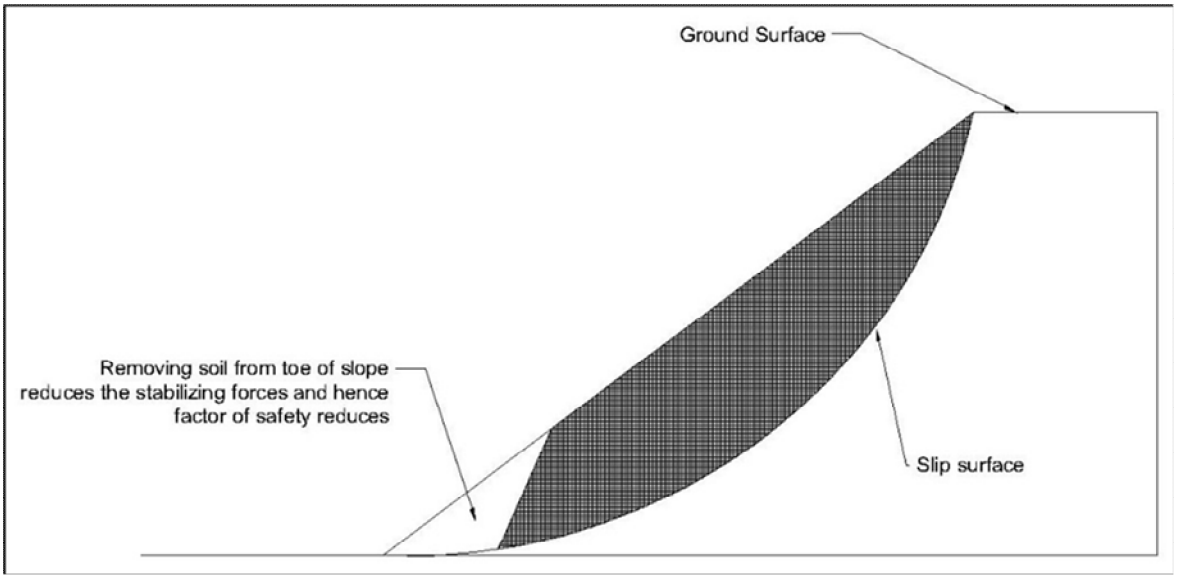

Figure 2.12: Illustration of the removing soil from the toe of a slope

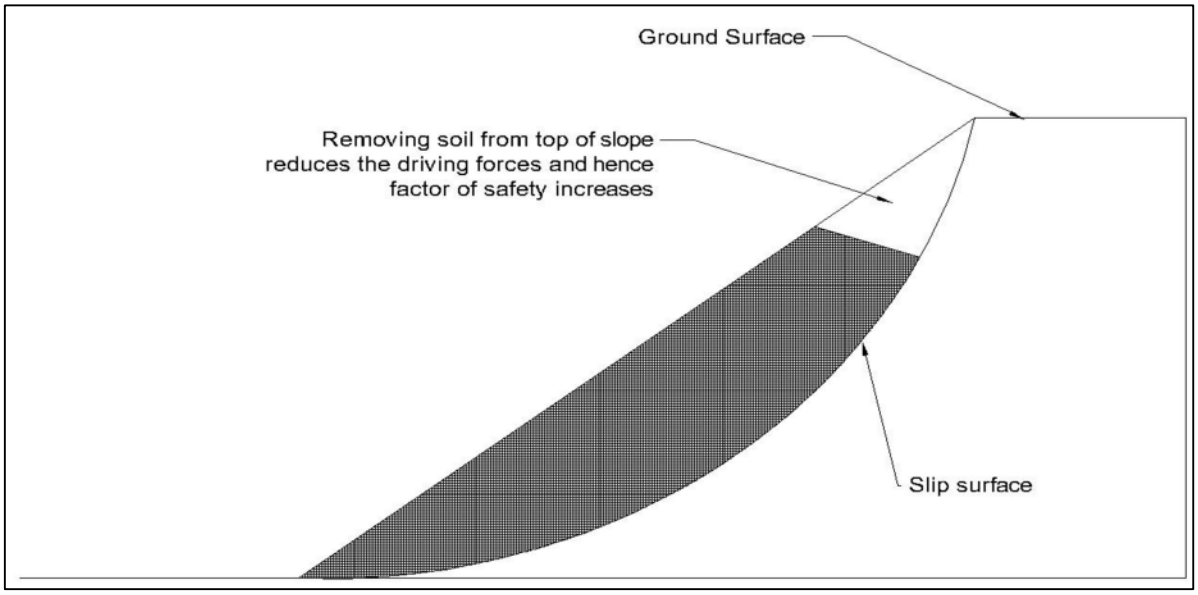

Figure 2.11: Illustration of the removing soil from the top of a slope

2.3.3.7 Reinforcement for Slope Stability

An efficient and dependable method for enhancing the stability and strength of soils is soil reinforcement. The effects of randomly oriented discrete inclusions (Fibres, mesh elements, waste products like plastic strips and tyre chips, etc.) on highly compressible clayey soils, including soils that are prone to landslides, have been the subject of several studies (Gobinath et al. 2020; Huang et al. 2010). Utilizing retaining walls is one method of stabilizing slopes.

The purpose of retaining walls is to provide continuous support for soil masses. Additionally, retaining walls are utilized to stop or reduce the toe erosion caused by river scour or to delay creep. However, they cannot be utilized to prevent landslides from happening. Timber cribs, steel pins, piles, cantilevers, sheet piles, plastic mesh, and reinforced earth are a few fundamental wall kinds. Each of these types has benefits in specific circumstances, although the choice of type is typically based on cost. Installing rows of drilled shafts for slope stabilization has shown to be a dependable and effective method throughout the years to prevent excessive slope movement (Chaple and Dhatrak, 2013; Ellis et al. 2010; Lirer 2012; Kourkoulis et al. 2011). In the stable soil layer underneath the sliding surface, piles are inserted through the brittle soil layer. A portion of the force from the collapsing mass can be transferred to the stable soil layer via piles, which stabilize the slope. For passive piles, soil movement, which is in turn impacted by the existence of the piles, determines the soil-pile pressure that the unstable layer applies to the piles (Won et al. 2005a; Chen and Poulos, 1997; Ausilio et al. 2001). For the study of slope stabilization, it is crucial to assess the soil pile pressure that is operating on the stabilizing piles. These techniques have predicted satisfactory outcomes and have been used and developed in later studies (Joorabchi et al. 2014; Li and Liang, 2014; Yamin and Liang, 2010a; Joorabchi et al. 2013). Reinforcing structures can be installed to boost resistance forces and enhance FOS. Examples of stabilizing constructions include soil nailing, retaining walls, ground anchors, and mechanically stabilized earth walls. For many stabilizing structures, there are conventional design methods, although they are often an expensive choice. For projects where there is a lack of area, retaining walls are an option. In some highway projects, a well-designed and built retaining wall enables design teams to work around drastic slope changes. Retaining walls can control grade changes during road construction, prevent salt, oil, and other highway pollutants from getting on nearby vegetation, and shield drivers from rocks, wildlife, and other potential hazards.

2.3.3.7.1 Micro piles

Micropile installation is a technique that has been used to increase embankment stability. Micropile is a small diameter replacement pile, often reinforced, usually less than 300 mm in diameter (Bruce and Juran, 1997a). Micropiles are created by drilling a borehole, inserting reinforcements, and grouting the hole. Since Fernando Lizzi first developed micropile technology in the 1950s, it has evolved continuously. Over the last 60 years, improvements in drilling technology have led to increased application of micropiles in infrastructure repair and

seismic retrofitting projects (Tsukada et al. 2006); (Pinyol and Alonso, 2012). Additionally, micropiles can be easily erected in areas where heavy equipment access is restricted, such as landslides that occur in hilly, steep, or mountainous areas. Several researchers have reported the effective use of this technique to stabilize slopes (Lizzi 1978; Cantoni et al. 1989; Pearlman and Wolosick 1992; Juran et al. 1996; Loehr et al. 2000; Sun et al. 2009a). Despite these uses, stabilized micropiles are constructed using a variety of techniques. According to (Lizzi 1978), micropiles can be used as a web-like network system to construct stable reinforced soil 'gravity retaining walls' that provide the critical lateral stresses required for unstable slope motion. Since none of the micropiles are stressed, Lizzi (1982) proposed a micropile group design strategy based on the idea of a highly redundant system. The system is subjected to compression and shear, and the micropiles confine the soil in situ, increasing its shear strength and improving its modulus of deformation. The "node effect" and the concept of reinforced concrete comparison Lizzi (1978) and Plumelle (1984) have a great influence on the behaviour of this system.

According to Palmerton (1984), and Pearlman and Wolosick (1992), micropiles can be constructed to carry axial and lateral loads from soft or weak soils to more capable formations. These micropiles are typically used to withstand applied loads directly. To stop the sliding body, it is a design concept that mainly replaces conventional large-diameter piles with small-diameter and high-strength piles. San et al. (2009) did a comparative study of micropile and conventional anti-skid piles, revealing that the loading mechanisms of micro-pile and anti-skid piles are quite different. Since conventional piles have high bending rigidity, pitch distortion occurs due to compressive failure of the soil behind the piles. Low flexural stiffness causes the micropiles to deform more easily, causing soil plastic zones to intersect and overlap between them. As a result, the sliding surface and the top of the micropile experienced greater lateral displacement. Therefore, it is difficult to apply conventional pile solutions to micropiles.

For use in stabilizing small slopes, Loehr et al. (2000) proposed a simplified procedure for estimating the ultimate load-bearing capacity of reinforcements made from recycled plastics. Their method was based on elastic analysis to determine the distribution of lateral boundary resistance along rebars, which considers two common failure mechanisms: Soil failure around or between rebars and structural failure of rebars caused by forces mobilized from the surrounding soil. In addition, Reese (1992) guided the design of micropile-stabilized embankments. According to numerical studies by Duan et al. (2016), tunnels should be strengthened by maintaining slopes primarily through the construction of anti-skid piles, sealing cracks in slopes, and providing drainage as a by-product. The top of the tunnel exit and the front of the slide body are lined with non-slip pillars. This method evaluates the potential for ground failure due to soil flow between micropiles and calculates the resistance provided by micropiles, assuming micropile bending is a limit condition. This method is based on the key assumption that the axial force generated in the micropile affects stability only by increasing the lateral resistance of the micropile. Since the stability verification does not explicitly consider the axial component normal to the slip plane, effects such as the reduction in the normal force acting on the disk base are not taken into account. Design methods for embankment stabilization using micropile are generally in their infancy, and some designs have historically had to be fairly conservative. Figure 2.13 presents a schematic illustration of the slope stabilized using micro-piles.

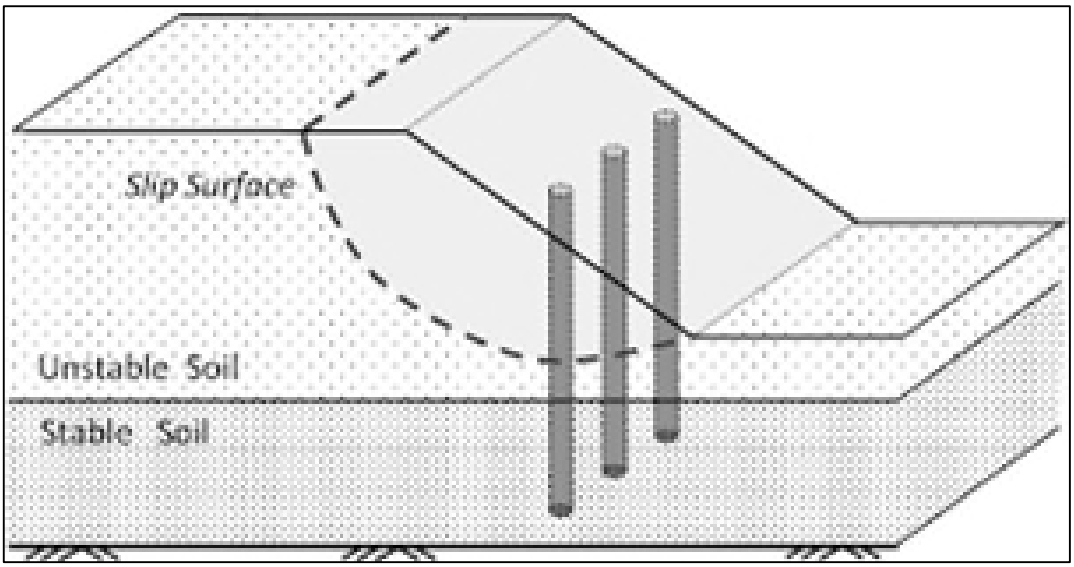

Figure 2.13: Schematic figure for typical slope stabilization using micro piles (Sun et al. 2009b)

When choosing the best strategy to stop a landslide, the geological, geomorphic, and geotechnical characteristics of the target area should be considered. Additionally, landslides might have many underlying causes in various nations or geographical areas. Therefore, it is important to carefully consider area peculiarities and local landslide mechanisms while selecting a viable countermeasure (Schuster, 1995; Hong 1999; Ho 2004). Around the world, stabilizing piles are being utilized more frequently to ensure slope stability or restore slopes that have already collapsed (Hong and Han, 1996; Anagnostopoulos and Georgiadis, 2004; Hungr et al. 2001; Kang et al. 2009; Popescu and Schaefer, 2008).

Some researchers have also examined the stability of slopes reinforced by piles and drilled shafts using computational techniques like the Limit Equilibrium Method (LEM) and the Finite Element Method (FEM). (Yamin and Liang, 2010b; Bellezza and Pasqualini, 2005; Won et al. 2005b; Day et al. 1999) and others have employed traditional LEMs. Liang and Yamin, 2010; Liang and Zeng, 2002; Ng et al. 2001; Cai, Ugai 2000; Matsui and San, 1992), among others, have all employed two- or three-dimensional FEMs.

2.3.3.7.2 Stone Columns

Stone columns are widely employed in various global projects as a technique for enhancing ground conditions and have multiple applications, such as slope stabilization. Slope instability can be caused by cyclic loading, such as earthquake loading, which can lead to the accumulation of excess pore water pressures in the soil. These pressures can have a negative impact on the shear strength of the soil. Stone columns can alleviate liquefaction by facilitating drainage, preventing the accumulation of excessive pore water pressures, and enhancing soil stiffness to reduce shear strain during cyclic loading. Stone columns are an effective technique for addressing problems related to the stability of slopes, providing an excellent means of preventing landslides and stabilizing slopes. The presence of these columns helps to dissipate pore water pressures more effectively inside the slope, resulting in an overall improvement in the stability of the terrain. The addition of additional permeable gravel columns to the slope enables the effective removal of surplus water via drainage. Stone columns strengthen the strength of the existing soils, mitigate saturation danger, and improve overall slope stability. Enhanced permeability facilitates improved water dissipation, hence minimizing the accumulation of pore water pressures that may lead to slope collapses (Abramson et al. 2001b). The applied load, which is sometimes referred to as normal stress, and the shear displacement

at the failure plane are the two factors that define the shear resistance of stone columns (Alfaro et al. 2009).

2.3.3.7.3 Bolts and Anchors

It is normal practice to use soil nails for the purpose of reinforcing soil masses, providing tension and bending resistances, and helping to the stabilisation of slopes. Most of the time, these nails are made of metallic or polymeric components that are secured to the ground. Grouting may be done in pre-drilled holes, or insertion can be done using displacement techniques using static push or dynamic forces, including vibration, percussion, and/or rotation. These are all examples of installation procedures. Depending on the geometry of the slope, the orientation of the soil nails will vary. Installing them may be done in a horizontal orientation or at a variety of angles relative to the horizontal. When it comes to creating large tension resistance, horizontal nails are an effective method, while nails that are parallel to a probable failure plane and contribute to major bending resistance are also beneficial. The history of soil nailing may be traced back, at least in part, to developments in rock-bolting, multi-anchorage systems, and methods for soil reinforcement. This geotechnical approach, known for its adaptability and practicality, has become an essential component of slope stabilization schemes, providing reliable reinforcement and enhanced stability to soil masses (Phear et al. 2005). In the early 1960s, numerous retaining walls in France were constructed using bars as rock anchors (Bonazzi 1984). The first known soil nail wall was built in Versailles, France, in 1972 (Bruce and Juran, 1997b). By 1988, France had constructed soil-nailed walls and steep slopes covering at least 50,000 m² (Bruce et al. 2013a; Bruce and Jewell 1986). In Germany, over 500 soil-nailed walls had been built by the mid-1990s (Bruce et al. 2013). Similarly, in the United States, more than 500 soil-nailed barriers were constructed for highway projects by 2001. In the late 1980s, soil nailing was first applied in the United Kingdom to reinforce walls and slopes. Soil nailing was first used as an excavation support technique in Canada in the early 1980s (Bruce et al. 2013b). Initially, steel nails were grouted into almost horizontally drilled holes immediately after each additional cut level to apply soil nails to nearly vertical cut slopes. Although slope failure data show that nails experience significant bending resistance near the failure surface, conventional design methods still presume that the nails only function in tension.

On the other hand, the slopes of unstable soil that already exist are often flatter than 45 degrees. In these circumstances, nail insertion is frequently possible without drilling or grouting. These

nails are typically positioned perpendicular to the surface of the slope (Phear et al. 2005). Due to its quick installation and ability to be used in situ without requiring the reconstruction of existing slopes or embankments, this technology has appeal from both an economic and environmental standpoint. The soil nail technique used in these case studies was initially created to come up with a quicker, better, and more affordable solution for unstable slopes that already exist. The necessity for a quick insertion technique without expensive drilling or grouting, finding a replacement for the conventional mesh and shotcrete facing, addressing long-term corrosion, and creating analytical methods for bending resistance were the main development obstacles. With the introduction of effective splicing methods and percussion technologies, insertion was made possible. The facing was created by extending the nail head and developing a natural biotechnical facing of shallow vegetative roots. Long-term corrosion was treated sacrificially, much like piles.

2.3.3.7.4 Geosynthetic Textile Reinforcement

Another stability method is geosynthetic reinforcement. A permeable textile is referred to as a "geotextile." The word "geogrid" usually refers to a synthetic material with a lattice pattern that is sandwiched between layers of fill material. Extensive research has been conducted on the utilization of geosynthetic materials for slope stabilization. Geotextiles were the subject of substantial research as early as three decades ago (Fowler and Koerner, 1987), while geocell materials were the subject of research undertaken (Bush et al. 1990). The objective of this research was to investigate the possibility of using geosynthetic materials in the building of embankments on soft soils when they are used. Since that time, a wide variety of geosynthetic materials have been produced and used in a variety of projects that are centred on the stabilization of slopes and the reclamation of land.

One example of these cutting-edge materials is the three-dimensional polyethene geocell material, which was explored by Wu and Austin (1992). Another material that deserves mention is heavy-duty polyester woven geotextile, which was explored by (Guerra et al. 2015). Furthermore, geosynthetic mulch mats, which were investigated by (Ahn et al. 2002), have been shown to be beneficial in slope stabilization operations. Slurry-filled geotextile mats, which were investigated by (Yan and Chu, 2010), are an additional recent development in this area of research. In conclusion, biological geotextiles, which were also brought to light by Guerra et al. (2015), have emerged as a potentially useful solution in the field of slope stabilization and land reclamation. The dynamic character of geotechnical engineering is

shown by the ongoing development and introduction of these geosynthetic materials, which also demonstrate a commitment to enhancing and extending the toolset that is available for slope stabilization projects.

In more recent advances, a geosynthetic cementitious composite mat (GCCM) has been presented. This was brought to light in research conducted by Jirawattanasomkul et al. (2018). Both geotextiles and cement powder are used in the construction of GCCMs, which allows for the combination of the beneficial qualities of both materials. It is important to note that after they have been fixed to a consistent thickness, GCCMs demonstrate exceptional strength and stiffness, which makes them suitable for a wide range of applications. One of the most significant benefits of GCCMs is the simplicity with which they may be installed in the field. Because of this property, the application of GCCMs in a variety of engineering projects is made easier. Consequently, GCCMs have shown a great deal of promise in applications that are associated with the stabilization of slopes, the management of erosion, the containment of water, and the lining of ditches. A novel solution in the field of geosynthetics, the combination of geotextiles and cement powder in GCCMs offers increased strength and adaptability for a variety of geotechnical applications. This is a solution that marks a breakthrough in the field. The continuous development and application of various geosynthetic materials highlight their significance in addressing slope stability challenges. These materials offer innovative solutions for slope stabilization projects, providing enhanced strength, erosion resistance, and ease of installation compared to traditional methods. As research in this field progresses, geosynthetic materials are likely to play an increasingly important role in sustainable slope stabilization and land management practices. Figure 2.14 illustrates the installation of geosynthetic textiles for the stability of the slope at the Northampton Gateway Project site. The photo was taken by the author during the site inspection visit.

Figure 2.14: Installation of Geo-synthetic textile to stabilise slope at Northampton Gateway Site Project (Reference: image taken by the Author during site visit in June 2024)

2.3.4 Summary

Slope stabilization encompasses a range of techniques, broadly classified into structural, vegetative, and bioengineering methods. Structural stabilization employs physical structures like retaining walls, soil nails, and geogrids to reinforce slopes and redistribute lateral pressure. Vegetative stabilization leverages plant cover to bind soil particles, reducing erosion and enhancing stability through the natural reinforcement provided by root systems. Bioengineering techniques integrate both structural and vegetative elements, employing methods like live crib walls and coir rolls to combine the benefits of living plant materials with engineered structures.

The selection of a slope stabilization method depends on factors such as slope geometry, soil conditions, environmental considerations, and project requirements. Combining these methods often yields the most effective and sustainable solutions. Retaining walls support vertical slopes, soil nails and rock bolts reinforce masses, and geogrids enhance load-bearing capacity. Meanwhile, vegetation, including grass, shrubs, and trees, mitigates erosion and anchors soil. Bioengineering techniques, such as brush layering and coir rolls, merge living plant materials with structural elements for a holistic approach. Overall, integrating structural, vegetative, and bioengineering methods offers a comprehensive strategy to address slope instability, ensuring the safety of infrastructure and communities while promoting environmental sustainability.

2.4 PARTICLE IMAGE VELOCIMETRY

2.4.1 Introduction

In the context of this PhD project, the Particle Image Velocimetry (PIV) technique has been employed to measure displacements, specifically capturing soil movement on model slopes during controlled laboratory experiments (refer to Chapter 5, section 5.5 for detailed insights). The application of PIV to measure soil slope movements within the specific framework of this research is innovative. Additionally, a newly proposed technique, ASPS (refer to Chapter 5 for detailed explanations), has been adopted and successfully applied to this project to capture the soil movement displacement of the slope surface. The following sections present a detailed explanation of the working principles, limitations, accuracy, and applications of Particle Image Velocimetry (PIV) in Civil Engineering.

In experimental mechanics, particle image velocimetry (PIV) is frequently employed as a non-intrusive method to quantify displacements. Without using sensors that can damage the material being seen, incremental displacement fields can be estimated to subpixel accuracy by relating two digital pictures of an item before and after deformation. A digital snapshot is divided into a small virtual subset (sometimes known as “patches”), each of which is a collection of pixels with a particular colour intensity. The complete collection of pixels is divided up into regions or subsets that represent points. For each subgroup, the observed displacement vectors between two images captured at various times are calculated. The difference between the reference subset centre's position and the matching subset centre's position in the deformable image is the displacement. Research on the technique has improved displacement and strain measurements over the past several years, and a number of image-processing methods and methodologies have been created to meet a variety of application needs. Pan et al. (2009) describe DIC and survey the many approaches employed and offered, and more recently, Take (2015). The reader is directed to these contributions for an explanation of the approach and a thorough examination of the variables that affect the technique's accuracy and precision.

Digital Particle Image Velocimetry (DPIV) is a popular method for quantitative and qualitative flow and non-intrusive visualization. Several research articles (Adrian 1991a; Buchhave 1992; Willert and Gharib, 1991; Raffel et al. 2007a; Stamhuis and Videler, 1995; Grant 1997) discuss the application and improvement of the DPIV technology. Here, a MATLAB, DPIV analysis GUI-based open-source tool (PIVlab) is introduced. The application makes use of a number of

MATLAB's built-in features and simplifies further data handling by maintaining a close joining to MATLAB's well-known user interface.

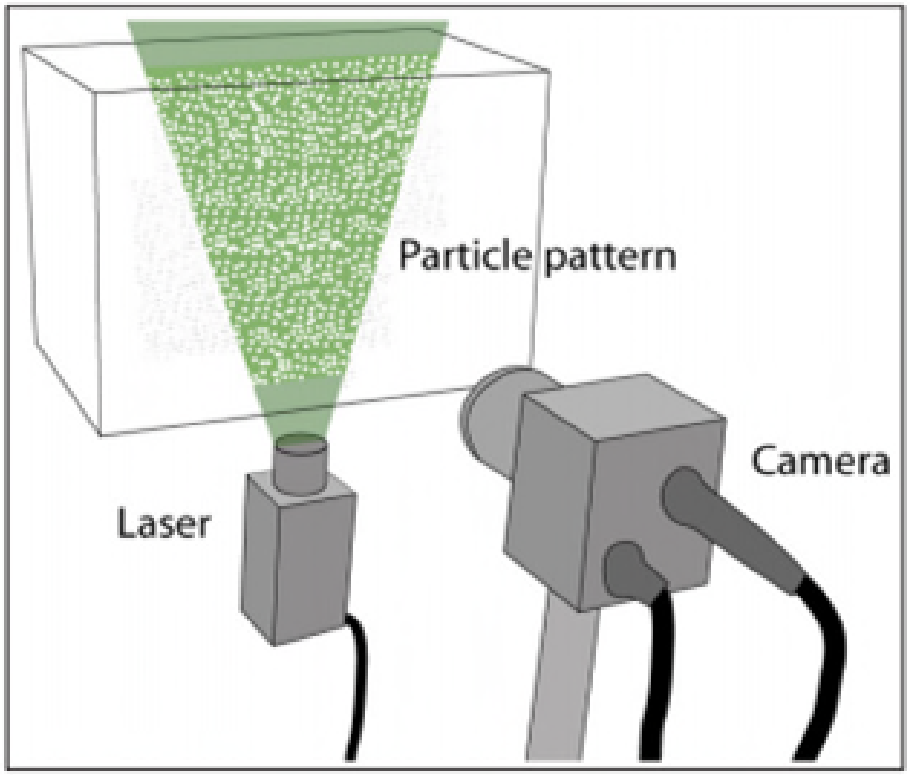

Figure 2.15: Principle of DPIV: A Laser sheet illuminates the particles contained in the fluid (Brücker 1996).

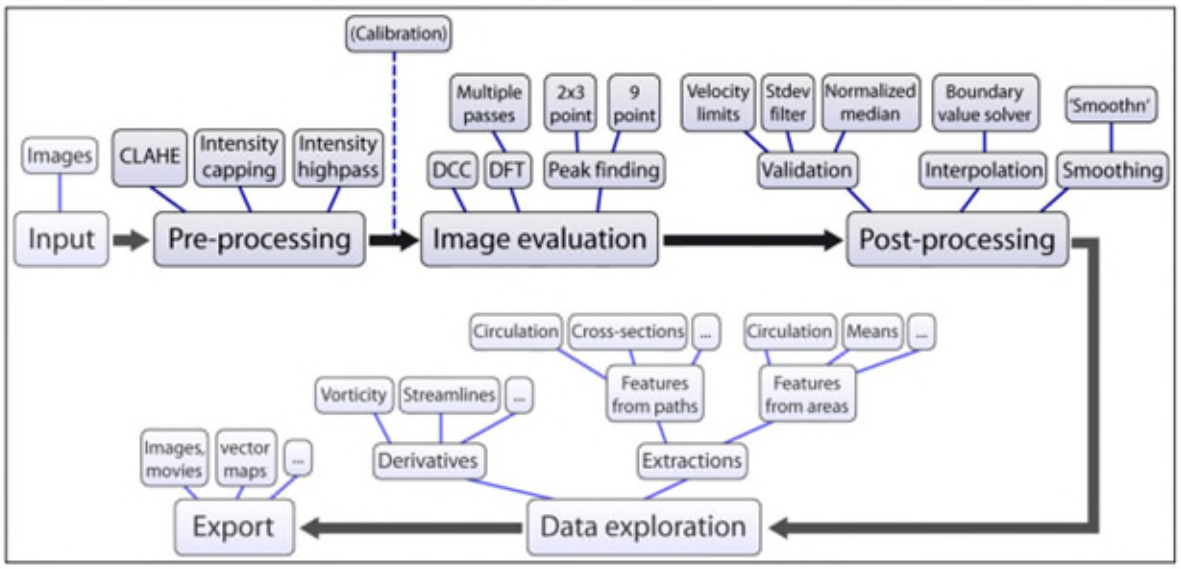

Figure 2.16: DPIV analyses in PIVlab. Overview of the workflow and the implemented features (Thielicke and Stamhuis, 2014)

The Digital Image Correlation (DIC) method is a surface deformation measurement technique that is observed as a commanding and multipurpose tool for measuring strains and is being adopted worldwide (Shavit et al. 2007a). For the DIC method, a subset known as PIV is available. In literature, this method will precisely calculate strains of provided 'particles' (of specific colour and texture) by identifying them with the help of algorithms, which is totally dependent on the image quality taken during an experiment (Pizer et al. 1987). The same authors explained that focus, shutter speed, and level of light must be maintained appropriately, and the camera should be kept stationary and smooth by using a tripod while excluding other intrusion.

2.4.2 Basic elements of PIV

2.4.2.1 Seeding

In general, PIV requires a higher seeding density than LDV (Laser Doppler Velocimetry), which is considered to be the standard. Ten particles should be connected with each velocity vector that is measured, according to a good rule of thumb. Melling (1997) has written an excellent review study on tracer particles and seeding in PIV systems. Although many scientific studies have extensively described the properties and attributes of seeding particles, there is a clear lack of information in the literature about the practical methods of introducing these particles into the flow being studied. The process of seeding is often seen as simple or even considered superfluous, resulting in a lack of knowledge about the effective methods used to

introduce particles into the flow. The transportation of seeding particles is a crucial element in experimental arrangements, particularly in the field of fluid dynamics and related research, where seeding is used for the purposes of visualisation or measurement. The literature may not place much importance on delivery techniques due to the notion that seeding is a normal and straightforward process. However, it is crucial to acknowledge and tackle the difficulties related to particle distribution in order to guarantee precise and dependable experimental results. Additional investigation and reporting on effective methods for introducing seeding particles into fluid flows would provide useful knowledge to the experimental approach in many scientific fields. Spontaneous seeding may be acceptable if there are sufficient visible particles to act as PIV tracers. In virtually all other cases, the addition of a tracer helps provide adequate image contrast and tune particle size. For most liquid streams, inoculation is a simple process in which solid particles are suspended in a liquid and mixed to achieve a uniform distribution. LDV and PIV are two particles that can be used for flow visualization.

The particles used are difficult to handle as many droplets evaporate quickly. Solid particles agglomerate and are difficult to disperse. Particles should be introduced into the flow periodically just before the gaseous medium enters the test area. Injections should be made in such a way and at points that the tracer is evenly distributed without significantly interrupting the flow. The current turbulence in many test environments is insufficient for adequate mixing of the fluid and particles, so the particles must be delivered from multiple orifices. Therefore, particles that can be transported through small pipelines are required. Various processes are used to prepare and provide particles for seeding gas streams (Thielicke and Stamhuis, 2014; Willert 1996; Shavit et al. 2007b).

2.4.2.2 Light Sources

Rays (lasers) are commonly utilized in PIV for their capacity to produce a single type of light with higher energy that may be readily packaged in tiny sheets of light for lighting and monitoring the particles irrespective of chromatic deviations. This may be performed with either constant wave (CW) laser or, more ideally, (pulse laser) PL. For PIV, typical CW lasers with a few watts of power are employed for less challenging presentations with pulse rates in the tens of hertz.

A continuous-wave laser can be used to generate pulses, or a rotating polygonal mirror with all but two of its facets covered can be used to reflect the complete laser beam across the test area quickly. A sheet-forming module is still required to create a light sheet for the chopped beam.

The light sheet is not an instantaneous entity, and as a result, even extremely rapid particles are successfully slowed.

2.4.3 Image Capturing

Particle Image Velocimetry (PIV) recording modalities may be classified into two distinct categories. The first approach entails producing a solitary illumination picture for every illumination pulse, while the second method captures the lighted stream in a solitary frame. There are two branches of PIV, namely 'multi-frame/single-exposure PIV and 'single-frame/multiple-exposure PIV, as described by Adrian (1991b). In the technique known as 'multi-frame/single-exposure PIV,' an individual picture is generated for every lighting pulse. Conversely, the 'single-frame/multiple-exposure PIV' technique catches the lighted stream in a single frame. The main difference between these approaches is based on the sequential timing of the light pulses. In the previous case, there is no intrinsic data on the order of light pulses, which might result in uncertainty when calculating the direction of the reconstructed displacement vector. In order to resolve this uncertainty in a direction, many methods have been created, such as pulse marking or colour coding. These solutions aid in resolving errors in the reconstruction process and improve the precision of PIV measurements. The selection of these modalities is contingent upon the particular demands of the experiment and the intended degree of information on the chronological order of events in the lighted flow (Hinsch 1995; Reuss et al. 1986; Gogineni et al. 1998).

2.4.4 Recording Hardware

Recent advances in electronic image processing have changed the way photography is done. The distinct advantages of electronic imaging include immediate image availability and feedback during acquisition, as well as the complete avoidance of photochemical processing. Current trends suggest that electronic recording may replace large-format film cameras and holographic discs in the near future. Therefore, although development in this area is progressing very rapidly, there is an increasing emphasis on writing electronic records.

PIV images are typically captured with film or charge-couple device (CCD) sensors. CCD cameras are increasingly being used for PIV imaging. However, where very high resolution is required, especially when high flow velocities, small imaging areas, and small grains place special demands on the camera used, photographic film may be a viable option. There is. In the first two scenarios, the need arises for the camera to rapidly capture two images, ensuring

that the same individual particles are visible in both frames. Attaining brief intermediate exposure durations is crucial for this objective, and high-speed cameras play a pivotal role in achieving this endeavour. These cameras possess the capacity to consistently collect pictures at a frequency of a few kilohertz, allowing for the recording of rapid occurrences.

Currently, high-speed cameras may attain an intermediate time as short as around 10 microseconds. This is achieved by synchronizing the time of laser pulses with the camera's exposure cycle. In this configuration, the first laser pulse coincides with the end of the first image's exposure, while the second pulse is timed to match the start of the second image's exposure. Cameras with progressive scan design may record two pictures per second. Upon capturing the first picture, the electrical charge of every individual pixel is effectively relocated to its assigned position inside the interline shift register. This allows the pixel to capture a fresh picture, guaranteeing quick image acquisition. The second picture is thereafter shown until the first image is extracted from the interline shift register and sent to the buffer using a similar procedure. It is important to mention that this sequential process leads to the second picture being exposed for a longer period of time compared to the first image. In order to reduce the possibility of excessive exposure caused by surrounding light, a filter may be attached to the camera lens, allowing only the laser wavelength to transmit. This precise filtering guarantees that the camera catches the intended laser-induced pictures without any disruption from extraneous light sources.

2.4.5 Image Processing

Initially, this query was performed manually on selected images using sparse seeds, allowing individual particle tracking (Agüí and Jimenez, 1987; Dracos 1996). However, tracking the image of a single tracer particle from exposure to exposure is only practical for low image densities. Low image densities often occur in highly three-dimensional, high-velocity flows (such as turbo machinery) that fail to provide sufficient tracer particles or in two-phase flows where the transport of the particles themselves is studied.

This requirement requires an intermediate concentration of tracer particle images within the PIV image. Especially in airflow, high image densities are not possible because, above a certain level, increasing the tracer density in the flow does not increase the number of recognizable images (Adrian and Yao, 1985). Average image density is defined. Visual inspection of PIV recordings is not possible, and we are unable to detect matching pairs of particle images induced by subsequent illumination. As a result, it was necessary to develop a statistical

approach. After statistical evaluation, tracking algorithms can be used to achieve a sub-window spatial resolution of the measurements, called 'super-resolution' PIV (Keane et al. 1995). However, because extracting displacement information from individual particle images requires a spatially well-resolved image of the particle image, these techniques increase the spatial resolution of photographic PIV images over digital images (Raffel et al. 2007b).

2.4.5.1 Errors in PIV

Multiple sources of inaccuracy are present in PIV measurements (Prasad 2000):

- Noise in captured photographs is the cause of random mistakes;
- Bias mistakes that occur when signal peak locations are calculated with sub-pixel accuracy;
- Radial errors brought on by rotation and deformation of the flow within the query location, which cause correlation to be lost;
- Lag mistakes brought on by particles' incapacity to follow the flow without slipping;
- Acceleration errors from the Lagrangian motion of the tracer particles to approximate the local Euler velocity.

2.4.5.2 Performance: Accuracy, Precision and Resolution

Accuracy and resolution are crucial factors in deformation measuring systems since they determine the dependability and precision of the readings.

Accuracy, in this sense, pertains to the stochastic disparities detected across numerous measurements of the same magnitude. It indicates the degree of congruence between the measured values and the real values or actual situations. Precision is essential for guaranteeing the accuracy of deformation measurements, particularly when monitoring target markers in pictures or digital images. Resolution, however, is the minimum interval that may occur in a measurement. It assesses the system's capacity to perceive and depict subtle intricacies or variations in the observed magnitude. High resolution is crucial in deformation measuring systems to accurately capture delicate deformations or motions. The precision of a deformation measuring system that relies on monitoring target markers is affected by the method used to detect targets in pictures or digital images. The accuracy of the system is also influenced by the technique used to link measured places in the picture (image space coordinates) to equivalent positions in the physical element or model test. Representing accuracy as a

percentage of the field of vision (FOV) offers a dimensionless portrayal. This metric indicates the percentage of the field of view (FOV) that properly reflects the actual circumstances or motions being recorded. It provides a uniform method for expressing precision, enabling significant comparisons across various systems or studies.

Phillips (1991) showcased a remarkable level of precision in measurement, achieving an accuracy of 1/10,000 of the field of view (FOV) by direct tracking of the target marker's location on the X-ray film. This accomplishment demonstrated the exactness with which deformation or changes in position may be measured within the observed area.

Similarly, Butterfield et al. (1970) and Andrawes and Butterfield (1973) achieved a similar degree of precision, accurately reaching 1/11,000 of the field of vision. Their approach consisted of using stereophotogrammetry to measure photographic film. Stereophotogrammetry is a method that utilizes the concepts of triangulation from several photographs to accurately ascertain the three-dimensional coordinates of places in space. In this instance, it was used to examine photographic film, yielding very precise measurements inside the designated field of view. These works emphasize the progress and proficiency attained in accurately measuring deformation, namely in the realm of X-ray film and stereophotogrammetry. The capacity to attain accuracies at the scale of 1/10,000 or 1/11,000 of the field of view (FOV) highlights the advanced and precise measuring procedures used, which enhance the dependability of deformation assessments in diverse sectors.

Unlike traditional target tracking systems, stereo photogrammetry does not require markers to be embedded in soil particles can be detected. In neither case was an accuracy assessment performed. Instead, it was intended that measurements in picture space might be scaled directly to coordinates in object space. In other words, the image scale (defined as the length of the object space within the image or X-ray image compared to its length) was assumed to be constant across the field of view.

2.4.6 Application of PIV in Engineering

Planar velocity fields can be calculated using particle image velocimetry (PIV). Both qualitative and quantitative investigations of the flow's velocity distribution can be done using PIV. PIV is a potent instrument for measuring optical surface velocities that was initially created in the study of experimental fluid and gas dynamics.

2.4.6.1 Application of PIV in Civil Engineering

Several researchers have published findings about the use of PIV in civil engineering, and some relevant findings are reported in this section. Mirzababaei et al. (2016) conducted a laboratory study on strip foundations of fibre-reinforced slopes and used particle image velocimetry to estimate settlement and soil deformations. According to the results, a complete and systematic laboratory study was conducted on the effects of Fibre content and basal edge distance ratio on slope behaviour under surface loading. A particle image velocimetry technique was used throughout the study to assess the embankment deflection pattern. Furthermore, the behaviour of excess pore water pressure and the increase in overall stress were measured at predetermined locations on the slope using a series of devices. Using the experimental results, the following conclusions were reached:

- The model slope's load-bearing capacity increases significantly with the reinforcement of fibre. With a tread distance ratio of 3, the tread force on the 5% fibre-reinforced model slope was improved by 145% compared to the unreinforced model slope.
- Fibre is used to increase the strength of reinforced soil slopes and reduces vertical and lateral slope deformation as the soil particles are entangled with the Fibres. Additionally, the Fibres improved fill integrity and reduced the occurrence of stress cracks upon failure. Increasing the Fibre content significantly increased the stiffness of the levee, resulting in a decrease in deformation of the Fibre-reinforced levee at the same pedalling pressure.
- The degree of stress transfer is greater on the slope of the Fibre-reinforced model. This is due to the increased shear strength and restraint.
- Fibre-reinforced embankments with a Fibre content of 5% showed highly elastic behaviour with a nearly linear relationship between foundation pressure subsidence rates over a subsidence rate range of up to 25%.

Fujita et al. (1998) performed a comprehensive investigation on large-scale particle image velocimetry (LSPIV), specifically targeting the characterization of flow in hydraulic engineering applications. Their study investigated the use of video-based Large Scale Particle Image Velocimetry (LSPIV) in three specific hydraulic engineering situations, including areas ranging from 4,000 square metres to 45,000 square metres. The many applications included the examination of ice transportation at a simulated river junction, the exploration of gas transfer mechanisms after a simulated spillway, and the analysis of floodplain flow in an actual river.

The researchers faced distinct obstacles in each of these applications, which led them to make precise decisions and modifications to parameters in order to efficiently overcome these hurdles. LSPIV has shown to be a dependable, adaptable, and economical method for diagnosing flow, notwithstanding the many situations in which it is used. The effective use of this technology has been witnessed in different areas of water-related operations, such as surveillance planning, design, danger warning, operation, and management. The adaptability of LSPIV was especially apparent in situations where conventional measuring methods were either unfeasible or dangerous, such as in proximity to bridges, river training structures, powerhouses, and spillways. The researchers determined that LSPIV exhibited a high level of effectiveness in instances where rapid and efficient measurements were crucial, with a low need for site preparation. The research proposed that the use of LSPIV in extensive situations is a feasible and encouraging method. This technology provides an engaging method for obtaining two-dimensional flow field data in many areas of hydraulic engineering, demonstrating its potential for being very efficient and applicable in numerous water-related contexts.

In 2004, Meselhe et al. (2004) conducted a study pertaining to LSPIV in the context of low velocity and shallow water flows. The findings indicate that the precision of the LSPIV methodology remains unaffected even when the flow rate decreases to as low as 0.015 m/s, given that appropriate seeding and optimal time difference between images are chosen. The findings indicate that LSPIV is a suitable method for analyzing flow fields characterized by low velocities, which frequently fall below the detection threshold of conventional devices. The researchers arrived at the conclusion that LSPIV exhibits promise in the measurement of low velocities and, given suitable assumptions, flow rates within laboratory settings. It is also believed to be potentially applicable in field tests.

Hosseini et al. (2014) conducted a study to explore the use of particle image velocimetry (PIV) to measure displacement and strain fields in steel and reinforced concrete beams. The researchers concluded that PIV can effectively replace traditional displacement and strain measurement methods in bending tests, as supported by various validation experiments conducted in the study. Moreover, the PIV technique demonstrated significant potential for investigating the fracture mechanism in Reinforced Concrete (RC) beams during testing. It can be considered as a virtual strain gauge, enabling the monitoring of macro-crack propagation in reinforced concrete structures. By utilizing PIV, the researchers were able to obtain load-crack

width curves for the three flexural macrocracks of the RC beam specimen without prior knowledge of crack locations or the need for mechanical instruments. This highlights the superiority of PIV over conventional instruments. The Particle Image Velocimetry (PIV) method has the potential to serve as a suitable alternative to traditional measurement techniques in typical structural tests, especially in bending tests. It offers cost-effectiveness and robust capabilities for assessing midspan displacement, overall displacement, and strain fields.

Jayalat and Gallage (2021) performed a study to evaluate the tensile characteristics of geogrids utilizing particle image velocimetry (PIV) as a technology. The GeoPIV-RG software was used especially to monitor the localized axial and lateral strain development of composite geogrid specimens during a wide-width tensile test. The programme was essential in assessing the load-strain response of the composite geogrid material.

The analysis revealed that the stiffness values produced with the GeoPIV-RG approach exceeded the manufacturer's stipulated nominal strength. The determination of this nominal strength is commonly conducted using the crosshead technique. The researchers proposed that using the GeoPIV-RG approach, as opposed to the conventional crosshead method, enables the cost-effective design of geotechnical structures by leveraging precise evaluation of tensile characteristics. This discovery highlights the advantages of using the GeoPIV-RG approach to accurately assess the strain development of geosynthetic materials during wide-ranging tensile tests. The GeoPIV-RG approach, because of its capacity to record localized strain development, provides a more precise and perceptive comprehension of geogrid behaviour under tensile loading circumstances, thereby offering useful information for geotechnical engineering applications.

The research undertaken by (Huang et al. 2015) used Particle Image Velocimetry (PIV) to examine the factors responsible for the elevation of pipes that are buried in sand with a medium density. The study was focused on two states: a stationary state and a changing one. The PIV technology was used to acquire displacement vector fields and strain contours in the soil around the pipes. The objective of the research was to understand the processes by which the soil around the pipes and the ground surface deforms under various situations, taking into account external pressures and soil liquefaction as factors that initiate the deformation. During the post-peak phase, the study documented a shear failure plane that extended all the way to the ground surface, creating a trumpet-shaped formation at an inclined angle. The magnitude of ground surface deformation escalated in proportion to the depth at which the pipe was buried. Within

a liquefied field, the soil displayed a flow pattern confined to a heart-shaped area around the pipe. The zone of soil distortion encompassing a pipe buried at a shallow depth, with a width ranging from 5 to 6 times the diameter of the pipe (5D-6D), was notably bigger in comparison to a pipe sunk at the same depth in an unchanging environment. The ground surface displayed both upward and downward movements. The investigation yielded excellent insights into the intricate interplay of subterranean pipes, soil deformation, and liquefaction, underscoring the usefulness of PIV in recording intricate deformation patterns.

Baba and Peth (2012) conducted a study focusing on soil deformation and creep movement on slopes using a large-scale soil box test. The soil box used in the test had dimensions of 3.0 m in length, 1.0 m in width, and 1.2 m in height. The main objective of the study was to investigate the creep movement that occurs along slopes. The researchers found that by employing PIV, it was possible to detect soil movements with high precision, down to the scale of micrometres, simply by analyzing the natural texture of the soil captured in the images. This non-invasive method proved to be effective in studying the interaction between hydraulic (related to water flow) and mechanical stresses and their impact on slope stability. Overall, the study demonstrated that PIV has significant potential for systematically analyzing the intricate relationship between hydraulic and mechanical factors affecting slope stability. It offers a valuable tool for understanding soil deformation and creep movements on slopes, providing insights that can contribute to better slope management and stability assessment.

Slominski et al. (2007) conducted research to investigate the possible use of Particle Image Velocimetry (PIV) in monitoring deformations that occur when granular materials flow in silos. The primary objective was to quantitatively assess the strain fields in dry and cohesionless sand as it undergoes gravity flow in planar strain silos. The researchers performed small-scale experimental studies employing both mass flow and funnel flow silos to examine the deformation patterns in the sand. Additionally, they conducted trials using a funnel flow silo that was supplied with inserts in order to evaluate their impact. An investigation was conducted to analyse the impact of flow type, insert type, starting sand unit weight, and silo wall roughness on the material's kinematics. The researchers determined that the PIV approach is a proficient optical tool for quantifying deformations on the surface of granular materials. This is achieved by processing successive digital images without the need for physical contact. However, they also pointed out a limitation of PIV: it is unable to trace strains within the material itself, only capturing surface deformations. This discrepancy is particularly relevant in the case of silo flow

due to wall friction between the granulated material and the transparent wall. It results in differences between strains observed on the surface and those occurring inside the material. Furthermore, they also demonstrated the usefulness of PIV for surface deformation measurements in granular materials within silos. However, they noted the inability of PIV to trace internal strains within the material, which is important to consider when analyzing silo flow due to the impact of wall friction.

Matziaris (2019) did research aimed to investigate the threshold at which rainfall-induced landslides occur on sandy slopes. The research used physical modelling experiments to investigate the beginning of landslides triggered by rainfall in unsaturated soil slopes. The experiments were conducted in a plane-strain centrifuge box that was equipped with integrated devices for regulating rainfall and groundwater conditions. The primary aim of the research was to examine the optimal precipitation thresholds necessary to initiate landslides under different circumstances. Slope models composed of finely granulated silica sand were originally created at various densities when in an unsaturated condition under the influence of 1g of normal gravity. Subsequently, the models were positioned inside the centrifuge container, and a rainfall simulator was used to administer rainfall episodes with varying durations and intensities. Additionally, the groundwater conditions varied during the centrifuge flight at an acceleration of 60g. The results of the study revealed that more intense rainfall events led to greater soil displacement, indicating a stronger response. However, it was observed that full slope collapse did not always occur, even with intense rainfall. Failure and landslide initiation only transpired in models where the groundwater table rose above the toe of the slope. This indicated that higher groundwater table levels played a crucial role in triggering slope failure. Furthermore, the study demonstrated that the reduction in permeability of the soil played a significant role in initiating instability under different combinations of rainfall intensity and duration. The results highlighted the complex relationship between rainfall, groundwater conditions, and soil properties in the context of landslide initiation. Overall, the study contributed to a better understanding of the rainfall thresholds required for landslide initiation in sandy slopes and emphasized the importance of groundwater conditions and permeability in slope stability assessment.

The work done by Yuan et al. (2017) aimed to analyse the deflection of a laterally loaded pile and the associated soil deformation using Particle Image Velocimetry (PIV). This required computing displacement fields of both the ground surface and the profile based on a sequence

of photographs. By using this methodology, a more accurate estimate of the pile deflection was achieved in contrast to the typically used Double Integration (DI) method. The acquired photos clearly showed that the sand inside the pile had a rotating motion at a depth of about 160 mm, which aligns with the findings obtained using the DI approach. In order to confirm the correctness of the PIV approach, a finite-element analysis was used to replicate the model test. The results of this investigation confirmed the dependability and accuracy of the PIV approach in capturing the complexities of soil-pile interaction issues. Thus, the findings of this study unequivocally demonstrate that the PIV technique, in conjunction with the optical setup utilized, is well-suited for addressing challenges associated with the interaction between soil and piles. The implications of this research hold significance in the academic and practical realms, as it provides valuable insights into the behaviour of laterally loaded piles and contributes to the development of more effective engineering approaches in dealing with soil-pile interactions.

2.4.7 Summary

Particle image velocimetry (PIV) is a technique employed in geotechnical engineering to study the movement of particles within soil or fluid systems. It involves tracking and analysing the displacement and velocity of particles using high-resolution imaging. In geotechnical engineering, PIV has several applications. It enables the measurement of fluid flow characteristics, such as velocity fields and turbulence, which are crucial in understanding soil behaviour and erosion processes. PIV helps in assessing the stability and performance of structures like retaining walls, dams, and slopes by providing insights into the flow patterns and forces exerted by the soil or water. PIV can be employed to study the flow patterns and velocities of soil particles on slopes during rainfall events. By analysing the displacement and velocity fields, PIV helps in understanding the erosion mechanisms, identifying potential failure zones, and assessing the stability of slopes. By capturing detailed particle motion data, PIV aids in analysing phenomena like soil erosion, sediment transport, and pore-water pressure distribution. This information assists in designing erosion control measures, optimizing drainage systems, and improving the stability of geotechnical structures. PIV also allows researchers to validate and refine numerical models and simulations, providing a means to validate assumptions and improve the accuracy of predictions. It helps in calibrating parameters, validating boundary conditions, and gaining a better understanding of the complex interactions between soil, water, and structures. Overall, PIV serves as a valuable tool in geotechnical engineering, providing quantitative and visual data that contribute to a deeper

understanding of soil-fluid interactions, improving design practices, and ensuring the safety and performance of geotechnical systems.

CHAPTER 3: RESEARCH METHODOLOGY

3.1 Introduction

This chapter presents the detailed methods and procedures adopted in this research project to achieve the targeted aim and objectives as described in Chapter 1. The research methodology for this research project consists of 5 different phases: (i) laboratory-based testing of soil properties, (ii) the numerical modelling using finite element tool (PLAXIS 2D), (iii) the design and fabrication and use of physical slope model and (iv) image analysis of slope model results and (v) a case study of Azad Pattan road landslide. These stages have been discussed in the following sections.

Figure 3.1 outlines the methodology employed in this comprehensive study. After thoroughly formulating the research question and objectives, a detailed review of the existing literature was conducted, investigating a wealth of information and research findings on the complex subject of slope failures induced by rainfall.

Originally, the project was designed to start with experimental work, followed by the development of finite element models tailored to the specific slope under consideration. The intention was to optimize critical parameters, such as slope angle, critical rainfall intensity and duration, the length of sand piles, and diameters from the experimental testing phase.

Unfortunately, unforeseen circumstances arose in the form of the COVID-19 pandemic, which led to nationwide lockdowns during 2020-21. During this period, no access was allowed to NTU laboratories. Consequently, a strategic decision was made to pivot the projected trajectory, first initiating the finite element modelling. Thus, a revised intention was to optimize slope and geometry parameters through numerical analysis and, subsequently, employ these optimized parameters in the planned experimental and laboratory testing phases. Despite the unexpected adjustment to the project timeline, the overarching aim remained to contribute significantly to understanding rainfall-triggered slope failures and their mitigation strategies.

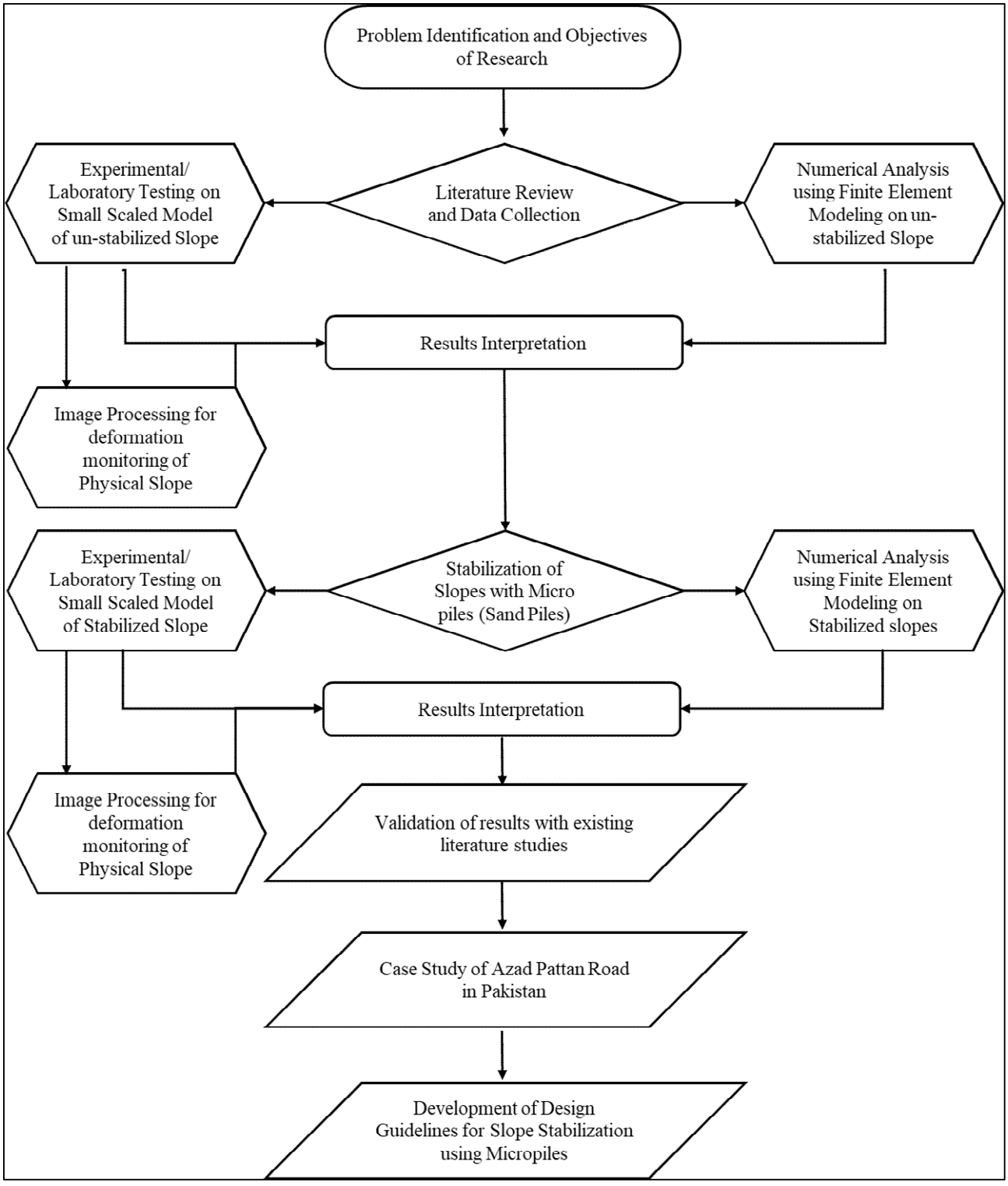

Figure 3.1: Research Methodology flow chart

3.2 Engineering Characteristics of Soil used for this Research

The physical testing program was conducted in the soil mechanics laboratory of the Civil Engineering department at Nottingham Trent University. Laboratory tests were performed to

determine the soil properties required for slope stability analysis (the test results are presented in Chapter 7). These tests were basic and index properties, including classification and compaction, as specifically described in the following sections.

- Soil Classification;
- Compaction.

The preparation of the soil slope model is also presented in this chapter. This includes the fabrication of a model tank/rig, setting up of an artificial rainfall system, installation of moisture monitoring instruments, and details of deformation measuring procedure using image processing technique.

3.2.1.1 Classification Tests (BS 1377-2:2022)

Soil classification is a fundamental aspect of geotechnical engineering, essential for understanding soil behaviour and its suitability for construction purposes. Two primary tests employed in soil classification are the sieve analysis and Atterberg Limits tests. Sieve analysis determines the particle size distribution of soil by passing it through a series of sieves with progressively smaller openings, which helps in identifying the soil's texture and gradation. Atterberg Limits, on the other hand, assesses the plasticity characteristics of fine-grained soils by measuring the liquid limit, plastic limit, and shrinkage limit. These tests provide critical insights into the soil's consistency, compaction potential, and structural stability, forming the basis for effective soil management and foundation design.

3.2.1.1.1 Sieve Analysis (BS 1377-2:2022)

The sieve analysis test of soil, conducted in accordance with British Standard BS 1377-2:2022 part 10, is a fundamental procedure in geotechnical engineering and soil science. This method provides essential information about the particle size distribution of a soil sample, which is crucial for understanding its engineering properties and suitability for various applications. During the test, a representative soil sample is carefully prepared and placed in a series of progressively finer mesh sieves. These sieves are then mechanically shaken, allowing particles to separate based on their size. The results are typically presented in a particle size distribution curve, showing the percentage of soil retained on each sieve. This data aids in classifying the soil, assessing its permeability, and predicting its behaviour under different load and drainage conditions. The sieve analysis test is a cornerstone in geotechnical investigations, guiding

engineers and researchers in making informed decisions related to construction, foundation design, and soil improvement techniques.

3.2.1.1.2 Atterberg Limits (BS 1377-2:2022)

Soil containing fine particles can manifest in different states, contingent on the moisture content within the soil system. In its dry state, each particle becomes surrounded by a thin layer of adsorbed water upon contact with water. The introduction of water to individual particles in any soil leads to an augmentation in the thickness of the water film enveloping each particle. This augmented film thickness promotes smoother sliding of particles past one another. As a result, the frictional behaviour of the soil is intricately linked to the quantity of water present in the system.

Casagrande (1932) later provided more precise definitions for these limits based on the water content corresponding to specific conditions:

- Liquid limit (LL): This is the moisture content at which the soil displays such low shear strength that it flows to close a groove of standardized width when subjected to a specific jarring procedure;
- Plastic limit (PL): It is the moisture content at which the soil starts to crumble when rolled into threads of specific length and diameter;
- Shrinkage limit (SL): This represents the moisture content necessary for the soil to fill its pores when it reaches its minimum volume during the drying process.

The quantity of water required to transition a soil from its plastic limit to its liquid limit serves as an indication of its plasticity. This plasticity is quantified by the "Plasticity index" (PI), which is calculated as the difference between the liquid limit and the plastic limit (PI = LL - PL). Figure 3.2 illustrates the relationship between each limit and moisture content. It can be seen as the percentage of moisture content increases, the state of the soil changes. The liquid limit and plastic limit were determined in laboratory settings according to the British standard (BS 1377-2).

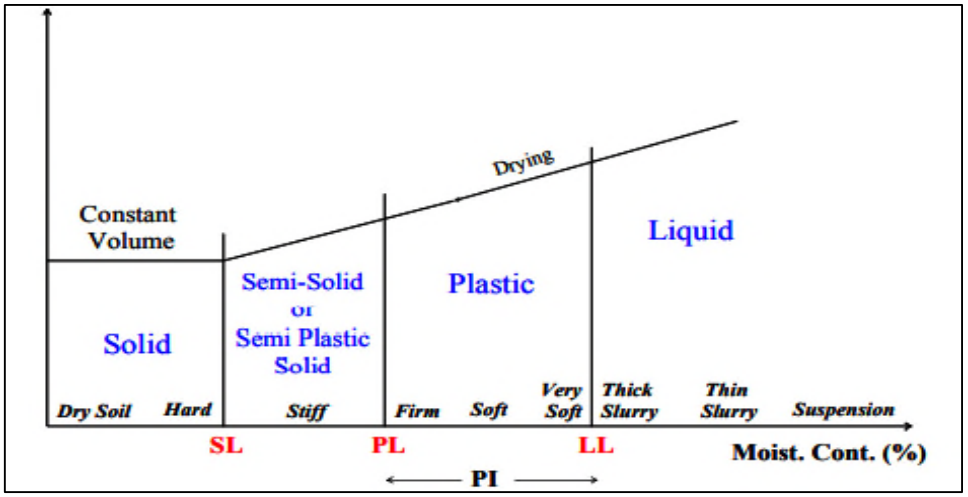

Figure 3.2: Moisture content and volume of soil relationship (Oh and Lu, 2015a)

3.2.1.2 Compaction Test (BS 1377-2:2022)

Soil compaction is a process whereby soil particles experience increased proximity and density through the application of impact energy delivered by a specified number of hammer blows falling from specific heights. This procedure, known as the Proctor Compaction test or Standard British Compaction test (BS 1377-2:2022), is commonly employed for fine and cohesive soils. The specific test conducted depends on the size and weight of the hammer and the compaction mould, leading to two variations: the Standard Compaction Test and the Modified Compaction Test. The underlying mechanism behind compaction, which results in increased soil density, is attributed to the reduction of air voids through mechanical means.

The compaction test is a frequently used laboratory process that aims to establish the correlation between the moisture content and the dry density of a soil sample. The procedure adheres to the Standard Proctor Test Procedure established by Proctor (1933). The Standard Proctor Test includes compacting the soil with a 2.5 kg hammer dropped from a height of 30.5 cm into a mould filled with three equally thick layers of soil. Every layer experiences 25 impacts from a hammer. The Modified Proctor Test is a modification of this process, utilizing a 4.5 kg hammer dropped from a height of 45.7 cm and using five equally thick dirt layers instead of three.

Two types of compaction moulds are used for these tests. The smaller mould, with a diameter of 105mm (internal) and a volume of approximately 1/30 ft^3 (944 cm^3), is utilized for the Standard Proctor Test. The larger mould, with a diameter of 150mm (internal and a volume of

approximately 1/13,333 ft³ (2123 cm³), is employed for the Modified Proctor Test. When using the larger mould for the Modified Proctor Test, each soil layer is subjected to 56 blows instead of the 25 blows required for the Standard Proctor Test. Figure 3.3 illustrates the process of the Standard Proctor Test. The compaction test was carried out to determine the optimum moisture content and maximum dry density of the selected soil type. This density was later used to prepare and compact the slope model for slope analysis.

(a) (b) (c)

Figure 3.3: The Process of Compaction test, (a) Soil mixing, (b) Soil compaction, (c) soil mass measurement.

After determining the physical properties of the soil, including its classification and density, the strength parameters were obtained from relevant literature sources, as detailed in section 3.3.4. These parameters were subsequently utilized for numerical modelling using PLAXIS software. The numerical modelling facilitated the optimization of slope parameters, which were then applied in small-scale laboratory testing. A comprehensive description and discussion of the numerical modelling process are presented in the following sections.

3.3 Numerical Modelling

Numerical modelling is a powerful tool in geotechnical engineering, offering precise and comprehensive analysis of complex soil-structure interactions that are challenging to assess using traditional methods. It enables the simulation of various scenarios and conditions, providing insights into the behaviour of soil under different loads and environmental influences. PLAXIS, a specialized finite element software for geotechnical applications, is particularly beneficial in slope stability analysis. It allows for detailed modelling of soil properties, groundwater conditions, and structural elements, enabling accurate prediction of

potential failure mechanisms and stability factors. By using PLAXIS, researchers can conduct thorough analyses, optimize design parameters, and enhance the safety and reliability of geotechnical structures, contributing significantly to advanced research and practical engineering solutions. PLAXIS is a widespread finite element programme utilised by geotechnical engineers and researchers in the field of soil and rock analysis for over twenty years. The software was initially created at The Technical University of Delft in 1987 to analyse the characteristics of soft soils in the lowlands of Holland (Brinkgreve and Vermeer, 2001). The software was subsequently expanded to encompass all facets and uses of geotechnical engineering simulations, employing a user-friendly interface that harnesses the capabilities of finite element analysis. The initial version of PLAXIS was commercially released in 1998. PLAXIS incorporates various soil models along with a flexible library of structural elements. The program's automated mesh generation tool facilitates the production of soil models by providing both 6-node and 15-node triangular elements, making the process easy and practical. The programme uses the Mohr-Coulomb (MC) methodology to compute the safety factors of slopes.

This computer program may be used to solve a wide variety of geotechnical issues, such as stability studies and computations of steady-state groundwater flow. Several Finite Element (FE) models and four primary sub-routines are included in this package for convenience. Inputs, computations, outputs, and curve charts are included in these subroutines. The curve plots sub-routine is used to generate a plot of the factor of safety (FOS) vs displacement. It is the input sub-routine that analyzes the slope models. For a particular soil layer, the material attributes, which include the shear strength parameters, are provided as input, and their definition is established.

For the purpose of performing the generation of the finite element mesh, a plain strain model consisting of fifteen nodded triangular elements was chosen (Ambily and Gandhi, 2007). Furthermore, an M-C material model was used to conduct stability assessments. It is the elastic-perfectly plastic theory of soil mechanics that serves as the foundation for the M-C model that was chosen. As a result, the model incorporates both elastic parameters (E, v) and plastic parameters (c', φ', Ψ) in order to accurately represent the system (Bentley Systems, 2020). In a similar manner, the model has integrated a plastic potential function (g) in addition to the yield function (f). This function is related to the plastic behaviour of soils, and the dilatancy angle (Ψ) is the variable that represents this relationship.

3.3.1 Computation of the Factor of Safety (FOS)

The 'c-φ reduction' approach was used in order to calculate the FOS algorithm. As stated by PLAXIS (2021), this particular strategy entails gradually decreasing the soil strength parameters c' and tan φ' until the point when failure takes place. The parameters of the strength are automatically decreased until the final calculation is completed, which results in a failure mechanism that has been completely established. Furthermore, a soil body is recognised to fail if a particular strength drop happens (Nordal and Glaamen, 2004). This is accomplished by gradually decreasing the strength of the soil from its initial state. In this way, PLAXIS computes the FOS as the ratio of the available shear strength to the strength at failure by summing up the incremental multiplier (M_{sf}) as defined by Equation 3.1:

$$\sum M_{sf} = \frac{tan\emptyset_{input}}{tan\emptyset_{reduced}} = \frac{c_{input}}{c_{reduced}} = \frac{S_{u,input}}{S_{u,reduced}} \text{----------(Equation 3.1)}$$

$$= \frac{tensile\ strength_{input}}{tensile\ strength_{reduced}} \text{----------(Equation 3.2)}$$

$$\text{Safety Factor} = \frac{available\ strength}{strenght\ at\ failure} \text{----------(Equation 3.3)}$$

$$= \text{value of } \sum M_{sf} \text{ at failure} \text{----------(Equation 3.4)}$$

3.3.2 Coupled Flow-Deformation Analysis

A prevalent approach in designing slope failure forecasting models involves integrating a hydrology model with a stability model to evaluate the factor of safety. Constitutive models for the hydro-mechanical behaviour of unsaturated soils may be categorised into two distinct groups: Elastic models (Thomas and He, 1998) and elastoplastic models (Chiu and Ng, 2003; Georgiadis et al. 2005; Thomas and He, 1998; Wheeler and Sivakumar, 1995). The fully coupled flow deformation section was introduced into the (PLAXIS 2021) finite element (FE) program. Haxaire et al. (2011) Provided a comprehensive description and validation of finite element formulations for the study of coupled hydro-mechanical systems. In the coupled analysis, the two computing processes mentioned above are effectively combined. This allows for the simultaneous calculation of both the soil's hydraulic and mechanical responses. Oh and Lu (2015a) said that performing a coupled analysis has the potential to enhance the precision of evaluating slope stability in the presence of rainfall. The primary emphasis was on forecasting hydrological reactions and determining the slope factor of safety, notwithstanding the execution of many hydromechanical investigations. An acceptable approach to capture the

interaction between fluid and solid in unsaturated soils is to use a coupled analysis, where flow modelling and mechanical modelling are done concurrently. The stability of this unsaturated slope in its native terrain was assessed using the safety factor, which is the predominant method for assessing slope stability under different environmental circumstances (Qi and Vanapalli, 2015).

3.3.3 The Benefits of Using PLAXIS for Simulating Model Slopes

Using advanced Finite Element (FE) programs like PLAXIS offers several benefits in the analysis of slopes:

- Calculation of Displacements: PLAXIS can calculate both horizontal and vertical displacements of the entire model slope. This is essential for understanding how the slope deforms under different conditions.
- No Predefined Failure Surface: Unlike some traditional methods that require a distinct failure surface to be predefined, PLAXIS can analyse slopes without such predetermined surfaces. This allows for more flexibility in modelling complex geological conditions.
- Progressive Failure: PLAXIS has the capability to capture progressive failure. This means that the analysis considers how failure propagates through the slope gradually, providing a more realistic representation of the slope behaviour.
- Distributed Deformations: The program can simulate distributed deviatoric deformations. This is valuable for understanding how different regions of the slope deform and fail independently, contributing to a more detailed analysis.
- Dynamic Responses: PLAXIS can simulate dynamic responses, allowing for the analysis of how slopes behave under dynamic loads, such as seismic events. This is crucial for assessing the stability of slopes in regions prone to earthquakes.

3.3.4 Slope Model

In order to develop a deep understanding of slope behaviour against a combined effect of rainfall infiltration and gravitational forces, six different slope angles (α) were assumed to investigate the failure pattern under the coupled flow-deformation analysis concept. These values were selected based on previous studies that defined slope steepness (Shiferaw 2021a; Baazouzi et al. 2015; He et al. 2015). Slopes with higher angles will experience high

gravitational forces, whereas slopes with lower angles will experience less gravitational forces. Considered slope dimensions for the FEM analyses are as follows.

- Slope Model 1: α_1=25º
- Slope Model 2: α_2=30º
- Slope Model 3: α_3=35º
- Slope Model 4: α_4=45º
- Slope Model 5: α_5=50º
- Slope Model 6: α_6=55º

Once the slope geometry was established, the specific parametric values corresponding to the soil type being evaluated were inputted into the Finite Element (FE) program. The soil characteristics, including index values and compaction properties, were derived from experiments conducted at the NTU - Soil Mechanics Laboratory. In addition to such completed tests, some parameters were calculated/taken based on those tests, such as permeability coefficient (k), consolidation parameters, internal friction angle (φ), Young Modulus (E), and the Poisson Ratio (ν) from Table 2-3, Table 2-5, Table 2-6, Table 2-7 and Table 2-8 of Foundation Analysis and Design by (Bowles 1988) respectively. For the simulation of different rainfall intensities, various intensities were assumed, i.e. 10mm/hr, 20mm/hr, 60mm/hr, 90mm/hr and 120mm/hr lasting for 01hr, 06hrs, 12hrs, 24hrs and 24hrs. These intensities were assumed based on the literature. Various researchers (Cruden and Varnes, 1996; Li et al. 2015; Suemitsu et al. 2024; Dunkerley 2021) have classified rainfall intensities as low (<20mm/hr), mid (<60mm/hr) and high (>70mm/hr) intense rainfall events.

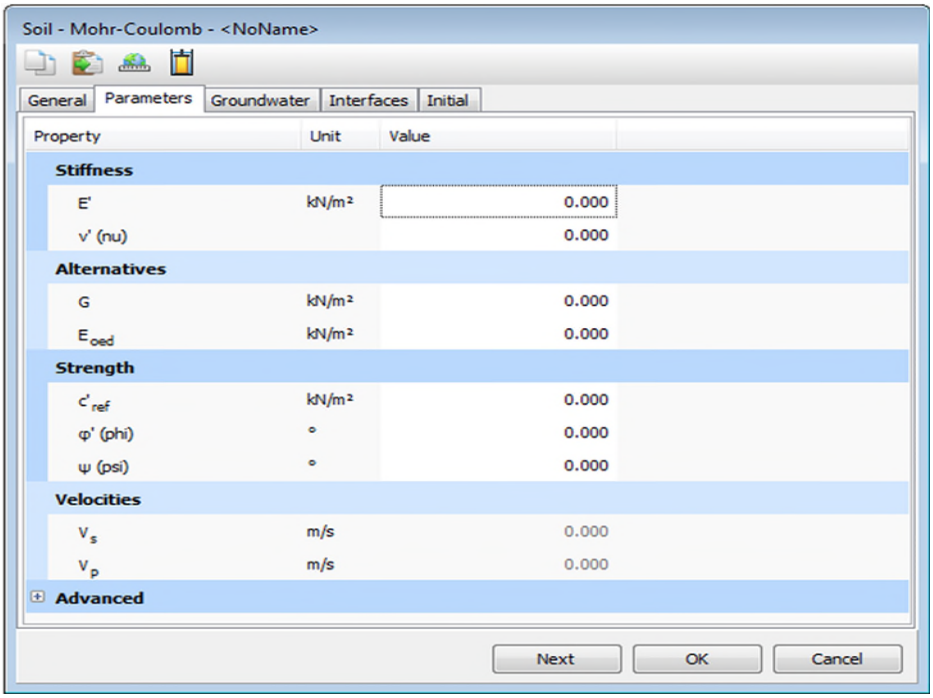

Figure 3.4: Parameter tabsheet for Soil Models

3.3.5 Slope Analysis

Step 1 - Model development: Once the shape of the slope model is chosen, the material properties for the model slope are specified. Figure 3.4 illustrates the parameters required for soil modelling. The physical properties (i.e. classification, density and strength parameters) were obtained from laboratory testing and also from empirical relationships.

Step 2 - Mesh Generation: PLAXIS software includes a "Global Coarseness" feature in the "Mesh" menu, allowing users to select various mesh sizes, ranging from coarse to ultrafine. Reducing the mesh size enhances the detail and accuracy of the analysis results. To ensure a thorough and reliable analysis, users can select an appropriate level of mesh refinement. This refinement enables the generation of a more detailed and precise mesh, which is essential for capturing the intricacies of the modelled system. By adjusting the mesh size to a finer level, users can achieve a higher resolution in their simulations, leading to more accurate and comprehensive outcomes.

Step 3 - Initial and Boundary Conditions: This stage provides details on the exact position of the groundwater table (GWT) level, requirements for the impermeable boundary, and the phreatic level. The GWT level corresponds to the whole incline surface at which the generation of hydrostatic pressure ceases. Figure 3.5 shows the typical geometry and boundary conditions

for finite element modelling of different slopes. The inclusion of an impermeable rock layer at the slope's base imposes a foundational constraint. Seepage conditions are specified for both the left and right flanks of the slope, while an infiltration condition is allocated to the upper portion. This approach aims to replicate the infiltration of rainwater into the slope, providing a comprehensive simulation of the complex interactions and dynamics involved in such scenarios.

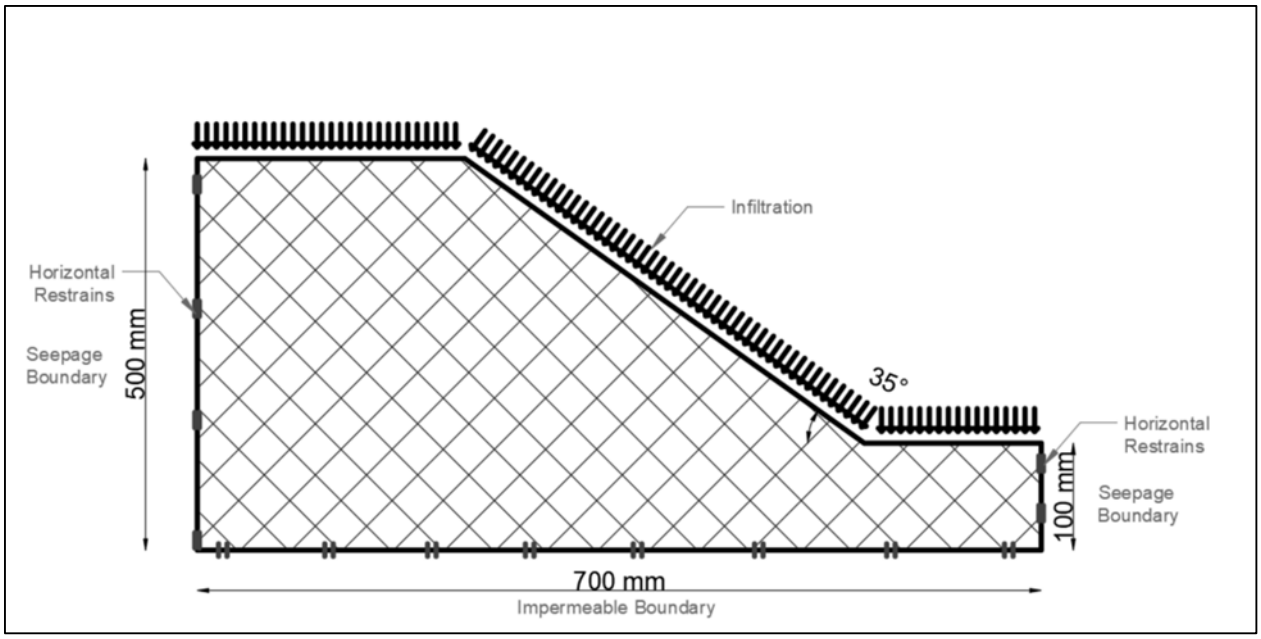

Figure 3.5: Typical Slope geometry and boundary conditions

Step 4 - Calculations: The computation component is the concluding phase that employs diverse calculation methodologies for distinct soil models. The Shear Strength Reduction (SSR) technique is used in this research to ascertain the minimal factor of safety for the specified slope model. The SSR approach relies on the Mohr-Coulomb (M-C) soil model parameters, namely the effective stress terms for cohesion (c') and internal friction angle (φ'). The SSR approach operates in the following manner: first, soil strength parameters are established, and subsequently, the finite element programme computes the current soil strength. Subsequently, the programme automatically reduces the values of the soil shear strength parameters while simultaneously calculating the factor of safety (FOS) until it reaches a value less than 1. If the FOS is less than 1, the slope is said to be in a state of collapse.

Step 5 - Analysis of Results: After the completion of the analytic process, PLAXIS enables the user to visualize the results using graphical representations, tables, and figures. The FE programme marks probable slip surfaces as "deformations" in the main menu. Additionally, the values of the safety factors may be obtained for the tested model slopes using the display menu.

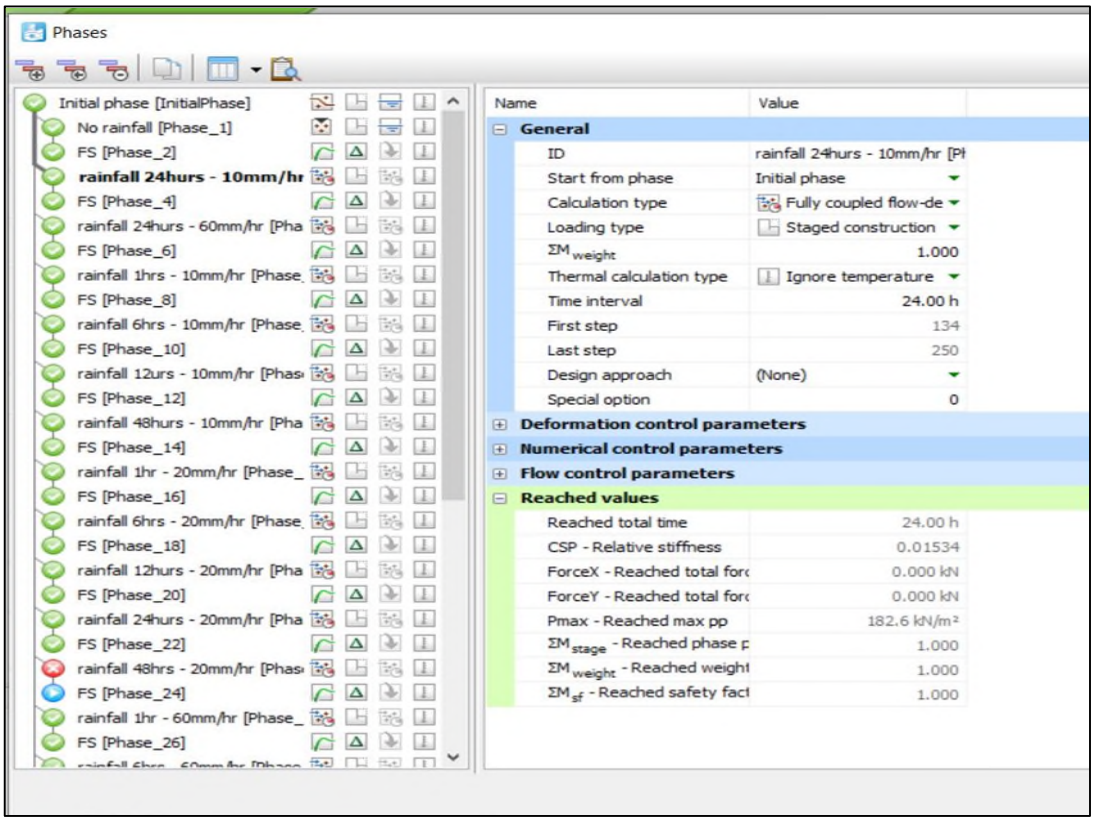

Figure 3.6: Illustration of different stages formed in PLAXIS for slope analysis.

3.4 Laboratory-based Experimental Testing

Based on the optimization of slope configuration, a detailed experimental setup was designed and fabricated in the Geotechnical lab at NTU. Creating a laboratory-based slope model within a specially designed soil container involves several critical steps and considerations. The process began with a comprehensive literature review to understand existing methodologies and best practices for laboratory-based slope models. The design phase focused on creating a transparent tank with a specific geometry that mimics the desired slope conditions. Materials chosen for the tank provide transparency for clear observation of soil behaviour, ensuring durability to withstand experimental conditions. A strong steel base was implemented to provide stability and support without compromising the transparency of the tank. In parallel, an artificial rainfall system was designed and set up to simulate precipitation on the slope. This involved considerations such as rainfall intensity, duration, and distribution. A data collection

system was integrated to measure soil parameters like moisture, displacement, and other relevant factors during artificial rainfall. A monitoring system, including cameras or imaging devices, was implemented to observe the slope's response. The experimental rig, comprising the transparent tank, steel base, and artificial rainfall system, was assembled based on the designed specifications. Calibration of instruments and sensors was performed to ensure accurate data collection. Safety measures were implemented to prevent accidents, and the entire setup, including tank dimensions, materials used, and details of the artificial rainfall system, was thoroughly documented. This laboratory-based slope model is expected to provide valuable insights into slope behaviour under controlled conditions, contributing to a better understanding of slope stability.

3.4.1 Fabrication of Experimental Rig

The soil experimental rig used in this slope model is a rectangular steel frame measuring 2000 mm in length, 1000 mm in width, and 1000 mm in height. The process of fabrication is illustrated in Figure 3.7. To sustain the lateral earth pressure, acrylic Perspex panels of 5mm thickness were used for all four sidewalls, while a 12.5mm thick metal plate was used for the bottom side. By making the side walls of the soil container from plexiglass, displacement and infiltration could be observed throughout the experiment. An additional significant rationale for employing plexiglass is to reduce the resistance against friction along the sidewalls of the soil container. This allows for a more accurate approximation of plane strain conditions by utilizing a low friction surface along the container's sides.

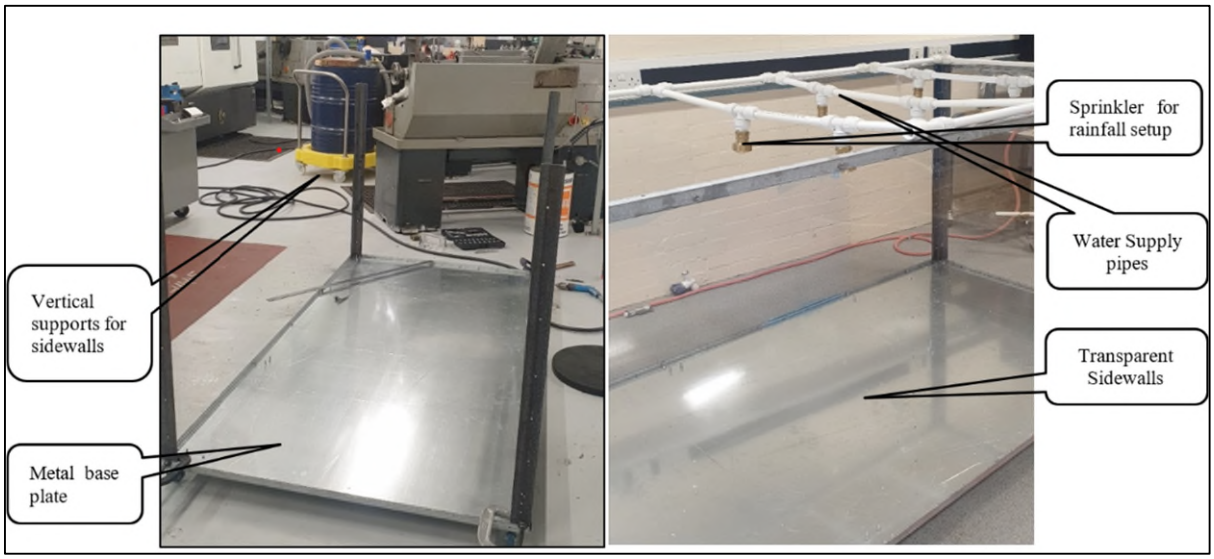

Figure 3.7: Experimental testing rig with a water supply and rainfall setup

3.4.2 Artificial Rainfall System

A specially designed sprinkler system was used to generate artificial rainfall, allowing for consistent and adjustable simulation of both intensity and duration. This system includes a main water supply, a water flow meter, sprinklers, and rainfall hoses. Figure 3.8 illustrates the arrangement of the sprinklers. The sprinklers, each with a diameter of 50mm, were organized into three rows, with three sprinklers per row. Each sprinkler effectively covered a circular area with a diameter of 300mm. This strategic arrangement ensured uniform water distribution across the designated area, enhancing the efficiency of the artificial rainfall system. By placing the sprinklers in a precise grid pattern, the system maximized coverage and allowed for accurate control over the simulated rainfall, thereby ensuring consistent and replicable experimental conditions. A similar kind of rainfall setup was designed and applied by various researchers (Suradi 2015; Ahmadi-Adli, 2014; Lirer 2012; El-Hazek et al. 2020; Oh and Lu, 2015; Malla and Dahal, 2021).In order to achieve uniform and consistent rainfall intensity, the main water supply valves (Figure 3.9) were used. Prior to commencing the experiment, the uniform rainfall intensity capability of each nozzle was regulated. To address the issue of uneven rainfall intensity from the nozzle, screw valves were used as a solution. To avoid potential water seepage between the primary water supply and the valve system, it is necessary to regulate the connection points. Teflon tape was used to prevent any water leakage.

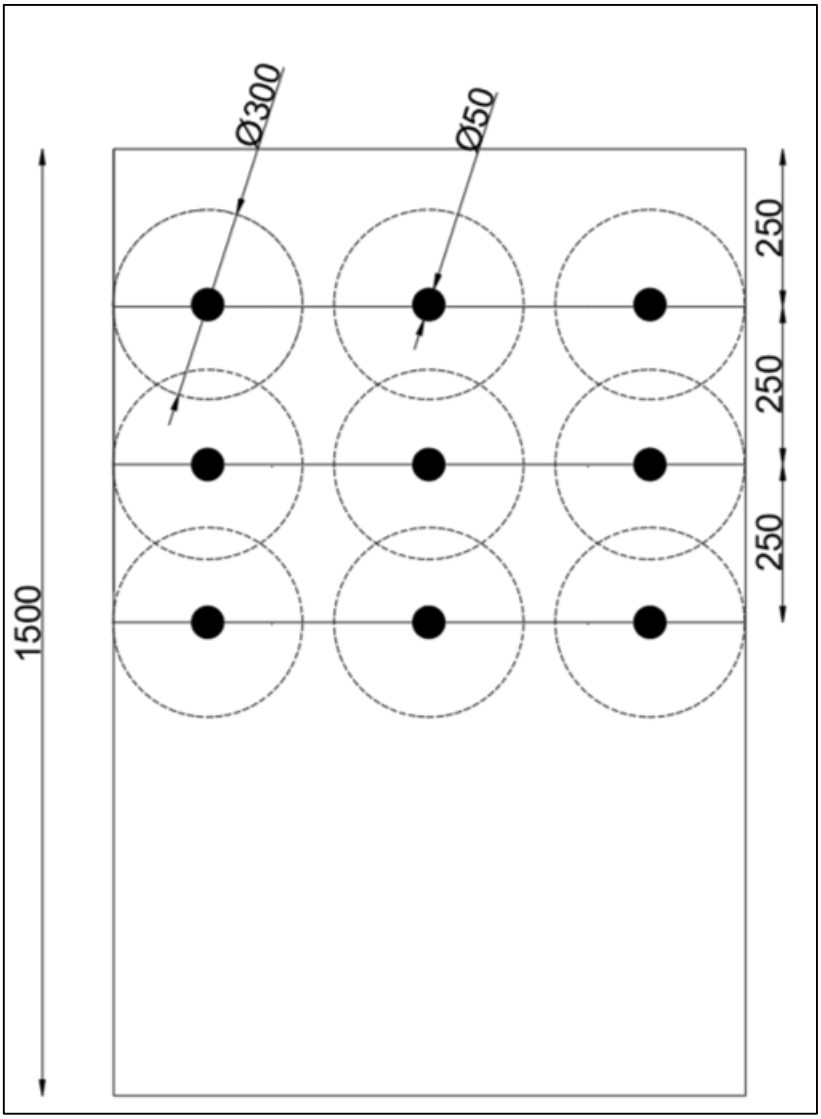

Figure 3.8: Schematic of Sprinkler setup and surface area coverage for slope

Figure 3.9: Main water supply valve (left) and flow meter (right) to record the water flow rate

Hoses and sprinklers were used to carry out the primary function of the artificial rainfall system. The system was built using PVC tubing with a diameter of 12.5 mm, and a basic frame was used to support the sprinklers above the soil container. The sprinkler frame consists of three rows, with each row containing three nozzles (Figure 3.10).

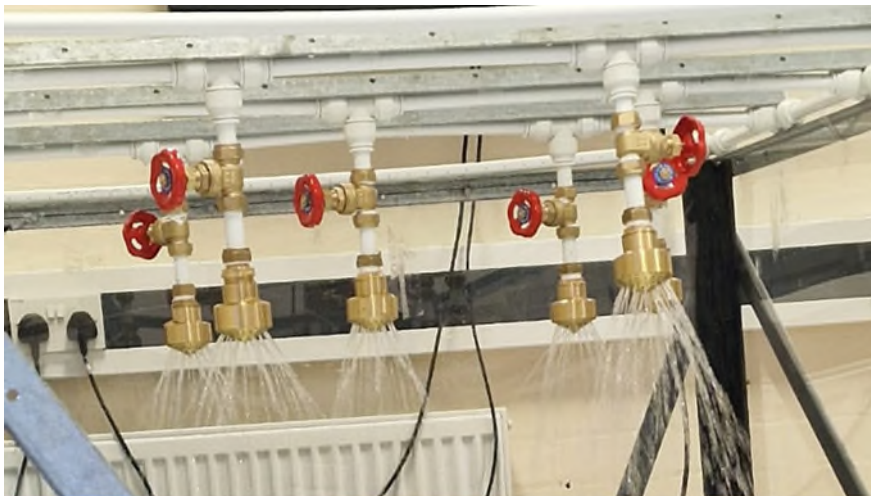

Figure 3.10: Rainfall hose and Sprinklers showing uniform rainfall activity

3.4.3 Slope Preparation

The most critical and sensitive phase in the entire experimental program was the preparation of the slope. The key requirement was to ensure an even distribution of soil material within the glass container or test rig while achieving a specified dry density. To meet this criterion, the procedure was carefully designed to involve layering the soil material in thicknesses exceeding 5cm and then compacting it to reach the desired density (Relative density, D_r, between 30% -

40%) by repeatedly tamping it on a steel plate (Suradi 2015; Day et al. 1999; Jing et al. 2019). Before conducting the actual tests, extensive trial and error experimentation was conducted to determine the optimal thickness for each deposition layer, the required number of drops, and the height of each drop necessary to achieve the specified density. Figure 3.11 depicts the process, illustrating the procedure of deposition of soil layers and compaction.

Figure 3.11: Compaction process of model slope

Figure 3.12: Model Slope after compaction

3.4.4 Instrumentation

The pore water pressure within the soil slope was measured using a vibrating wire piezometer, with a pressure measuring range up to 4000kPa, and the data was recorded using the GTech

Link datalogger (see Figure 3.13). Three different locations were selected (near the surface, middle of the slope, and near the bottom of the slope) to measure the pore water pressure.

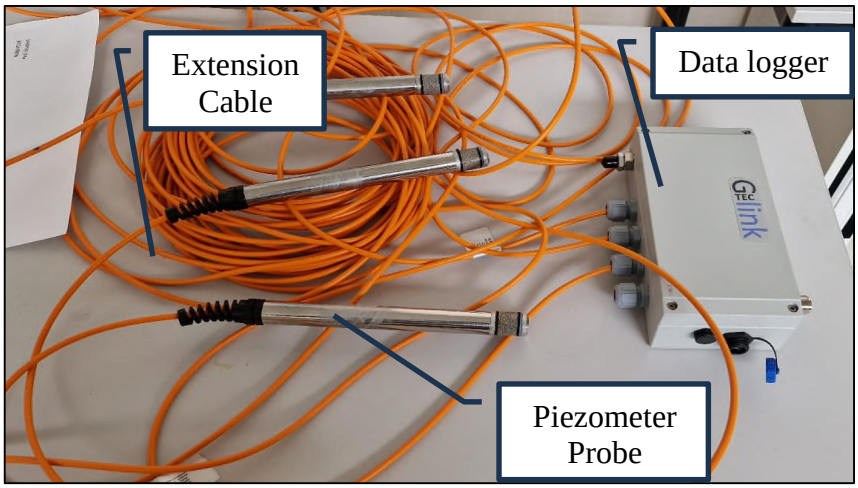

Figure 3.13: Piezometers used to measure the pore water pressure within the slope

3.4.5 Installation of Sand Piles

The replacement technique is used in the fabrication of sand columns. This procedure entails the installation of columns using a seamless steel pipe that is open at both ends, with an outside diameter of 37 mm and an interior diameter of 35 mm. The steel pipe was inserted into the slope surface with a gentle force until it reached the desired depth. To ensure that the pipe was straight, a steel weight attached to a string was lowered into the borehole to measure the alignment. To prevent disturbance to the surrounding soil and facilitate smooth penetration, the outer surface of the steel pipe was lightly greased. Soil removal was conducted at an increment of 50 mm depth at a time to minimize suction effects. A soil extruder was used to remove the soil from the steel pipe. Following each soil removal, the column material was systematically introduced into the hole from the top in 50 mm layers. This methodical approach ensured that the insertion and alignment of the steel pipe were precise and that the surrounding soil structure remained undisturbed. Once the borehole was prepared, sand was poured into it in successive layers, and compaction was achieved by employing a 1.25 kg circular steel tamper. This tamper was dropped from a height of 100 mm, delivering 15 blows on each layer to ensure uniform density. Careful attention was paid during compaction to prevent any lateral bulging that could disturb the surrounding soft clay, as illustrated in Figure 3.15. Figure 3.14 presents the

schematic of the sand pile location for the laboratory model. The sand piles were installed in a triangular pattern with center-to-center spacing of 3 times the diameter of the sand piles. Studies have shown that sand piles are more effective if the spacing between the piles is 3 to 5 times the diameter of the sand piles (Ambily and Gandhi, 2007; Naseer et al. 2019).

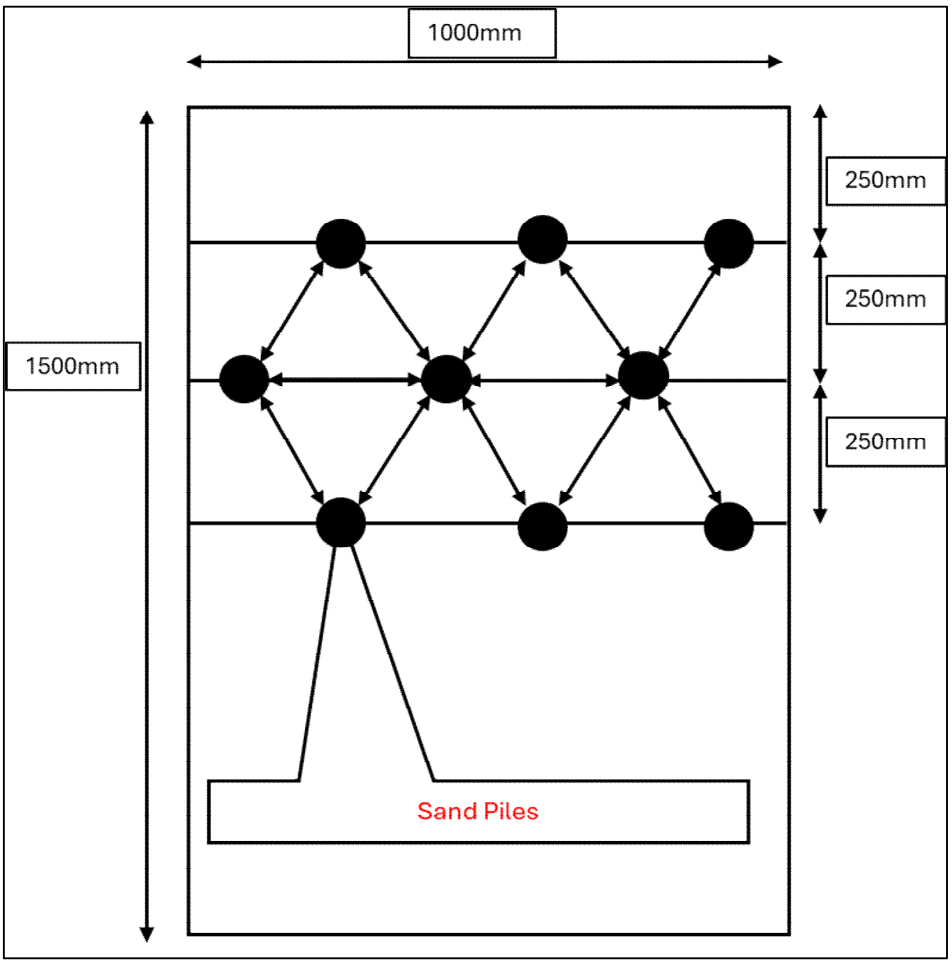

Figure 3.14: Schematic od Sand Piles location

(a) (b) (c)

Figure 3.15: Installation of Sand Piles (a) drilling of borehole, (b) sand compaction into the borehole, (c) Sand piles with Piezometers for pore water pressure measurement

3.5 Image Processing for Detection of Soil Movements

Upon completion of the experimental phase and the acquisition of necessary images, the subsequent step involves subjecting these images to processing to extract pertinent information or features. The images are classified into two categories: low displacement images and high displacement images, the latter containing information indicative of a potential failure of soil slope. Typically, raw images captured by cameras lack significant useful information.

3.5.1 Designing the Suggested ASPS Approach for Monitoring of Slope Movements/Failures

The proposed automated sensor and signal processing selection system (ASPS) for slope deformation/soil displacement builds upon the original ASPS approach, which was previously studied, designed, and validated by (Al-Habaibeh and Gindy, 2000). Addressing a noted gap in monitoring systems for slope failure, wherein existing solutions are typically based on either single techniques or multiple techniques without integration into a fusion system, the new ASPS approach employs a fusion of multiple sensors and cameras. This novel approach aims to extract the most informative Characteristic Features (CFs) to recognise the changes that happened during a rainfall event on a slope and identify deformations as a result of rainfall.

Following the preparation of images, the subsequent step involves subjecting them to advanced image processing techniques, including Fast Fourier Transform (FFT) and Discrete Wavelet Transform (DWT). These techniques are employed to extract the necessary features that facilitate a clear differentiation between the state of the monitored system before and after the occurrence of the event under investigation. The application of FFT and DWT enhances the discernibility of relevant characteristics in the images, aiding in the identification and classification of the system's status.

Upon processing the data, a mathematical approach, including linear regression or a simple calculation of percentage differences, along with statistical functions, is employed to distinguish between the two conditions: high deformation and low deformation in a slope. Statistical measures, including mean, standard deviation, maximum, minimum, and others, are utilized to quantify values for both conditions (Table 3-1). The magnitude of the slope or the percentage difference serves as the criterion for selecting sensitive features from the cameras. This feature indicates whether a camera can detect changes in the system's condition. Moreover, it guides the selection of the optimal image processing technique, as different techniques may yield varied results for the same image. The extracted features are ranked in ascending order based on sensitivity, forming groups referred to as systems. Artificial intelligence techniques, such as Neural Networks, are then applied to the collected information to determine the condition of the designed system.

Table 3-1: Statistical/Mathematical Equation used in image processing (Al-Habaibeh et al. 2024).

Definition	**Equation**
Max	$E_1 = \max(x_i)$
Min	$E_2 = \min(x_i)$
Mean	$E_3 = \frac{1}{n}\Sigma_{i-1}^{n} x_i$
STD	$E_4 = \sqrt{\frac{\Sigma_{i=1}^{n}(x, -E_3)^2}{n-1}}$
Absolute Mean	$E_5 = \left(\frac{1}{n}\sum_{i=1}^{n}\sqrt{\lfloor x_i \rfloor}\right)^2$
RMS	$E_6 = \sqrt{\frac{\sum_{i=1}^{n}(x_i)^2}{n}}$
Absolute Max	$E_7 = max\lfloor x_i \rfloor$
Variance	$E_8 = \frac{\sum_{i=1}^{n} s(n) - \left(\frac{1}{n}\sum_{i=1}^{n} s(n)\right)}{n-1}$
Skewness	$E_9 = \frac{\sum_{i=1}^{n}(x_i - E_3)^3}{(n-1)E_4^3}$
Kurtosis	$E_{10} = \frac{\sum_{i=1}^{n}(x_i - \lvert x \rvert)^4}{(n-1)E_2^4}$
RSS (Root sum of squares level)	$E_{11} = \sum_{i-1}^{n}(y_i - f(x_i))^2$
Covariance	$E_{12} = \sum_{i=1}^{n}\frac{(x_i - \lvert x \rvert)(y_i - \lvert y \rvert)}{n}$
IQR (interquartile range of time)	$E_{13} = Q_3 - Q_1$
Range (Range of radio wave propagation)	$E_{14} = E_1 - E_2$
Crest Factor	$E_{15} = \frac{E_7}{E_6}$
Clearance Factor	$E_{16} = \frac{E_7}{E_5}$

3.5.2 Linear Regression Analysis

Linear Regression Analysis is a mathematical method employed for modelling the relationship between dependent and independent variables. Linear regression of the extracted CFs serves as a quantitative measure of sensitivity. CFs with substantial changes in response to parameter variations yield higher linear regression values, categorizing them as highly sensitive CFs. Conversely, CFs with random or less pronounced changes result in lower linear regression values, classifying them as low-sensitive CFs. The slope value of the trend line further highlights this sensitivity assessment, with a higher slope indicative of higher sensitivity. Figure 3.16 and Figure 3.17 provide two examples, illustrating the extracted features and

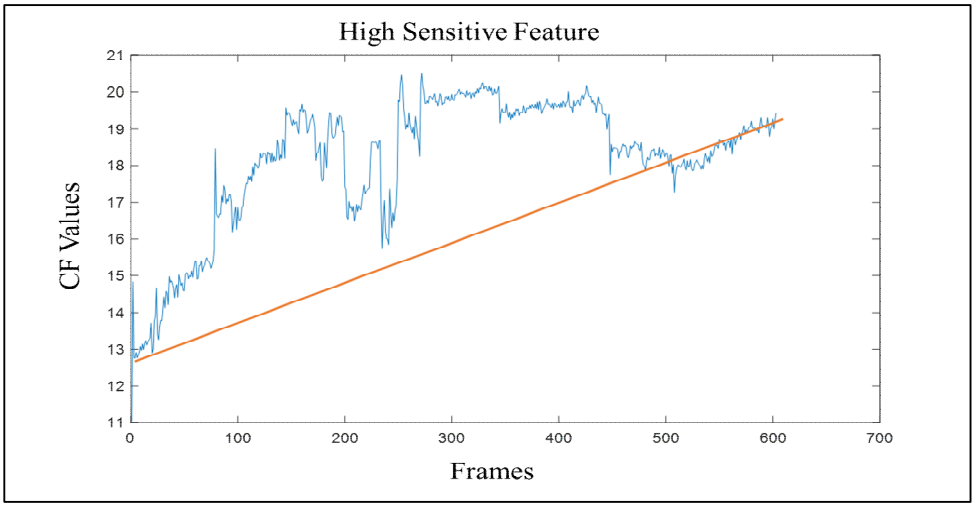

Figure 3.16: High Sensitive feature for soil movement detection

interpreting the concept of CF sensitivity from this study. Highly sensitive CFs, identified through their higher linear regression values and steeper slopes, play a pivotal role in the design and implementation of an effective monitoring system, serving as integral components within the fusion system for ongoing monitoring purposes. These frames were captured over the whole experiment (a total of 02 hours of continuous rainfall event).

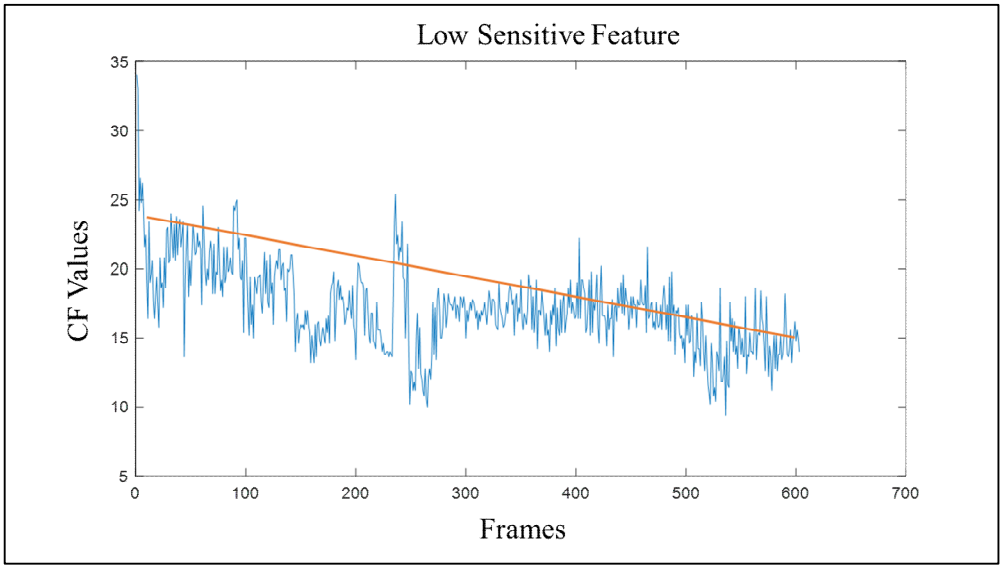

Figure 3.17: Low Sensitive feature for soil movement detection

The chosen Characteristic Features (CFs) are deemed highly sensitive when they yield higher slope values in response to changes in the system's condition. These features are derived from both raw and processed data, with the processing involving techniques such as Fast Fourier Transform (FFT) and Discrete Wavelet Transform (DWT). In essence, each set of images undergoes multiple methods for extracting useful features, encompassing various approaches for processing raw data. The utilization of FFT and DWT enables the extraction of distinctive features that enhance the system's ability to detect and respond to changes in the monitored conditions.

3.5.3 Use of Percentage in Calculating the Sensitivity (%)

The sensitivity of Characteristic Features (CFs) to changes in the monitored system's condition is quantified by assessing the difference in values between the old and new conditions. The sensitivity calculation involves determining the percentage difference (Δ) between the two situations. A higher percentage value indicates a higher sensitivity feature (CF). The percentage is computed by taking the absolute value of the difference and dividing it by the maximum difference. The equation below is utilized for this purpose. This methodology is precise in discerning the two conditions of the sample, providing normalized data that ranges from 0 to 1.

$$\Delta = Max - Min \qquad (3\text{-}5)$$

$$the\ percentage = |Max - Min| / Max\ diff \qquad (3\text{-}6)$$

The maximum difference in Equation (3-5) refers to the maximum distance between the two peaks of the samples. There are three distinct cases for calculating the maximum difference, each illustrated in the following figures. The first case pertains to situations where both samples of data are positive. In this instance, the maximum difference corresponds to the maximum value, as depicted in Figure 3.18.

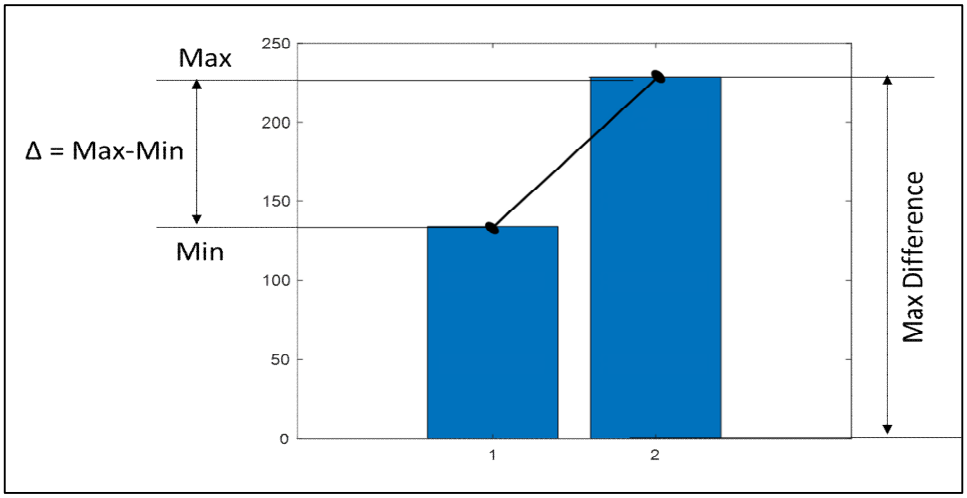

Figure 3.18: Maximum difference is equal to maximum value.

In the second case, where both samples are negative, the maximum difference is equal to the absolute minimum value, as illustrated in Figure 3.19.

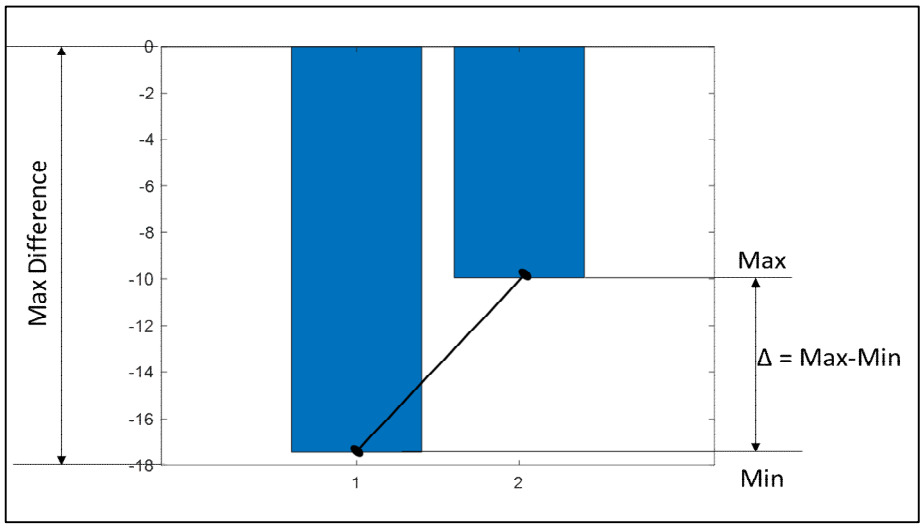

Figure 3.19: Maximum difference is equal to absolute minimum value.

In the third case, where two samples have different signs, the maximum difference is larger than both the maximum positive value and the absolute minimum negative value. It is equal to Δ, signifying that the percentage of difference is at its peak value and equals one. This scenario is depicted in Figure 3.20.

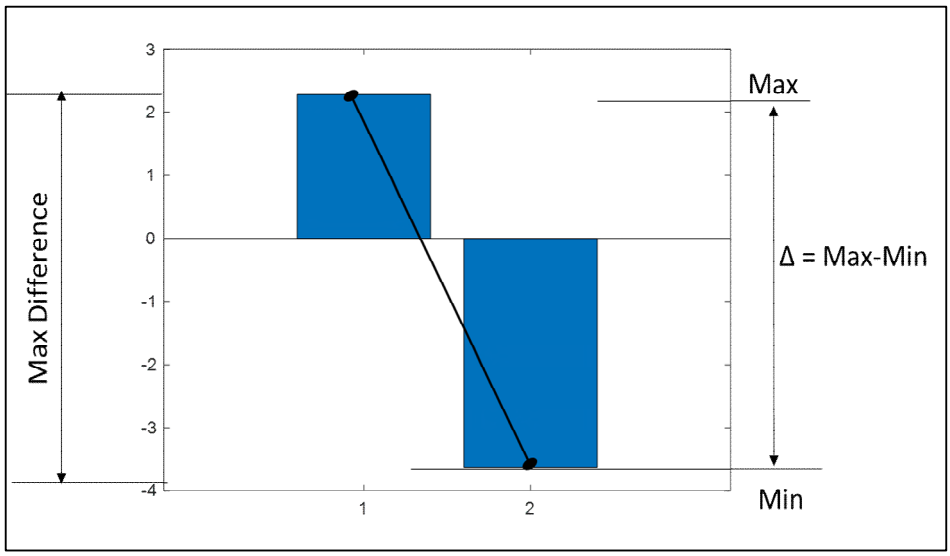

Figure 3.20: Maximum difference is equal to distance between the two peaks.

3.5.4 Image/Signal Processing Techniques

In the domain of image analysis and processing, the transformation of images is a fundamental step to facilitate their processing, thereby easing the extraction of valuable information. Signals are broadly categorized as either continuous or discrete and further distinguished based on whether they exist in the time or frequency domain. Fourier transform and wavelet transform emerge as pivotal tools in signal processing applications. These transforms play a crucial role in converting signals between time and frequency domains, enabling a more effective analysis and extraction of pertinent information from the signals under consideration.

3.5.4.1 Time Domain Analysis

Signals are typically captured and represented in the time domain, describing events over a specific period. However, time-domain signals often do not convey sufficient information, with crucial details concealed in the frequency domain (Ahadi and Bakhtiar, 2010). To extract features from a time domain signal, statistical analysis functions, including maximum,

minimum, mean, and standard deviation, are commonly employed. These statistical measures contribute to a more comprehensive understanding of the signal's characteristics and aid in revealing pertinent information embedded within the frequency spectrum.

3.5.4.2 Frequency Domain Analysis

The transformation of a signal from the time domain to the frequency domain is employed to reveal concealed information not readily apparent in the original time domain representation. When a real-world signal, or raw signal, undergoes this transformation, it manifests as a combination of multiple sine waves. In the frequency domain representation resulting from the raw signal, each sine wave is distinctly represented by a vertical line (Amit and Khalid, 2012).

3.5.4.3 Fourier Transform

The Fourier Transform, also known as Fourier Analysis, serves as a conversion technique that shifts a signal from the time domain to the frequency domain (Al-Habaibeh and Gindy, 2000). This transformative process restructures signals, organizing them based on their frequency values rather than representing them as a chronological sequence of temporal data. In contrast to the raw signals, which may exhibit unclear singularities, the Fourier Transform enhances clarity by presenting them in the frequency domain. The Fourier Transform can reveal variations in the amplitude of the frequency of specific singularities within the signal, serving as a valuable indicator of changes in system parameters. Such alterations may signify a transition from an intact system to a compromised system, as explored in the context of this research. Equations (3-7) and (3-8) describe the mathematical formulations for the Fourier Transform and the Inverse Fourier Transform, respectively (Heckbert 1995).

$$F(w) = \int_{-\infty}^{\infty} F(x) e^{-iwx} dx \qquad (3\text{-}7)$$

$$f(x) = \frac{1}{2\pi} \int_{-\infty}^{\infty} F(x) e^{iwx} dx \qquad (3\text{-}8)$$

3.5.4.4 Wavelet Transform

The Wavelet Transform (WT) involves the decomposition of a signal into multiple components characterized by distinct frequencies while retaining temporal information, thereby preserving crucial features that hold significance (Al-Habaibeh and Gindy, 2000). Functioning as a time-frequency analysis method (Ahadi and Bakhtiar, 2010), the Wavelet Transform is distinguished among time-frequency domain analysis techniques due to its proficiency in conducting multi-

scale analyses (Wang et al. 2013). The decomposition tree of the Wavelet Transform, as depicted in Figure 3.21, illustrates the iterative nature of signal decomposition, wherein each subsequent level mirrors the original signal's decomposition. This process can be inverted to reconstruct the signal. The approximation decomposition, termed low pass, utilizes a scaling function coefficient, while the detail decomposition, termed high pass, employs the wavelet function coefficient (Weeks and Bayoumi, 2003).

$$w(j,n) = \sum_{m=0}^{2n} \mathrm{w(j-1,m)}h(2n-m) \qquad (3\text{-}9)$$

$$w(j,n) = \sum_{m=0}^{2n} \mathrm{w(j-1,m)}g(2n-m) \qquad (3\text{-}10)$$

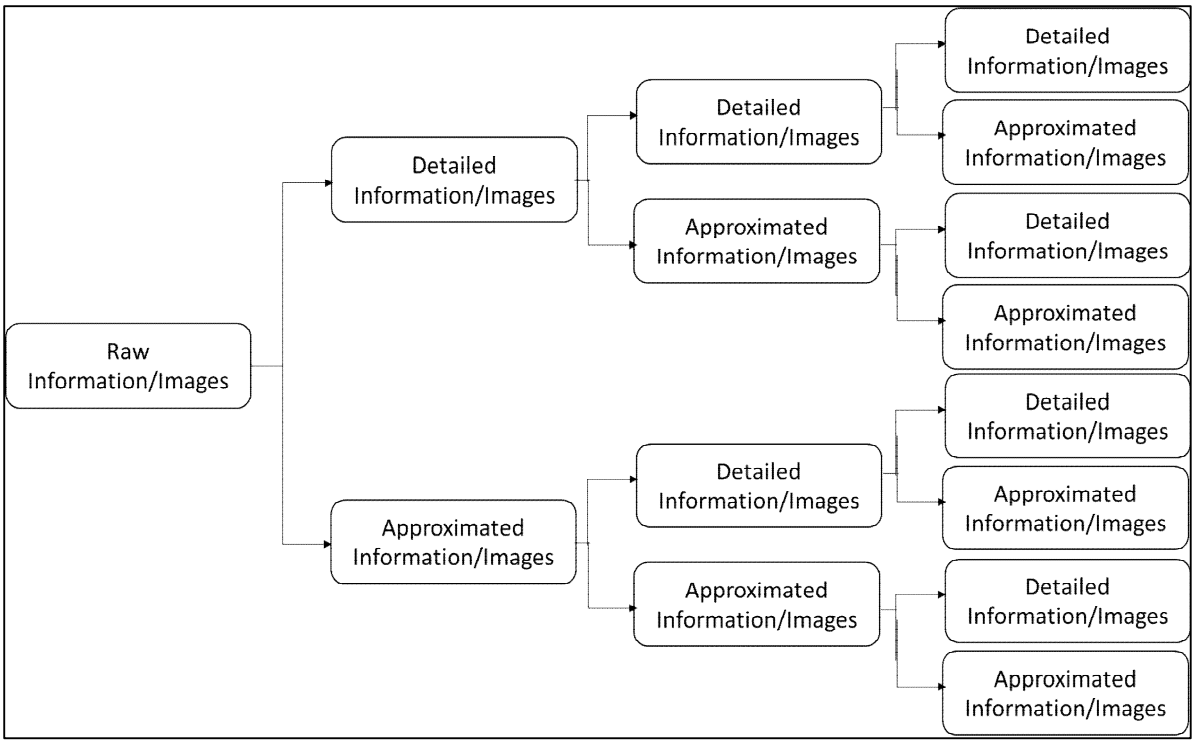

Figure 3.21: Decomposition Tree for Wavelet Transformation (Weeks and Bayoumi, 2003)

3.5.4.5 Image Processing

Image processing constitutes the investigation into the representation and manipulation of visual information (Martin and Tosunoglu, 2000). It involves the refinement, alteration, and transformation of images to extract information or features that may not be discernible in their original states. In the current research, various image processing techniques have been employed to enhance the visualization of images and facilitate the extraction of Characteristics Features (CFs). Matlab software, recognized for its efficiency in image processing, is utilized

for these processing tasks (Thielicke and Stamhuis, 2014). Figure 3.22 illustrates the overall approach used in this research.

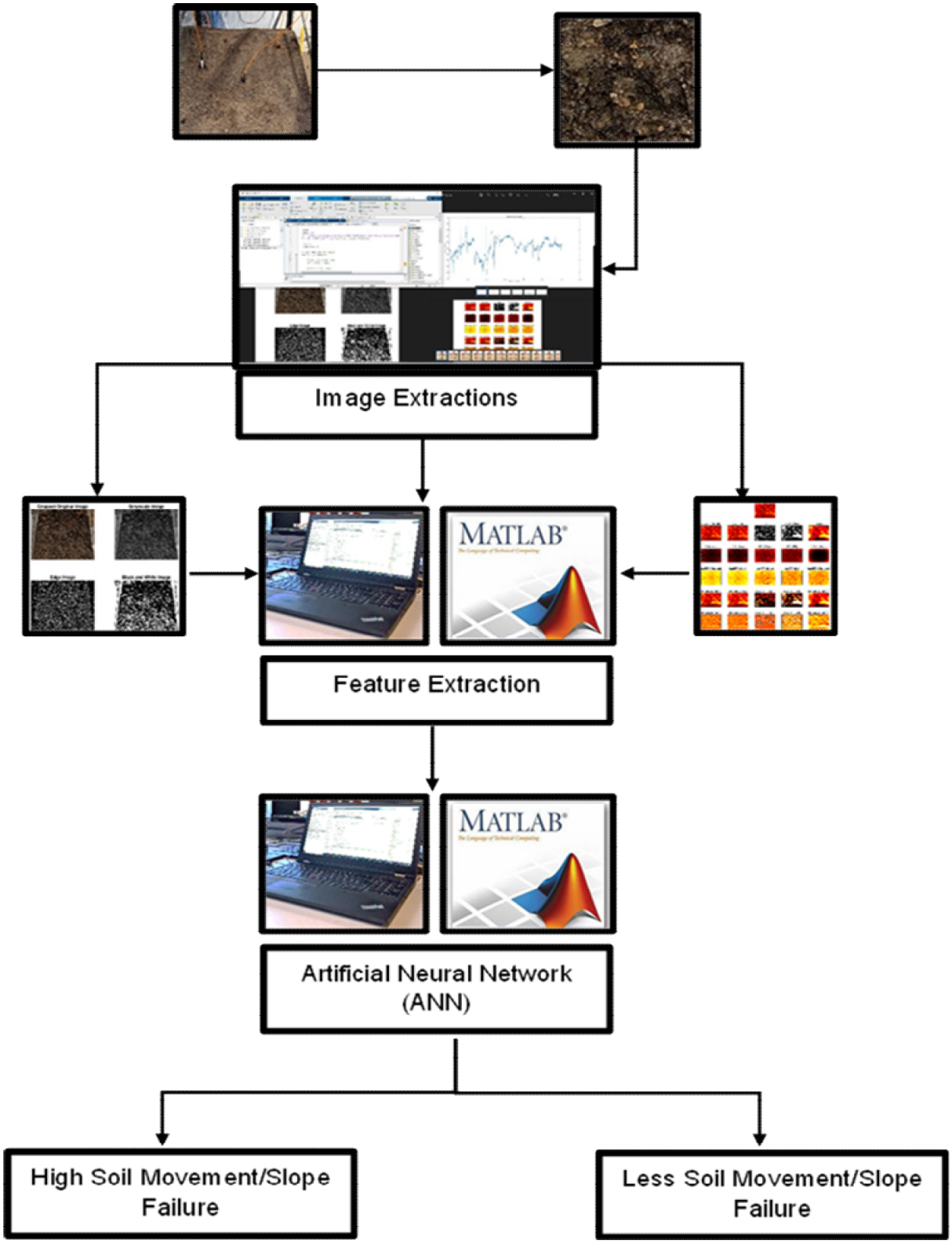

Figure 3.22: Schematic diagram for image processing to monitor the soil slope.

3.5.5 Artificial Neural Networks (ANN)

Computer scientists have perennially drawn inspiration from the human brain, specifically the biological neural network, observing its problem-solving capabilities (Romero et al. 2016). Artificial Neural Networks, commonly referred to as Neural Networks, represent an endeavour to replicate the information processing and problem-solving mechanisms of the human brain by establishing correlations through initial training objectives. This paradigm shift in programming development is rooted in the emulation of human cognitive processes (Bhattacharya and Solomatine, 2000). The conceptualization of neural networks stems from endeavours initiated over half a century ago, seeking to create artificial tools grounded in mathematical modules (Martin and Tosunoglu, 2000). Over the past three decades, the applicability of neural networks has proliferated across diverse domains, encompassing functions such as recognition, estimation, automation, prediction, and classification (Gerstner 1998).

Neural networks are specifically tailored to address tasks categorized as "easy for a human, difficult-for-a-machine" (Romero et al. 2016). They exhibit proficiency in handling intricate nonlinear data, accommodating missing information, and managing a substantial number of parameters. Notably, their inherent learning capacity enables self-adjustment to dynamic conditions and discernment of relationships among diverse parameters (Dolinsek et al. 1999). An appealing characteristic of neural networks lies in their reliance on training with existing data rather than conventional analytical models and statistical assumptions (Fadare and Ofidhe, 2009). Furthermore, their ability to learn is a distinctive attribute (Romero et al. 2016).

The neural network, functioning as an intelligent tool, discerns relationships within complex and nonlinear input data, generating outputs swiftly and accurately based on training (Fadare and Ofidhe, 2009). Numerous studies indicate that sophisticated data-driven tools, such as neural networks, yield significantly lower error rates compared to conventional methodologies (Bhattacharya and Solomatine, 2000). The adoption of neural networks not only expedites data processing but also proves cost-effective, contributing to enhanced quality (Al-Habaibeh and Parkin, 2004). The learning strategies within the network are categorized into several approaches (Romero et al. 2016).

3.5.5.1 Neural Networks Structure

Neural networks, in a broad sense, comprise essential components such as input layers, hidden layers, output layers, weights, and biases. Network configurations can range from simplicity, featuring a singular input layer, a solitary hidden layer, and a lone output layer, to complexity, involving multiple inputs, numerous hidden layers, and multiple outputs. The feedforward network, commonly employed with a single layer incorporating the sigmoid activation function, exemplifies a simpler architecture (Romero et al. 2016). Conversely, more intricate structures may involve various inputs, multiple hidden layers, and multiple outputs. Figure 3.23 illustrates one representing an artificial neural network configuration.

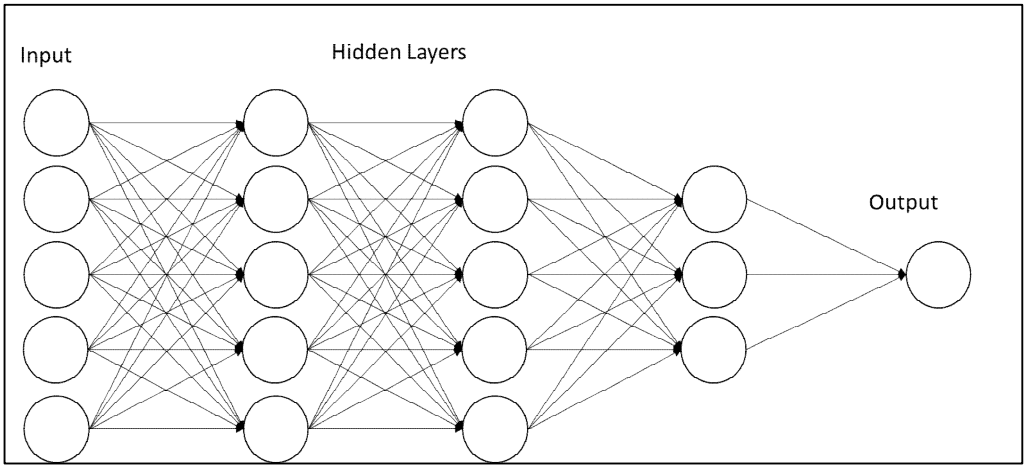

Figure 3.23: Structure of Artificial Neural Network (ANN)

3.6 Summary

This chapter provides an extensive overview of the methodology and procedures utilized in the current research. Commencing with a comprehensive explanation of laboratory-based soil testing, the aim was to ascertain the physical characteristics of the soil employed in this study. The primary focus of the investigation centred on slopes featuring fine soil, given their high susceptibility to failures resulting from rainfall infiltration when compared to slopes with coarser soils. Consequently, a series of index properties and classification tests for slope material and sand pile material were carried out at the Soil Mechanics Lab at NTU.

The subsequent phase delved into the determination of hydraulic and strength properties through various empirical calculations and correlations. The second section of this chapter explains the details of numerical modelling. The current study used the finite element analysis

tool PLAXIS 2D. This involved a detailed explanation of slope geometry, soil parameters, soil models, and the successive stages of calculations. The careful description of these aspects aimed to provide clarity and transparency in replicating the study and comprehending the distinctions of numerical simulations.

The third section unfolded the thorough process of designing and fabricating a test tank specifically fabricated for the slope model. The importance of this section lies in the critical role the test tank plays in replicating real-world conditions, ensuring the reliability and applicability of the ensuing results. Details pertaining to the construction materials, dimensions, and other relevant parameters were thoroughly expounded upon. In the final part of this chapter, the focus was on the methodologies and techniques employed for data collection and interpretation. Notably, a novel approach was introduced for processing images captured during laboratory-based experiments on a small-scale slope model. This innovative technique holds promise in enhancing the precision and depth of data analysis, potentially yielding novel insights into slope behaviour under different conditions.

CHAPTER 4: NUMERICAL MODELING OF SLOPES UNDER VARIOUS RAINFALL CONDITIONS

4.1 Introduction

This chapter presents the detailed procedure of modelling coupled flow-deformation analysis for slopes subjected to various rainfall durations and different intensities. Furthermore, results of finite element modelling of soil slope using the PLAXIS 2D tool are also presented. A coupled flow-deformation analysis was carried out, which allowed the slope model to simulate seepage and stability analysis simultaneously.

Figures 4.1 to 4.5 show the deformed mesh of the slope under rainfall infiltration of 60mm/hr lasting 24 hours, whereas Figures 4.6 to Figure 4.10 show the slip surfaces of the same slope. The gentle slope shows a deeper slip surface, while the steep slope fails with a shallow slip surface. The lower FOS was observed for higher slope angles, whilst the higher FOS was noted for less steep slopes. This is because the gravitational forces acting on the slope increase with the higher slope angle. As a result, the stresses applied to the slope become higher, which ultimately unstable the slope. The effect is particularly pronounced in steep slopes, where the soil is more likely to fail under the influence of gravity. Various researchers have reported that slope angle is a crucial parameter significantly influencing slope stability (Kayastha 2015; Wu et al. 2016; Çellek 2018; Alexakis et al. 2014; Shiferaw 2021b). A steep slope indicates high shear stress and a low safety factor for slope stability (Prodan et al. 2023; Shiferaw 2021b). This occurs because, as the slope increases, tangential stress in the clluvium and the residual or consolidated soil covering rises while axial tension decreases. Consequently, while shearing strength increases on steep slopes, overall stability deteriorates. Figure 4.11 to Figure 4.14 show the matric suction contours for the slope subjected to various rainfall intensities and duration with a slope angle of 25 degrees. It can be seen that there is a significant decrease in matric suction with prolonged and highly intense rainfall events. The analysis shows that matric suction rapidly decreases in the area close to the surface, and with the downward advance of the wetting front, the surface eventually vanishes. The decrease in matric suction due to rainfall infiltration and its impact on slope stability is well understood. Numerous studies have been conducted in this area of research (Fredlund 2006; Brooks 1965; Bao et al. 1998; Gavin and Xue, 2008; Shin et al. 2013; Rahardjo et al. 2010). These studies provide valuable insights into the infiltration of rainfall in saturated and unsaturated slopes and the mechanisms that lead to instability.

Mahmood et al. (2013) reported that geotechnical properties such as hydraulic conductivity and matric suction significantly influence the rate of infiltration, runoff, and the increase in pore-water pressure within the slope, which constitutes the hydrological response. Additionally, these properties affect the volume change, the rate of shear strength decrease, and the variation in the factor of safety during rainfall events, representing the geotechnical response

4.2 Slope Mesh Deformation Contours for Different Models with Varying Slope Angles

Figures 4.1 to 4.5**Error! Reference source not found.** shows the typical deformation contours f or 6mm/hr rainfall lasting for 24 hours with different slope angles. For gentle slopes, the deformed mesh shows slight vertical displacement with some lateral spread. The deformation is more uniform across the slope surface. However, in steeper slopes, the mesh shows more pronounced vertical displacement and localized lateral movement, especially in the middle to upper portions of the slope. The deformation often starts at the top and progresses downwards, with large sections of the slope potentially moving as a block. Studies such as those by Lin et al. (2016) and Wang et al. (2022) have used model tests and numerical simulations to analyze these effects, demonstrating that higher slope angles lead to greater instability and more significant deformation due to increased shear stress and pore water pressure from rainfall infiltration. Additionally, the work by Oh and Lu (2015b) and Chen and Wu (2018) supports these findings, showing that steeper slopes are more susceptible to deep rotational slides and other catastrophic failures under heavy rainfall conditions.

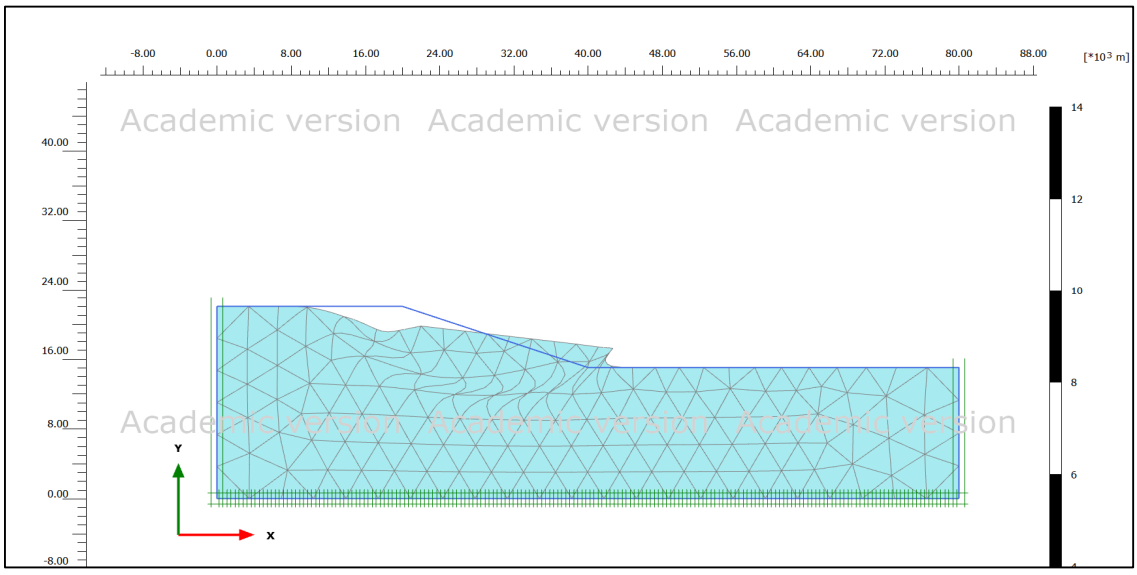

Figure 4.1: Deformed Mesh for rainfall infiltration of 60mm/hr lasting for 24hours and α = 25°

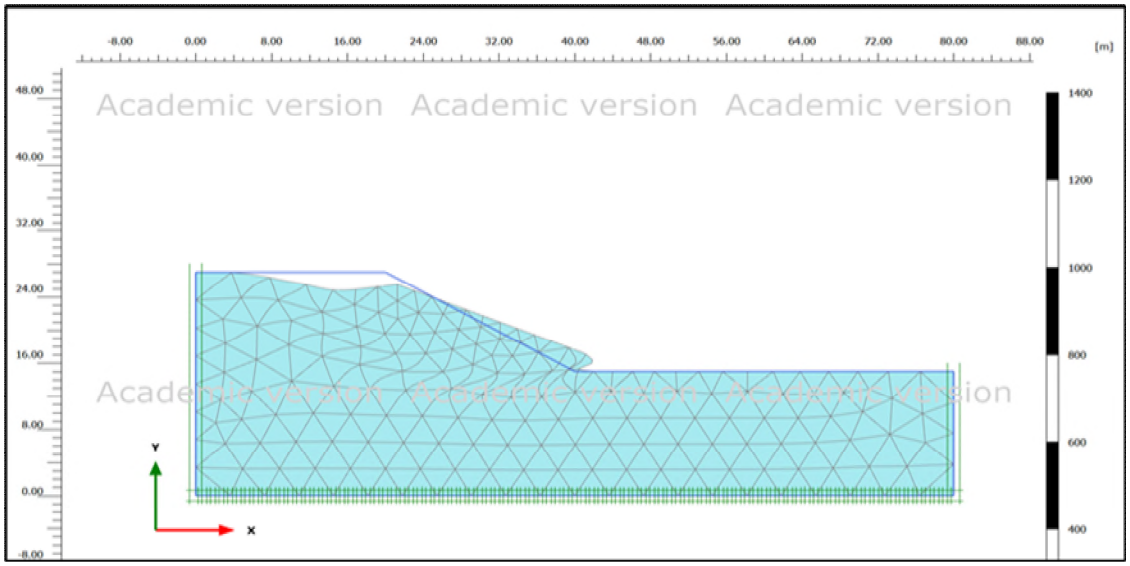

Figure 4.2: Deformed Mesh for rainfall infiltration of 60mm/hr lasting for 24hours and α = 30°

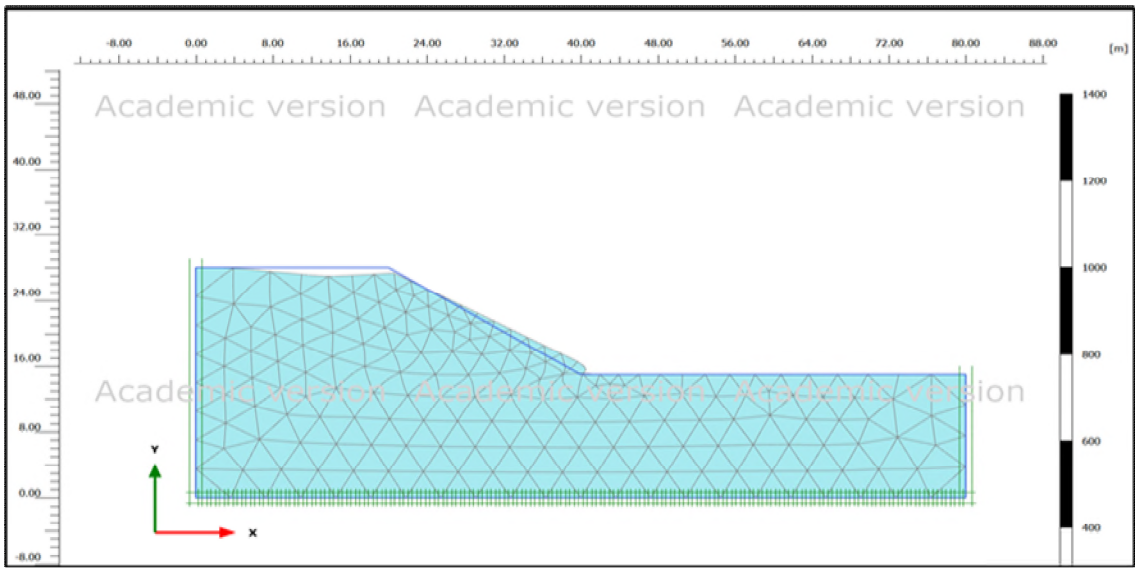

Figure 4.3: Deformed Mesh for rainfall infiltration of 60mm/hr lasting for 24 hours and α = 35°

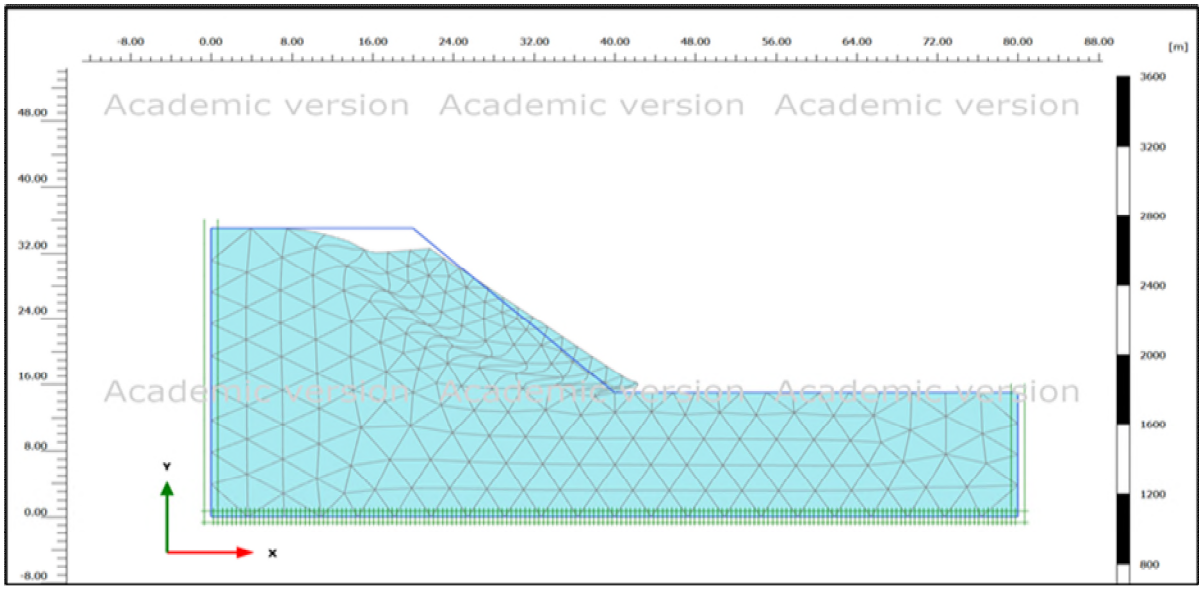

Figure 4.4: Deformed Mesh for rainfall infiltration of 60mm/hr lasting for 24 hours and α = 45°

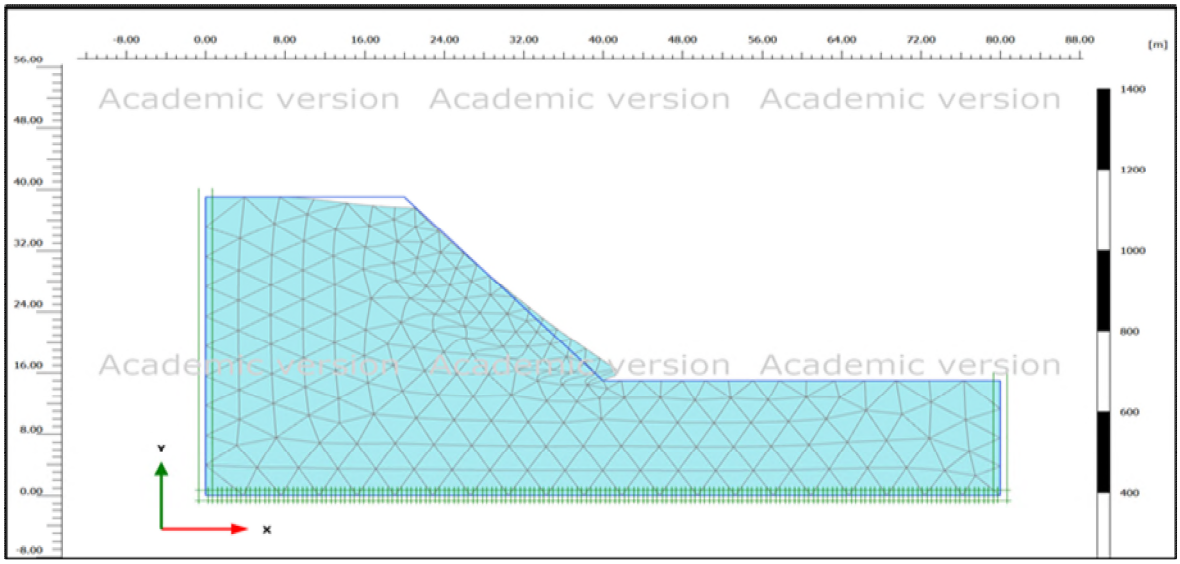

Figure 4.5: Deformed Mesh for rainfall infiltration of 60mm/hr lasting for 24 hours and α = 50°

4.3 Slip Surface Contours for Unreinforced Slope Models

Figures 4.6 to 4.10 illustrate the slip surface contours for unreinforced slope models with varying slope angles and 60mm/hr rainfall events lasting for 24 hours. The slip surface behaviour for gentle and steeper slopes under rainfall infiltration varies due to differences in soil saturation, shear stress distribution, and infiltration dynamics. In gentle slopes, rainfall has more time to infiltrate into the soil, leading to a reduction in shear strength at greater depths and resulting in deeper slip surfaces. This is because the longer infiltration period allows water

to penetrate further into the slope, increasing pore water pressure and reducing soil stability at deeper levels. Studies by Di et al. (2021) and Dong et al. (2017) confirm that gentle slopes tend to experience deeper slip surfaces due to prolonged infiltration times. In contrast, steeper slopes have shorter ponding times as most of the rainfall water quickly converts to surface runoff, limiting the amount of water that infiltrates the slope. This results in a reduction of shear strength, primarily at shallower depths, creating shallower slip surfaces. The rapid runoff and reduced infiltration depth in steeper slopes lead to quicker saturation near the surface, triggering shallow landslides. Oh and Lu (2015b) and Chen and Wu (2018) have demonstrated that steeper slopes are more prone to shallow slip surfaces due to these conditions.

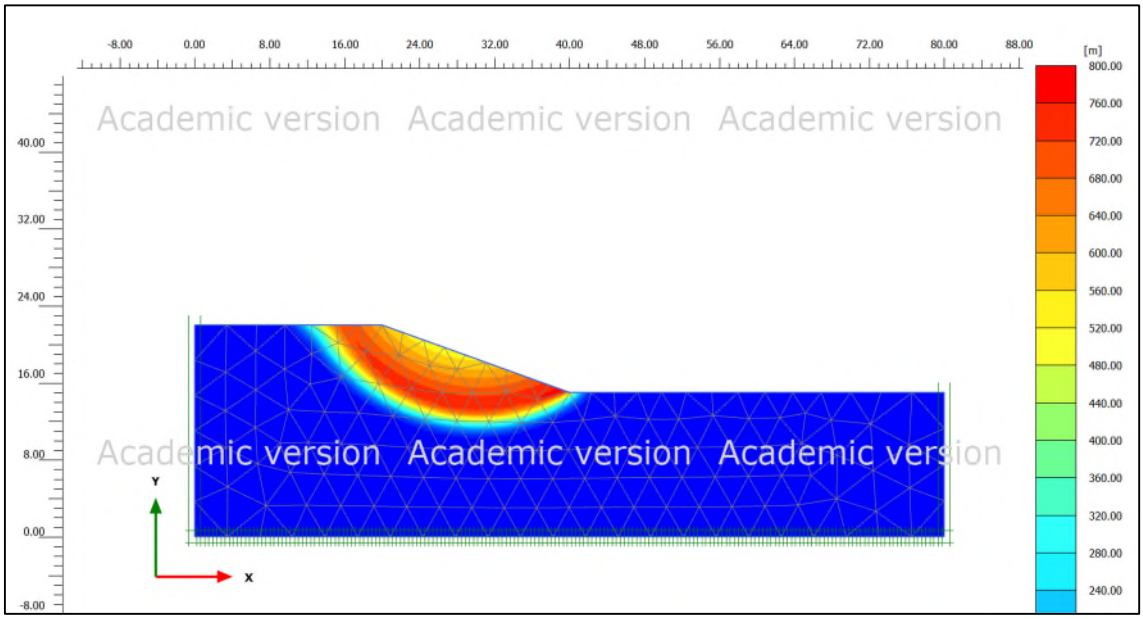

Figure 4.6: Slip surface of unreinforced slope against rainfall infiltration of 60mm/hr lasting for 24 hours and $\alpha = 25°$

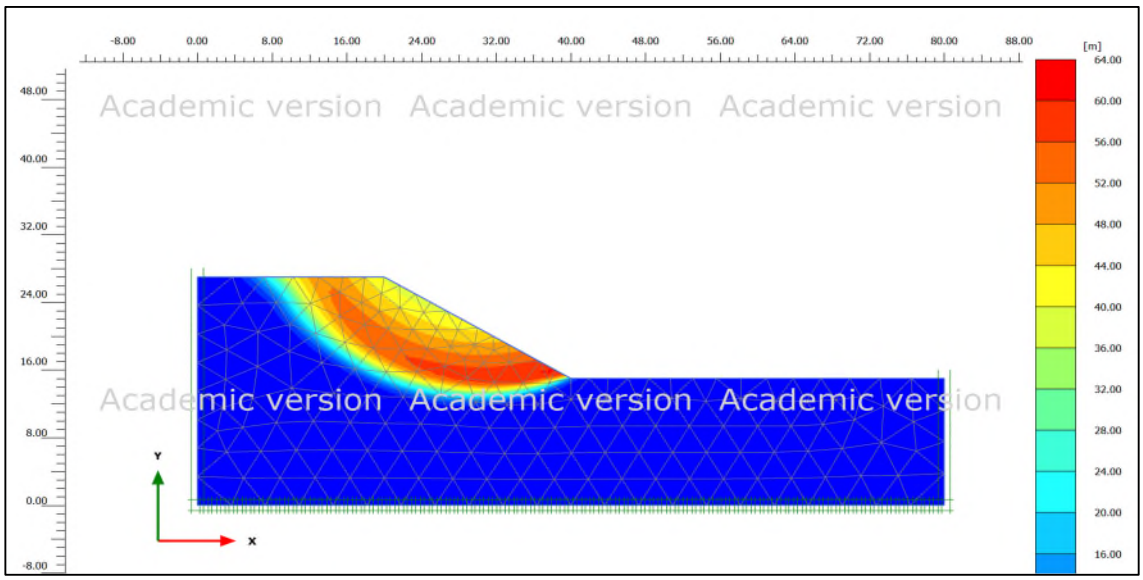

Figure 4.7: Slip surface of unreinforced slope against rainfall infiltration of 60mm/hr lasting for 24hours and α = 30°

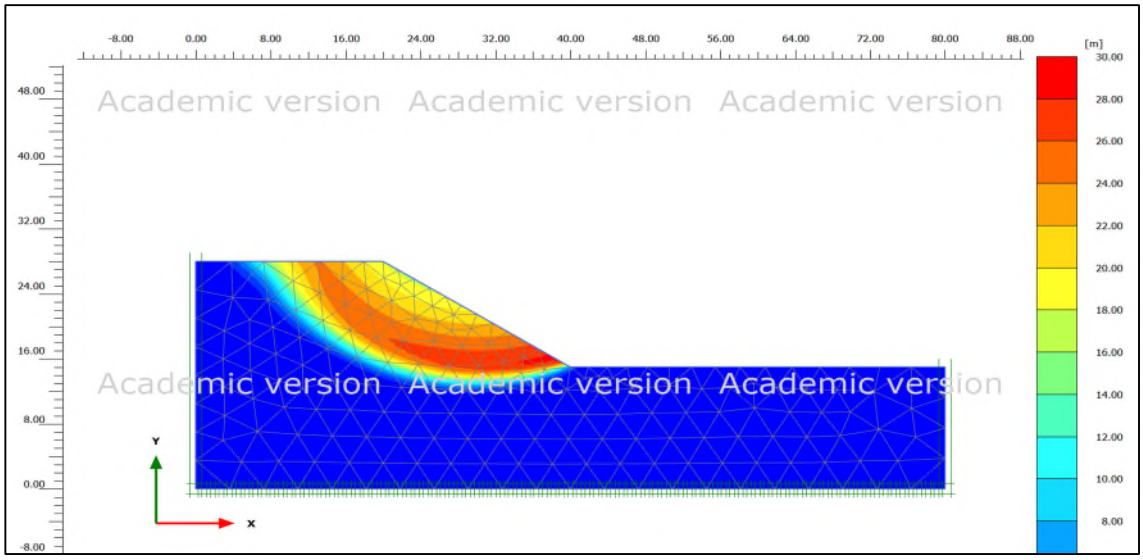

Figure 4.8: Slip surface of unreinforced slope against rainfall infiltration of 60mm/hr lasting for 24hours and α = 35°

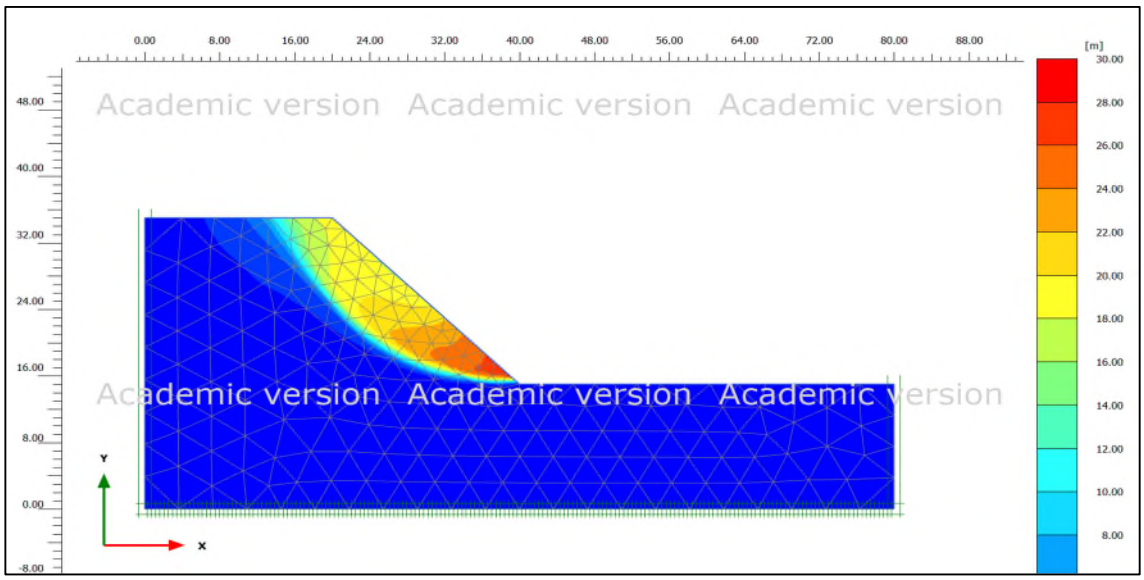

Figure 4.9: Slip surface of unreinforced slope against rainfall infiltration of 60mm/hr lasting for 24 hours and α = 45°

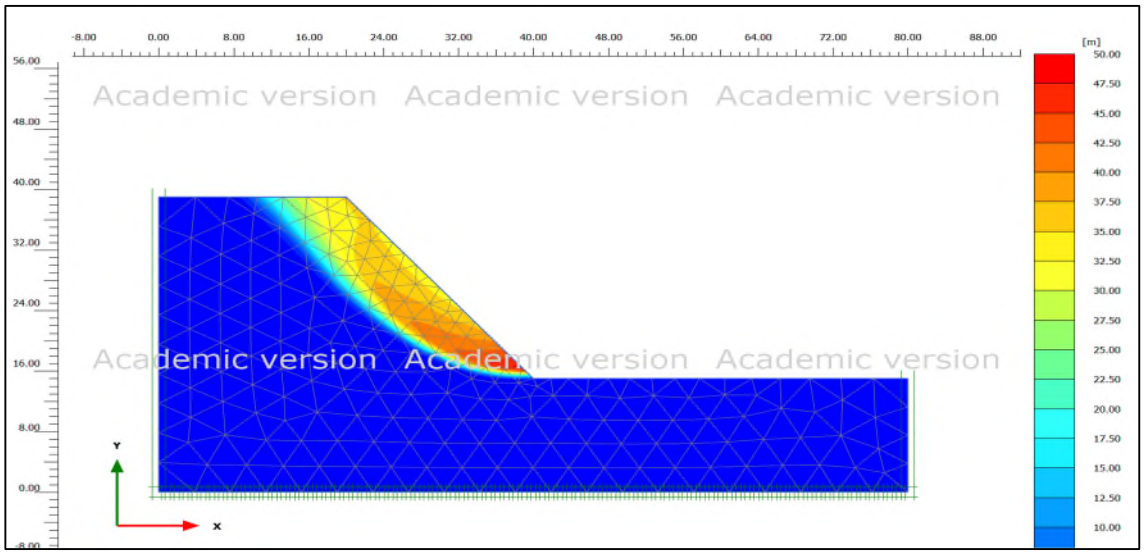

Figure 4.10: Slip surface of unreinforced slope against rainfall infiltration of 60mm/hr lasting for 24 hours and α = 50°

4.4 Matric Suction Contours for Different Rainfall Intensities

Figure 4.11 to Figure 4.14 presents the matric suction contours for different rainfall intensities lasting for 24 hours for a 25^{o} slope. Matric suction decreases as rainfall intensity increases due to the rapid infiltration and subsequent saturation of the soil pores. High-intensity rainfall leads to a quick rise in pore water pressure, thereby reducing the matric suction and weakening the soil structure. This reduction in matric suction lowers the shear strength of unsaturated soils, making them more susceptible to landslides and other forms of slope instability. Studies by Lu

and Godt (2013) and Lu et al. (2013) have shown that intense rainfall events can drastically diminish matric suction, triggering slope failures. Additionally, Rahardjo et al. (2005) demonstrated through field experiments that higher rainfall intensities lead to faster reductions in matric suction, significantly impacting the stability of slopes composed of unsaturated soils

.

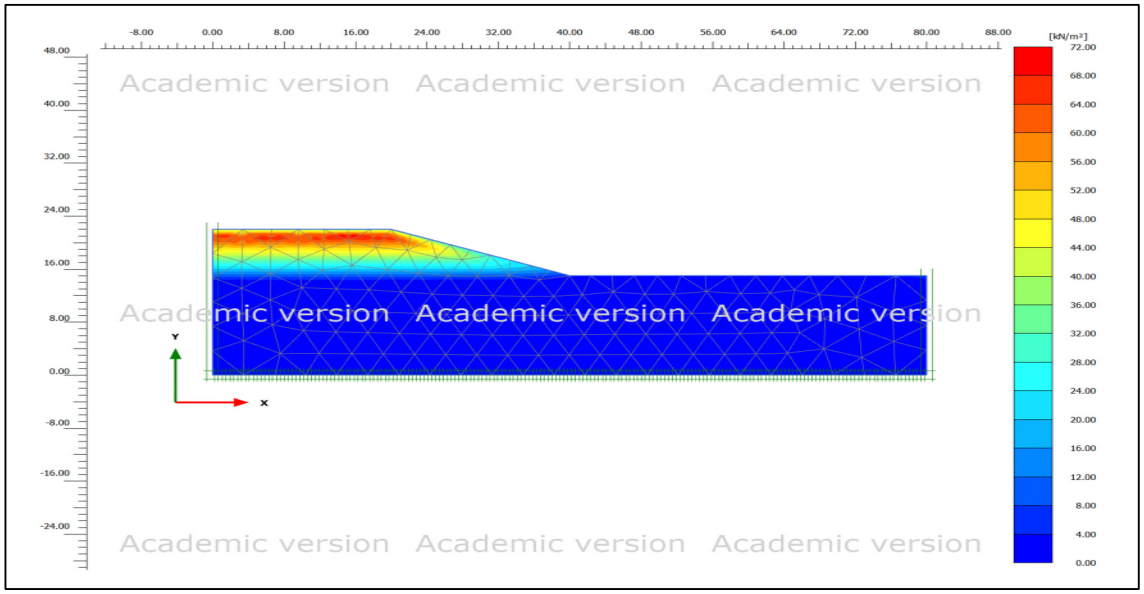

Figure 4.11: Matric suction contours for 10mm/hr rainfall intensity lasting for 01 hour and α = 25°

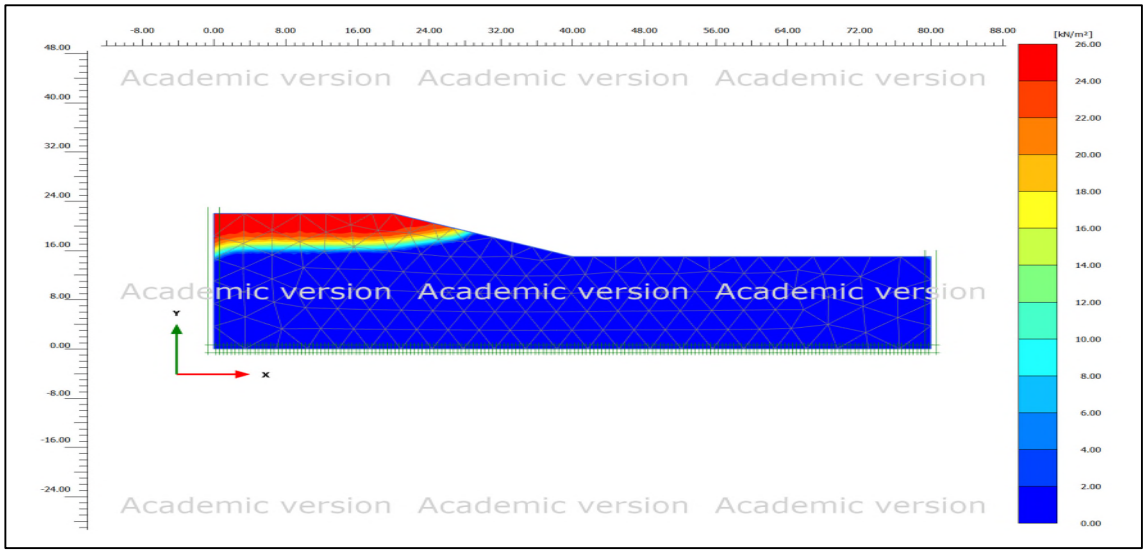

Figure 4.12: Matric suction contours for 10mm/hr rainfall intensity lasting for 24 hours and α = 25°

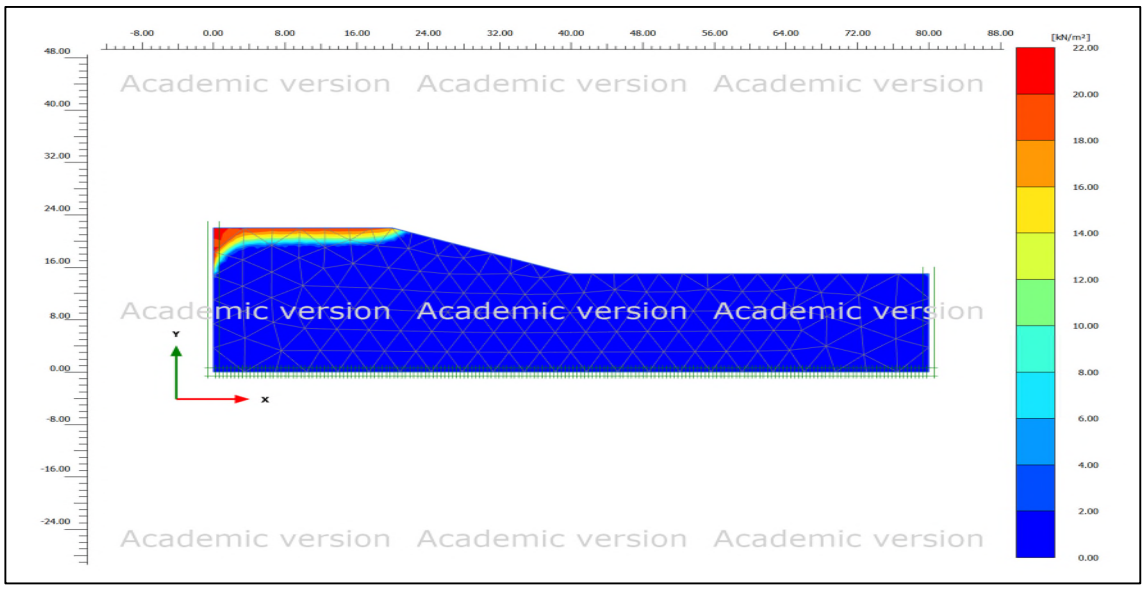

Figure 4.13: Matric suction contours for 20mm/hr rainfall intensity lasting for 24 hours and α = 25°

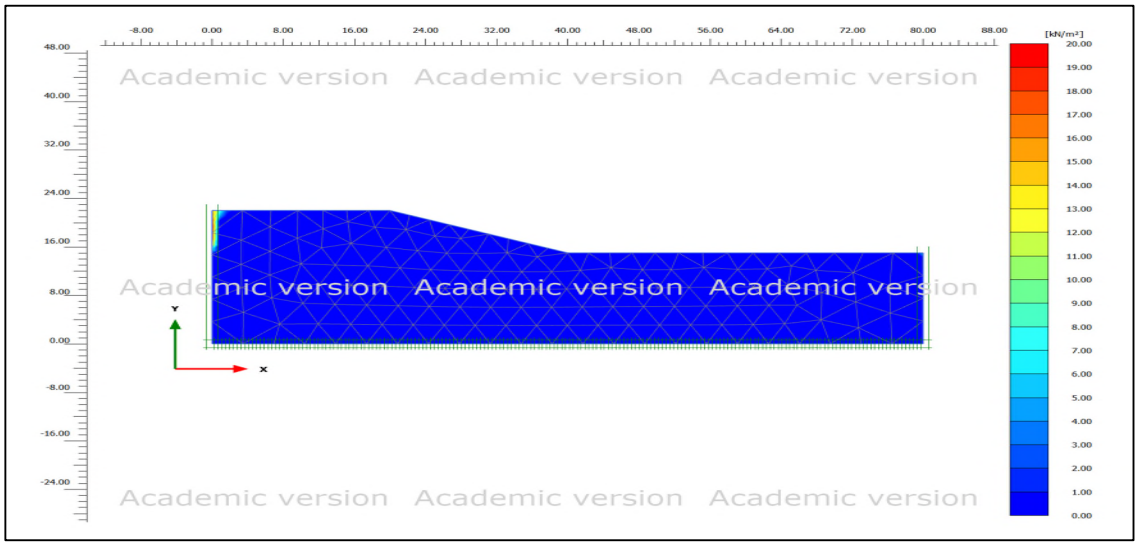

Figure 4.14: Matric suction contours for 60mm/hr rainfall intensity lasting for 24 hours and α = 25°

4.5 Deformation of Slope Contours for Unreinforced Slope

Figure 4.15 to Figure 4.16 present the deformation contours of the slope for different rainfall events but with the same slope angle. Deformation contours of a slope, which represent the displacement or strain within the slope material, vary significantly with higher intensities of rainfall events. As rainfall intensity increases, the infiltration of water into the slope's soil or rock material enhances, leading to a rise in pore water pressure. This elevated pore water pressure reduces the effective stress within the slope, thereby reducing its shear strength and increasing the likelihood of deformation (Wang et al. 2022; Chen and Wu, 2018).

Consequently, the deformation contours show more pronounced displacement gradients and more extensive areas of deformation. These contours likely indicate greater movement near the slope's surface and toe, where the water infiltration is most concentrated. In extreme cases, intense rainfall can lead to the formation of new deformation zones or the expansion of existing ones, resulting in significant slope instability or even landslides. Thus, higher rainfall intensities directly correlate with more severe and widespread deformation within a slope, as depicted by the deformation contours (Li et al. 2017; Soga et al. 2016).

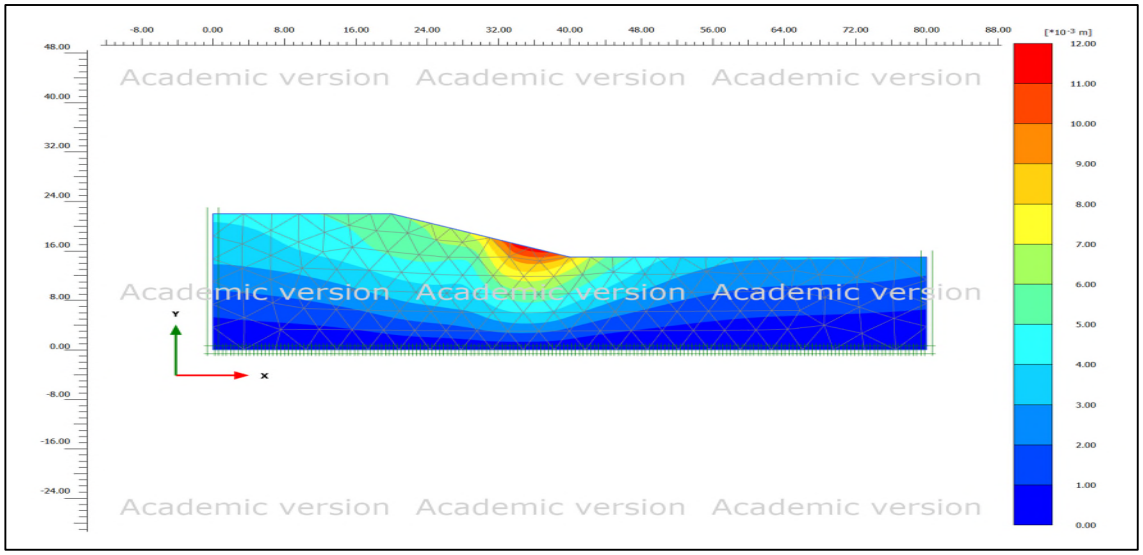

Figure 4.15: Deformation contours in slope subjected to 10mm/hr rainfall intensity lasting for 24 hours and α = 25°

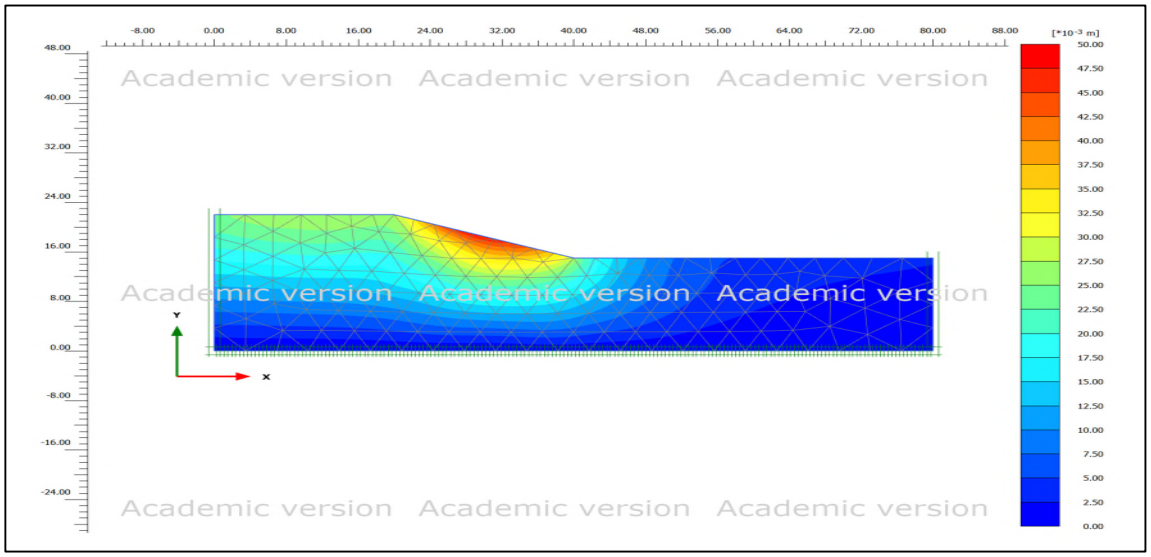

Figure 4.16: Deformation contours in slope subjected to 90mm/hr rainfall intensity lasting for 24 hours and α = 25°

4.6 Results and Discussions of Finite Element Analysis

Figure 4.17 to Figure 4.21 presents the factor of safety (FOS) for different slopes (i.e. slope angles of 25, 30, 35, 45, 50, and 55 degrees) for 10mm/hr. 20mm/hr, 60mm/hr and 90mm/hr rainfall infiltration, respectively, lasting for 01 hours, 06 hours, 12 hours, 24 hours and 48 hours. It can be easily seen that there is a significant reduction in FOS with higher slope angle, for longer duration of rainfall events and for high amounts of infiltration. Further discussion and explanation are presented in the following sections.

4.6.1 Effect of Rainfall Intensity on Slope Instability

Rainfall intensity directly governs the pace at which the factor of safety (FOS) decreases in slope stability. Increasing the magnitudes of the forces applied to the slope results in a more rapid decrease in the FOS during analysis. Nevertheless, when the intensity of rainfall exceeds the saturated hydraulic conductivity (Ks) of the top layer of soil, a fraction of the rainfall converts into runoff, leading to a decrease in infiltration. An investigation was conducted on a situation characterised by a consistent pattern of rainfall, where the intensity of rainfall varied throughout a range of values, including low (e.g., 10mm/hr), moderate (e.g., 20mm/hr), high (e.g., 60mm/hr), and very high (e.g., 90mm/hr) intensities.

The results show that rainfall intensities around the value of saturated hydraulic conductivity (Ks = 60mm/hr) had a stronger influence on instability. The FOS experiences a considerable decline until a rainfall intensity of 60mm/hr, after which any increases in rainfall intensity do not result in a significant reduction of the FOS. This may be due to the lack of any new infiltration into the slope. When rainfall intensity exceeds 60mm/hr, the main outcome is an increase in runoff. Similarly, a small drop in rainfall intensity has only a minimal impact on the FOS since the less intense rainfall is unable to fully penetrate and reduce the matric suction of the topsoil to a critical level. If the length of rainfall is sufficiently long, low-intensity rainfall might cause slope instability in some instances. Nevertheless, the infiltration via slopes with high hydraulic conductivity has little impact on slope stability. During such occurrences, precipitation easily seeps into the soil because of its porous composition, resulting in little change in suction pressure. During periods of light rainfall, the rates of infiltration and drainage are balanced. The infiltration of precipitation into the soil slope is the determining factor in its saturation level and susceptibility to failure. Figure 4.17 shows the low-intensity rainfall event (I = 10mm/hr) for different durations and different slope angles. The minimum FOS was observed as 1.45 for a 55-degree slope with rainfall events lasting for 48 hours, which is a 62%

reduction in FOS as compared to the slope without rainfall infiltration. Furthermore, only a 0.13% reduction in FOS was observed after 01 hours of rainfall event, which is negligible. Also, approximately a 13% reduction in FOS is observed against rainfall lasting for 24 hours.

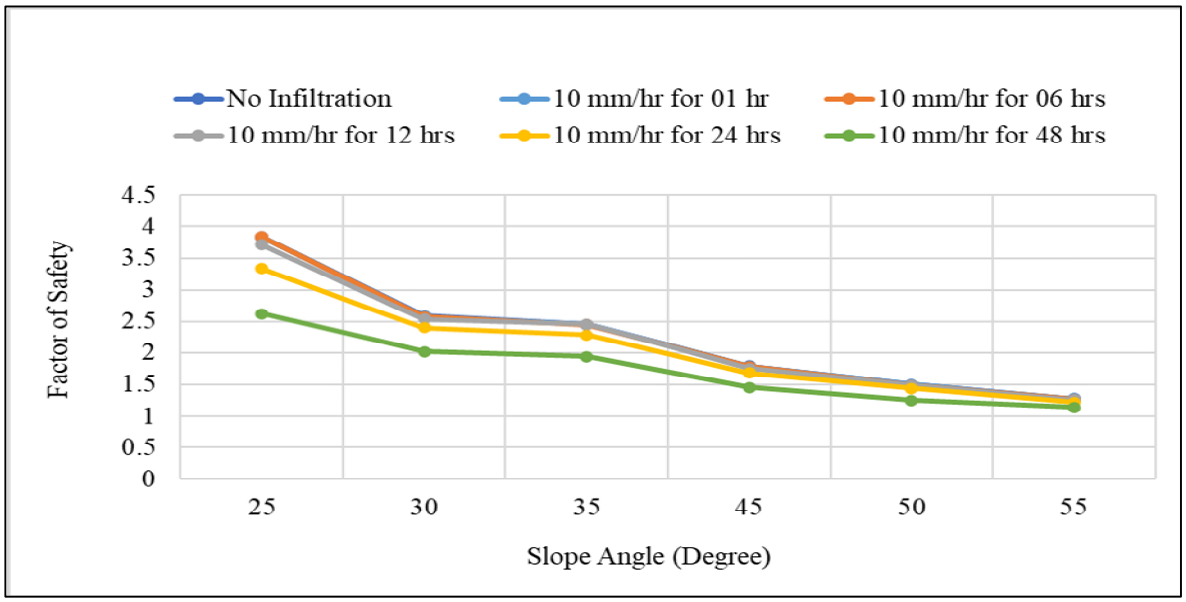

Figure 4.17: Factor of Safety for slope with different slope angles and rainfall durations of 10mm/hr infiltration

Figure 4.18 shows the FOS for different soil slopes subjected to 20mm/hr rainfall events lasting for different durations between 01 hours to 48 hours. It is observed that FOS decreased by 31% against the 20mm/hr rainfall infiltration lasting for 24 hours., while a 36% reduction was observed after 48 hours. The percentage of FOS reduction after 24 hours is higher due to the higher rainfall intensity. Figure 4.19 depicts the FOS for soil slopes subjected to a 60mm/hr rainfall event lasting for 01 hours up to 48 hours. An almost 36% decrease in FOS was observed for rainfall events lasting for 24 hours and the same for 48 hours, which indicates the full saturation of the slope and there is no further infiltration into the soil.

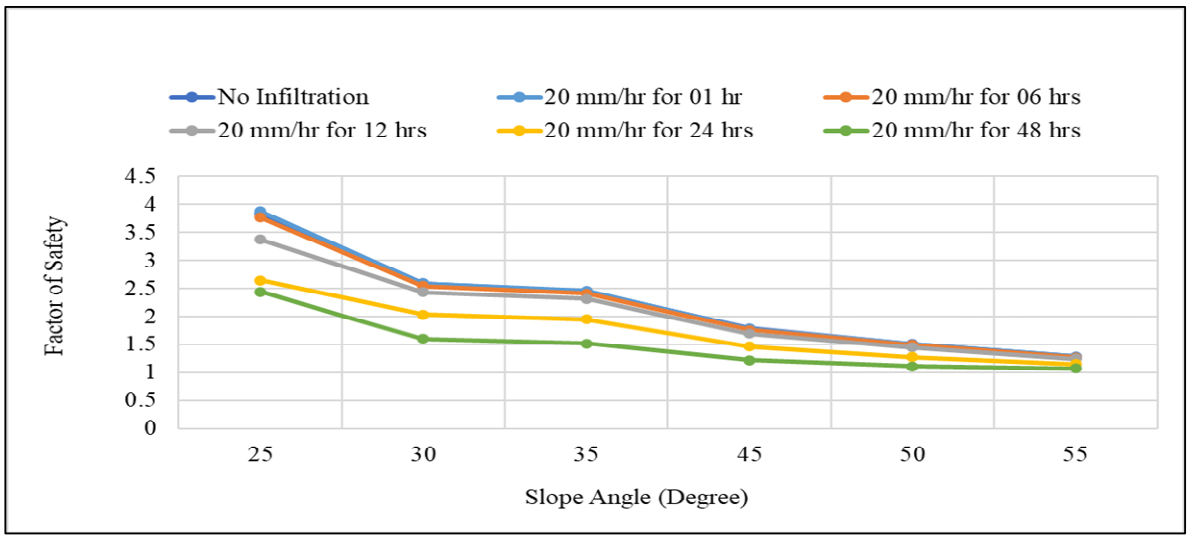

Figure 4.18: Factor of Safety for slope with different slope angles and rainfall durations of 20mm/hr infiltration

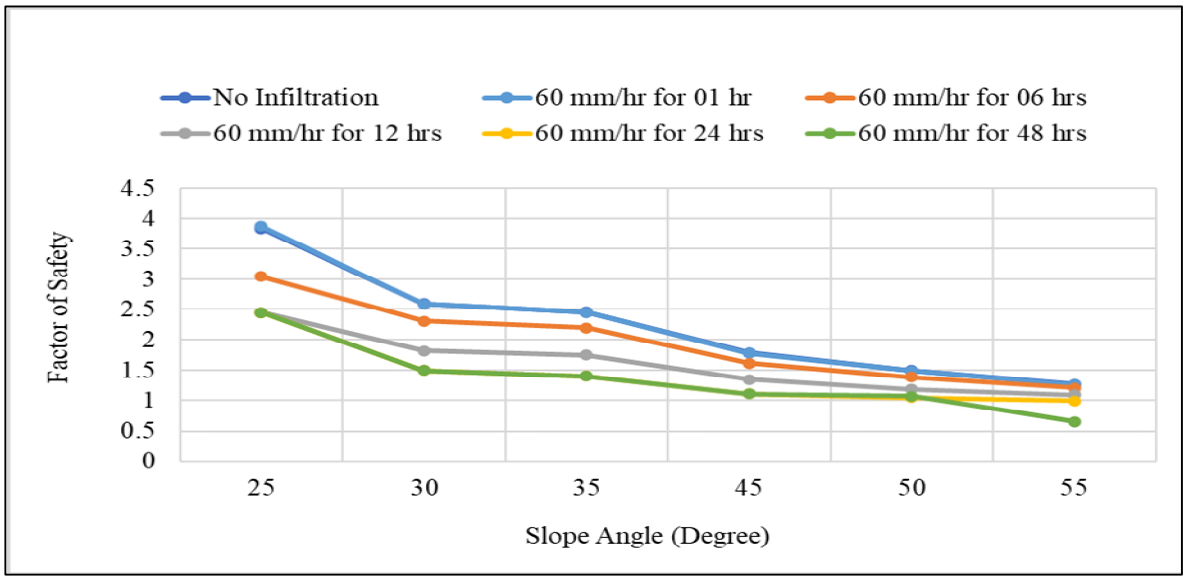

Figure 4.19: Factor of Safety for slope with different slope angles and rainfall durations of 60mm/hr infiltration

Figure 4.20 shows the FOS for slopes subjected to 90mm/hr rainfall intensity for different slopes and different rainfall durations. FOS decreased from 3.8 to 2.4, which is approximately a 36.5% reduction as compared to the slope with no infiltration. It can be seen that FOS decreased with an increase in duration up to 12 hours and remained the same afterwards. FOS This is due to the full saturation of the soil slope and no further infiltration into the soil. These analyses reveal the rainfall intensity of 60mm/hr is found to be a critical intensity limit in terms of influencing the slope instability.

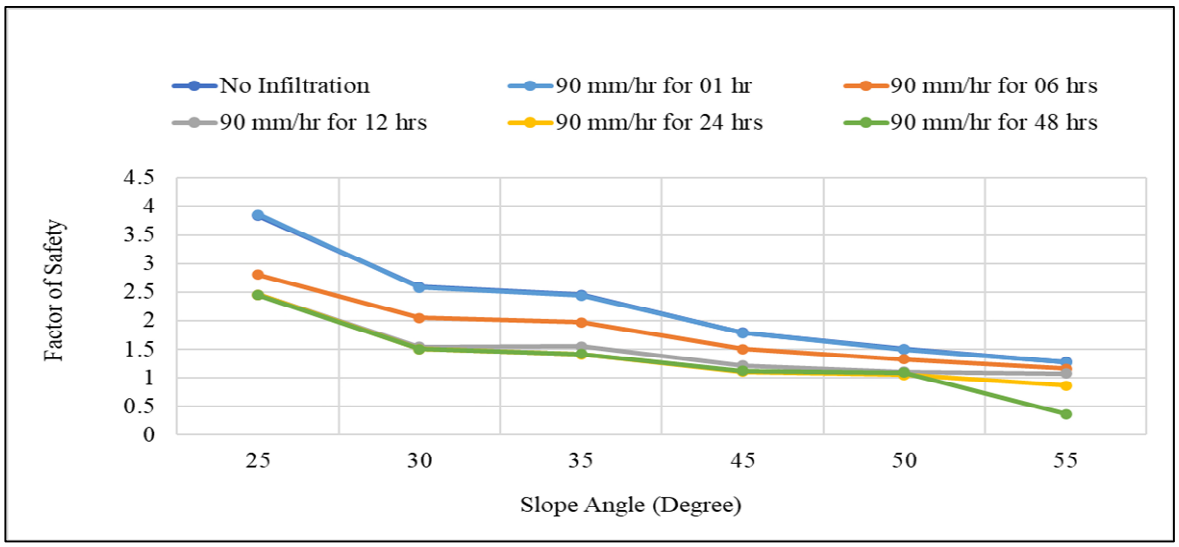

Figure 4.20: Factor of Safety of slope for different slope angles and rainfall duration for 90mm/hr infiltration

4.6.2 Effect of Slope Angle on the Instability of Slopes

When analysing slope stability, it is important to consider many elements, including the shape of the slope, the type of soil, the features of shear strength, the arrangement of soil layers, the circumstances of groundwater, and the flow of water through the soil. The combined influence of these characteristics is essential in determining the probability of slope failure, as emphasised by (Halder et al. 2020). The influence of slope geometry on slope stability has been emphasised by (Shiferaw 2021c). Given this, the building of slopes requires meticulous and exacting focus on detail, particularly with regard to slope geometry, in order to minimise the potential for instability. By ensuring that the geometry of the slope is designed to have a high safety factor, the potential for slope failure can be minimized. This implies that the dimensions, shape, and overall layout of the slope must be meticulously planned and executed to ensure its stability. 6 different slopes were analysed to develop a better understanding of stability response against various rainfall infiltrations. Furthermore, Table 4-1 summarises the percentage reduction in FOS for different slopes, and It can be seen that with no infiltration, the FOS significantly decreased with increasing the slope angle. About a 62.5% reduction in FOS was recorded in the slope of 55 degrees as compared to the slope of 25 degrees, while a 32.3% decrease in FOS was observed when the slope angle was changed from 25 degrees to 30 degrees. Figure 6-22 presents the comparison of FOS for different slopes with no infiltration and various infiltration rates lasting 24 hours. Slopes with no infiltration have the highest FOS as compared to the different infiltration rates. The highest FOS was observed for a 25-degree slope with no infiltration, which is 3.81, while the lowest FOS was noted for a 50 and 55

degrees slope with 90mm/hr infiltration lasting for 24 hours which is 1.05. Furthermore, 13%, 30.8% and 36.2% reduction in FOS was observed for 25 degrees slope for 10mm/hr, 20mm/hr, and 60mm/hr infiltration, respectively, lasting for 24 hours rainfall event. Similarly, for 30 degrees slope, maximum reduction was observed as 42.0% for 60mm/hr infiltration lasting for 24 hours.

Table 4-1: Percentage reduction in FOS for different slopes under various rainfall infiltrations lasting for 24 hours.

Slope Angle	Rainfall Infiltration (mm/hr)				
(degree)	0	10	20	60	90
25	-	13.0	30.8	36.2	36.0
30	32.3	7.6	21.3	42.0	42.1
35	35.9	7.1	20.3	42.5	42.6
45	53.2	5.9	18.5	37.7	38.3
50	60.8	4.3	18.5	30.1	30.0
55	62.5	4.5	18.5	26.3	26.0

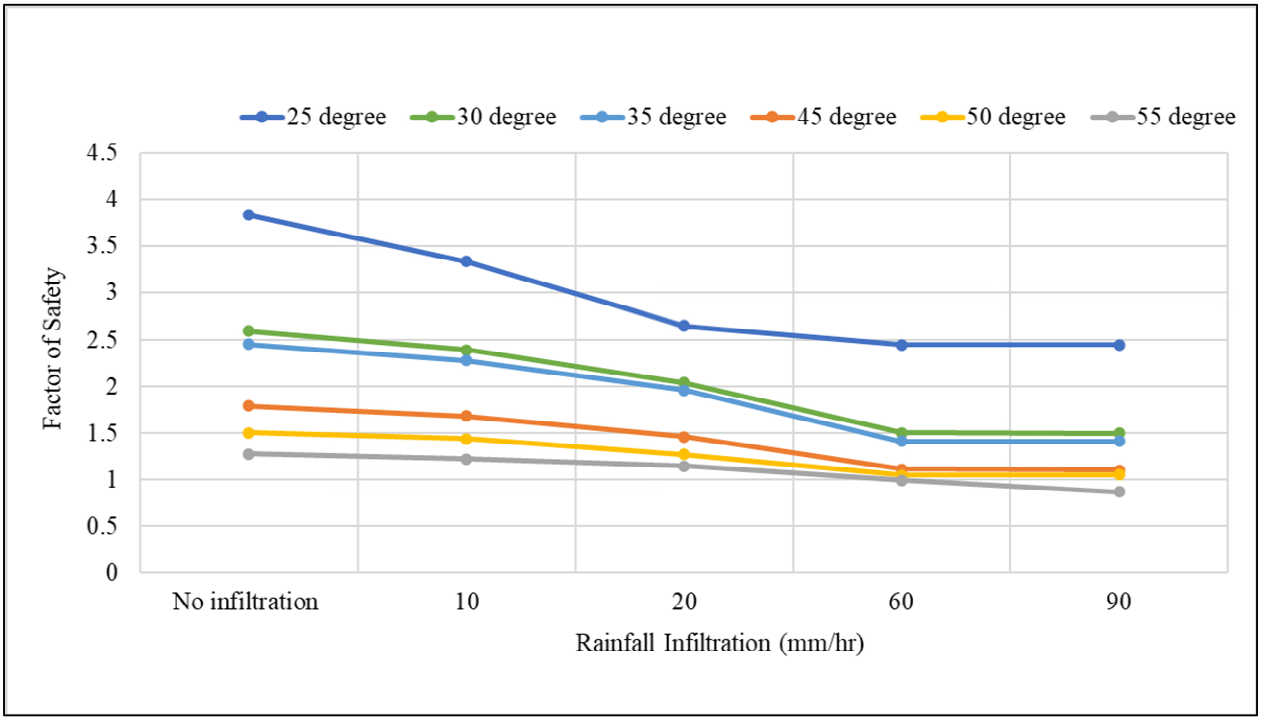

Figure 4.21: Comparison of Safety Factors for Different Slopes and Different Infiltration lasting 24 hours.

4.6.3 Response of Matric Suction Against Rainfall Events

Changes in the pressure of water inside slopes are an important factor that affects stability, especially when it comes to the start of landslides in soils that are not saturated with water. Performing computational simulations of seepage in slopes that are not fully saturated and only partly saturated enables the investigation of how the pressure of water in the pores varies as a result of rainfall penetration. Figure 4.22 illustrates the relationship between the variation in matric suction and different slopes exposed to a rainfall intensity of 10 mm/hr over a duration of 48 hours. It has been observed that an increase in slope angle leads to a corresponding increase in matric suction. This can be attributed to the reduced ponding time, which limits the infiltration of rainfall water into the slope as matric suction is inversely proportional to infiltration. A decrease in infiltration results in higher matric suction levels. Furthermore, Figure 4.23 and Figure 4.24 demonstrate the changes in matric suction for rainfall intensities of 20 mm/hr and 60 mm/hr, respectively, over the same 48-hour period. Both figures exhibit a similar trend, reinforcing the observations made in the case of the 10 mm/hr rainfall intensity. These findings contribute to the understanding of the relationship between slope angle, rainfall intensity, and matric suction. By investigating the effects of different slopes and rainfall intensities on matric suction, it becomes evident that slope angle plays a crucial role in influencing matric suction levels.

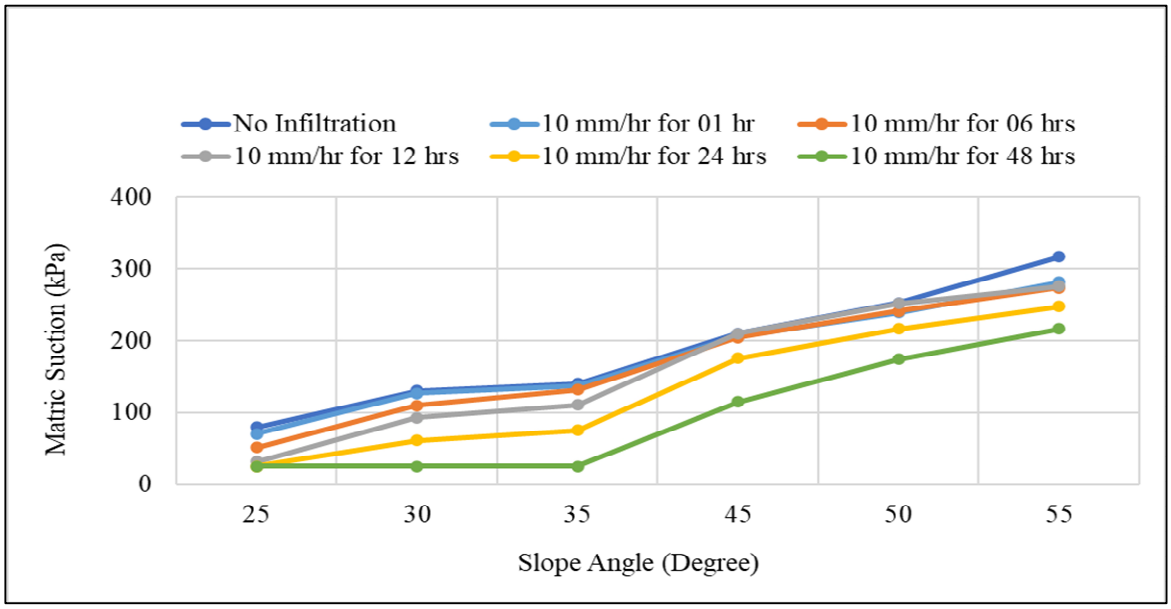

Figure 4.22: Variation in matric suction within slope subjected to 10mm/hr rainfall

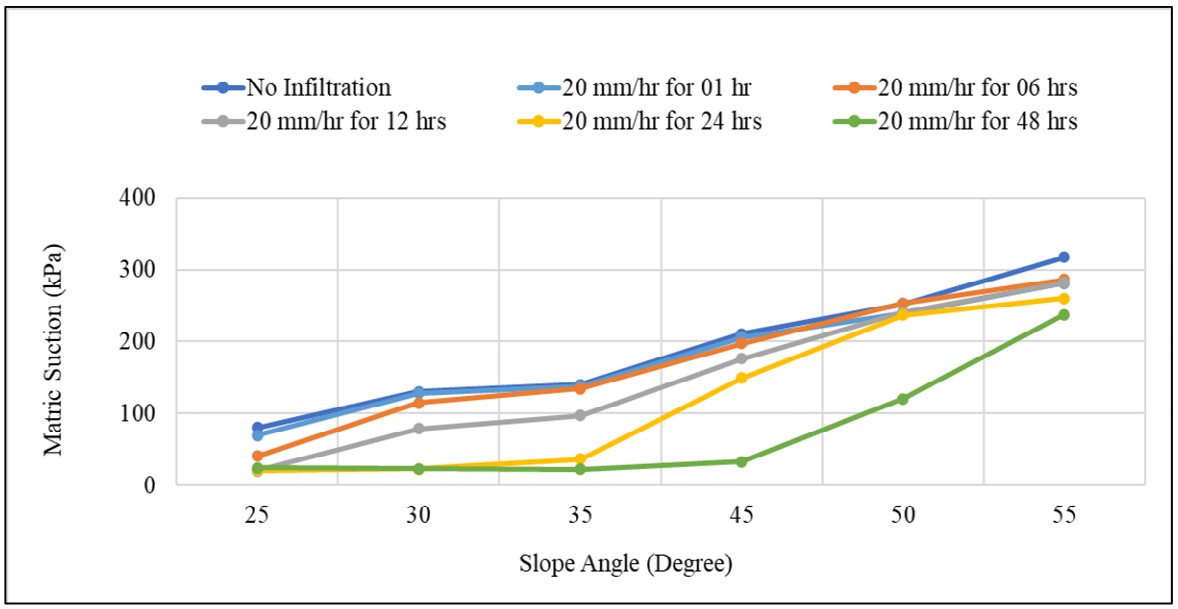

Figure 4.23: Variation in matric suction within slope subjected to 20mm/hr rainfall

Table 4-2 presents a summary of the percentage decrease in matric suction within slopes exposed to various rainfall events lasting for a duration of 24 hours. In the case of a rainfall intensity of 10 mm/hr, the highest reduction in matric suction was observed for a slope angle of 25 degrees. Interestingly, as the slope angle increases, the percentage reductions along the slope decrease. This observation suggests that a greater proportion of rainwater becomes runoff on steeper slopes compared to gentler slopes. Consequently, less water infiltrates into the slope, leading to a smaller reduction in matric suction.

Conversely, gentle slopes facilitate a significant amount of water infiltration, resulting in a higher reduction in matric suction. This finding emphasizes the role of slope angle in influencing the infiltration capacity of rainfall water. Steeper slopes tend to impede infiltration, causing a higher percentage of rainwater to become surface runoff, which limits the reduction in matric suction. In contrast, gentle slopes offer less resistance to infiltration, enabling a larger volume of water to penetrate the slope, thereby contributing to a greater reduction in matric suction.

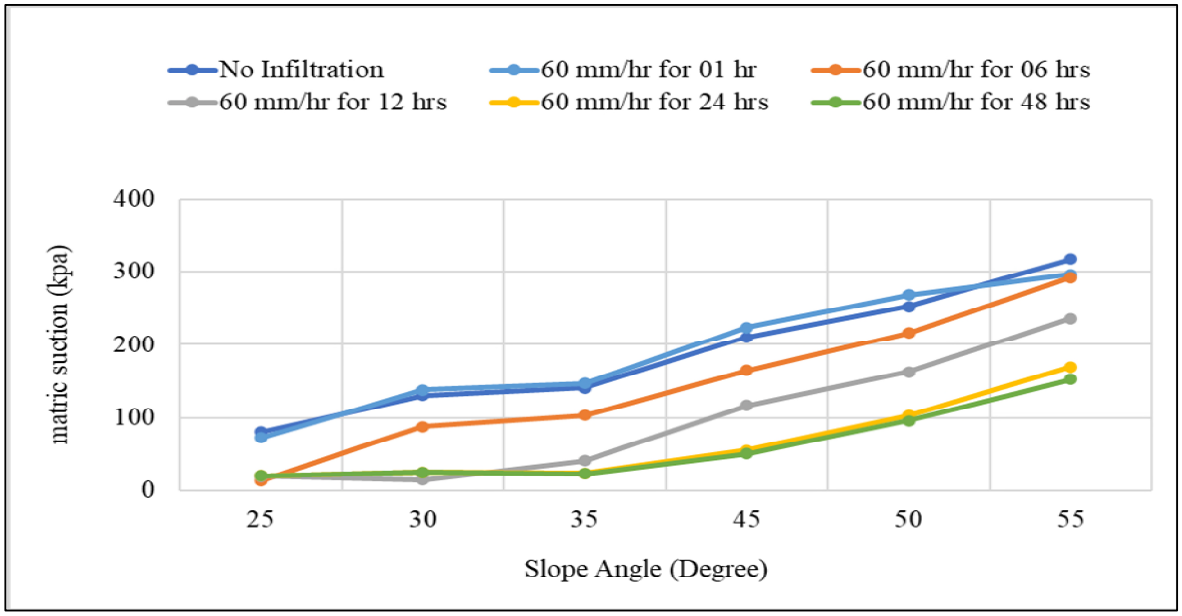

Figure 4.24: Variation in matric suction within slope subjected to 60mm/hr rainfall

Table 4-2: Percentage reduction in matric suction within slope subjected to various rainfall events lasting for 24 hours.

Slope Angle (degree)	Rainfall Infiltration (mm/hr)		
	10	20	60
25	68.4	73.6	75.2
30	52.8	82.3	80.9
35	46.2	74.3	83.4
45	16.4	29.2	73.8
50	14.0	6.1	59.0
55	21.9	18.0	46.6

Additionally, the findings of the study indicate that as the intensity of rainfall increases, the matric suction decreases due to a higher volume of water infiltrating into the slope. The most substantial reduction in matric suction was observed for a slope angle of 35 degrees subjected to a rainfall intensity of 60 mm/hr. In this particular scenario, the matric suction experienced an 83.4% decrease compared to the slope where no infiltration occurred. This observation highlights the influence of rainfall intensity on the hydrological response of slopes. Higher rainfall intensities result in a greater influx of water into the slope, which disrupts the matric suction equilibrium. The significant reduction in matric suction for the 35-degree slope

subjected to the intense rainfall event suggests that a substantial amount of water infiltrated the slope, causing a notable decrease in matric suction levels.

4.6.4 Slope Stabilization using Sand Piles

Several researchers have investigated methods for enhancing soil quality to study the stability of reinforced slopes using different materials (Aksoy et al. 2021; Anvari et al. 2017; W. Li et al. 2020). Researchers have analysed case studies of slope failure using numerical and analytical approaches, including static and dynamic analyses. These studies aim to understand the causes behind slope failure. The researchers who have undertaken these analyses are (Awlla et al. 2020; Gör et al. 2022; Huvaj and Oğuz, 2018; Moayedi et al. 2019; Tien Bui et al. 2019). The use of sand columns for slope stabilisation in highway construction has been seen in several states, such as Alaska, California, Florida, Iowa, Kentucky, Mississippi, New York, South Dakota, Texas, Virginia, and Wisconsin. This approach has been recognised as significant (Xanthakos et al. 1994). Research conducted by Christoulas et al. (1997) examined the immediate impacts of sand column-reinforced slopes. The findings indicated that clay slopes with lower shear strength (cu = 10 kPa) saw a threefold rise in the safety factor compared to slopes with greater shear strength (cu = 30 kPa). In addition, (Abusharar and Han, 2011) conducted a study on the influence of sand column reinforcement on slopes. They found that the presence of sand columns greatly improved the performance of soil slopes. The researchers found that the sand columns, due to their superior hardness and strength compared to the surrounding soil, play a pivotal role in improving slope stability. The study revealed several key findings. Firstly, an increase in the friction angle of the columns by approximately 14% was observed, leading to improved resistance to sliding. Additionally, the presence of sand columns resulted in a substantial increase in embankment cohesion, approximately 41%, which further contributed to slope stability. Moreover, the researchers discovered that reducing the height of the embankment had a profound impact on the safety factor. Specifically, when the embankment height was reduced by half, the safety factor increased significantly. This finding underscores the significance of considering embankment height reduction as a valuable strategy for enhancing slope stability. The study conducted by Abusharar and Han (2011) highlights the paramount importance of sand columns in improving the performance and stability of soil slopes. Their results emphasize the benefits of increasing the friction angle and cohesion through the implementation of sand columns, as well as the critical role of embankment height reduction in ensuring slope safety. In this study the slopes were stabilised with sand piles with different stiffnesses/friction angles of sand material. The analysis results

have been described in detail in following sections. Figure 4.25 presents a typical deformed mesh for slope stabilized with sand piles.

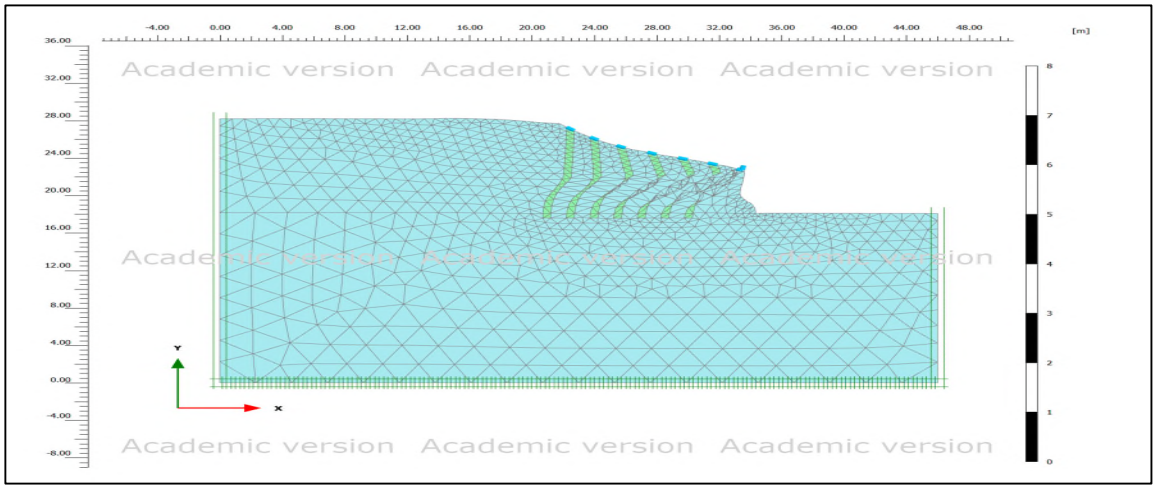

Figure 4.25: Deformed Mesh of slope stabilised with sand piles under rainfall infiltration of 60mm/hr lasting for 24 hours, $\alpha = 35°$

4.6.5 Variation in Matric Suction for Slopes Stabilized with Sand Piles.

Figure 4.26 to Figure 4.31 illustrates the change in matric suction in slope ($\alpha = 35°$) stabilized with sand piles, subjected to 10mm/hr, 60mm/hr and 90mm/hr rainfall infiltration lasting for up to 24 hours. It can be observed that as tie rainfall duration increases, the matric suction significantly decreases within slope but not in sand piles, which led to stabilize the slope against rainfall. As water infiltrates into the soil, the pore spaces become filled with water which results in high porewater pressure and hence reduces the matric suction. However, as the water drained out of the larger pores, leaving behind the smaller capillary pores. The remaining water is held under the tension, resulting negative porewater pressure or suction, as can be seen within the sand piles in Figure 4.27, Figure 4.29 and Figure 4.31.

Figure 4.32 to Figure 4.34 shows the variation in matric suction for slopes stabilized with sand piles subjected to rainfall infiltration of 10mm/hr, 20mm/hr and 60mm/hr respectively. It can be observed that matric suction increases as slope angle increases due to the less time available for water to infiltrate into the slope, whereas matric suction decreases as rainfall infiltration increases.

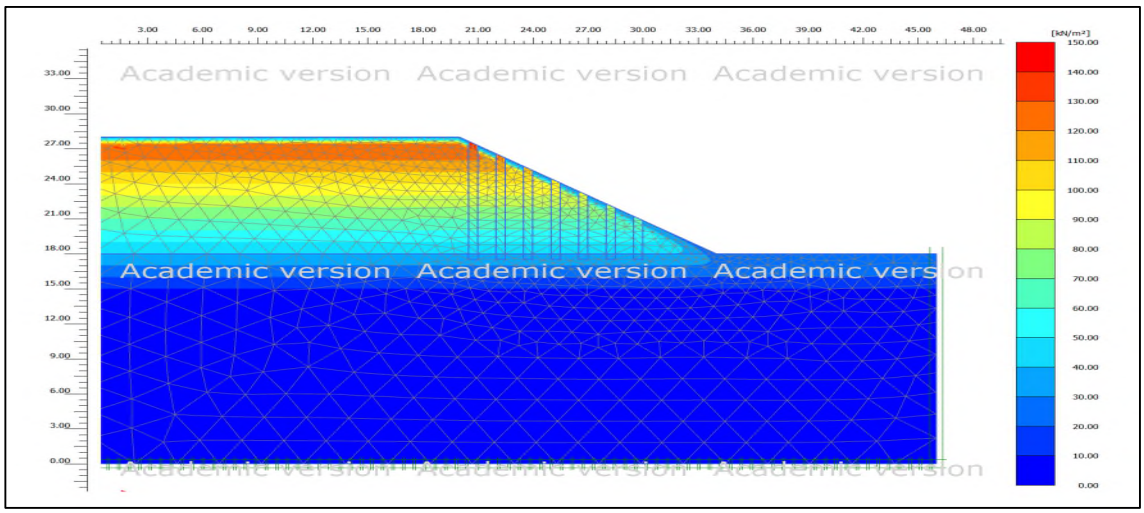

Figure 4.26: Matric Suction in slope stabilised with sand piles under rainfall infiltration of 10mm/hr lasting for 01 hour, α = 35°

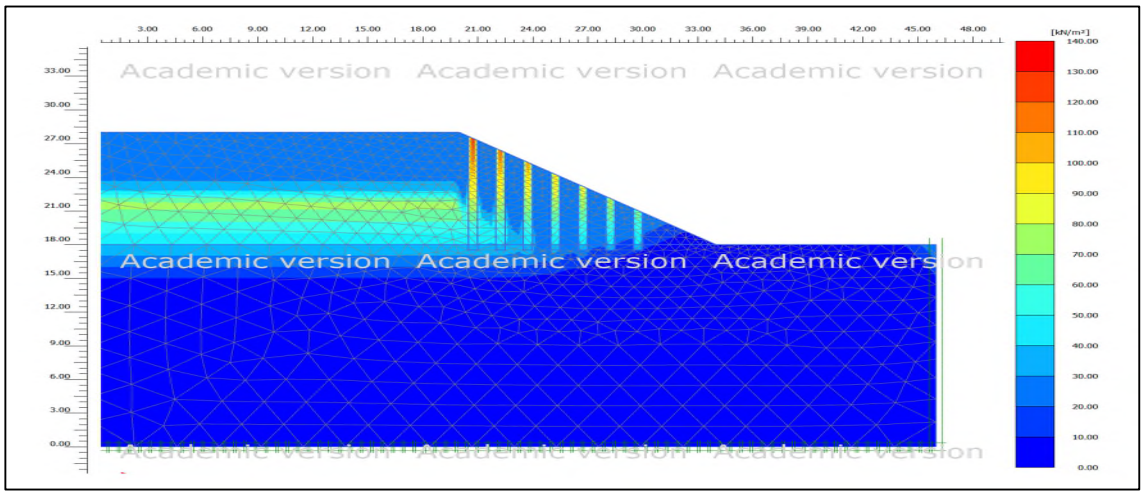

Figure 4.27: Matric Suction in slope stabilised with sand piles under rainfall infiltration of 10mm/hr lasting for 24 hours, α = 35°

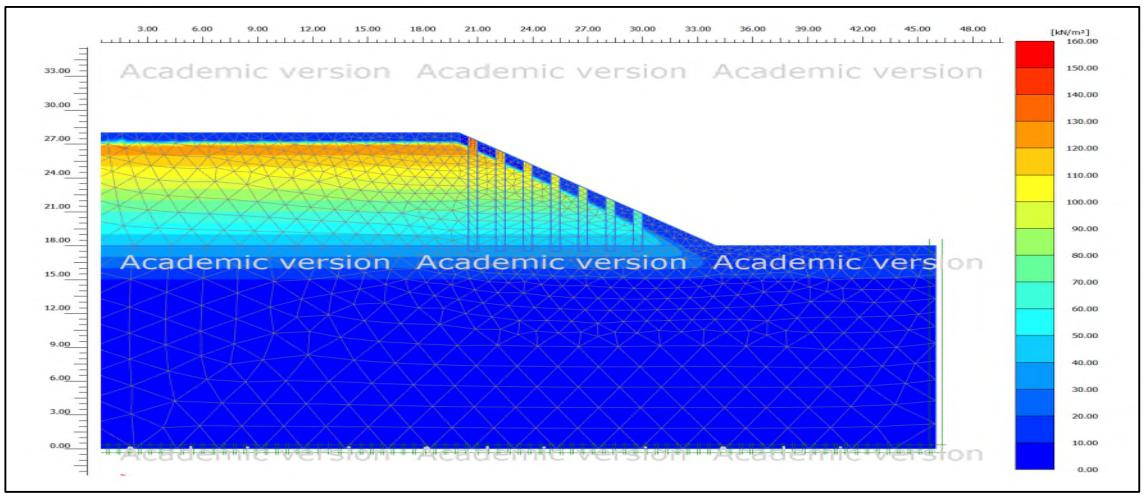

Figure 4.28: Matric Suction in slope stabilised with sand piles under rainfall infiltration of 60mm/hr lasting for 01 hour, α = 35°

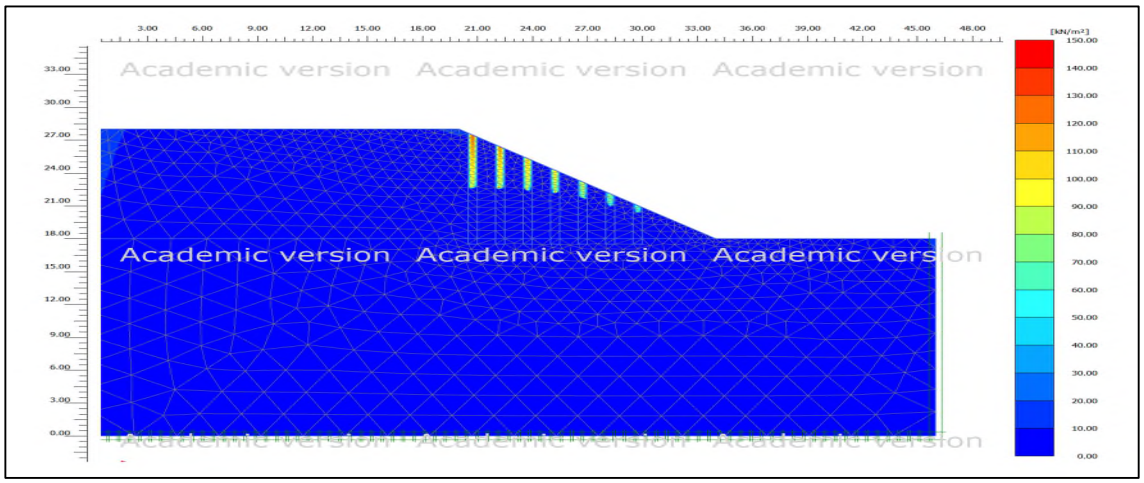

Figure 4.29: Matric Suction in slope stabilised with sand piles under rainfall infiltration of 60mm/hr lasting for 24 hours, α = 35°

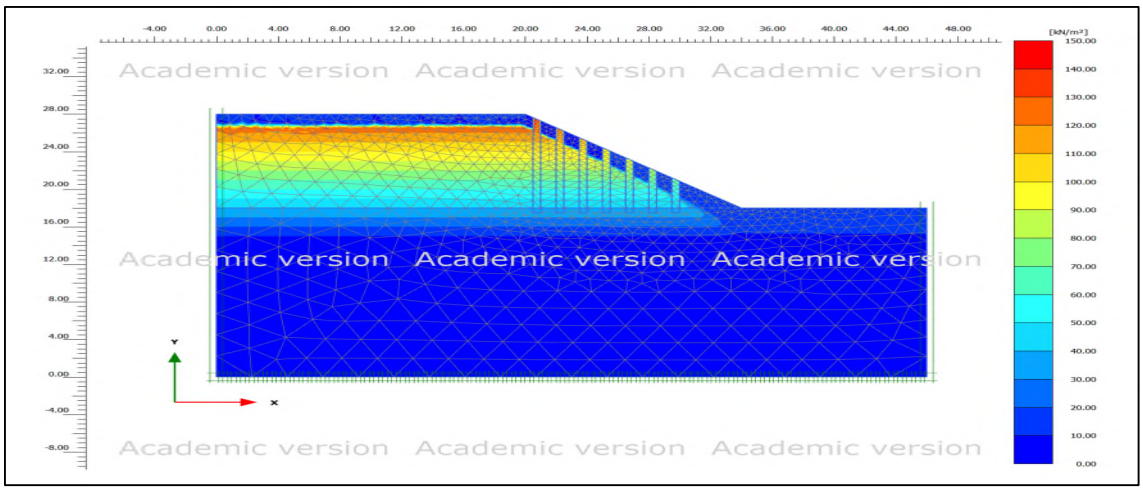

Figure 4.30: Matric Suction in slope stabilised with sand piles under rainfall infiltration of 90mm/hr lasting for 01 hour, α = 35°

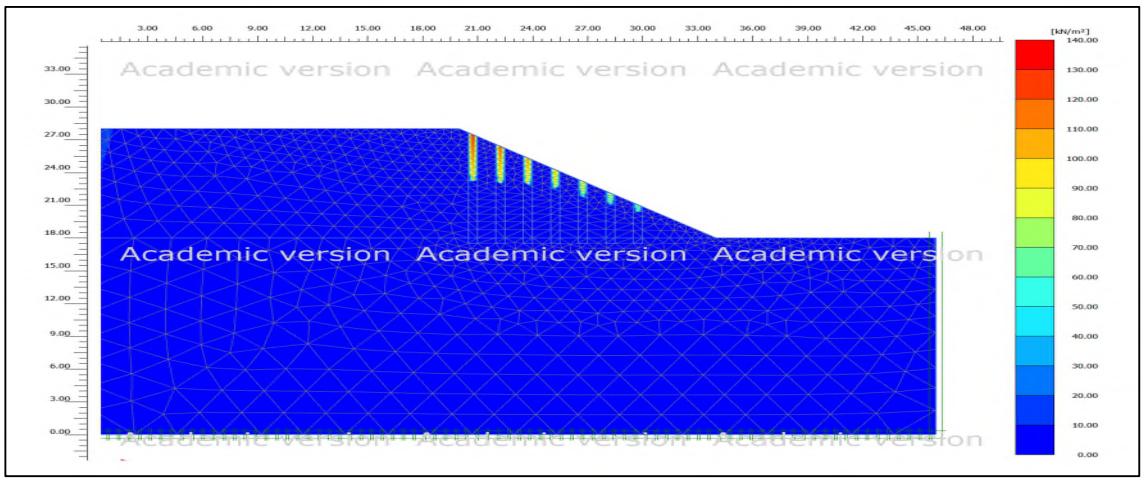

Figure 4.31: Matric Suction in slope stabilised with sand piles under rainfall infiltration of 90mm/hr lasting for 24 hours, α = 35°

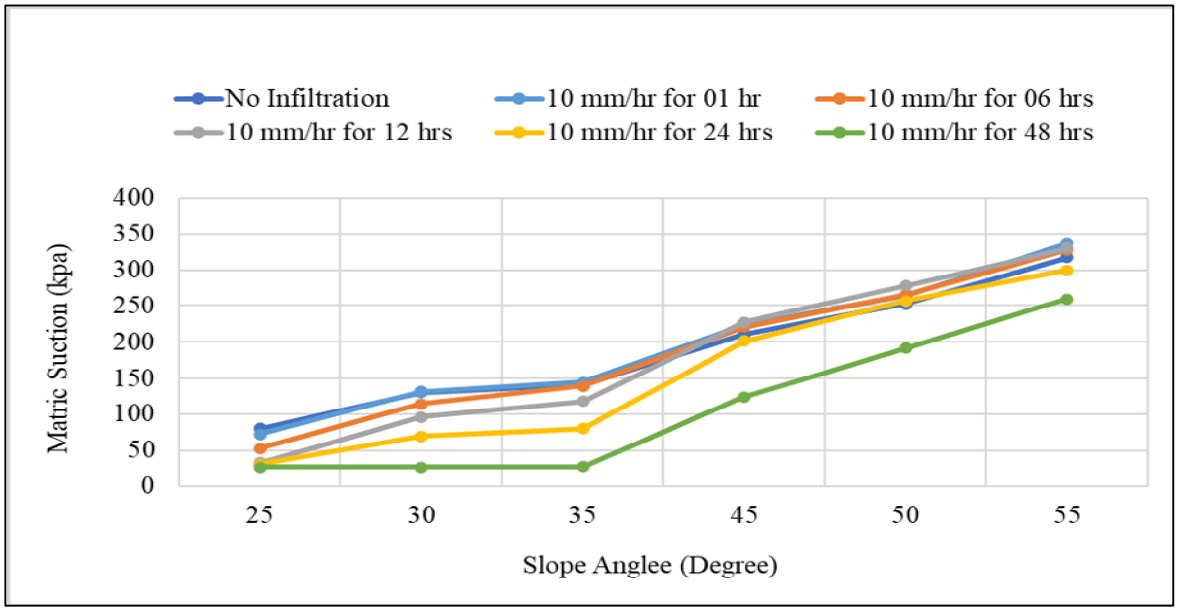

Figure 4.32: Change in matric suction for slope stabilized with sand piles subjected to 10mm/hr rainfall infiltration.

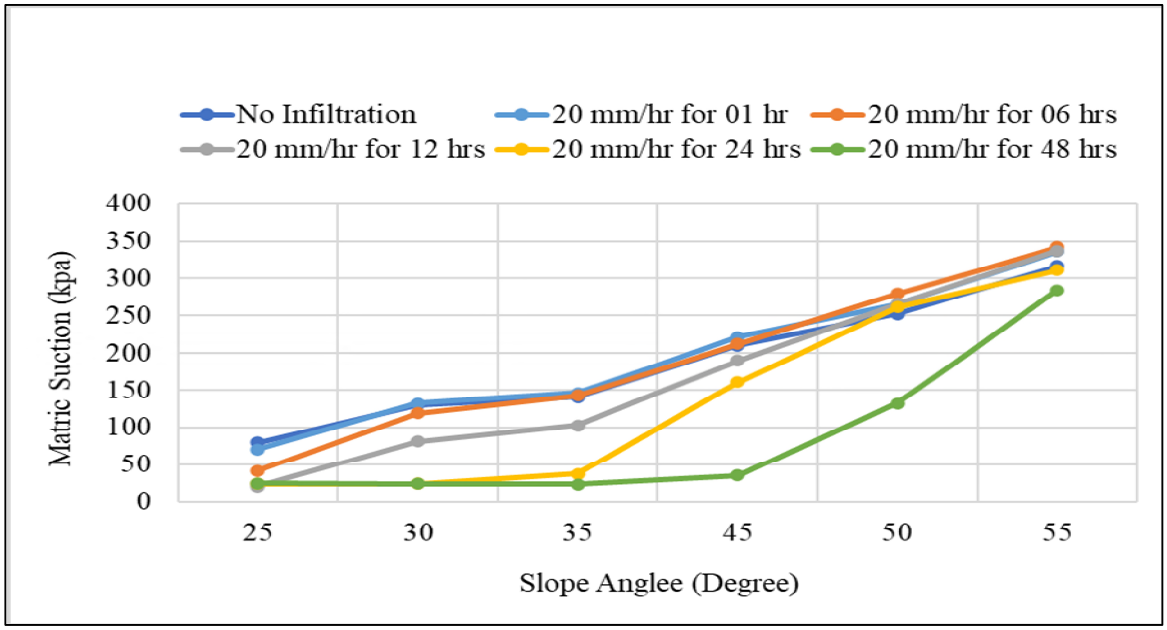

Figure 4.33: Change in matric suction for slope stabilized with sand piles subjected to 20mm/hr rainfall infiltration.

Table 4-3 provides a comprehensive summary of the percentage increase in matric suction that was observed within slopes that were stabilized using sand piles. The results revealed that the inclusion of sand piles in slopes, which were exposed to various rainfall events lasting for 24 hours, led to a notable increase in matric suction. Specifically, the study observed a significant maximum increase of up to 21% in matric suction.

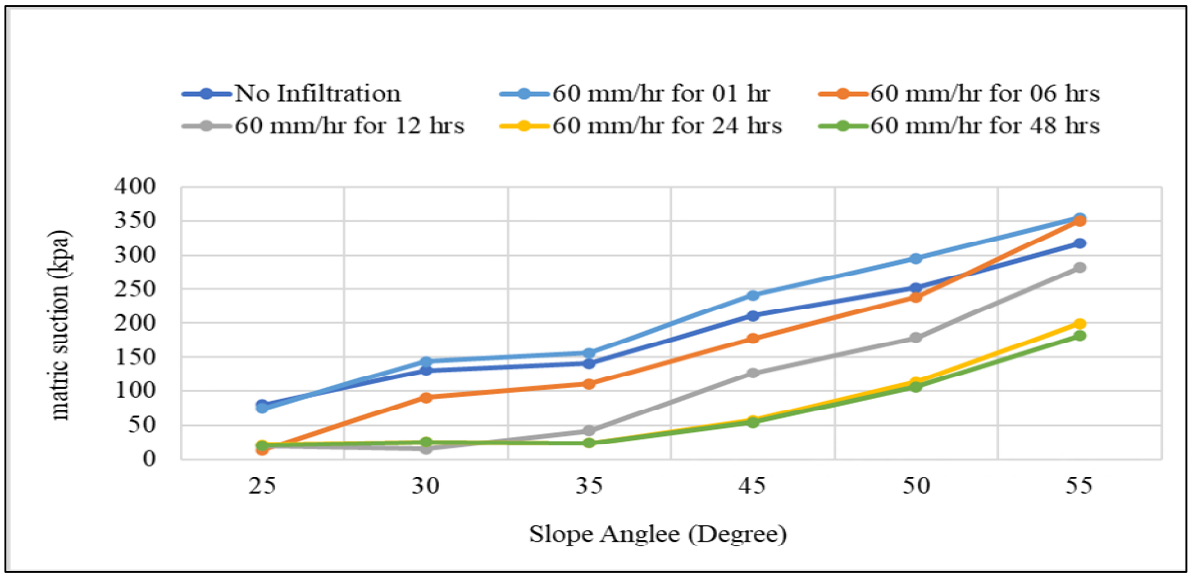

Figure 4.34: Change in matric suction for slope stabilized with sand piles subjected to 60mm/hr rainfall infiltration.

Table 4-3: Percentage increase in matric suction for slopes stabilized with sand piles.

Slope Angle (degree)	Rainfall Infiltration (mm/hr)		
	10	20	60
25	19.6	15.5	11.0
30	12.6	4.3	3.6
35	6.3	3.3	3.2
45	14.4	7.8	3.6
50	18.1	10.2	8.8
55	20.9	19.6	17.4

4.6.6 Effect on Factor of Safety

Figure 4.35 to Figure 4.37 illustrate the variation in the factor of safety for slopes that were stabilized using sand piles and were exposed to diverse rainfall events of varying durations. These figures provide a detailed depiction of how the factor of safety changed over time in response to the rainfall events. Additionally, Figure 4.38 depicts a comprehensive comparison between slopes that were stabilized with sand piles and those left unstabilized. The comparison clearly demonstrates a remarkable improvement in the stability of slopes that were reinforced with sand piles, in contrast to the unstabilized slopes. The findings highlight the effectiveness of sand piles in enhancing slope stability under varying rainfall conditions. Table 4-4 summarize the percentage reduction in factor of safety for slopes stabilized with sand piles. Maximum reduction in FOS was observed for 55-degree slope without infiltration.

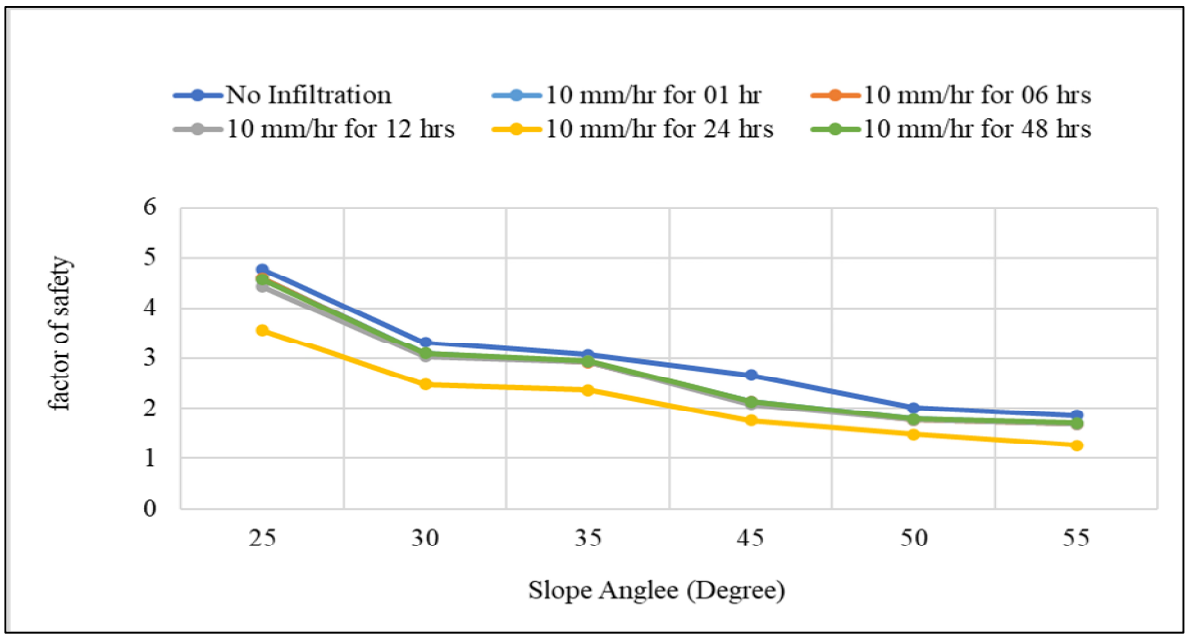

Figure 4.35: Change in factor of safety for slopes stabilized with sand piles subjected to 10mm/hr rainfall infiltration

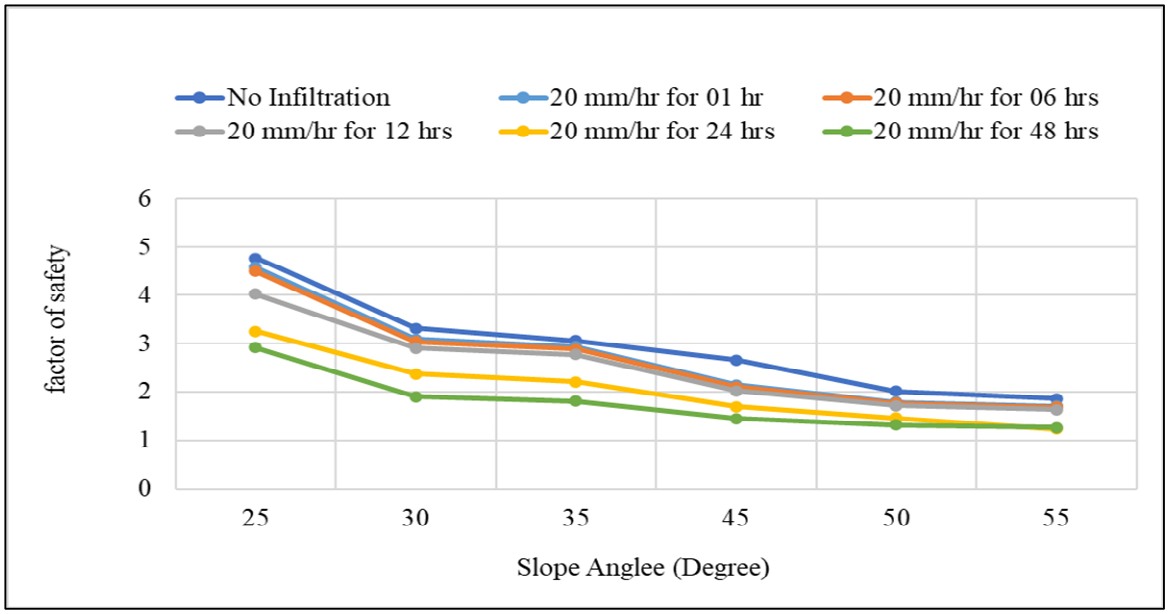

Figure 4.36: Change in factor of safety for slopes stabilized with sand piles subjected to 20mm/hr rainfall infiltration

Upon conducting a comparative analysis of Table 4-1 and Table 4-4, it is evident that the incorporation of sand piles has yielded notable improvements in the Factor of Safety (FOS) for slopes. The results indicate that slopes stabilized with sand piles exhibit a significant increase in FOS, with a recorded enhancement of up to 26% when compared to the unstabilized slope conditions. In addition to providing a drainage path, sand piles also contribute to an increase in

the resistance to soil movement, thereby leading to a higher Factor of Safety (FOS). The inclusion of sand piles in slope stabilization measures offers multiple benefits that positively impact the overall stability of the slope.

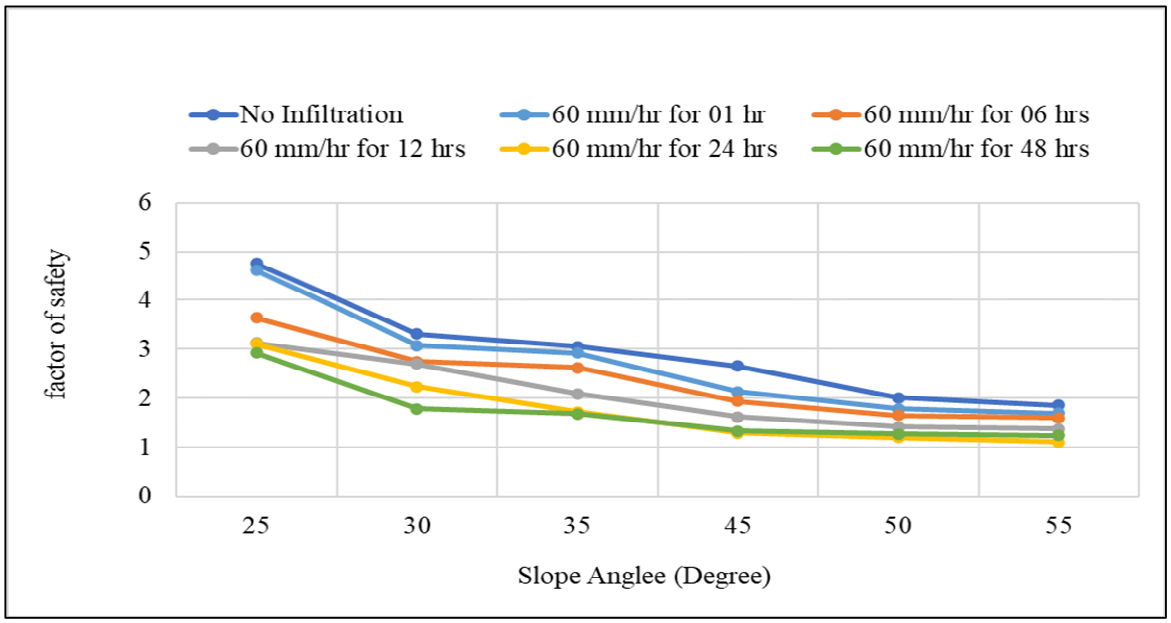

Figure 4.37: Change in factor of safety for slopes stabilized with sand piles subjected to 60mm/hr rainfall infiltration

Table 4-4: Percentage reduction in factor of safety for slopes stabilized with sand piles.

Slope Angle (degree)	Rainfall Infiltration (mm/hr)				
	0	10	20	60	90
25	24.3	6.8	22.6	26.8	30.4
30	27.7	3.5	16.1	22.5	27.3
35	24.4	3.4	12.6	21.9	20.1
45	34.0	4.4	16.0	16.2	32.3
50	45.9	3.3	14.8	14.3	19.0
55	48.3	2.3	7.9	11.3	18.1

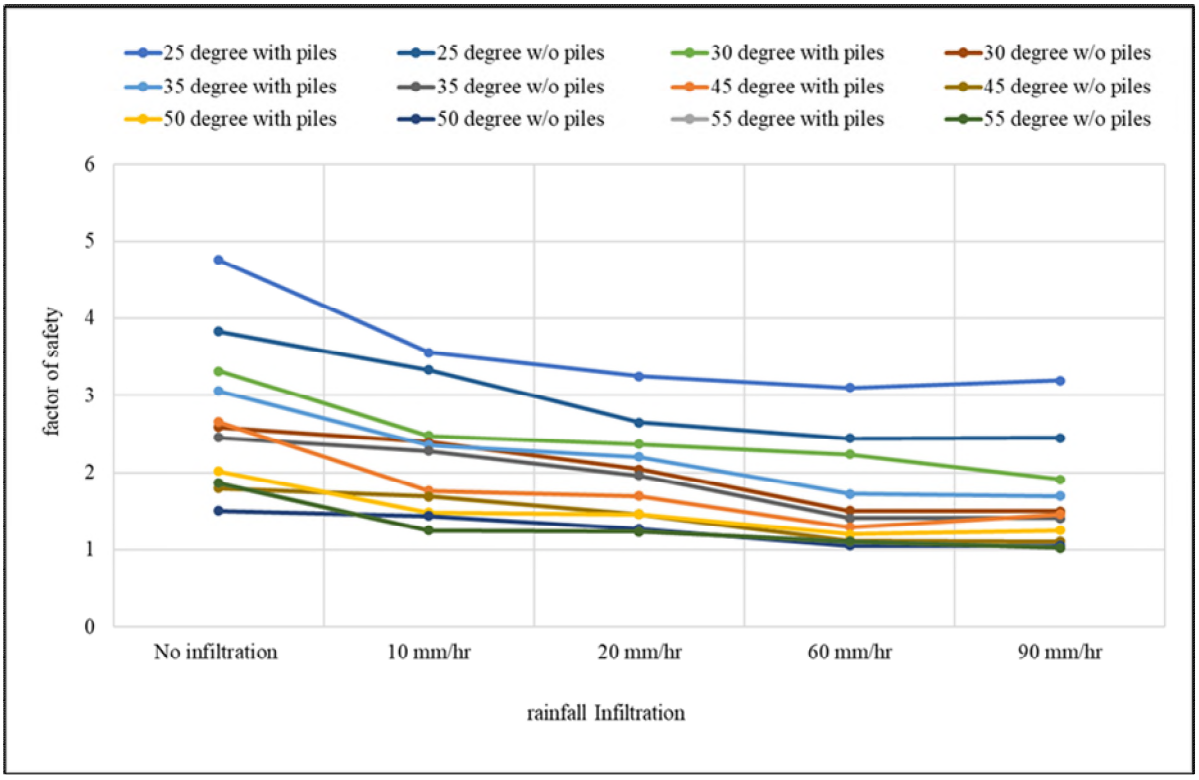

Figure 4.38: Comparison of factor of safety for un-stable and stabilized slope with sand piles

4.7 Discussion on Analysis Results

Slope stability is a critical aspect of geotechnical engineering, influencing the safety and integrity of various infrastructures. The infiltration of rainfall water into slopes significantly affects their stability, as it impacts pore water pressures and the resultant shear strength. Matric suction (or surface tension between the soil particle, also known as negative pore water pressure) plays a vital role in the overall slope behaviour. Understanding the relationship between slope angle, infiltration, and matric suction is crucial for effective slope management and hazard mitigation. Slope collapses or landslides often happen after extended periods of intense rainfall or previous rains. The main cause of these failures is the depletion of matric suction in soils caused by rainfall. When precipitation seeps into slopes, it causes the soil to become saturated, resulting in a decrease in matric suction. The infiltration of precipitation into the soil persists after the cessation of rainfall, eventually reaching a condition of balance or stability. Matric suction, a fundamental stress parameter in the theory of unsaturated soil (Fredlund and Morgenstern, 1977; Fredlund and Rahardjo, 1987), enhances the soil's mechanical resistance. The presence of negative pore water pressure, also known as matric suction, plays a vital role in regulating the shear strength of soil and has a significant impact on the stability of steep slopes. Heavy and continuous rainfall often triggers minor landslides

in steep residual soil slopes. As water seeps into the soil, the matric suction, especially close to the surface, progressively decreases and eventually reaches zero as the soil becomes saturated. The significant fall in matric suction causes a decline in the soil's ability to resist shear forces, leading to the occurrence of shallow landslides. Surface runoff is more common on steep slopes, which limits the amount of time water has to soak into the soil. Conversely, on mild inclines, water flows at a reduced pace and gathers, allowing enhanced water penetration into the soil.

The analysis revealed a consistent pattern of increased matric suction with higher slope angles. This observation can be attributed to the reduced ponding time for rainfall water to infiltrate into the slope. As the slope angle increases, the gravitational force acting on the infiltrating water enhances the speed at which it flows downslope. Consequently, the time available for water to infiltrate into the soil decreases, resulting in decreased infiltration rates. The inverse relationship between matric suction and infiltration further reveals the impact of slope angle. Matric suction, being inversely proportional to infiltration, exhibits an increase as infiltration decreases. Conversely, gentle slopes facilitate a significant amount of water infiltration, resulting in a higher reduction in matric suction. This finding emphasizes the role of slope angle in influencing the infiltration capacity of rainfall water. Steeper slopes tend to impede infiltration, causing a higher percentage of rainwater to runoff, which limits the reduction in matric suction. In contrast, gentle slopes offer less resistance to infiltration, enabling a larger volume of water to penetrate the slope, thereby contributing to a greater reduction in matric suction (Zaki et al. 2020; Wang et al. 2024; Guo et al. 2021; Mahmood et al. 2016).

These observations have implications for understanding the hydrological behavior of slopes subjected to rainfall events. By examining the percentage decrease in matric suction across different slope angles, we gain insights into the preferential flow paths of rainwater and the subsequent impact on soil moisture content. This knowledge is crucial for assessing slope stability, erosion risks, and the overall performance of slopes in geotechnical and environmental engineering applications. The slope's geometry interacts with other factors such as soil type and its shear strength properties. The slope angle, for instance, can impact the distribution of stresses within the soil mass. Steeper slopes tend to exert higher forces on the soil, potentially exceeding its shear strength and leading to instability. On the other hand, the slope's curvature and configuration also influence how external forces, such as groundwater and seepage, interact with the slope. Understanding the stratification of the soil and its potential

interaction with groundwater is crucial in evaluating slope stability. Variations in soil layers and their permeability can affect the flow of water through the slope, leading to changes in pore pressure and potentially reducing soil shear strength. These factors must be carefully considered to assess the stability of the slope accurately (Huat et al. 2006; Lu and Likos, 2006; Vergani and Graf, 2016; Matsushi et al. 2006).

The study's findings suggest that as the intensity of rainfall increases, the matric suction, which refers to the tension in the soil that holds water, decreases. This is attributed to a larger volume of water infiltrating into the slope. The most significant reduction in matric suction was observed in a specific scenario: a slope angle of 35 degrees subjected to a rainfall intensity of 60 mm/hr. In this particular case, the matric suction experienced a substantial decrease of 83.4% compared to a slope where no infiltration occurred. To provide more context, matric suction plays a crucial role in slope stability. When water infiltrates into a slope, it increases the pore water pressure within the soil. This increased pressure can weaken the soil's shear strength and contribute to slope failures, such as landslides or slope instability(Tsaparas et al. 2003; Gasmo et al. 2000; Gofar and Rahardjo, 2017). Matric suction acts as a stabilizing force by retaining some of the water within the soil and reducing the pore water pressure. However, higher rainfall intensity can overcome the matric suction and result in decreased stability. The observed reduction in matric suction of 83.4% in the specific scenario highlights the vulnerability of slopes with a 35-degree angle to heavy rainfall. It suggests that such slopes may experience a significant loss in stability when subjected to intense rainfall events. These findings could have implications for slope design, construction, and management, emphasizing the need for appropriate drainage systems or stabilization measures in areas prone to heavy rainfall. This observation highlights the influence of rainfall intensity on the hydrological response of slopes. The significant reduction in matric suction for the 35-degree slope subjected to the intense rainfall event suggests that a substantial amount of water infiltrated the slope, causing a notable decrease in matric suction levels. Understanding the impact of rainfall intensity on matric suction variations is essential for assessing the stability and performance of slopes. The infiltration of excessive amounts of water can lead to changes in pore water pressures and soil properties, potentially compromising slope stability and triggering soil erosion processes. By quantifying the extent of matric suction reduction under different rainfall intensities, engineers and researchers can develop more accurate models and guidelines for slope design, construction, and maintenance. One of the key mechanisms through which sand piles enhance resistance to soil movement is by acting as reinforcement elements. The presence

of sand piles within the slope creates internal friction and cohesion, which effectively counteracts the shear forces acting on the soil mass. This reinforcement mechanism improves the overall shear strength and resistance to soil deformation, thereby increasing the FOS.

Furthermore, sand piles create a composite structure with the surrounding soil, effectively altering the stress distribution within the slope. By redistributing the applied loads and reducing stress concentrations, the sand piles help to stabilize the slope and minimize the potential for soil movement (Fan et al. 2017; Kornejady et al. 2017; Guo et al. 2014; Ullmann et al. 2017). This redistribution of stresses helps to improve the overall load-bearing capacity and resistance to slope failure. Moreover, the sand piles act as vertical drains, facilitating the dissipation of excess pore water pressures within the slope. By providing an efficient drainage path, the sand piles help to reduce the buildup of pore water pressures, which can weaken the soil and increase the risk of instability. By maintaining lower pore water pressures, the sand piles contribute to an increase in the effective stress within the soil mass, further enhancing the FOS. The combined effects of reinforcement and drainage provided by the sand piles contribute to an overall increase in the resistance to soil movement and slope stability. By reducing the potential for soil deformation and failure, the sand piles effectively improve the FOS and enhance the safety of the slope. It is worth noting that the specific design and implementation of sand piles should consider various factors, including soil properties, slope geometry, and project requirements (Abusharar and Han, 2010; Bergado et al. 1990; Vekli et al. 2012). Detailed geotechnical investigations and analysis are crucial in determining the optimal arrangement, spacing, and dimensions of sand piles to maximize their stabilizing effects. In contrast, sand piles exhibited relatively stable matric suction values, regardless of the duration of rainfall. The inherent characteristics of sandy soils, such as higher permeability and larger particle sizes, allow for faster drainage and less significant pore pressure build-up. Consequently, the matric suction within sand piles remained relatively constant, contributing to their stability against prolonged rainfall events. Bergado et al. (1990) conducted large-scale experiments on Bangkok clay to evaluate and compare the effect of sand column and its vertical drainage. The researchers reached significant conclusions regarding the effectiveness of sand columns and their vertical drainage in enhancing slope stability and bearing capacity. The study findings demonstrated that the inclusion of sand columns in soil slopes resulted in a substantial increase in the safety factor, improving it by approximately 25%. Furthermore, the bearing capacity of the slopes experienced an impressive four-fold increase with the incorporation of sand columns. Interestingly, the researchers (Bergado et al. 1990) also observed that the settlement

of slopes reinforced with vertical drainage was 20% to 40% higher compared to those reinforced with sand columns. This indicates that while vertical drainage plays a crucial role in facilitating the dissipation of excess pore water pressure and minimizing settlement, sand columns provide reinforcement benefits in addition to their drainage function. The results of study conducted by (Bergado et al. 1990) highlight the multifaceted role of sand piles in soil slope reinforcement. Sand piles not only contribute to improved drainage and reduction of pore water pressure but also provide significant reinforcement, leading to enhanced slope stability, increased safety factors, and improved bearing capacity.

CHAPTER 5: LABORATORY BASED EXPERIMENTAL MODELING OF SOIL SLOPE – RESULTS AND DISCUSSIONS

5.1 Overview

This chapter explains the outcomes derived from comprehensive testing of soil characteristics and slope model experiments conducted at the laboratory facilities of NTU. The investigations encompassed essential soil attributes, including classification tests, density measurements, hydraulic property analyses, and assessments of the soil's strength characteristics, all of which were of significant relevance in the context of the slope model. Analyses of hydraulic properties delved into the dynamic behavior of the soil under varying moisture conditions, a critical consideration given its direct implications for slope stability. Furthermore, assessments of the soil's strength characteristics furnished crucial insights into the material's mechanical response under controlled conditions. All tests were conducted in accordance with the British Standards prescribed for soil testing. This commitment to standardized protocols ensures the reliability and credibility of the derived results, establishing a robust foundation for subsequent analytical and interpretative endeavors.

5.2 Physical Characteristics of Soil

Figure 5.1 presents the outcomes of liquid limits tests conducted on locally available soil through the utilization of a penetrometer, following the guidelines outlined in BS 1377-2:2022. The test results indicate a liquid limit (LL) of 36.5%, providing a quantitative measure of the soil's susceptibility to transition from a plastic to a liquid state. Also, the plastic limit (PL) was found as 28.5%, hence plasticity index was calculated as 8% (PI = LL – PL). This information is crucial in characterizing the soil's behavior and has significant implications for various engineering applications, particularly in understanding its response to changes in moisture content and potential implications for slope stability.

Figure 5.2 illustrates the results obtained from compaction tests conducted to assess the soil's behavior under varying moisture conditions. The data reveals that a maximum dry density of 1.450 g/cm³ was attained at an optimum moisture content of 22%. This information is pivotal in determining the quantity of soil needed to prepare the slope for subsequent physical slope testing. The maximum dry density signifies the soil's highest achievable density under compaction, while the optimum moisture content represents the moisture level at which the

soil can be compacted most effectively. The utilization of this data ensures a well-informed and optimized approach to the preparation of the slope for flume testing, contributing to the precision and reliability of subsequent experiments and analyses.

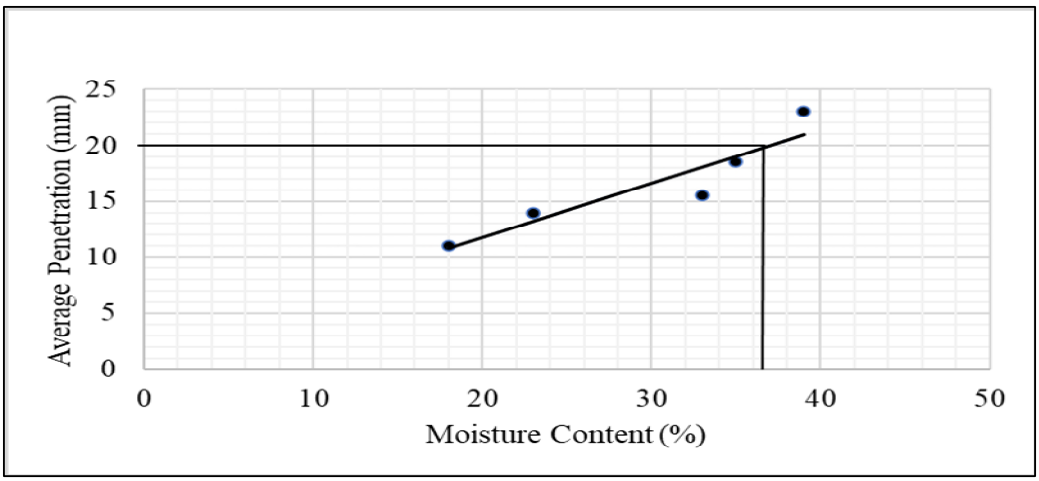

Figure 5.1: Liquid Limit graph

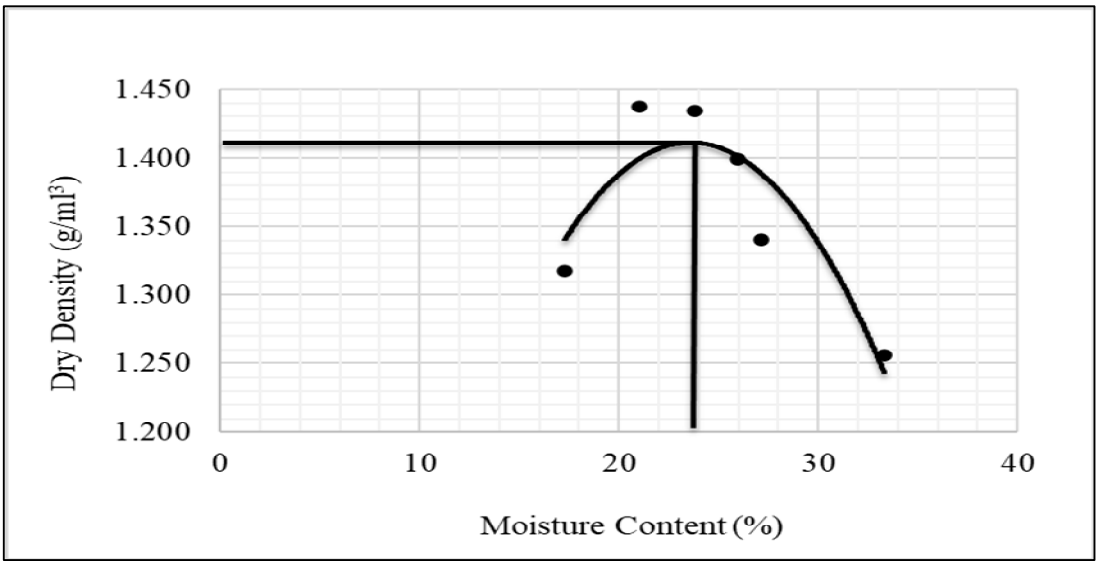

Figure 5.2: Dry density vs optimum moisture content

Figure 5.3 and Figure 5.4 respectively present the classification and particle size distribution curve of the soil utilized in laboratory testing, including slope preparation. The classification gradation curve, along with the determination of liquid limit, plastic limit, and plasticity index, collectively categorizes the soil as a low plastic silt with fine sandy contents. The classification gradation curve offers insights into the relative proportions of different particle sizes within the soil, aiding in its systematic categorization. The determination of liquid limit, plastic limit, and

plasticity index further refines the classification, providing valuable information about the soil's plasticity and cohesive properties. In this specific case, the classification as a intermediate plastic silt with fine sandy contents indicates a soil type that is characterized by relatively low plasticity, predominantly composed of silt particles with additional fine sandy components.

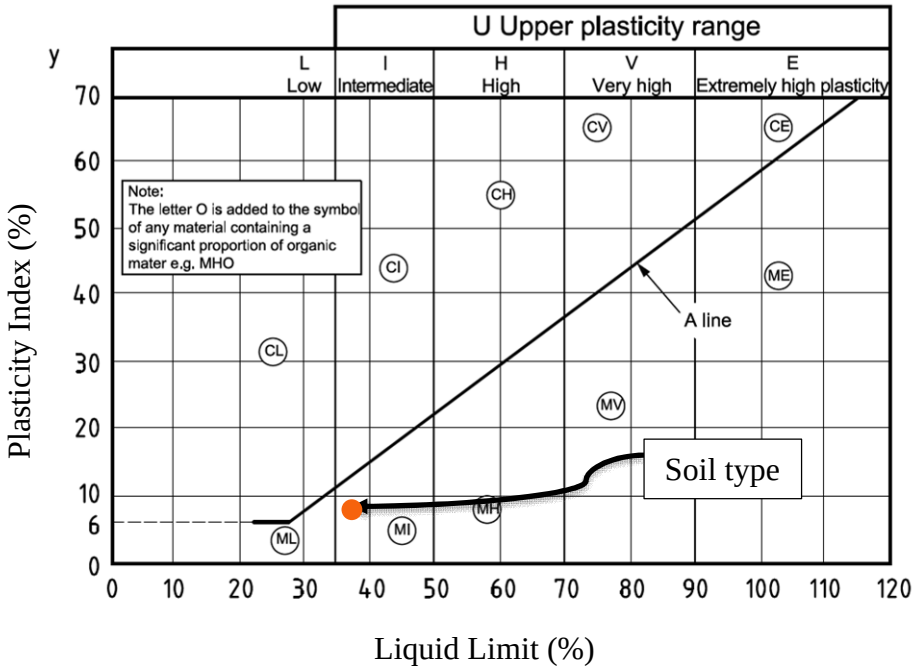

Figure 5.3: Soil Classification using Plasticity Chart (BS 5930:2015)

Locally available Leighton Buzzard Sand was employed as backfill material for the construction of sand piles, also referred to as micro piles. The physical characteristics of the Leighton Buzzard Sand are comprehensively outlined in Table 5-1. In Figure 5.4, where the gradation curve is illustrated, it becomes evident that the Leighton Buzzard Sand exhibits an overall coarse particle size nature. This characteristic is particularly advantageous as it inherently provides ample drainage paths for water to efficiently drain from within the soil slope. The coarse particle size facilitates enhanced permeability, allowing for the effective movement of water through the soil mass. This attribute is crucial for the mitigation of excess water, contributing significantly to the overall drainage and stability of the soil slope.

Table 5-1: Physical Properties of Leighton Buzzard Sand (Yang et al. 2012)

Property	Value
Uniformity coefficient, Cu	1.32
Coefficient of Curvature, Cc	0.96
Specific gravity, Gs	2.64
Minimum Void ratio	0.498
Maximum void ratio	0.769

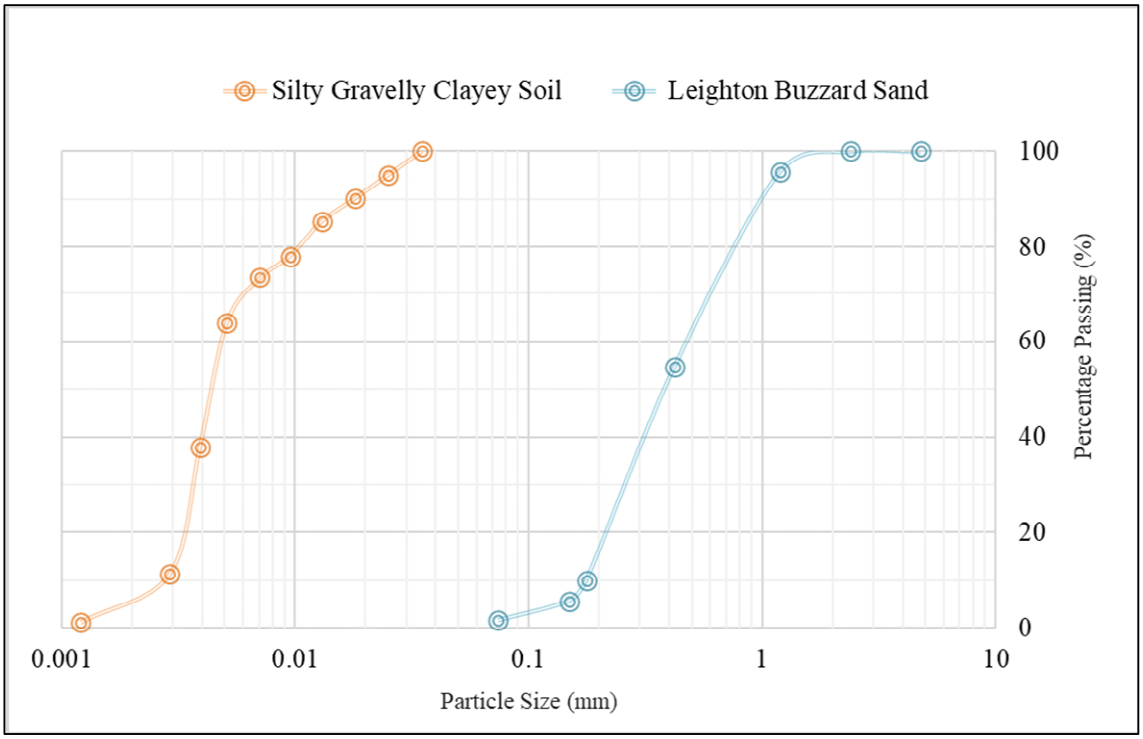

Figure 5.4: Particle size curve for soil and sand used for slope modelling.

5.3 Pore Water Pressure Measurement

As it is quite understood that pore water pressure plays an important role in strength characteristic of soil and hence effects the stability of soil. To measure the variations in pore water pressure within the slope, three piezometers, namely Point A (PA), Point B (PB), and Point C (PC), were installed at distinct locations within the slope, as indicated in Figure 5.5. In Figure 5.6, the depicted graph shows the variations in pore water pressure (PWP) within the slope, both with and without the incorporation of sand piles. The graph highlights significant differences in PWP values between the slope reinforced with sand piles and the unreinforced

slope. Specifically, the highest PWP values were observed at Point B, situated in the middle of the slope, for the unreinforced condition. In contrast, the lowest PWP values were noted at

Point C, positioned on the right side of the slope, for the slope reinforced with sand piles.

Figure 5.5: Piezometers Locations for both unreinforced and reinforced slope

These variations in PWP are indicative of the influence of sand pile reinforcement on the distribution and magnitude of pore water pressures within the slope. The observed differences highlight the effectiveness of sand pile inclusion in mitigating pore water pressures, particularly at critical points within the slope.

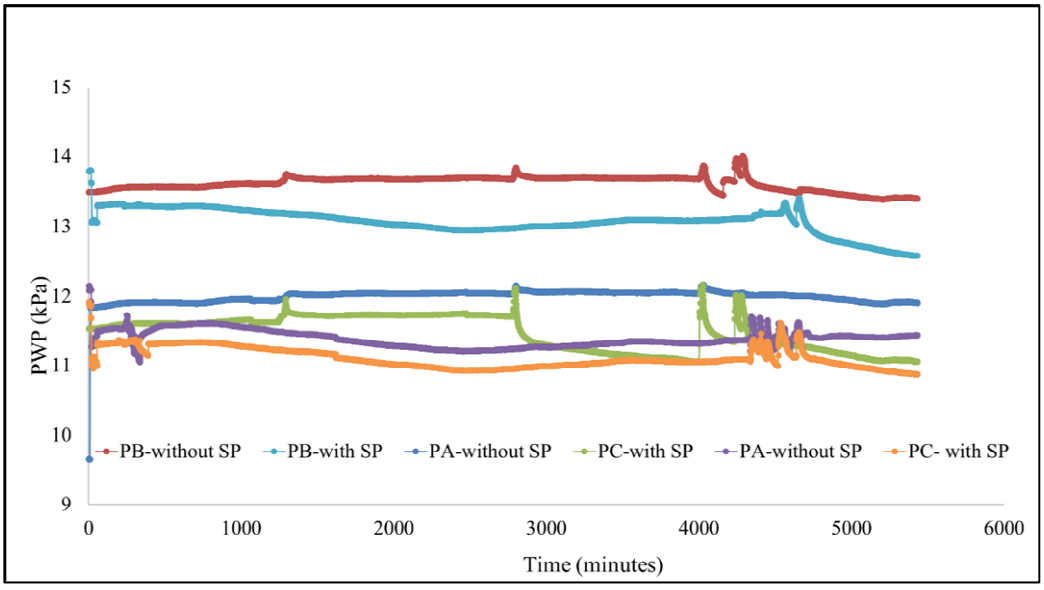

Figure 5.6: Comparison of PWP with and without Sand piles

5.4 Moisture Profile within Slope

Figure 5.7 provides a graphical representation of the moisture profiles of slopes, comparing those with and without the integration of sand piles. Wet samples were systematically collected from equivalent depths within each slope, and their respective moisture contents were subsequently determined after the slope failed (at the end of experiment). The results conspicuously indicate a significant reduction in moisture content, with a notable decrease of up to 18.8% observed in the slope reinforced with sand piles compared to unreinforced slope. This reduction in moisture content assumes a critical role in mitigating pore water pressure within the soil mass. The consequential increase in matric suction levels is particularly noteworthy, as it contributes substantially to the stabilization of soil slopes. The enhanced matric suction is indicative of a more resilient and self-draining soil structure, reducing the likelihood of slope failures associated with excessive water content. These findings underscore the effectiveness of sand pile reinforcement in influencing the moisture dynamics of slopes and, consequently, enhancing their overall stability.

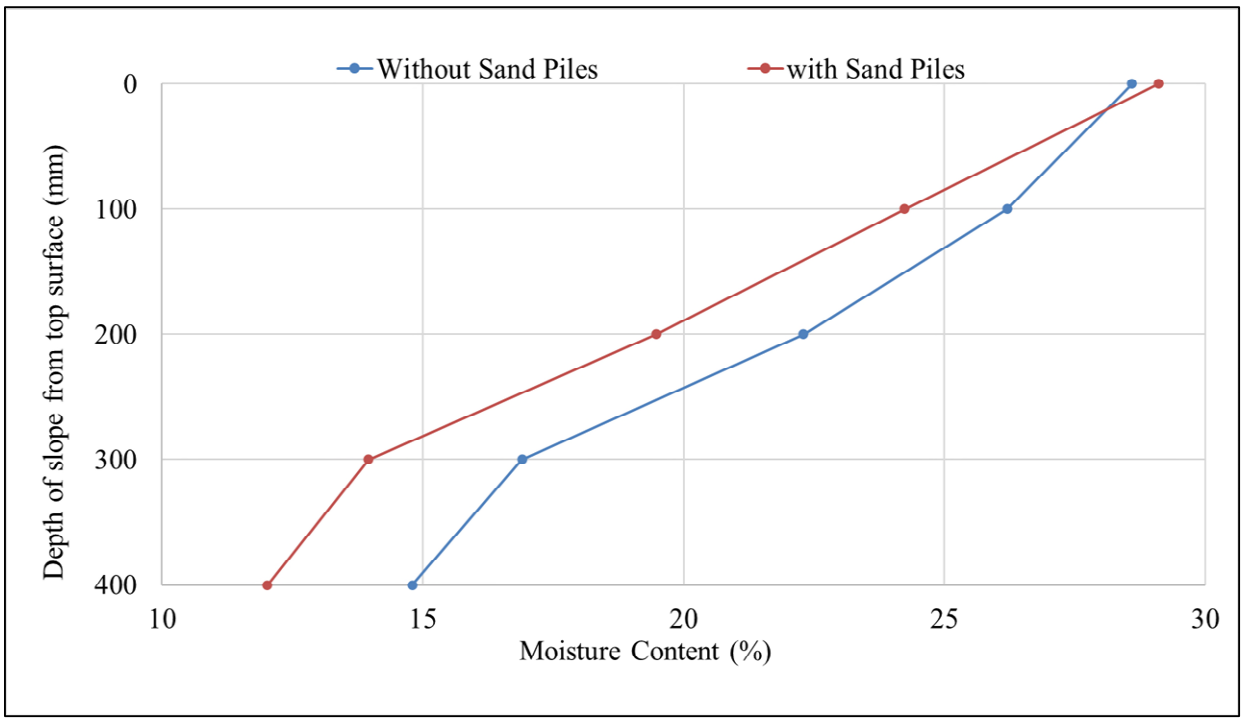

Figure 5.7: Moisture profile of slope with and without Sand Piles

5.5 Slope Deformation using Image Processing

The previous chapter detailed the novel approach, the Automated Signal and Sensory Processing System (ASPS) method, for measuring slope deformations using image processing.

This section elaborates on the findings derived from the image processing analysis. Initially, each image was resized to 100x100, focusing on the region of interest (ROI) that captures substantial changes in slope dynamics in response to rainfall infiltrations. Subsequently, through the application of various statistical equations outlined in the preceding chapter, 24 additional characteristic images were generated, as illustrated in Figure 5.8. Notably, a total of 16 characteristic features (CFs) were employed for each type of image, resulting in 400 features overall (i.e., 16 x 25 = 400). Figure 5.8 presents 25 distinct types of characteristic images depicting the unreinforced slope during the initial stages of the experiment (at the beginning of experiment where less significant variations were observed).

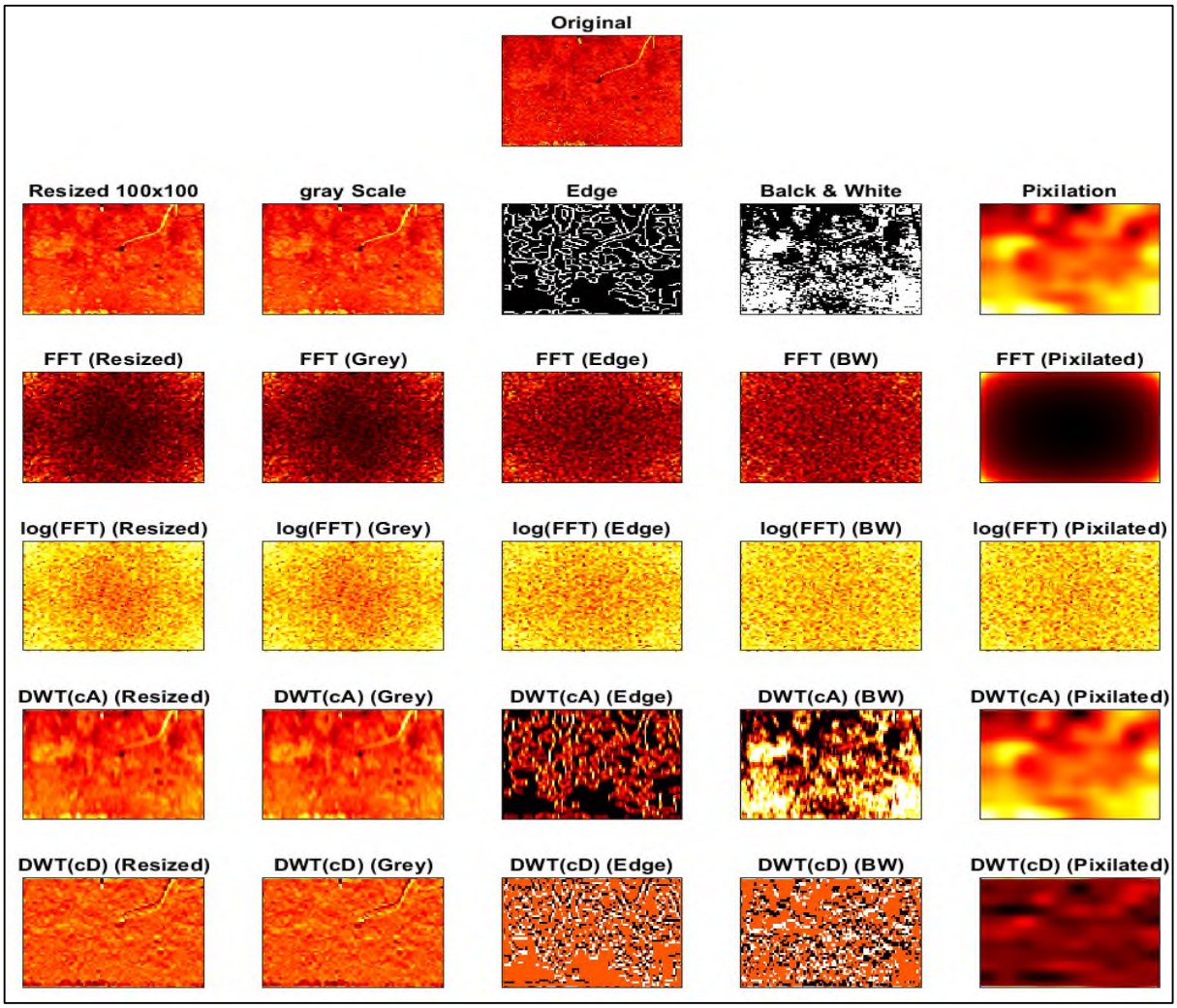

Figure 5.8: Illustration of various CFs on unreinforced slope at the start of experiment

In contrast, Figure 5.9 shows the corresponding characteristic images for the reinforced slope. The visual comparison reveals significant variations between the same types of slopes, with

and without the inclusion of sand piles. This observation highlights the evident impact of sand pile reinforcement on the slope's deformation characteristics during the initial phases of the experiment. The detailed analysis of these images and associated features provides valuable insights into the efficacy of sand pile inclusion in influencing and mitigating slope deformations under the influence of rainfall infiltrations.

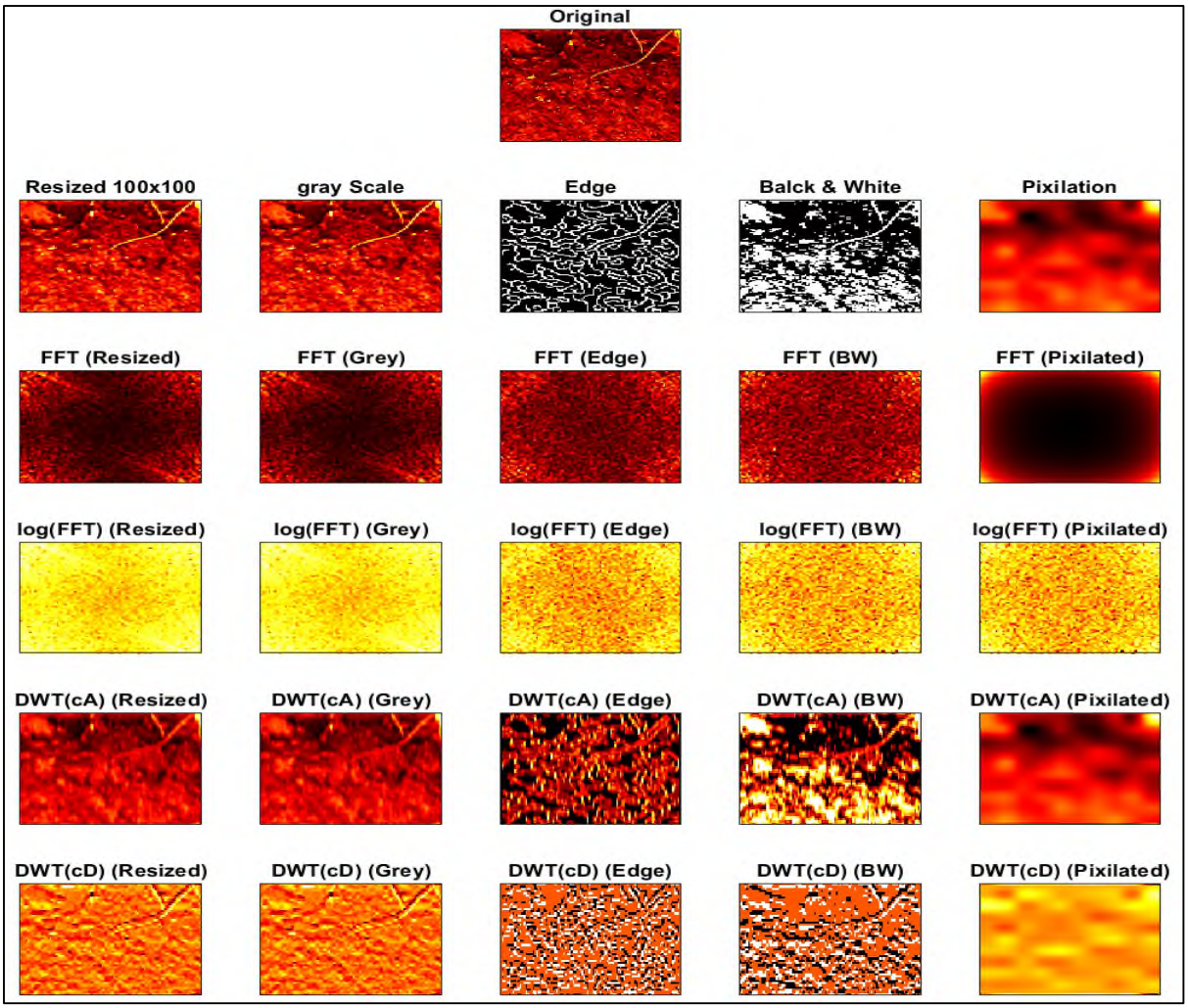

Figure 5.9: Illustration of various CFs on reinforced slope at the start of experiment

In Figure 5.10 and Figure 5.11, 25 characteristic images each are presented for the unreinforced slope and reinforced slope, respectively. These images capture the later stages of the experiment, characterized by a substantial amount of rainfall infiltration into the slope and consequent significant soil movement. The visual representation vividly portrays the impact of rainfall-induced deformations on both types of slopes. Crucially, the influence of sand piles in mitigating soil movements within the slope is readily apparent in both sets of characteristic

images. The comparative analysis suggests that the inclusion of sand piles has a discernible effect in reducing soil movements, indicating a positive influence on the slope's stability during the later stages of the experiment. These images serve as a visual testament to the efficacy of sand pile reinforcement in minimizing the impact of rainfall-induced deformations and enhancing the overall performance of the slope.

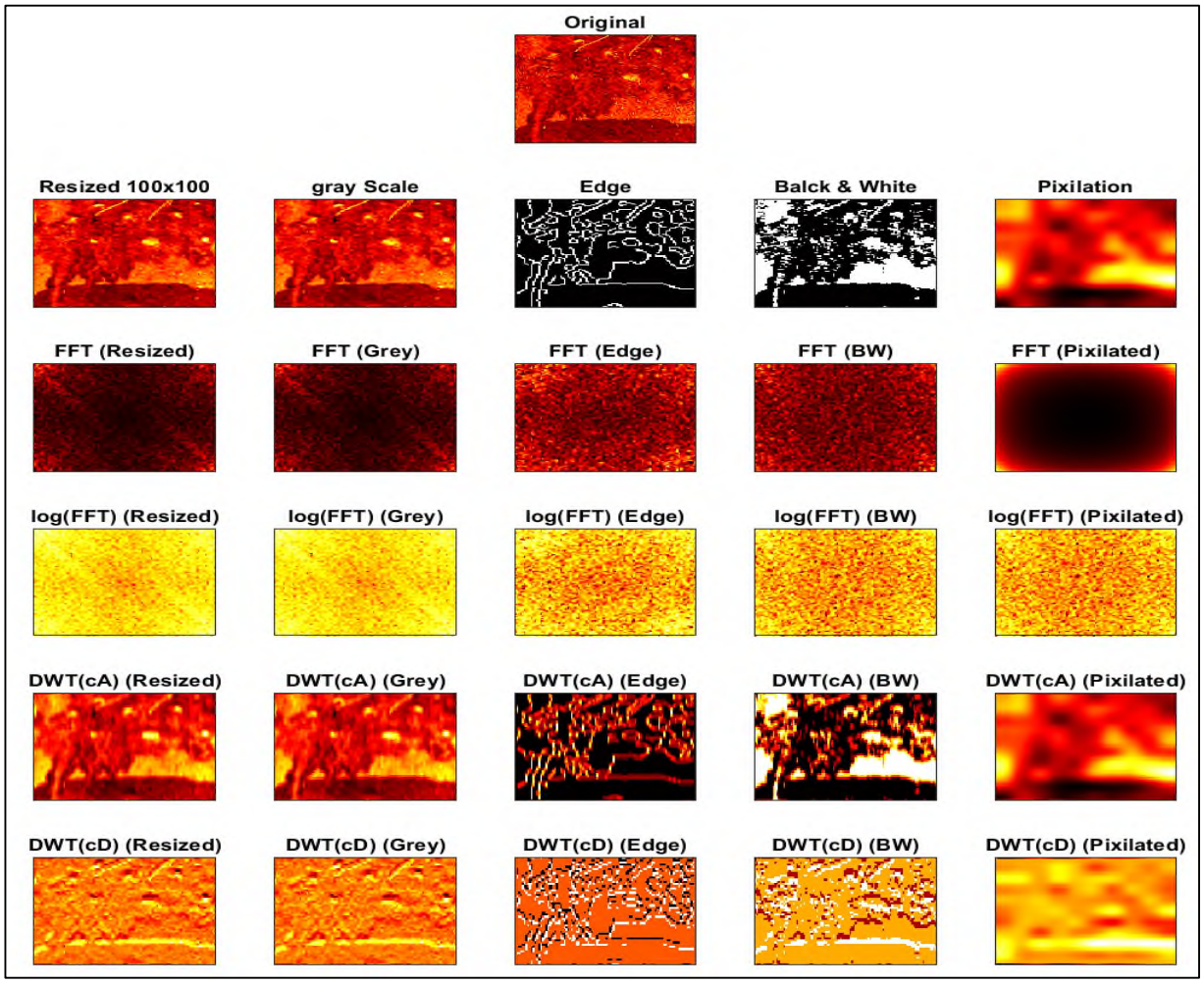

Figure 5.10: Illustration of various CFs on unreinforced slope at the end of experiment

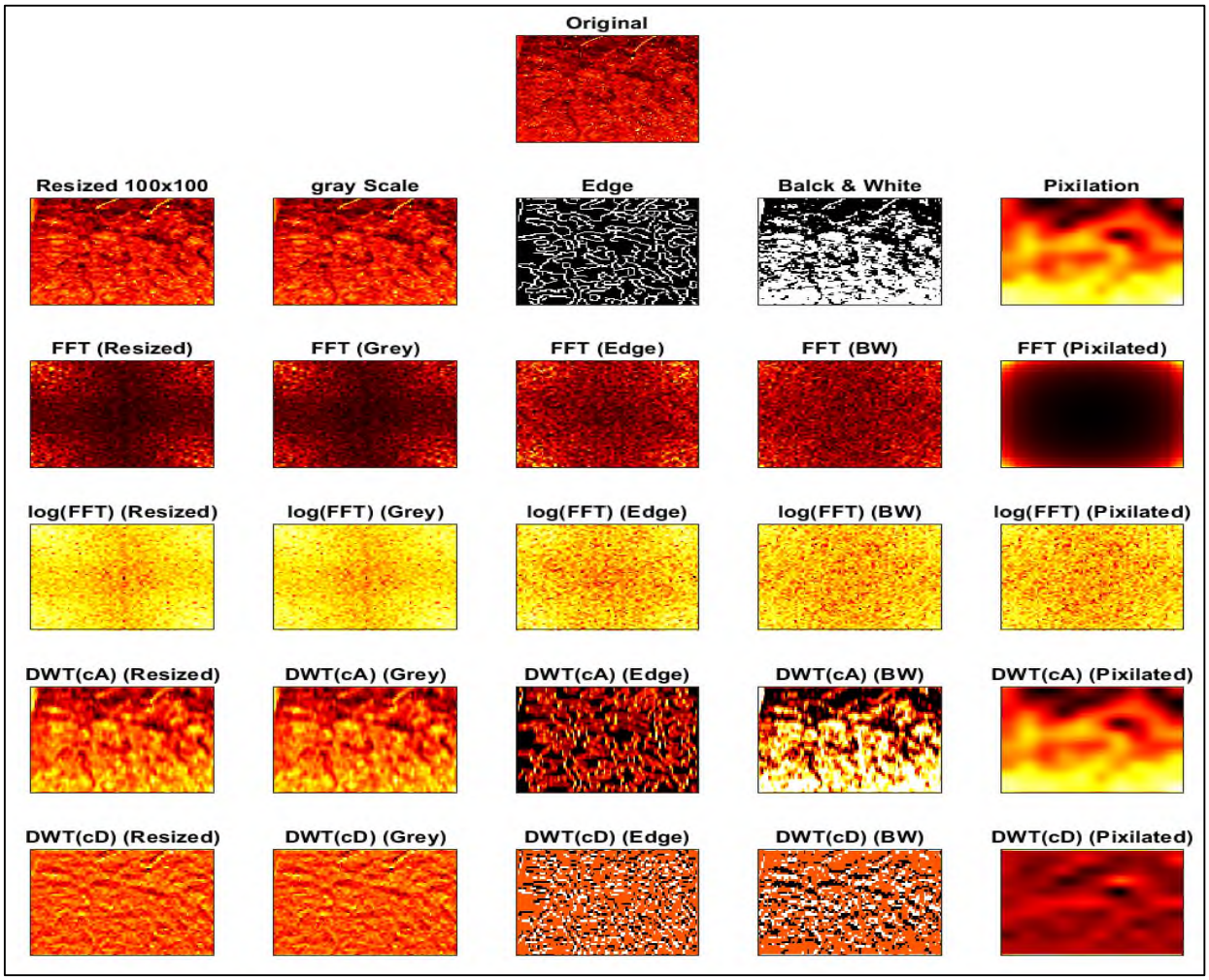

Figure 5.11: Illustration of various CFs on reinforced slope at the end of experiment

Figure 5.12 provides a comprehensive comparison of Feature 1 (maximum),, depicting maximum values, for both experimental conditions: the unreinforced slope and the slope reinforced with sand piles. A total of 600 frames were extracted from each experiment to facilitate a thorough comparative analysis. The interpretative key lies in understanding that higher values on the graph correspond to more pronounced slope movements, while lower values signify comparatively minimal slope movements. During the initial phases of the experiment, when the slope was either partially saturated or dry, the infiltration of rainfall triggered the erosion of soil particles, leading to higher Feature 1 values in both experiments. This phenomenon is attributed to the increased surface changes on the slope, evident in the numerous peaks observed. As the experiment progressed to later stages, the settling of soil particles resulted in a stabilization of slope conditions, leading to a decline in Feature 1 values. Significantly, towards the end of the experiment, a marked discrepancy in values becomes

evident. In the unreinforced slope, Feature 1 (maximum), values remain higher compared to the slope reinforced with sand piles. This noticeable difference highlights a significant reduction in deformations within the slope reinforced with sand piles, implying enhanced stability.

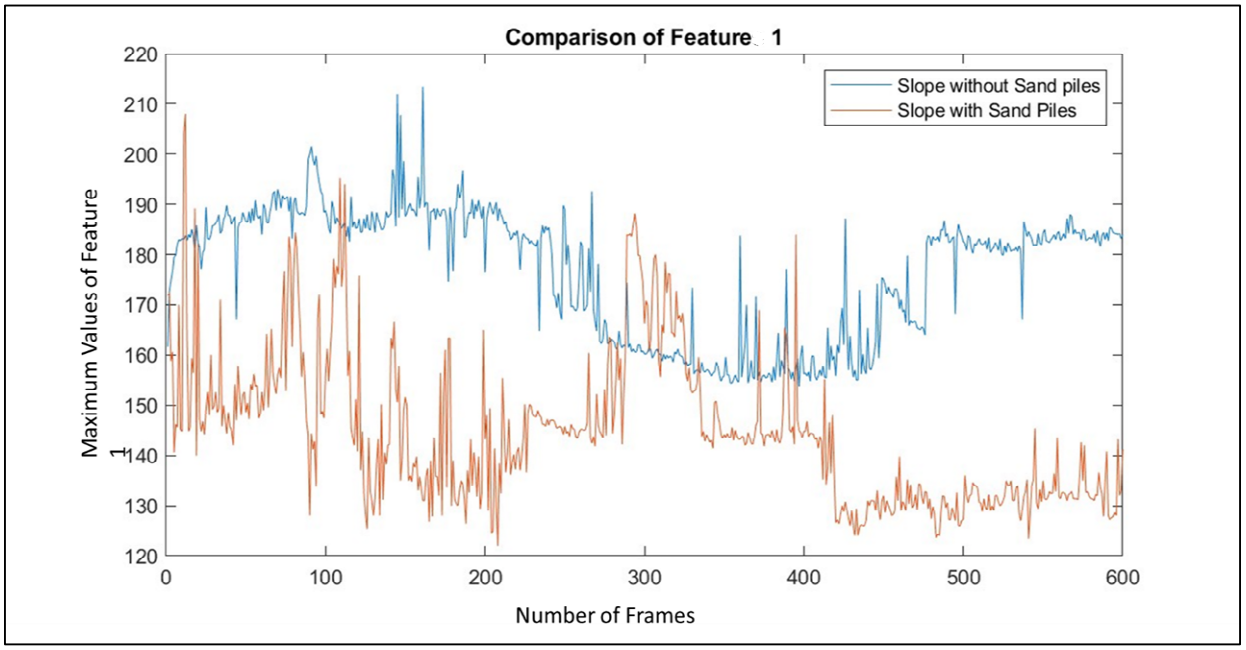

Figure 5.12: Comparison of CFs-1 (maximum) value for un-stabilised and stabilised slope

In Figure 5.13, a detailed comparative analysis is presented, focusing on Feature 9 (Skewness) concerning images numbered 5 (pixelations) for both experimental conditions – the unreinforced slope and the slope reinforced with sand piles. Skewness, a statistical function, provides insights into the symmetrical behaviour of a dataset. The features extracted from the image processing procedures exhibit as numerical sets, and skewness serves as a crucial metric for understanding the distribution's symmetry. The interpretative framework hinges on the following guideline:

- Wen skewness falls between -0.5 and 0.5, the data are considered fairly symmetrical;
- If skewness ranges between -1 and -0.5 or between 0.5 and 1, the data exhibit moderate skewness;
- When skewness is less than -1 or greater than 1, the data are deemed highly skewed.

In cases where the data distribution is skewed to the left, the mean tends to be less than the median, while in right-skewed distributions, the mean is generally greater than the median. Symmetric distributions anticipate the mean and median to be roughly equal. Analysing Figure

5.13 reveals that the majority of data points lie between -0.2 and 0.4, indicating highly symmetrical data for both slopes. These finding underlines consistent variation at the top surface of the slope. Higher ‘mean’ values are indicative of more substantial changes in the feature, as observed in the unreinforced slope experiment. Conversely, lower ‘mean’ values signify fewer changes at the surface of the slope, characteristic of the reinforced slope. This observation aligns with the consistent trend in the skewness metric, providing valuable insights into the comparative stability and deformation characteristics of the two slopes under consideration.

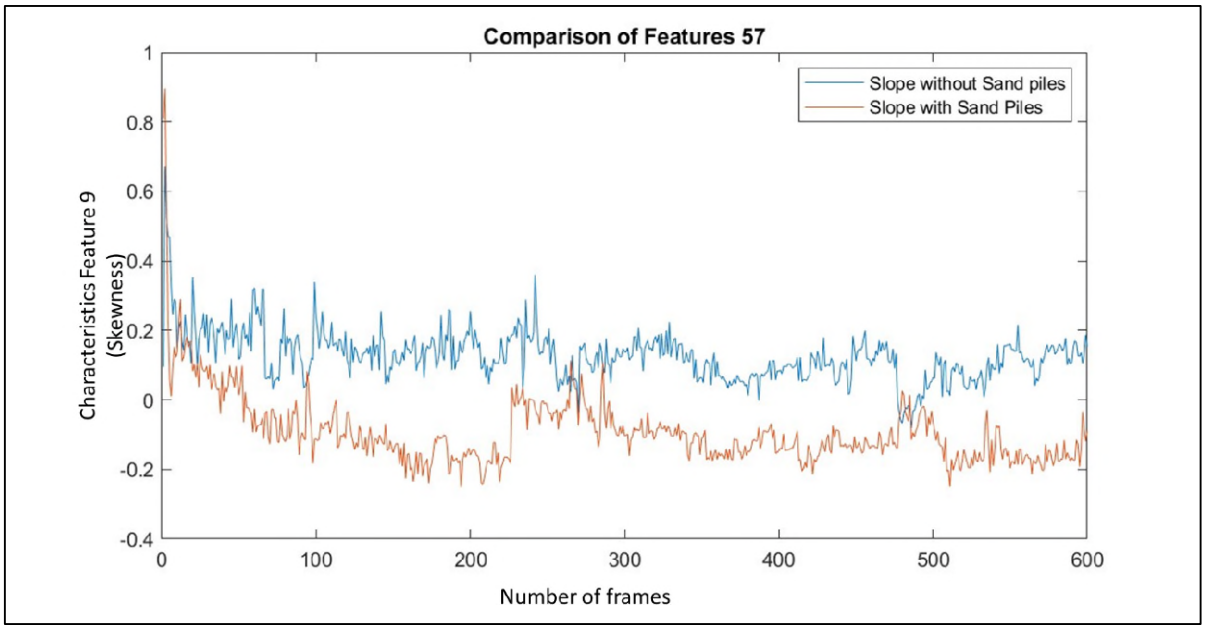

Figure 5.13: Comparison of CFs-9 (Skewness) value for un-stabilised and stabilised slope

Figure 5.14 through **Error! Reference source not found.** represents an in-depth comparison of CF-1 (maximum), CF-2 (Skewness), and CF-3 (standard deviation)—as observed in both unreinforced and reinforced slopes during the final stages of experimental investigations. To gain an in-depth understanding of the effectiveness of sand piles in slope stabilization, this analysis specifically focuses on the data from the last 100 frames captured during the final stages of both experiments. The comparison reveals a substantial difference in the magnitudes (values) of the characteristics features between the unreinforced and reinforced slopes. The numerical values summarized in these figures serve as quantitative markers of the surface characteristics, distinctly illustrating the consequential differences in slope stability. The predominant trend is clear: higher values are indicative of notable surface variations, a signal

of diminished stability, while lower values point to a more stabilized slope surface, evidenced by reduced variations.

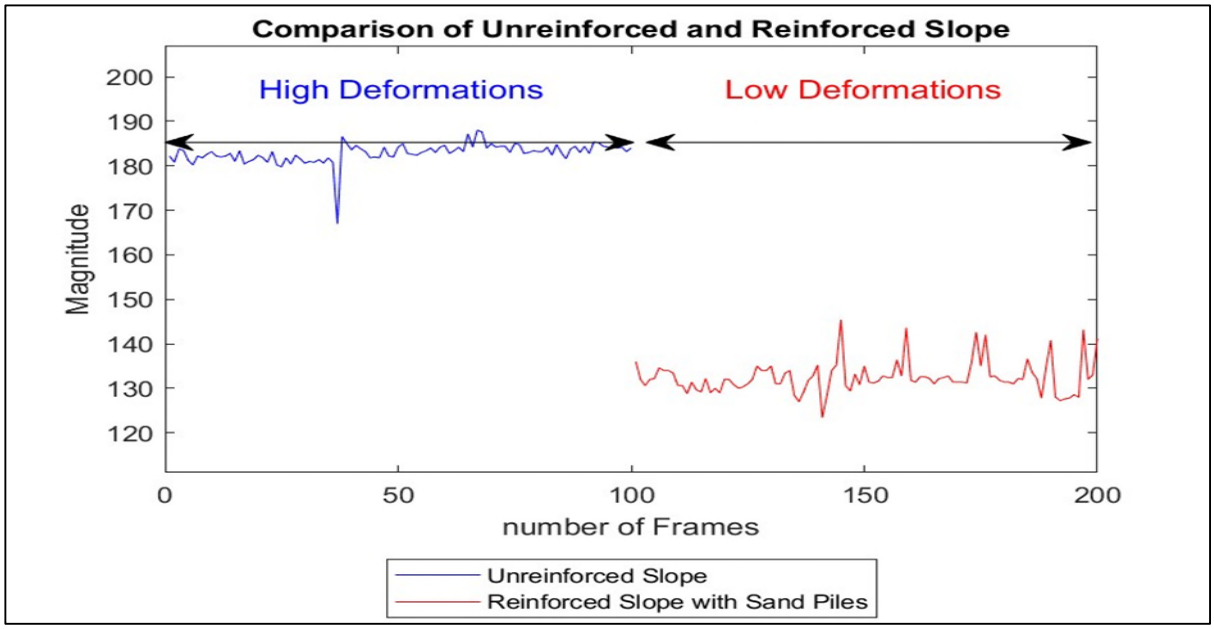

Figure 5.14: Comparison of CFs-1 (maximum) value for un-stabilised and stabilised Slope

Importantly, the figures illuminate the significant influence of sand piles on slope stability. As the comparison navigates through the last 100 frames of the experiments, the visual narrative coherently conveys the mitigating impact of sand piles on the surface variations. In essence, the incorporation of sand piles contributes to a noticeable reduction in surface fluctuations, effectively enhancing the overall stability of the slope. This empirical observation underscores the role of sand piles as a viable and efficacious reinforcement strategy in geotechnical engineering practices. This comparative assessment further validates the knowledge that the unreinforced and reinforced slopes, as illustrated by CF-1, CF-2, and CF-3, are characterized by distinct surface behaviour. The dynamic interaction between these characteristics and the presence of sand piles becomes clearly evident. The combination of these features affirms that the introduction of sand piles into the slope architecture plays a pivotal role in modifying the surface topography, thereby contributing to stability. In the broader context of geotechnical engineering, where slope stability is of paramount importance, these findings assume considerable significance. The reinforcement strategy involving sand piles, as explained by the numerical values and graphical representations in Figure 5.14 through **Error! Reference source not found.**, underscores its potential as a transformative approach. The evidence

presented here highlights the impact of sand piles on slope stability, thereby enhancing understanding and affirming their practical relevance in real-world applications. This exploration adds a layer of depth to the surrounding slope stability, providing valuable insights for researchers, engineers, and practitioners in the field.

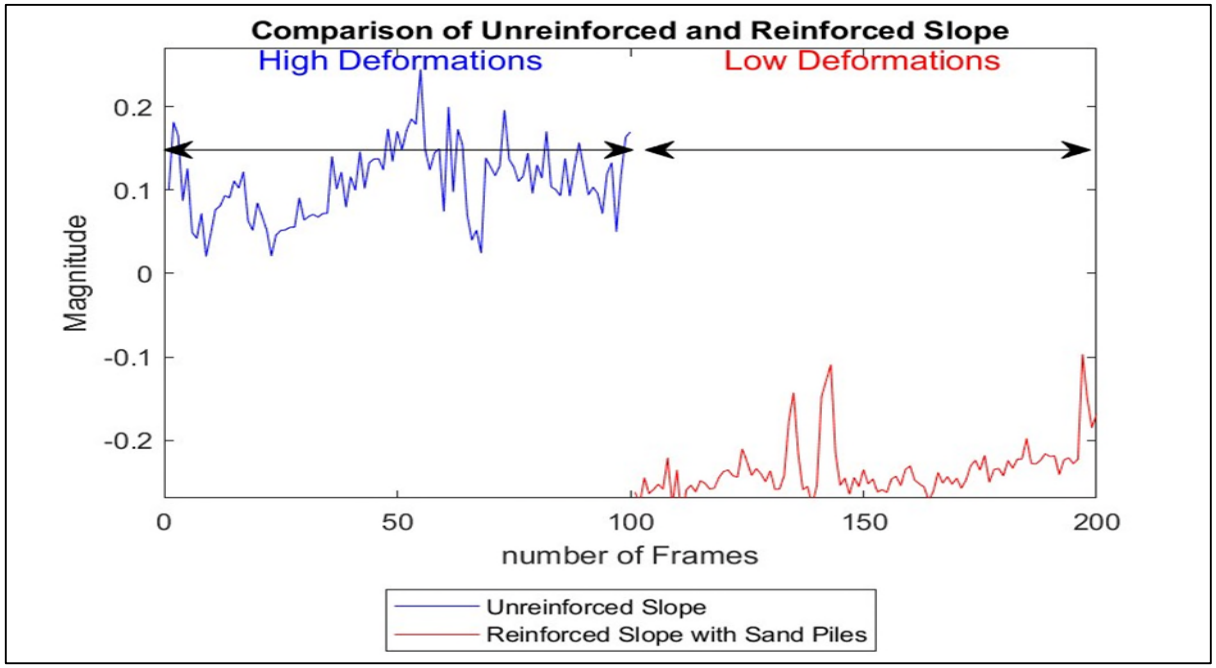

Figure 5.15: Comparison of CFs-9 (Skewness) value for un-stabilised and stabilised Slope

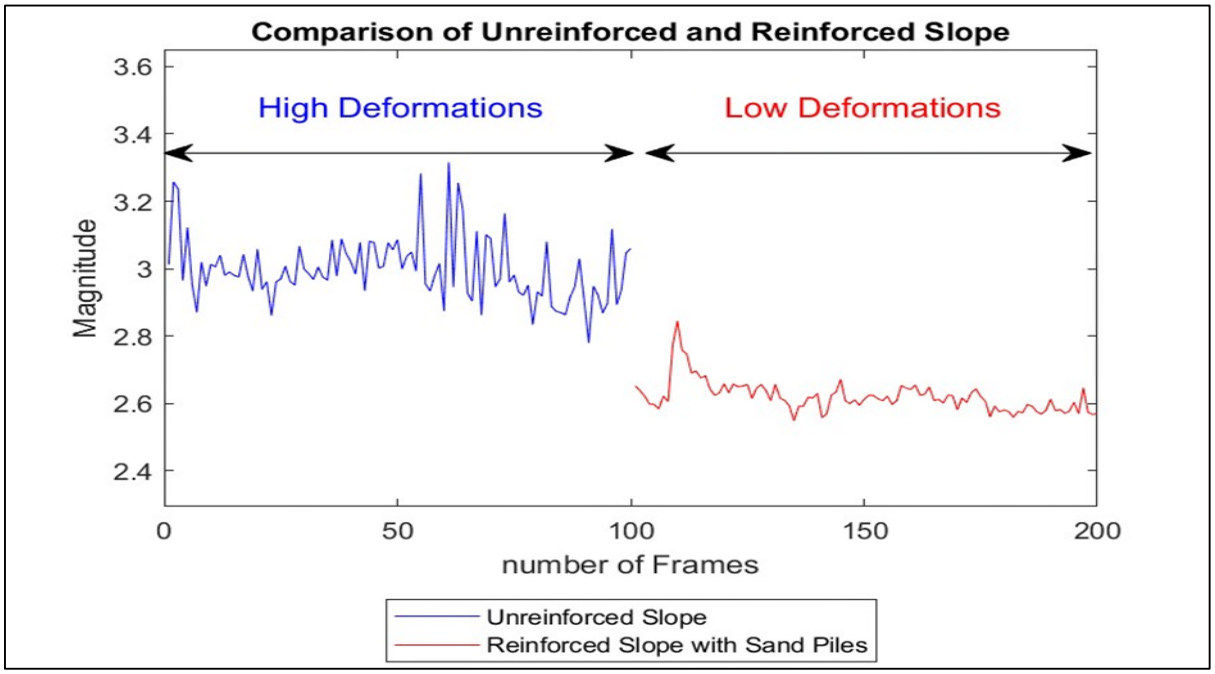

Figure 5.16: Comparison of CFs 4 (Standard Deviation) value for un-stabilised and stabilised Slope

5.6 Discussion on Results

In addition to slope geometry, rainfall infiltration emerges as a critical and influential factor significantly contributing to slope failures. Prolonged rainfall events trigger these failures by saturating the soil slope, thereby diminishing its shear strength and precipitating instability. While continuous and long-term slope monitoring during rainfall events is imperative, practical constraints such as cost, accuracy, and data interpretation associated with traditional instrumentation render it unfeasible. To overcome these challenges, an innovative approach, termed the ASPS approach, was conceptualized and tested in this study. The methodology involves capturing images throughout the entire duration of a laboratory-based small-scale slope model subjected to controlled artificial rainfall infiltration. These images are subsequently processed using the MATLAB tool, applying various mathematical equations to derive characteristics features that unveil variations on the slope surface. The observation post-processing revealed that certain features are less effective in gauging soil deformation, whereas others distinctly showcase variations on the slope surface, serving as clear indicators of soil movements during rainfall events. The study progressed through two phases: initially, the slope underwent testing without any stabilization, and subsequently, the slope was stabilized with strategically placed sand piles. Figure 5.17 illustrates the failed slope after rainfall activity of 60mm/hr lasting for 24 hours. Visible surface deformation and erosion can be noted in the upper layers of the slope. This is indicative of water infiltrating the soil, reducing its shear strength, and causing surface material to move downslope. The uneven surface and indentations indicate areas where potential slip surfaces may develop. These areas of localized deformation could be precursors to larger-scale slope failures. Monitoring these regions is crucial for predicting when and where a major slope failure might occur. The formation of failure surfaces is crucial in understanding slope stability. Rainfall infiltration can significantly affect these surfaces by reducing soil shear strength due to increased pore water pressure. Studies have shown that heavy rainfall can lead to the formation of deeper failure surfaces, especially when the rainfall intensity exceeds the soil's permeability. In such scenarios, the slope material becomes saturated quickly, leading to rapid failure initiation and deep-seated slide planes. Experiments and numerical simulations demonstrate that as rainfall intensity increases, so does the rate of surface erosion. This erosion can form channels and gullies, which concentrate runoff and further exacerbate slope instability. For instance, the migration of fine particles due to rainfall can alter the hydraulic properties of the soil, making it more prone to

erosion and subsequent failure (Aqib et al. 2023; Cheng et al. 2024; Yang, Huang 2023; Dai et al. 2024).

Figure 5.17: Top surface of an unstabilized slope after failure

Yang, Huang (2023) conducted an experimental study on slope stability and investigate how different rainfall intensities impact the infiltration behavior and stability of unsaturated soil slopes. The experiments revealed that the infiltration rate is significantly influenced by rainfall intensity, with higher intensities causing more rapid saturation of the soil, especially at the toe of the slope. This increased saturation leads to a wetting front that progresses upwards towards the crest. At lower rainfall intensities (80 mm/h), the slope exhibited a gradual increase in soil saturation, primarily affecting the slope's surface and causing moderate erosion. However, when subjected to higher rainfall intensities (160 mm/h), the slope experienced a significant increase in surface runoff due to the soil's low hydraulic conductivity. This high-intensity rainfall led to severe erosion, particularly at the crest, resulting in the formation of deep gullies and more pronounced slope failures.

Figure 5.18 illustrates failure surface of stabilised slope with sand piles. In comparison with the unstabilized slope presented in Figure 5.17, which exhibited significant surface deformation

and channel formation due to soil erosion, the image showing the stabilized slope with sand piles demonstrates a relatively more stable surface despite the presence of water flow. The unstabilized slope appears uneven, with pronounced indentations indicating areas where material has been displaced. This is a typical response to high-intensity rainfall, where the lack of support and cohesion leads to the rapid removal of soil particles and the formation of failure surfaces. However, in Figure 5.18, the sand piles likely provide additional drainage and reinforcement, reducing the extent of surface erosion. The surface appears more uniform, and the formation of deep channels or gullies is less evident. This suggests that the sand piles help distribute the infiltrating water more evenly and prevent concentrated flow paths that can exacerbate erosion. The sand piles act as stabilizing elements, interrupting the development of continuous failure surfaces by reinforcing the slope material and providing additional drainage paths. This results in a more stable slope profile with fewer signs of imminent failure (Patel et al. 2018; Nasiri, Hajiazizi 2021; Zheng et al. 2020; Rashma et al. 2024). In summary, the use of sand piles has significantly improved the slope's stability under artificial rainfall conditions. The sand piles mitigate erosion, enhance drainage, and prevent the formation of deep failure surfaces, leading to a more uniform and stable slope surface compared to the unreinforced slope in the first image. These observations align with findings in the literature that emphasize the importance of slope reinforcement and drainage improvement in preventing rainfall-induced slope failures (C. Li et al. 2020; Liu et al. 2023; Ghorbani et al. 2021). Additionally, a case study on the stabilization of expansive soil using lime sand piles demonstrated that these piles effectively controlled soil erosion and improved slope stability. The study indicated that lime sand piles helped in maintaining the structural integrity of slopes by enhancing drainage and reducing soil expansion and contraction, which are critical factors in preventing slope failures (Latha et al. 2018). Furthermore, a review on sustainable reinforcing techniques indicated that sand piles, among other methods, provide crucial reinforcement that improves the overall stability of slopes by offering additional drainage paths and increasing the soil’s shear strength. This reinforcement helps in mitigating the impact of heavy rainfall and preventing erosion. sand piles act as vertical drains, facilitating the removal of excess pore water pressure, which is critical during and after rainfall events. By improving drainage, sand piles reduce the risk of slope failure, which is often caused by the rapid buildup of pore pressure in the soil (Sujatha et al. 2023). This aligns with the observations from the experimental images where the slope stabilized with sand piles exhibited a more uniform surface with less evidence of deep channel formation or significant erosion.

Figure 5.18: To surface of stabilised slope after failure

5.7 Summary

This study investigates the critical role of rainfall infiltration in slope failures and introduces an innovative ASPS approach for monitoring slope stability during rainfall events. Traditional instrumentation for continuous and long-term slope monitoring is often impractical due to high costs, accuracy issues, and data interpretation challenges. The ASPS approach involves capturing and analyzing images of a small-scale slope model subjected to controlled artificial rainfall using MATLAB, effectively identifying soil deformation and variations on the slope surface, indicating potential failure zones.

The study was conducted in two phases: first, testing an unstabilized slope, and second, a slope stabilized with sand piles. The geometry of the slope and key parameters, including rainfall intensity, duration, and the dimensions of the sand piles, were optimized based on numerical

studies. To validate simulation results, moisture profiles of both the stabilized and unstabilized slopes were drawn, and piezometers were installed to measure pore water pressure within the slope. The findings indicated a noteworthy reduction of 18% in moisture content for the sand pile-reinforced slope compared to the unreinforced slope. This reduction underscores the efficacy of including sand piles, as they provide drainage pathways for water within the slope, diminishing pore water pressure. Consequently, this increase in matric suction stabilizes the slope, showcasing the potential of sand piles as a stabilizing measure against rainfall-induced slope failures.

Experimental results highlighted that higher rainfall intensities lead to rapid soil saturation, increased surface runoff, and severe erosion, especially at the slope crest. Sand piles provided additional reinforcement and drainage, reducing surface erosion and the formation of channels and gullies. The findings align with literature emphasizing the importance of slope reinforcement and drainage improvements in preventing rainfall-induced slope failures. The study concludes that sand piles effectively enhance slope stability under artificial rainfall conditions, mitigating erosion and maintaining a uniform and stable slope surface.

In essence, this study not only highlights the crucial role of rainfall infiltration in slope failures but also introduces a novel ASPS approach that overcomes the limitations of traditional monitoring. The successful integration of image processing, numerical simulations, and field measurements contributes to a comprehensive understanding of slope behavior during rainfall events, paving the way for innovative and effective slope stabilization strategies.

CHAPTER 6: CASE STUDY OF AZAD PATTAN ROAD LANDSLIDE - PUNJAB PAKISTAN

6.1 Introduction

The current study focuses on the failure of slopes composed of fine soil when subjected to rainfall events and their stabilization to reduce the risk of damages. In the first phase of this research, a detailed finite element analysis was conducted on slopes with varying inclination angles subjected to different rainfall activities lasting up to 96 hours. Subsequently, the slopes were stabilized with sand piles to assess the effectiveness of this stabilization technique. To validate the finite element analysis results, a small-scale laboratory slope was tested under the optimized parameters obtained from finite element analysis. The primary focus was on slopes composed of fine soils, as they are prone to failure under rainfall conditions. To further validate the findings from the finite element and laboratory tests, a real-life slope was selected as a case study. This slope, consisting of similar soil types, was located in a region with high rainfall. The geographical details and site conditions are described in the following sections.

6.2 Azad Pattan Road Landslide

Azad Kashmir is situated in geologically active regions, rendering it vulnerable to significant devastation caused by earthquakes. The Northern regions of Pakistan, including Azad Jamu and Kashmir (AJK), are regarded as highly vulnerable locations globally due to variables including fragile geological layers, intense monsoon rains, snowfall, steep slopes, and seismic activity (Basharat et al. 2016). Multiple studies (Basharat and Rohn, 2015; Ali et al. 2019; Shafique et al. 2016) have recorded many landslides that occurred in Kashmir because of the 2005 earthquake. These landslides caused a substantial number of fatalities, as reported by (Petley et al. 2005). One of the noteworthy incidents was the Hattian Bala landslide located in northern area of Pakistan. Significant casualties occurred in the Balakot region, which is near to the research site, as a result of extensive landslides (Jadoon et al. 2015). The occurrence of landslides in the research region presents hazards to human lives, communication infrastructure, buildings/structures, and industry. Consequently, the process of hazard zonation/susceptibility mapping is of utmost importance in predicting landslide occurrences, enabling the adoption of plans, preparedness, and administration to minimise significant harm. Geotechnical engineers have difficulties when evaluating the stability of soil slopes created by cutting into the ground for road building purposes, particularly along national roads and in mountainous regions. The main goal is to reduce the danger of slope collapse in road design,

with the purpose of preventing casualties and damage to infrastructure (Rafek et al. 2016). Although landslides along several highways in Azad Kashmir provide a substantial danger, there have been few studies conducted on key areas, particularly along the roadways in this region.

6.3 Site Location and Geology

Azad Jammu and Kashmir, located in the Northwestern region of the Himalayas, has borders with China, Pakistan, and India. Spanning 13,297 Square kilometers, it had a population of Around 4 million individuals in the year 2017. The area, being a constituent of the youthful Himalayan mountain range, undergoes intense overburden stress conditions, resulting in the formation of extensively compressed and deformed zones. The region is mostly made up of sedimentary rocks that form the outer layer of the Indian plate. It is known for its geological intricacies (Wadia 1928). Figure 6.1 presents the location map of Azad Pattan landslide.

Figure 6.1: Location Map of Azad Pattan Landslide

The slope in issue is situated on the Azad Pattan - Rawalakot Highway, which serves as a crucial thoroughfare linking the Poonch, Haveli, Bagh, and Kotli districts of AJK. The slope experienced collapse after a rainstorm event, as seen in Figure 6.2. The slope is composed of greenish-grey sandstone, siltstone, and mudstone. The sandstone on the slope is characterised by large layers and a texture that ranges from medium to coarse-grained. The geological makeup of the slope increases its susceptibility to instability. Figure 6.3 shows the soil profile of the slope area where it can easily be seen the different layers of clay, sandstone, and shale.

Figure 6.2: Azad Pattan Slope

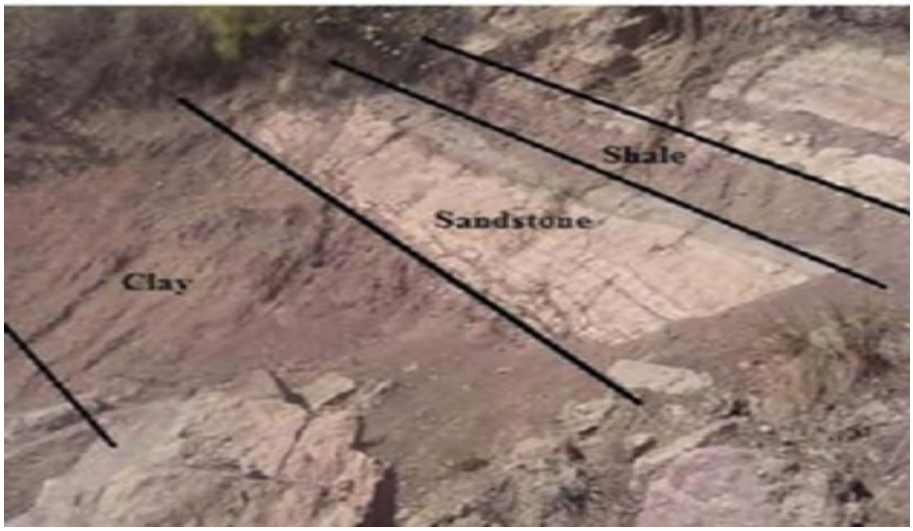

Figure 6.3: Soil Profile of Azad Pattan Slope (Islam, 2006)

6.4 Analysis of Rainfall Data

The annual rainfall data was collected from the weather stations installed in the surrounding areas of Azad Pattan Road. Figure 6.4 presents the rainfall data from 1970 to 2020. The average annual rainfall recorded was 1700 mm per year. Various rainfall scenarios were designed to simulate the rainfall activities, which were 5mm/hour, 10mm/ hour, 20mm/ hour, 60mm/ hour, 90mm/ hour, and 120mm/ hour lasting for 1 hour, 03hours, 06hours, 12 hours, 24 hours, 48 hours and 96 hours which represents the typical rainfall scenarios during the whole year, for this study.

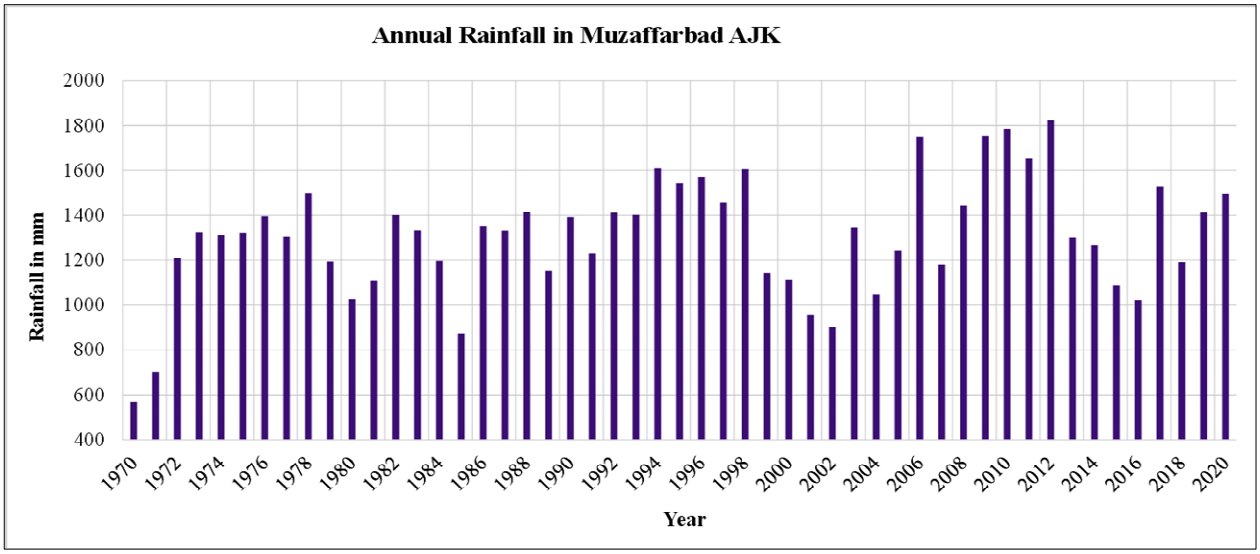

Figure 6.4: Rainfall data of Surrounding Areas of Azad Pattan Slope (Source: Pakistan Meteorological Department, 2020)

6.5 Material Type and Index Properties

The basic soil properties were calculated based on the investigations carried out by different geotechnical contractors in the local vicinity. Those properties included the classification, shear strength, and hydraulic properties which were summarized and repented in Table 6-1whilst the strength properties of sand material, used for piling is presented in Table 6-2. Some parameters were calculated/taken, based on those data collected from investigation reports, such as permeability coefficient (k), consolidation parameters, internal friction angle (φ) Young Modulus (E), and the Poisson Ratio (ν) from Table 2-3, Table 2-5, Table 2-6, Table 2-7 and Table 2-8 of Foundation Analysis and Design by (Bowles 1988) respectively.

Table 6-1: Index and strength properties of soil

Soil Type	Silty Clay with low plasticity
Average moisture content (%)	10.23
Specific gravity	2.66
Liquid Limit (%)	31
Plastic limit (%)	9
Plasticity Index	22
Unsaturated unit weight (kN/m^3)	16.50
Saturated unit weight (kN/m^3)	18.70
Initial void Ratio	2.4
Young's Modulus (MPa)	25
Poisson's Ratio	0.30
Cohesion (kPa)	20
Friction angle (degree)	21
K_x (cm/sec)	3.74E-06
K_y (cm/sec)	3.74E-06

6.6 Slope Modelling

Numerical modelling was used in the research to evaluate the factor of safety for the Azad Pattan slope. The user performed finite element analysis using PLAXIS 2D, a flexible software that allows for the study of coupled flow-deformation. This methodology takes into consideration the distortion and pore water pressure in soils that are fully saturated or partly saturated, while also considering the changes in hydraulic boundary conditions over time.

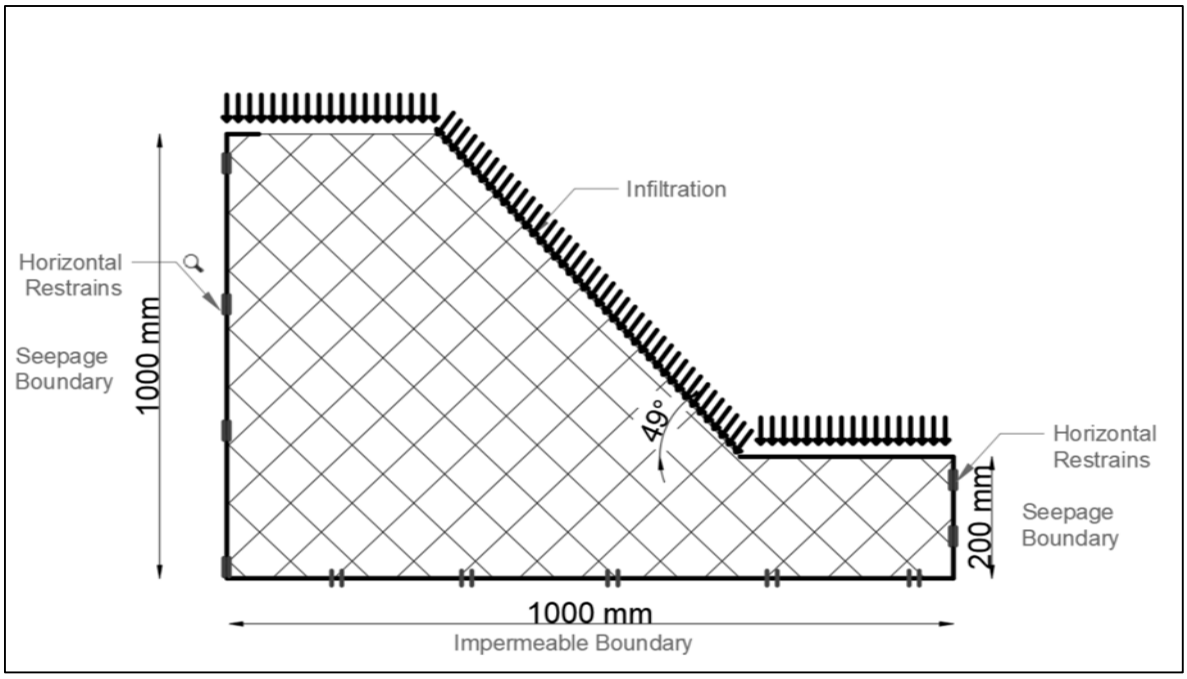

Figure 6.5: Schematic illustration of Slope Geometry with boundary conditions

The research used the Hardening Soil model, a sophisticated model capable of accurately reproducing the shear strength behaviour of unsaturated soil across different soil types. The model uses the notion of extended Mohr-Coulomb as proposed by (Rahardjo and Fredlund, 1993). In addition, the Soil Water Characteristic Curve (SWCC) was created to explain the hydraulic properties of groundwater flow in unsaturated areas. This was done using the model developed by (Van Genuchten, 1980) which is a commonly used method in groundwater research and is integrated in the PLAXIS software. After the investigation of failure mechanism, deformations, pore-water pressures, matric suction, and factor of safety, the model slope was stabilized with sand piles which also act as vertical drains. The sand piles were modelled as drains in PLAXIS, and interfaces were assigned to sand piles. The physical properties of sand material are presented in the Table 6-2. The Leighton Buzzard Sand was used as backfill material for sand piles and properties were taken from literature.

Table 6-2: Strength Properties of sand used for piles (Yang et al. 2012)

Unit weight kN/m^3	Stiffness kN/m^2	Poisson's ratio μ	Friction angle ϕ (°)	Cohesion kN/m^2	k_x (m/h)	k_y (m/h)
19	100	0.28	38	1	5.036E-3	5.036E-3

6.6.1 Slope Geometry and Boundary Conditions

Using the slope parameters presented in Table 6-1, the slope was modelled with boundary conditions shown in Figure 6.5. The bottom boundary was set to be impermeable Figure 6.6 (a-d) shows the typical undeformed and deformed mesh for studying the slope without and with sand piles stabilization. A significant change in the failure surface can be seen in the slope stabilized with sand piles.

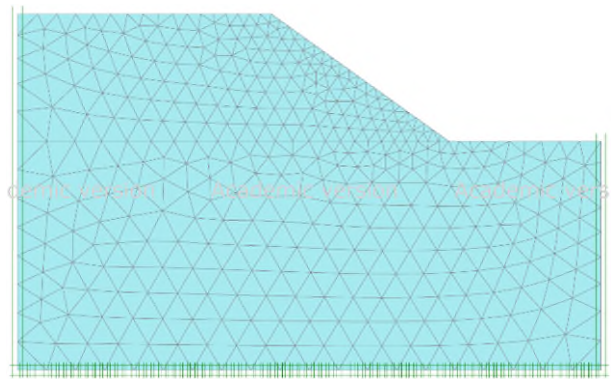

(a)

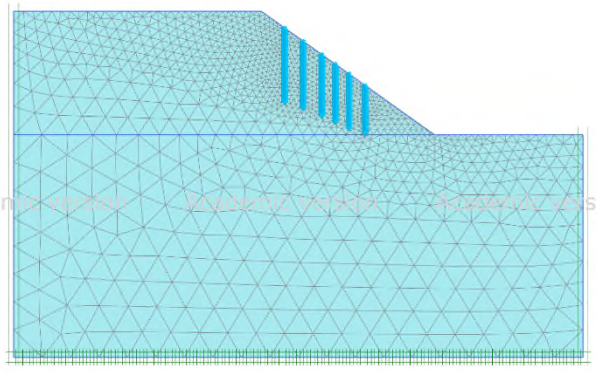

(b)

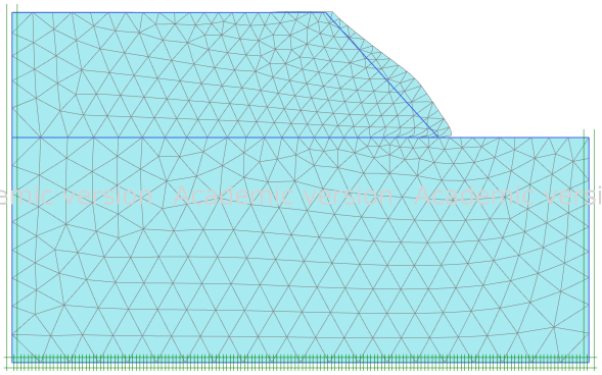

(c)

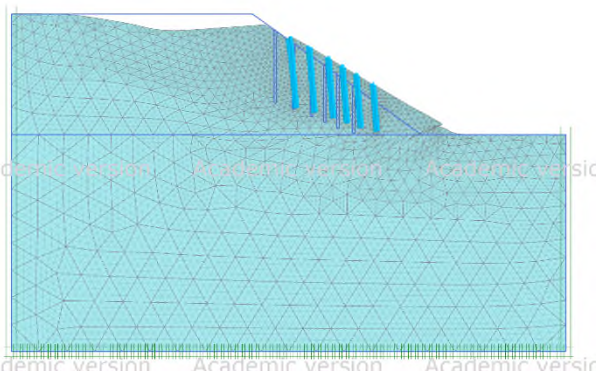

(d)

Figure 6.6: a) undeformed mesh without sand piles, b) undeformed mesh with sand piles, c) deformed mesh without sand piles, d) deformed mesh with sand piles

6.7 Results and Discussions

6.7.1 Effect of Rainfall on Matric Suction of the Soil Slope

Figure 6.7 presents the variation in matrix suction subjected to different rainfall intensities and time duration. At the start of the rainfall event (from 1 hour to 3 hours), the change in matric suction is not obvious, after that, there is a steep fall in matric suction. As the infiltration of rainfall water continued to increase, the soil matric suction decreased to a minimum level and became stable. Suction in the soil increased during dry periods and decreased during wet periods. The maximum change in suction occurred near the ground surface and the magnitude of the suction change decreased with depth. The reduction in suction after rainfall was observed to be a function of the initial suction just before the rainfall. It was observed that suction has been reduced up to 9.1 kPa against rainfall of 120mm lasting for 96 hours. The maximum suction value of 138.3kPa was recorded against 5mm rainfall lasting for 1 hour. After 96 hours of 5mm rainfall, the matric suction was reduced by 77%. For 10mm rainfall intensity lasting for 96 hours, the matric suction was reduced by 81%. Furthermore, 85.7%, 88.5%, 91.8%, and 92.47% of matric suction reduced for 20mm, 60mm, 90mm, and 120mm rainfall lasting for 96 hours respectively. In 171 below, it can be easily seen how matric suction varied with different infiltration rates and rainfall duration.

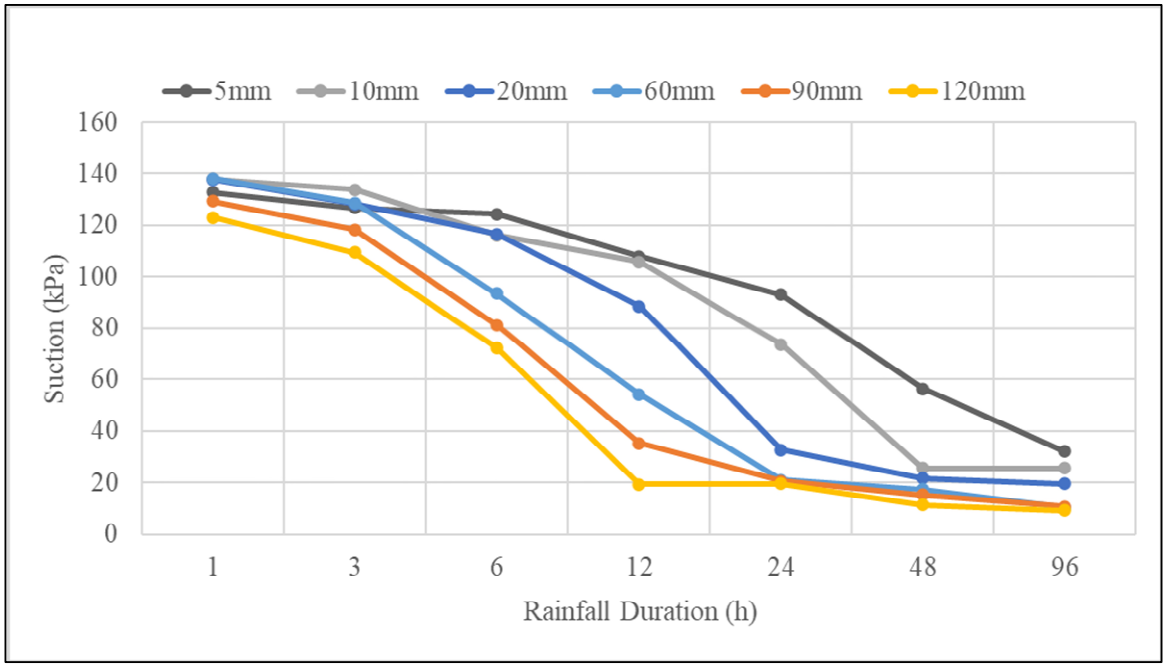

Figure 6.7: Variation in matric suction within slope under different rainfall duration and intensities

6.7.2 Strain Response of Slope During Rainfall

The variations of changes in total deformations, with low and high-intensity rainfall at different rainfall duration are presented in Figure 6.8. The highest deformation occurred with 120mm of rainfall lasting for 96 hours. With rainfall intensity of 5mm/hr for 96 hours, the maximum deformation was recorded as 15mm, while for 10mm/hr, 20mm/hr, 60mm/h, and 90mm/hr, the maximum deformations were recorded as 49.36mm, 59.52mm, 69.35mm, and 87.35mm respectively.

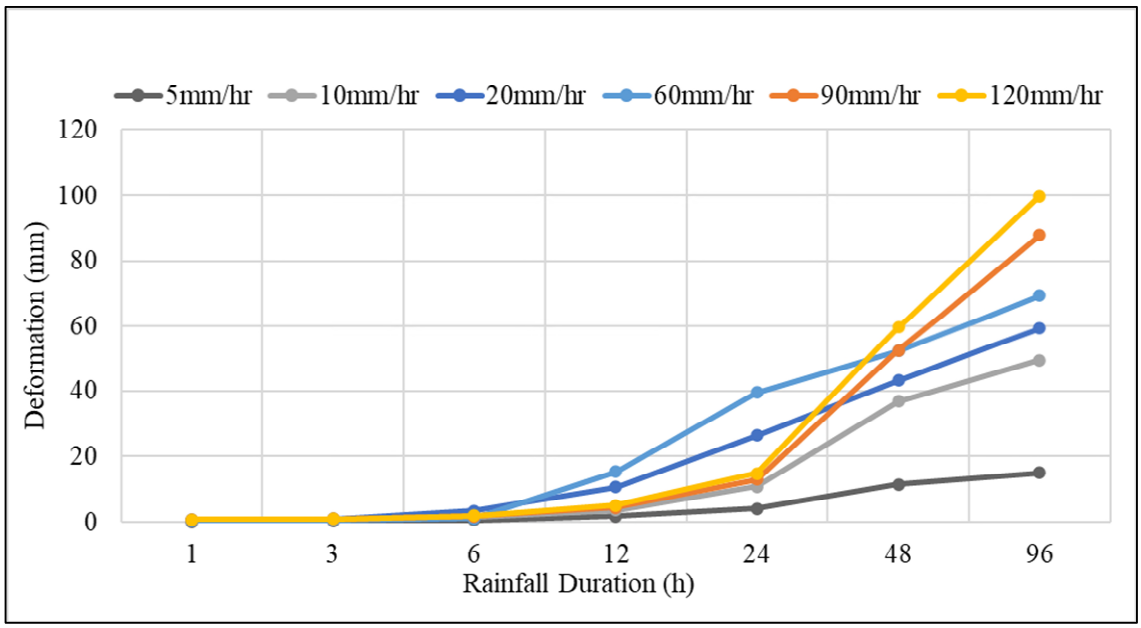

Figure 6.8: variation in total displacement within slope under different rainfall intensities and duration

6.7.3 Effect of Rainfall on Slope Stability

The factor of safety (FOS) is measured in PLAXIS in terms of available shear strength and strength at the time of failure. Figure 6.9 presents the factor of safety for the slope subjected to different rainfall intensities and rainfall duration. The minimum SF recorded was 1.11 against 120mm rainfall lasting for 96 hours. The initial factor of safety before the rainfall event was observed as 2.72, which was reduced up to 1.11 which is around a 60% reduction in the safety factor. Furthermore, the factor of safety was reduced by 17%, 24%, 36%, 43%, and 52% for 5mm, 10mm, 20mm, 60mm, and 90mm rainfall intensities lasting for 96 hours respectively.

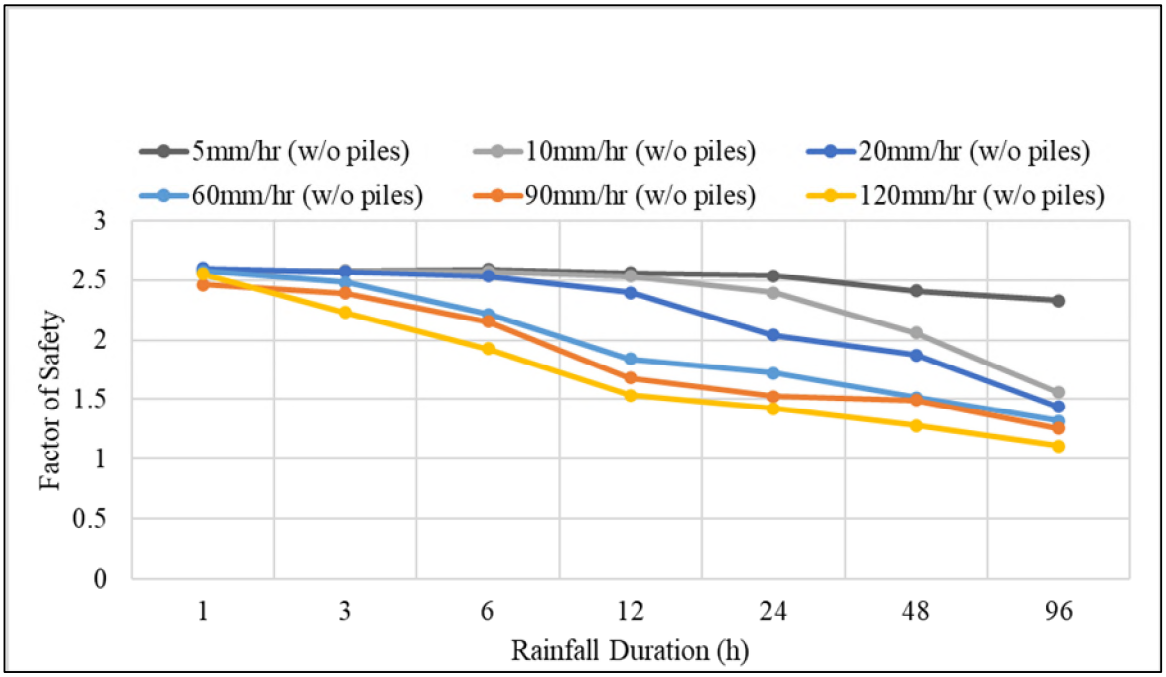

Figure 6.9: Change in safety factors of slope

The slip surface for the slope analysed under different rainfall intensities and duration was investigated. From FEM analysis results, it can be noted that the factor of safety is decreasing with higher rainfall intensities and longer duration. Moreover, based on the observations, the slope with low intense rainfall and less duration experienced a shallow slope failure condition, whilst the slope with high rainfall intensity and long duration experienced a deeper slip surface.

6.8 Comparison with Sand Piles and without Sand Piles

Figure 6.11 and Figure 6.11 presents the comparison of the factor of safety for the unstabilized and stabilized slope. Around a 30% increment in safety, factor was observed in the slope stabilized with sand piles as compared to the unstabilized slope. The minimum factor of safety for the unstabilized slope was recorded as 1.11, which increased up to 26% in slope stabilized with sand piles for a 120mm/hr rainfall event lasting for 96 hours.

Figure 6.12 and Figure 6.13 presents the comparison of matrix suction for unstabilized and stabilized slopes with sand piles. A significant improvement has been observed in the slope stabilized with sand piles. The suction in the slope, when stabilized with sand piles, has been reduced by 61% under 5mm rainfall lasting for 96 hours which is 16% less as compared with the slope without sand piles. similarly, for 10mm rainfall, the suction was reduced by 73% in

the slope stabilized with sand piles, which is 8% less than in the slope without sand piles. Furthermore, approximately a 6% to 8% increment was observed in matrix suction in the slope stabilized with sand piles. This is due to the granular material of sand piles with allows drainage to pore water and as a result, pore water pressure is reduced which leads to increasing in matric suction. Sand piles also referred to as sand columns or sand compaction piles have been proven as effective and efficient ground improvement techniques (Aboshi et al. 1991; Naseer et al. 2019; Ambily and Gandhi, 2007).

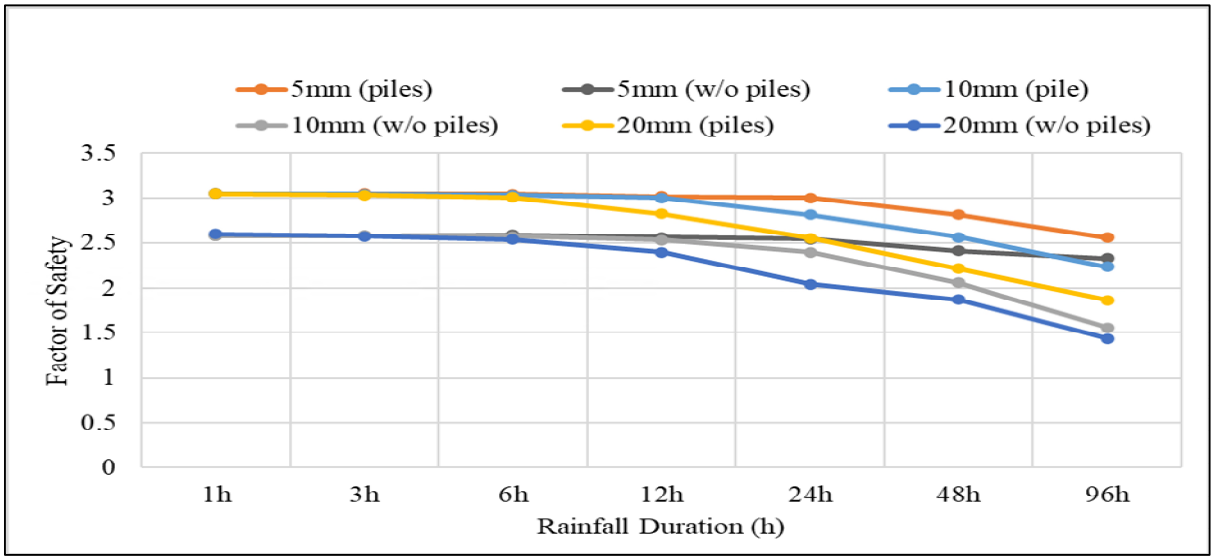

Figure 6.10: Comparison of Factor of Safety for un-stabilised and stabilised slope against 5mm/hr, 10mm/hr and 20mm/hr rainfall intensities lasting for 94 hours

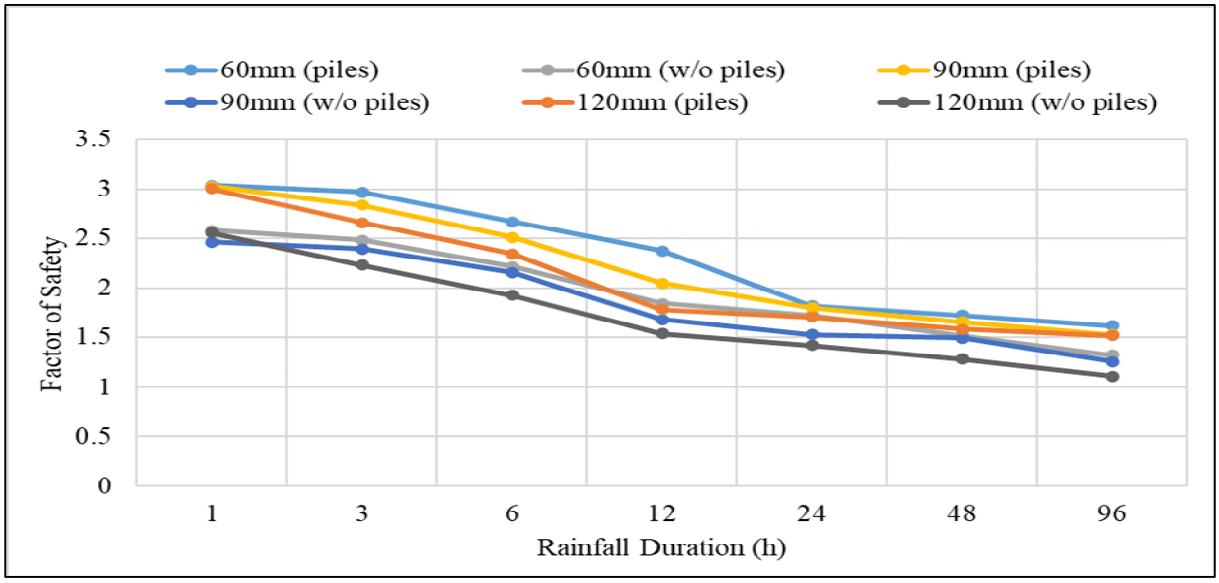

Figure 6.11: Comparison of Factor of Safety for un-stabilised and stabilised slope against 60mm/hr, 90mm/hr and 120mm/hr rainfall intensities lasting for 94 hours

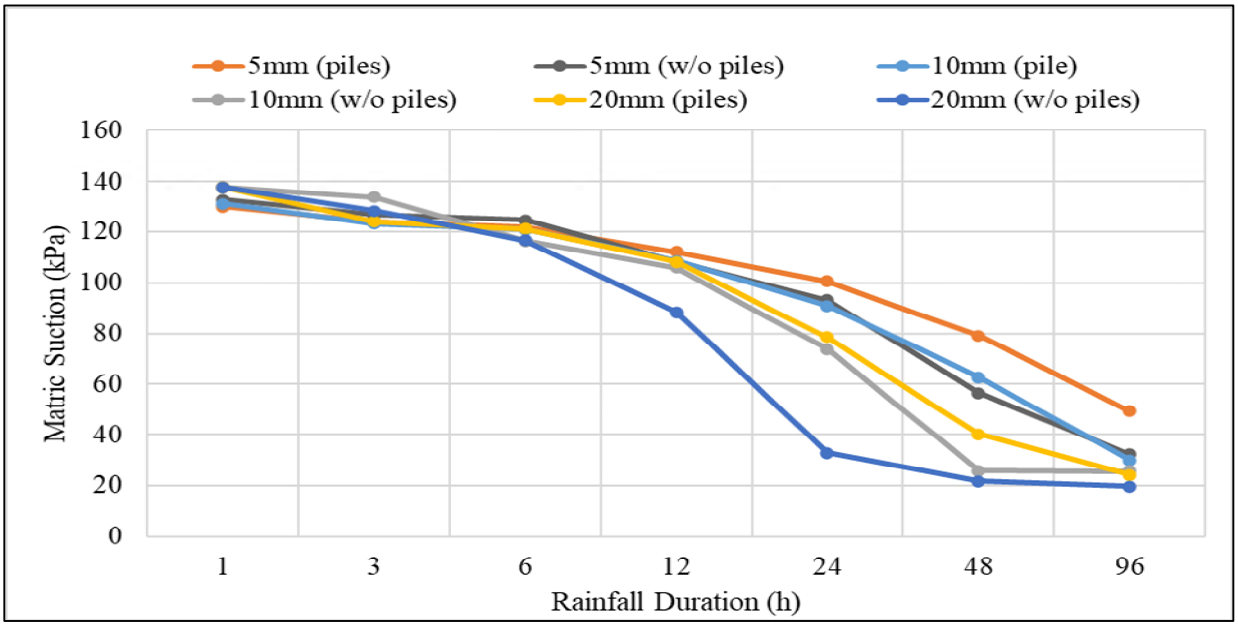

Figure 6.12: Comparison of Matric Suction for un-stabilised and stabilised slope against 5mm/hr, 10mm/hr and 20mm/hr rainfall intensities lasting for 94 hours

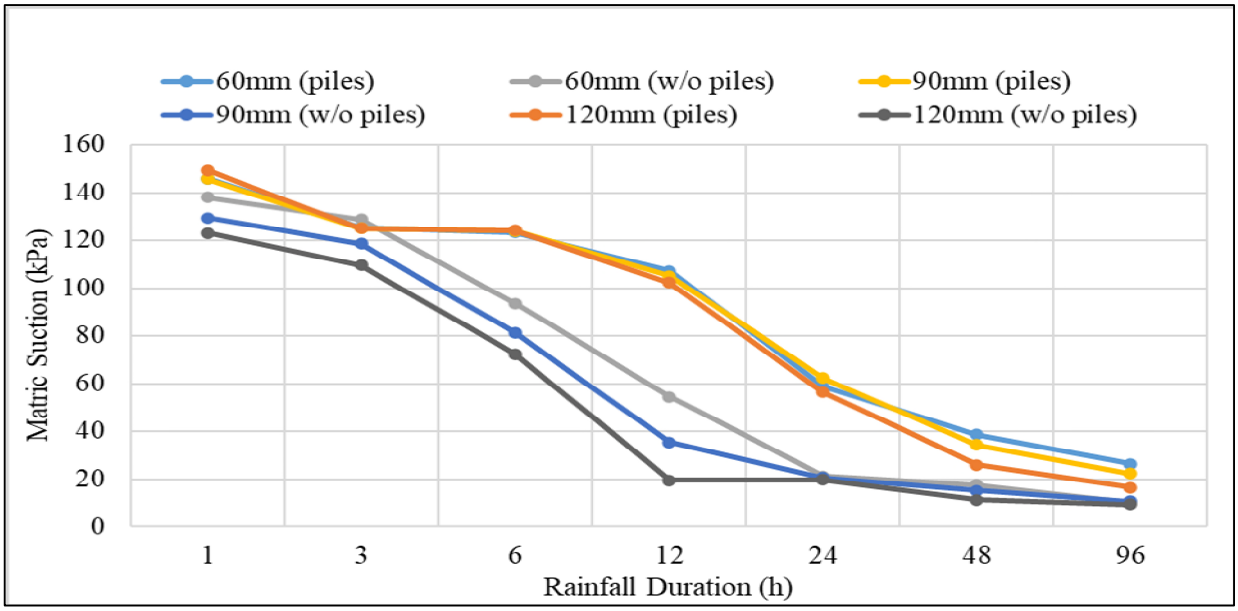

Figure 6.13: Comparison of Matric Suction for un-stabilised and stabilised slope against 60mm/hr, 90mm/hr and 120mm/hr rainfall intensities lasting for 94 hours

In Figure 6.14 and Figure 6.15, the comparison of total deformation in unstabilized vs stabilized slopes are presented. With the installation of sand piles, up to a 39% reduction in total deformation has been recorded. 10%, 30%, and 18% less deformation was recorded in slope stabilized with sand piles against 5mm/hr, 10mm/hr, and 20mm/hr rainfall respectively, lasting for 96 hours. Moreover, 39%, 34%, and 37% reduction in deformation was observed in slope subjected to 60mm/hr, 90mm/hr, and 37mm/hr rainfall respectively.

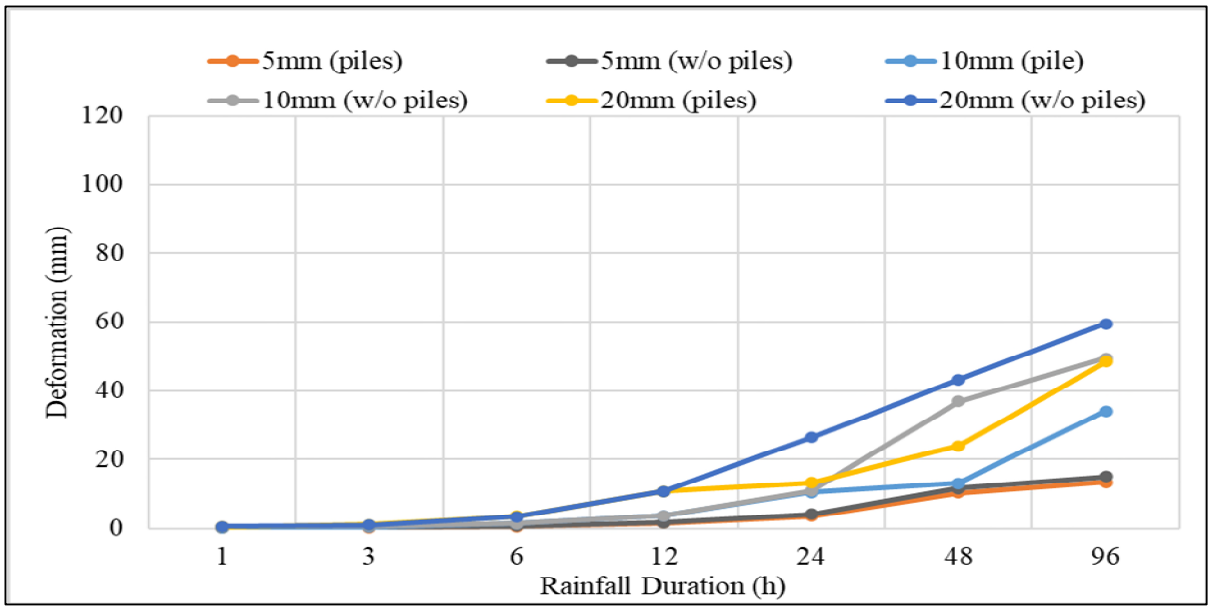

Figure 6.14: Comparison of deformations for un-stabilised and stabilised slope against 5mm/hr, 10mm/hr and 20mm/hr rainfall intensities lasting for 94 hours

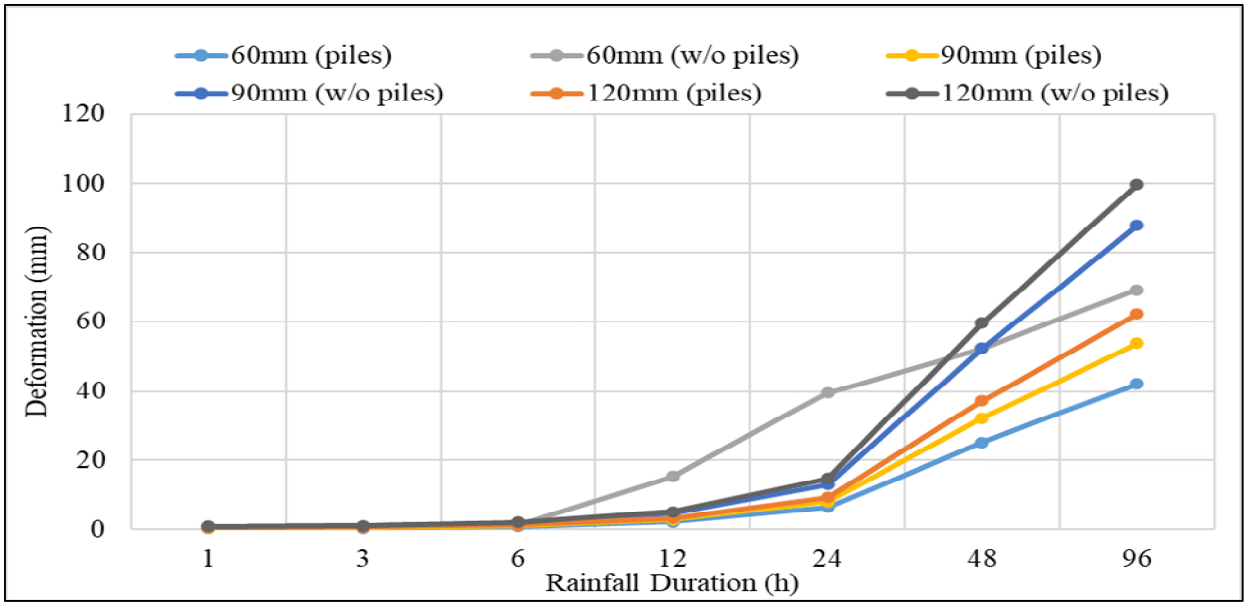

Figure 6.15: Comparison of deformations for un-stabilised and stabilised slope against 60mm/hr, 90mm/hr and 120mm/hr rainfall intensities lasting for 94 hours

6.9 Summary

The current study examines the relationship between soil slope stability and parameters such as the intensity and duration of rainfall. The numerical study of distinct soil slopes used consistent rainfall patterns of varying durations for analysis. This work used finite element calculations to calculate the water pressure inside the slopes during rainfall. The analysis took into consideration the transient water flow that occurs when water moves from unsaturated to saturated soils. The finite element approach was used to analyse slope stability, while including a shear strength reduction strategy. The primary discoveries and deductions derived from the outcomes of the finite element study of transient water flow and slope stability encompass:

- Prolonged events with less intense rainfall critically reduce the stability of the slope. The range of a factor of safety was observed from 2.72 to 1.11 with no rainfall event to 120mm/hour lasting for 96 hours respectively, which is a 60% reduction. On the other hand, only an 8% reduction in the factor of safety was observed for the same rainfall intensity lasting for 01 hour, and a 15% reduction in the factor of safety was recorded against the same rainfall intensity lasting for 24 hours. This reduction in the factor of safety is due to the increase in pore water pressure and reduction in matric suction which contributes toward the reduction in soil strength and fails soil slope.
- The sand piles can be used as an effective stabilizing technique to stabilize slopes with fine soils. Sand piles works on the same principle as vertical drains, which provide

drainage passage for water reducing the pore water pressure and increasing matric suction, which led to stabilizing the soil slope. Up to 16% increment in matric suction was observed in the slope stabilized with sand piles. Furthermore, up to 39% reduction in deformation was recorded in the slope stabilized with sand piles and a 26% improvement was noted in the factor of safety for stabilized slope

CHAPTER 7: CONCLUSIONS AND RECOMMENDATIONS

7.1 Overview

Slope failure is a common geotechnical problem affecting the built and sustainable environment. Among the various factors that can trigger slope failure, rainfall is considered particularly crucial due to its varying intensity and prolonged events. Rainfall infiltrates into the slope, increasing pore water pressure and reducing matric suction in partially to unsaturated soil slopes. This ultimately reduces the shear strength of the soil, leading to slope failure. Various techniques have been introduced to stabilize these slopes, including chemical stabilization using lime or cement piles, mechanical stabilization using reinforcement (such as anchors and soil nails), micro-piles, and retaining walls.

This study conducted detailed investigations to assess the efficiency of sand piles as a stabilization technique for fine soil slopes exposed to various rainfall events of differing intensities and durations. The investigation included both finite element modeling and small-scale laboratory experiments. Key parameters considered in this study were the land slope angle, rainfall intensity, rainfall duration, length-to-diameter ratio, and the spacing between sand piles.

7.2 Conclusions

Based on this research study, the following conclusions were made:

- Understanding the varying effects of rainfall patterns on different soil types is crucial for assessing slope stability and implementing appropriate measures, such as drainage systems or stabilizing techniques like sand piles, to mitigate the potential hazards of rainfall-induced slope failures. The intensity and duration of specific rainfall events significantly influence the destabilization of fine soil slopes.
- It has been observed that low-to-medium intensity rainfall events with prolonged durations can be more critical than heavy, intense rainfall events with shorter durations, especially for low-permeability soil slopes. This is due to the infiltration behavior of rainfall into the soil. Low-permeability soils have a limited capacity to quickly absorb and drain water due to their low hydraulic conductivity. As a result, during prolonged low-to-medium intensity rainfall events, the soil gradually becomes saturated. This continuous water ingress can lead to a gradual increase in pore water pressure within

the slope, significantly reducing the soil's shear strength and triggering slope instability. In contrast, heavy, intense rainfall events with shorter durations may produce a considerable volume of water, but the limited duration allows less time for the water to infiltrate deeply into the soil. Consequently, the overall increase in pore water pressure may not be as significant as during prolonged rainfall. Therefore, for low-permeability soil slopes, it is crucial to carefully consider the effects of extended periods of moderate rainfall, as they can pose greater destabilization risks than short-lived, intense downpours.

- Slope geometry, including the overall height of the slope and the slope inclination angle, plays a crucial role in slope destabilization. Steeper slopes experience higher gravitational forces, making them less stable compared to gentler slopes. These increased gravitational forces act as driving forces for potential slope failures, especially when external triggers like rainfall are present. However, the interaction between slope geometry and rainfall effects is complex and can exhibit contrasting behaviors. For steep slopes, the ponding time for rainfall water is relatively short due to rapid runoff. Consequently, less water can infiltrate into the slope, resulting in reduced saturation and pore water pressure build-up. As a result, the matric suction remains relatively higher in steep slopes, contributing to better retention of shear strength and overall slope stability. On the other hand, gentle slopes provide more extensive areas for water to accumulate, leading to longer ponding times during rainfall events. The increased ponding time allows more water to infiltrate into the slope, leading to higher levels of saturation and reduced matric suction. This reduction in matric suction, in turn, leads to a reduction in the shear strength of the soil, making gentle slopes more susceptible to failure under certain conditions. It is essential to recognize these differing behaviors based on slope geometry and rainfall characteristics while assessing slope stability and implementing suitable mitigation measures. Proper slope design, careful consideration of slope angles, and the incorporation of drainage systems are some of the strategies that can be employed to address the specific challenges posed by different slope geometries and rainfall patterns, ensuring the stability of engineered slopes.
- Sand piles have proven to be an effective and efficient technique for stabilizing fine soil slopes. These piles serve a dual role, functioning as both reinforcements and drainage elements within the soil slope. By strategically placing sand piles, engineers

can enhance the overall stability and safety of the slope. The principle behind the drainage effectiveness of sand piles lies in the natural flow of water from areas of higher hydraulic head (confined areas) to regions of lower hydraulic head (less confined areas). Water from surrounding soils tends to move towards the sand piles, taking advantage of the permeable nature of the sand material. This process allows water to migrate through the soil mass, eventually reaching the surface through capillary action or forming surface runoff. As water drains out of the slope through the sand piles, the excess pore water pressure within the soil decreases, leading to a reduction in hydrostatic forces acting on the slope. This decrease in pore water pressure is beneficial, as it effectively increases the matric suction, and hence the overall shear strength of the soil. The heightened shear strength contributes significantly to the slope's stabilization and resistance against potential failures. The use of sand piles thus represents a prudent approach to mitigating slope instability in fine soil. By managing the water content and pore water pressures, these piles facilitate enhanced slope stability, providing a reliable and versatile solution for geotechnical engineers dealing with challenging slope stabilization projects.

- Beyond the primary research objectives, this study investigated a novel approach for slope monitoring using image processing techniques. An innovative approach known as the Automated Sensory and Signal Processing Selection System (ASPS) was employed. This approach played a pivotal role in extracting valuable characteristic features from diverse types of images captured throughout the experimental procedures. The selected characteristic features were subsequently used to train and test an artificial neural network, thereby integrating advanced computational techniques into the slope monitoring framework. This novel methodology aimed not only to improve the accuracy and efficiency of slope monitoring but also to explore the potential of cutting-edge technologies in enhancing our understanding and management of geological features. The integration of image processing and artificial intelligence in this study represents a significant step forward in the domain of slope monitoring, offering a promising avenue for future advancements in geotechnical engineering research and practice.

7.3 Limitations of Current Research and Future Recommendations

As this research progresses, the need for extensive and comprehensive future investigations becomes apparent. New questions will emerge, requiring more detailed analyses and broader datasets for adequate resolution. This need stems from the desire to achieve greater accuracy, validity, and generalizability in the study's conclusions. Conducting thorough research can help identify potential limitations and areas needing further refinement or exploration. By engaging in detailed and extensive studies, researchers can strengthen the robustness of their findings and contribute significantly to the advancement of their field. The following suggestions are proposed for consideration in future studies:

- A comparative approach involving multiple soil types would enable researchers and practitioners to identify soil-specific nuances or trends that may influence the performance of sand piles. This would facilitate a more robust and nuanced understanding of their efficacy in geotechnical engineering practice.
- In this investigation, the stabilized slopes were analyzed without the influence of surcharge loading. Future research should consider incorporating surcharge loading conditions and further explore the effectiveness of sand piles as a stabilizing measure. This approach will enhance the depth and breadth of the study, providing greater insights into slope stability and the advantages of using sand piles in geotechnical engineering applications.
- The present study proposes the utilization of a geotechnical centrifuge facility to conduct an in-depth investigation into the initiation conditions governing rainfall-induced landslides. This facility offers the opportunity to subject multiple soil types to diverse rainfall regimes, enabling the determination of precise rainfall thresholds for landslide initiation. These thresholds hold potential correlations with soil type as well as initial and boundary conditions, thereby offering valuable insights to enhance early-warning systems pertaining to landslide initiation.
- Future studies should include long-term monitoring and field validation of the laboratory and modeling results. This would provide real-world data to verify the effectiveness of sand piles and other stabilization techniques under actual environmental conditions, contributing to the practical applicability of the research findings.
- In addition to sand piles, future research could explore the effectiveness of other stabilization techniques such as geosynthetics, vegetation, and bioengineering methods.

Comparing these methods with sand piles could provide a broader understanding of the best practices for slope stabilization in various geotechnical contexts.

- Investigate the potential impacts of climate change on slope stability, particularly with regard to changes in rainfall patterns, intensity, and frequency. Understanding these impacts will help in designing more resilient stabilization measures that can withstand future climatic variations.
- Assess the economic feasibility and environmental impact of using sand piles and other stabilization techniques. This would involve cost-benefit analyses and environmental impact assessments to ensure that the chosen methods are not only effective but also sustainable and economically viable.
- Explore the integration of advanced monitoring technologies such as remote sensing, drones, and real-time data acquisition systems. These technologies can provide continuous monitoring of slope conditions and early warning of potential failures, enhancing the safety and management of slopes.
- Develop and refine predictive models that incorporate various factors affecting slope stability, such as soil properties, slope geometry, rainfall characteristics, and stabilization measures. These models can serve as valuable tools for predicting slope behavior and planning effective mitigation strategies.

By addressing these recommendations, future research can build on the findings of this study, ultimately leading to improved slope stabilization techniques and a better understanding of the factors influencing slope stability.

Bibliography

Aboshi, H., Kuwabara, M., Mizuno, Y., 1991. *Present state of sand compaction pile in Japan*. ASTM International West Conshohocken, PA, USA.

Abramson, L.W. et al., 2001a. *Slope stability and stabilization methods*. John Wiley & Sons.

Abramson, L.W. et al., 2001b. *Slope stability and stabilization methods*. John Wiley & Sons.

Abusharar, S.W., Han, J., 2011. Two-dimensional deep-seated slope stability analysis of embankments over stone column-improved soft clay. *Engineering Geology*, 120(1–4), pp.103–110.

Adrian, R.J., 1991a. Annul. Rev. Fluid Mech. *Particleimaging techniques for experimental fluid mechanics*, pp.261–304.

Adrian, R.J., 1991b. Annul. Rev. Fluid Mech. *Particleimaging techniques for experimental fluid mechanics*, pp.261–304.

Adrian, R.J., Yao, C.-S., 1985. Pulsed laser technique application to liquid and gaseous flows and the scattering power of seed materials. *Applied optics*, 24(1), pp.44–52.

Agency, E.E., 2017. *Climate change adaptation and disaster risk reduction in Europe: enhancing coherence of the knowledge base, policies and practices*. Office for Official Publ. of the Europ. Communities.

Agüí, J.C., Jimenez, J., 1987. On the performance of particle tracking. *Journal of fluid mechanics*, 185, pp.447–468.

Ahadi, M., Bakhtiar, M.S., 2010. Leak detection in water-filled plastic pipes through the application of tuned wavelet transforms to acoustic emission signals. *Applied Acoustics*, 71(7), pp.634–639.

Ahmadi-Adli, M., 2014. *Shallow Landslides Triggered By Rainfall In Unsaturated Soils A Thesis Submitted To The Graduate School Of Natural And Applied Sciences Of Middle East Technical University In Partial Fulfillment Of The Requirements For The Degree Of Doctor Of Philosophy In Civil Engineering*.

Ahn, T.B., Cho, S.D., Yang, S.C., 2002. Stabilization of soil slope using geosynthetic mulching mat. *Geotextiles and geomembranes*, 20(2), pp.135–146.

Aksoy, H.S., TAHER, N., AWLLA, H., 2021. Shear strength parameters of sand-tire chips mixtures. *Gümüşhane Üniversitesi Fen Bilimleri Dergisi*, 11(3), pp.713–720.

Alexakis, D.D. et al., 2014. Integrated use of GIS and remote sensing for monitoring landslides in transportation pavements: The case study of Paphos area in Cyprus. *Natural Hazards*, 72(1), pp.119–141. 10.1007/s11069-013-0770-3.

Alfaro, M.C. et al., 2009. Evaluating shear mobilization in rockfill columns used for riverbank stabilization. *Canadian geotechnical journal*, 46(8), pp.976–986.

Al-Habaibeh, A. et al., 2024. A novel method of using sound waves and artificial intelligence for the detection of vehicle's proximity from cyclists and E-scooters [online]. *MethodsX*, 12, p.102534. Available at: https://www.sciencedirect.com/science/article/pii/S2215016123005307.

Al-Habaibeh, A., Gindy, N., 2000. A new approach for systematic design of condition monitoring systems for milling processes. *Journal of Materials Processing Technology*, 107(1–3), pp.243–251.

Al-Habaibeh, A., Parkin, R.M., 2004. A generic approach towards intelligent condition monitoring systems of machining operations.

Ali, A. et al., 2014. Boundary effects of rainfall-induced landslides. *Computers and Geotechnics*, 61, pp.341–354.

Ali, S. et al., 2019. Landslide susceptibility mapping by using a geographic information system (GIS) along the China–Pakistan Economic Corridor (Karakoram Highway), Pakistan. *Natural Hazards and Earth System Sciences*, 19(5), pp.999–1022.

Ambily, A.P., Gandhi, S.R., 2007. Behavior of stone columns based on experimental and FEM analysis. *Journal of geotechnical and geoenvironmental engineering*, 133(4), pp.405–415.

Amit, A., Khalid, S., 2012. Vibration analysis techniques for gearbox diagnostic. *International Journal of Advanced Engineering Technology*, 3(2).

Anagnostopoulos, C., Georgiadis, K., 2004. Stabilization of a highway with piles in a landslide area. In: *Proceedings of the 9th International Symposium on Landslides, Rio de Janeiro, Brazil*. pp. 1697–1700.

Anon, 1963. Subgrade improved with drill-lime stabilization. *Rural and Urban Roads.*, (October), pp.24–27.

Anvari, S.M., Shooshpasha, I., Kutanaei, S.S., 2017. Effect of granulated rubber on shear strength of fine-grained sand. *Journal of Rock Mechanics and Geotechnical Engineering*, 9(5), pp.936–944.

Aqib, M. et al., 2023. Experimental and numerical analysis of rainfall-induced slope failure of railway embankment of semi high-speed trains. *Journal of Engineering and Applied Science*, 70(1). 10.1186/s44147-023-00188-7.

Van Asch, T.W.J., Buma, J., Van Beek, L.P.H., 1999. A view on some hydrological triggering systems in landslides. *Geomorphology*, 30(1–2), pp.25–32.

Au, S.W.C., 1998. Rain-induced slope instability in Hong Kong. *Engineering Geology*, 51(1), pp.1–36.

Ausilio, E., Conte, E., Dente, G., 2001. Stability analysis of slopes reinforced with piles. *Computers and Geotechnics*, 28(8), pp.591–611.

Awlla, H.A., Taher, N.R., Mawlood, Y.I., 2020. Effect of fixed-base and soil structure interaction on the dynamic responses of steel structures. *International Journal of Emerging Trends in Engineering Research*, 8(9).

Azeze, A.W., 2020. Assessments of Geotechnical Condition of Landslide Sites and Slope Stability Analysis Using Limit Equilibrium Method around Gundwin Town Area, Northwestern Ethiopia.

Baazouzi, M. et al., 2015. 2D Numerical Analysis of Shallow Foundation Rested Near Slope under Inclined Loading [online]. *Procedia Engineering*, 143(April), pp.623–634. Available at: http://dx.doi.org/10.1016/j.proeng.2016.06.086.

Baba, H.O., Peth, S., 2012. Large scale soil box test to investigate soil deformation and creep movement on slopes by Particle Image Velocimetry (PIV). *Soil and Tillage Research*, 125, pp.38–43. 10.1016/j.still.2012.05.021.

Bao, C.G., Gong, B., Zhan, L., 1998. Properties of unsaturated soils and slope stability of expansive soils. In: *Keynote Lecture, Proceedings of the 2nd International Conference on Unsaturated Soils (UNSAT 98). Beijing, China*. pp. 71–98.

Basharat, M., Rohn, J., 2015. Effects of volume on travel distance of mass movements triggered by the 2005 Kashmir earthquake, in the Northeast Himalayas of Pakistan. *Natural Hazards*, 77, pp.273–292.

Basharat, M., Shah, H.R., Hameed, N., 2016. Landslide susceptibility mapping using GIS and weighted overlay method: a case study from NW Himalayas, Pakistan. *Arabian Journal of Geosciences*, 9, pp.1–19.

Bellezza, I., Pasqualini, E., 2005. Parametric study of the stability of slopes reinforced with piles. In: *Proceedings Of The International Conference On Soil Mechanics And Geotechnical Engineering*. p. 1319.

Bentley Systems, 2020. PLAXIS CONNECT Edition V21.00 2D Tutorial Manual. , pp.1–243.

Bergado, D.T. et al., 1990. Improvement of soft Bangkok clay using vertical geotextile band drains compared with granular piles. *Geotextiles and Geomembranes*, 9(3), pp.203–231.

Bhattacharya, B., Solomatine, D.P., 2000. Application of artificial neural network in stage-discharge relationship. In: *Proc. 4th International Conference on Hydroinformatics, Iowa City, USA*. pp. 1–7.

Bishop, A.W., 1955. The use of the slip circle in the stability analysis of slopes. *Geotechnique*, 5(1), pp.7–17.

Bordoni, M. et al., 2016. Quantifying the contribution of grapevine roots to soil mechanical reinforcement in an area susceptible to shallow landslides. *Soil and Tillage Research*, 163, pp.195–206.

Bowles, J.E., 1988. *Foundation analysis and design*.

Bračko, T., Žlender, B., Jelušič, P., 2022. Implementation of Climate Change Effects on Slope Stability Analysis. *Applied Sciences (Switzerland)*, 12(16). 10.3390/app12168171.

Brand, E.W., 1984. Landslides in Southeast Asia, A state-of the art report. In: *Proc. 4th Int. Symp. Landslides, Toronto, Canada, 1984*.

Brooks, R.H., 1965. *Hydraulic properties of porous media*. Colorado State University.

Bruce, D.A., Juran, I., 1997a. *Drilled and grouted micropiles: state-of-practice review. US Federal Highway Administration*. Publication FHWA-RD-96-017, Washington, DC.

Bruce, D.A., Juran, I., 1997b. *Drilled and grouted micropiles: state-of-practice review. US Federal Highway Administration*. Publication FHWA-RD-96-017, Washington, DC.

Bruce, M.E.C. et al., 2013a. *Federal Highway Administration design manual: Deep mixing for embankment and foundation support*.

Bruce, M.E.C. et al., 2013b. *Federal Highway Administration design manual: Deep mixing for embankment and foundation support*.

Brücker, C., 1996. 3-D PIV via spatial correlation in a color-coded light-sheet. *Experiments in fluids*, 21(4), pp.312–314.

Buchhave, P., 1992. Particle image velocimetry—status and trends. *Experimental Thermal and Fluid Science*, 5(5), pp.586–604.

Bush, D.I., Jenner, C.G., Bassett, R.H., 1990. The design and construction of geocell foundation mattresses supporting embankments over soft grounds. *Geotextiles and Geomembranes*, 9(1), pp.83–98.

Cai, F., Ugai, K., 2000. Numerical analysis of the stability of a slope reinforced with piles. *Soils and foundations*, 40(1), pp.73–84.

Cai, Y. et al., 2014. An investigation of flow characteristics in slope siphon drains. *Journal of Zhejiang University SCIENCE A*, 15(1), pp.22–30.

Campbell, R.H., 1975a. *Soil slips, debris flows, and rainstorms in the Santa Monica Mountains and vicinity, southern California*. US Government Printing Office.

Campbell, R.H., 1975b. *Soil slips, debris flows, and rainstorms in the Santa Monica Mountains and vicinity, southern California*. US Government Printing Office.

Cantoni, R. et al., 1989. A design method for reticulated micropile structures in sliding slopes. *Ground engineering*, 22(4).

Carminati, A. et al., 2010. Dynamics of soil water content in the rhizosphere. *Plant and soil*, 332(1), pp.163–176.

Casagrande, A., 1932. Research on the Atterberg limits of soils. *Public roads*, 13(8), pp.121–136.

Çellek, S., Effect of the Slope Angle and Its Classication on Landslide [online]. Available at: https://doi.org/10.21203/rs.3.rs-61660/v1.

Chang, C. et al., 2023. The influence of seismic frequency spectrum on the instability of loess slope. *Scientific reports*, 13(1), p.10949. 10.1038/s41598-023-38016-w.

Chaulya, S.K., Prasad, G.M., 2016. Slope failure mechanism and monitoring techniques. *Sensing and Monitoring Technologies for Mines and Hazardous Areas. Elsevier, doi*, 10, pp.1–86.

Chen, H., Lee, C.F., Law, K.T., 2004. Causative mechanisms of rainfall-induced fill slope failures. *Journal of geotechnical and geoenvironmental engineering*, 130(6), pp.593–602.

Chen, K.-T., Wu, J.-H., 2018. Simulating the failure process of the Xinmo landslide using discontinuous deformation analysis. *Engineering Geology*, 239, pp.269–281.

Chen, L.T., Poulos, H.G., 1997. Piles subjected to lateral soil movements. *Journal of Geotechnical and Geoenvironmental Engineering*, 123(9), pp.802–811.

Cheng, Q. et al., 2024. Numerical Simulation of Rainfall-Induced Erosion on Infiltration and Slope Stability. *Water (Switzerland)*, 16(11). 10.3390/w16111517.

Cheng, Y.M., Lansivaara, T., Wei, W.B., 2007. Two-dimensional slope stability analysis by limit equilibrium and strength reduction methods. *Computers and geotechnics*, 34(3), pp.137–150.

Chiu, C.F., Ng, C.W.W., 2003. A state-dependent elasto-plastic model for saturated and unsaturated soils. *Géotechnique*, 53(9), pp.809–829.

Christoulas, S.T., Giannaros, C.H., Tsiambaos, G., 1997. Stabilization of embankment foundations by using stone columns. *Geotechnical & Geological Engineering*, 15, pp.247–258.

Ciabatta, L. et al., 2016. Assessing the impact of climate-change scenarios on landslide occurrence in Umbria Region, Italy. *Journal of Hydrology*, 541, pp.285–295.

Cornforth, D.H., 2005. Landslides in practice. *Investigation, analysis, and remedial/preventative options in soils*.

Corominas, J., 2000. Landslides and climate. In: *Proceedings of the 8th International Symposium on Landslides*. AA Balkema Cardiff, Wales, pp. 1–33.

Crosta, G.B., Frattini, P., 2008. Rainfall-induced landslides and debris flows. *Hydrological Processes: An International Journal*, 22(4), pp.473–477.

Cruden, D.M., Varnes, D.J., 1996. Landslides: investigation and mitigation. Chapter 3-Landslide types and processes. *Transportation research board special report*, (247).

DAHAL, R.K., 2012. Rainfall-induced landslides in Nepal. *International Journal of Erosion Control Engineering*, 5(1), pp.1–8.

Dai, Z. et al., 2024. Model test study on the deformation and stability of rainfall-induced expansive soil slope with weak interlayer. *Bulletin of Engineering Geology and the Environment*, 83(3). 10.1007/s10064-024-03576-2.

Dailey, P. et al., 2009. The financial risks of climate change. *ABI Research Paper*, (19).

Davies, O., 2011. *Numerical Analysis of the Effects of Climate Change on Slope Stability*.

Day, R.W. et al., 1999. Design method for stabilization of slopes with piles. *Journal of Geotechnical and Geoenvironmental Engineering*, 125(10), pp.910–914.

Dehn, M. et al., 2000. *Impact of climate change on slope stability using expanded downscaling* [online]. Available at: www.elsevier.nl/locate/enggeo.

Deng, D., Li, L., Zhao, L., 2017. Limit equilibrium method (LEM) of slope stability and calculation of comprehensive factor of safety with double strength-reduction technique. *Journal of Mountain Science*, 14(11), pp.2311–2324.

Djordjevic, N. et al., 1999. *Effect of blast vibration on slope stability* [online]. Available at: https://www.researchgate.net/publication/43485860.

Dolinsek, S. et al., 1999. An intelligent AE sensor for the monitoring of finish machining process. In: *Proceedings of the Second International Conference on Intelligent Processing and Manufacturing of Materials. IPMM'99 (Cat. No. 99EX296)*. IEEE, pp. 847–853.

Dracos, T., 1996. *Three-Dimensional Velocity and Vorticity Measuring and Image Analysis Techniques: Lecture Notes from the Short Course held in Zürich, Switzerland, 3–6 September 1996*. Springer Science & Business Media.

Duan, L., Huang, M., Zhang, L., 2016. Differences in hydrological responses for different vegetation types on a steep slope on the Loess Plateau, China. *Journal of Hydrology*, 537, pp.356–366.

Duncan, J.M., Wright, S.G., Brandon, T.L., 2014. *Soil Strength and Slope Stability* [eBook]. Wiley. Available at: https://books.google.co.uk/books?id=LtAXBAAAQBAJ.

Dunkerley, D.L., 2021. Light and low-intensity rainfalls: A review of their classification, occurrence, and importance in landsurface, ecological and environmental processes [online]. *Earth-Science Reviews*, 214, p.103529. Available at: https://www.sciencedirect.com/science/article/pii/S0012825221000283.

El-Hazek, A.N., Abdel-Mageed, N.B., Hadid, M.H., 2020. Numerical and experimental modelling of slope stability and seepage water of earthfill dam. *Journal of Water and Land Development*, 44.

Emberson, R., Kirschbaum, D., Stanley, T., 2020. New global characterization of landslide exposure. *Natural Hazards and Earth System Sciences Discussions*, 2020, pp.1–21.

Fadare, D.A., Ofidhe, U.I., 2009. Artificial neural network model for prediction of friction factor in pipe flow. *Journal of Applied Sciences Research*, 5(6), pp.662–670.

Fell, R.H., Lacasse, Kks., S e Leroi, E. 2005. A Framework for Landslide Risk Assessment and Management. In: *Proceedings International Conference on Landslide Risk Management*. pp. 3–25.

Fellenius, W., 1936. Calculation of the stability of earth dams. In: *Proc. of the second congress on large dams*. pp. 445–463.

Fisher, R. V, 1971. Features of coarse-grained, high-concentration fluids and their deposits. *Journal of Sedimentary Research*, 41(4).

Fourie, A.B., Rowe, D., Blight, G.E., 1999. The effect of inæltration on the stability of the slopes of a dry ash dump. *Geotechnique*, 49(1), pp.1–13.

Fowler, J., Koerner, R.M., 1987. Stabilization of Very Soft Soils Using Geosynthetics.

Fredlund, D.G., 2006. Unsaturated soil mechanics in engineering practice. *Journal of geotechnical and geoenvironmental engineering*, 132(3), pp.286–321.

Fujita, I., Muste, M., Kruger, A., 1998. Large-scale particle image velocimetry for flow analysis in hydraulic engineering applications. *Journal of Hydraulic Research*, 36(3), pp.397–414. 10.1080/00221689809498626.

Gallipoli, D., Wheeler, S.J., Karstunen, M., 2003. Modelling the variation of degree of saturation in a deformable unsaturated soil. *Géotechnique*, 53(1), pp.105–112.

Gariano, S.L., Guzzetti, F., 2016. Landslides in a changing climate. *Earth-Science Reviews*, 162, pp.227–252.

Gasmo, J.M., Rahardjo, H., Leong, E.C., 2000. Infiltration effects on stability of a residual soil slope. *Computers and geotechnics*, 26(2), pp.145–165.

Gavin, K., Xue, J., 2008. A simple method to analyze infiltration into unsaturated soil slopes. *Computers and Geotechnics*, 35(2), pp.223–230.

Van Genuchten, M.T., 1980. A closed-form equation for predicting the hydraulic conductivity of unsaturated soils. *Soil science society of America journal*, 44(5), pp.892–898.

Georgiadis, K., Potts, D.M., Zdravkovic, L., 2005. Three-dimensional constitutive model for partially and fully saturated soils. *International Journal of Geomechanics*, 5(3), pp.244–255.

Gerstner, W., 1998. Supervised learning for neural networks: A tutorial with Java Exercises. *Recurso disponible on-line: http://diwww. epfl. ch/mantra/tutorial/english/supervised. pdf*.

Ghasemi, E., 2017. Particle swarm optimization approach for forecasting backbreak induced by bench blasting. *Neural Computing and Applications*, 28(7), pp.1855–1862. 10.1007/s00521-016-2182-2.

Gholamzade, M., Khalkhali, A.B., 2021. Slope Stability Analysis Under Pore-Water Pressure: A Case Study in Zarm-Rood Earthfill Dam, Iran.

Ghorbani, A., Hosseinpour, I., Shormage, M., 2021. Deformation and stability analysis of embankment over stone column-strengthened soft ground. *KSCE Journal of Civil Engineering*, 25(2), pp.404–416.

Gillarduzzi, A., 2008. Sustainable landslide stabilisation using deep wells installed with Siphon drains and electro-pneumatic pumps. In: *Proceedings of The Tenth International Symposium on Landslides and Engineered Slopes*.

Gobinath, R. et al., 2020. Soil erosion protection on hilly regions using plant roots: an experimental insight. *Gully Erosion Studies from India and Surrounding Regions*, pp.321–335.

Gofar, N., Rahardjo, H., 2017. *Saturated and unsaturated stability analysis of slope subjected to rainfall infiltration*.

Gogineni, S. et al., 1998. Two-color digital PIV employing a single CCD camera. *Experiments in Fluids*, 25(4), pp.320–328.

Goh, J.R. et al., 2020. Stability analysis and improvement evaluation on residual soil slope: building cracked and slope failure. In: *IOP Conference Series: Materials Science and Engineering*. IOP Publishing, p. 072017.

Gonzalez-Ollauri, A., Mickovski, S.B., 2017. Hydrological effect of vegetation against rainfall-induced landslides. *Journal of Hydrology*, 549, pp.374–387. 10.1016/j.jhydrol.2017.04.014.

Gör, M. et al., 2022. Effect of geogrid inclusion on the slope stability. In: *Proceedings of the V-International European Conference on Interdisciplinary Scientific Research, Valencia, Spain*. pp. 28–29.

Grant, I., 1997. Particle image velocimetry: a review. *Proceedings of the Institution of Mechanical Engineers, Part C: Journal of Mechanical Engineering Science*, 211(1), pp.55–76.

Griffiths, D. V, Lane, P.A., 1999. Slope stability analysis by finite elements. *Geotechnique*, 49(3), pp.387–403.

Griffiths, D. V, Marquez, R.M., 2007. Three-dimensional slope stability analysis by elasto-plastic finite elements. *Geotechnique*, 57(6), pp.537–546.

Guerra, A.J.T. et al., 2015. The effects of biological geotextiles on gully stabilization in São Luís, Brazil. *Natural Hazards*, 75, pp.2625–2636.

Guo, L. et al., 2021. Analysis of Rainfall-induced Landslide Using the Extended DDA by Incorporating Matric Suction. *Computers and Geotechnics*, 135. 10.1016/j.compgeo.2021.104145.

Gureghian, A.B., Youngs, E.G., 1975. The calculation of steady-state water-table heights in drained soils by means of the finite-element method. *Journal of hydrology*, 27(1–2), pp.15–32.

Guzzetti, F. et al., 2008. The rainfall intensity–duration control of shallow landslides and debris flows: an update. *Landslides*, 5(1), pp.3–17.

Halder, A., Nandi, S., Bandyopadhyay, K., 2020. A comparative study on slope stability analysis by different approaches. In: *Geotechnical Characterization and Modelling: Proceedings of IGC 2018*. Springer, pp. 285–293.

Hammah, R., 2005. A comparison of finite element slope stability analysis with conventional limit-equilibrium investigation. In: *Proceedings of the 58th Canadian Geotechnical and*

6th Joint IAH-CNC and CGS Groundwater Specialty Conferences–GeoSask 2005. Citeseer.

Handy, R.L., Williams, W.W., 1966. *Chemical stabilization of an active landslide*.

Haxaire, A., Galavi, V., Brinkgreve, R.B.J., 2011. Fully coupled thermo-hydro-mechanical analysis for unsaturated soils in Plaxis. *Delft University of Technology*.

Hazari, S., Ghosh, S., Sharma, R.P., 2020. Experimental and numerical study of soil slopes at varying water content under dynamic loading condition. *International Journal of Civil Engineering*, 18(2), pp.215–229.

He, Y. et al., 2015. Evaluating the effect of slope angle on the distribution of the soil-pile pressure acting on stabilizing piles in sandy slopes. *Computers and Geotechnics*, 69, pp.153–165. 10.1016/j.compgeo.2015.05.006.

Hearman, A.J., Hinz, C., 2007. Sensitivity of point scale surface runoff predictions to rainfall resolution. *Hydrology and Earth System Sciences*, 11(2), pp.965–982.

Heckbert, P., 1995. Fourier transforms and the fast Fourier transform (FFT) algorithm. *Computer Graphics*, 2(1995), pp.15–463.

Highland, L.M., 2006. Estimating landslide losses - preliminary results of a seven-State pilot project [online]. *Open-File Report 2006-1032*, p.11. Available at: http://pubs.er.usgs.gov/publication/ofr20061032.

Highland, L.M., Bobrowsky, P., 2008. *The landslide handbook-A guide to understanding landslides*. US Geological Survey.

Hinsch, K.D., 1995. Three-dimensional particle velocimetry. *Measurement Science and Technology*, 6(6), p.742.

HO, K.K.S., 2004. Recent advances in geotechnology for slope stabilization and landslide mitigation-perspective from Hong Kong. In: *Landslides: evaluation and stabilization*. pp. 1507–1560.

Hollingsworth, R., Kovacs, G.S., 1981. Soil slumps and debris flows: prediction and protection. *Bulletin of the Association of Engineering Geologists*, 18(1), pp.17–28.

Hong, W.P., 1999. Slope stabilization to control landslides in Korea. *Geotechnical Engineering Case Histories in Korea, Special Publication to Commemorate the 11th ARC on SMGE, Seoul, Korea*, pp.141–152.

Hong, W.P., Han, J.G., 1996. The behavior of stabilizing piles installed in slopes. In: *Landslides*. pp. 1709–1714.

Hosseini, A., Davood Mostofinejad, ;, Hajialilue-Bonab, M., 2014. Displacement and Strain Field Measurement in Steel and RC Beams Using Particle Image Velocimetry. 10.1061/(ASCE)EM.1943.

Huang, B. et al., 2015. Application of particle image velocimetry (PIV) in the study of uplift mechanisms of pipe buried in medium dense sand. *Journal of Civil Structural Health Monitoring*, 5(5), pp.599–614. 10.1007/s13349-015-0130-y.

Huang, J., Griffiths, D. V, Fenton, G.A., 2010. System Reliability of Slopes by RFEM [online]. *Soils and Foundations*, 50(3), pp.343–353. Available at: https://www.sciencedirect.com/science/article/pii/S0038080620302432.

Huat, B.B.K., Ali, F.H.J., Low, T.H., 2006. Water infiltration characteristics of unsaturated soil slope and its effect on suction and stability. *Geotechnical & Geological Engineering*, 24(5), pp.1293–1306.

Hungr, O., Evans, S.G., Hutchinson, I.N., 2001. A Review of the Classification of Landslides of the Flow Type. *Environmental & Engineering Geoscience*, 7(3), pp.221–238.

Hutchinson, J.N., 1988. General report: morphological and geotechnical parameters of landslides in relation to geology and hydrogeology. In: *International symposium on landslides. 5*. pp. 3–35.

Hutchinson, J.N., Bhandari, R.K., 1971. Undrained loading, a fundamental mechanism of mudflows and other mass movements. *Geotechnique*, 21(4), pp.353–358.

Huvaj, N., Oğuz, E.A., 2018. Probabilistic slope stability analysis: a case study. *Sakarya University Journal of Science*, 22(5), pp.1458–1465.

Ingles, O.G., Metcalf, J.B., 1972. Soil Stabilization—Principles and Practice Butterworths. *Sydney, NSW 374pp*.

Islam, M., 2006. Structure, stratigraphy, petroleum geology and tectonics of Mirpur, Khuiratta and Puti Gali areas of district Mirpur and Kotli, Azad Jammu and Kashmir. Pakistan. *Unpublished Thesis, Institute of Geology, University of Azad Jammu and Kashmir, Muzaffarabad, 170p.*

Ismail, M.A.M., Ng, S.M., Abustan, I., 2017. Parametric study of horizontal drains for slope stability measure: A case study in Putrajaya, Malaysia. *KSCE Journal of Civil Engineering*, 21, pp.2162–2167.

Istok, J.D., Harward, M.E., 1982. Clay mineralogy in relation to landscape instability in the Coast Range of Oregon. *Soil Science Society of America Journal*, 46(6), pp.1326–1331.

Jadoon, I.A.K. et al., 2015. Structural interpretation and geo-hazard assessment of a locking line: 2005 Kashmir Earthquake, western Himalayas. *Environmental Earth Sciences*, 73, pp.7587–7602.

Janbu, N., 1954. Stability analysis of slopes with dimensionless parameters. *(No Title)*.

Jayalath, C., Gallage, C., 2021. Evaluating the Tensile Properties of Geogrids Using the Particle Image Velocimetry Technique. *Journal of Materials in Civil Engineering*, 33(11). 10.1061/(asce)mt.1943-5533.0003909.

Jing, X. et al., 2019. Erosion failure of a soil slope by heavy rain: laboratory investigation and modified GA model of soil slope failure. *International journal of environmental research and public health*, 16(6), p.1075.

Jirawattanasomkul, T. et al., 2018. Finite element modelling of flexural behaviour of geosynthetic cementitious composite mat (GCCM). *Composites Part B: Engineering*, 154, pp.33–42.

Joorabchi, A.E. et al., 2014. Yield acceleration and permanent displacement of a slope reinforced with a row of drilled shafts. *Soil Dynamics and Earthquake Engineering*, 57, pp.68–77.

Joorabchi, A.E., Liang, R.Y., Li, L., 2013. Yield acceleration of a slope reinforced with a row of drilled shafts. In: *Geo-Congress 2013: Stability and Performance of Slopes and Embankments III*. pp. 1987–1996.

Juran, I., Benslimane, A., Bruce, D.A., 1996. Slope stabilization by micropile reinforcement. In: *Landslides*. pp. 1715–1726.

Kang, G.-C., Song, Y.-S., Kim, T.-H., 2009. Behavior and stability of a large-scale cut slope considering reinforcement stages. *Landslides*, 6(3), pp.263–272.

Kanjanakul, C., Chub-uppakarn, T., 2013. Comparison between numerical and limit equilibrium methods for slope stability analysis. In: *Published in 18th National Convention on Civil Engineering*.

Kayastha, P., 2015. Landslide susceptibility mapping and factor effect analysis using frequency ratio in a catchment scale: a case study from Garuwa sub-basin, East Nepal [online]. *Arabian Journal of Geosciences*, 8, pp.8601–8613. Available at: https://api.semanticscholar.org/CorpusID:128883193.

Keane, R.D., Adrian, Rj., Zhang, Y., 1995. Super-resolution particle imaging velocimetry. *Measurement Science and Technology*, 6(6), p.754.

Kim, J. et al., 2004. Influence of rainfall-induced wetting on the stability of slopes in weathered soils. *Engineering Geology*, 75(3–4), pp.251–262.

Kim, S.K., Hong, W.P., Kim, Y.M., 1992. Prediction of rainfall-triggered landslides in Korea. In: *International symposium on landslides*. pp. 989–994.

Kitsugi, K., 1982. Lime-column technique in the improvement of clay ground. In: *Symp. on Soil and Rock Improvement Techniques including Geotextiles, Reinforced Earth and Modern Piling Methods*.

Kolathayar, S. et al., *Lecture Notes in Civil Engineering Climate Change and Water Security Select Proceedings of VCDRR 2021* [online]. Available at: https://link.springer.com/bookseries/15087.

Latha, M., Raghuveer, G.P., Editors, R., 2018. *Lecture Notes in Civil Engineering Problematic Soils and Geoenvironmental Concerns Proceedings of IGC 2018* [online]. Available at: http://www.springer.com/series/15087.

Lau, K.C., Kenney, T.C., 1984. Horizontal drains to stabilize clay slopes. *Canadian Geotechnical Journal*, 21(2), pp.241–249.

Le, T.M.H., 2014. Reliability of heterogeneous slopes with cross-correlated shear strength parameters. *Georisk: Assessment and Management of Risk for Engineered Systems and Geohazards*, 8(4), pp.250–257.

Li, C. et al., 2020. Optimal Location of Piles in Stabilizing Slopes Based on a Simplified Double-Row Piles Model. *KSCE Journal of Civil Engineering*, 24(2), pp.377–389. 10.1007/s12205-020-0712-z.

Li, L., Liang, R.Y., 2014. Limit equilibrium based design approach for slope stabilization using multiple rows of drilled shafts. *Computers and Geotechnics*, 59, pp.67–74.

Li, Q. et al., 2015. Soil moisture response to rainfall in forestland and vegetable plot in Taihu Lake Basin, China. *Chinese Geographical Science*, 25(4), pp.426–437. 10.1007/s11769-014-0715-0.

Li, W., Kwok, C.Y., Senetakis, K., 2020. Effects of inclusion of granulated rubber tires on the mechanical behaviour of a compressive sand. *Canadian Geotechnical Journal*, 57(5), pp.763–769.

Li, Z. et al., 2017. Deformation features and failure mechanism of steep rock slope under the mining activities and rainfall. *Journal of Mountain Science*, 14(1), pp.31–45.

Liang, R., Zeng, S., 2002. Numerical study of soil arching mechanism in drilled shafts for slope stabilization. *Soils and foundations*, 42(2), pp.83–92.

Liang, R.Y., Yamin, M., 2010. Three-dimensional finite element study of arching behavior in slope/drilled shafts system. *International Journal for Numerical and Analytical Methods in Geomechanics*, 34(11), pp.1157–1168.

Lin, H., Cao, P., 2012. Limit Equilibrium Analysis for the Relationships Among Slope c, phi and Slip Surface. *Electronic Journal of Geotechnical Engineering*, 17.

Lirer, S., 2012. Landslide stabilizing piles: Experimental evidences and numerical interpretation. *Engineering Geology*, 149–150, pp.70–77. 10.1016/j.enggeo.2012.08.002.

Liu, H. et al., 2023. Centrifuge modeling of stability of embankment on soft soil improved by rigid columns. *Journal of Geotechnical and Geoenvironmental Engineering*, 149(9), p.04023069.

Liu, S.Y., Shao, L.T., Li, H.J., 2015. Slope stability analysis using the limit equilibrium method and two finite element methods. *Computers and Geotechnics*, 63, pp.291–298.

Lizzi, F., 1978. Reticulated root piles to correct landslides.

Lizzi, F., 1982. The pali radice (root piles)" symposium on soil and rock improvement techniques including geotextiles reinforced earth and modem piling Methods Bangkok D3.

Llorens, P., Domingo, F., 2007. Rainfall partitioning by vegetation under Mediterranean conditions. A review of studies in Europe. *Journal of hydrology*, 335(1–2), pp.37–54.

Loehr, J.E. et al., 2000. Slope stabilization with recycled plastic pins. *Transportation research record*, 1714(1), pp.1–8.

Loo, Y.Y., Billa, L., Singh, A., 2015. Effect of climate change on seasonal monsoon in Asia and its impact on the variability of monsoon rainfall in Southeast Asia. *Geoscience Frontiers*, 6(6), pp.817–823.

Lu, H.H. et al., 2013. Comparison of 3D finite element slope stability with 3D limit equilibrium analysis. In: *18th International conference on soil mechanics and geotechnical engineering*.

Lu, N., Godt, J.W., 2013. *Hillslope hydrology and stability*. Cambridge University Press.

Lu, N., Likos, W.J., 2006. Suction stress characteristic curve for unsaturated soil. *Journal of geotechnical and geoenvironmental engineering*, 132(2), pp.131–142.

Lutenegger, A.J. t, Dickson, J.R., 1984. Experiences with drilled lime stabilisation in the mid-west USA. In: *Proceedings of the Fourth International Symposium on Landslides*. pp. 289–293.

Mahmood, K. et al., 2016. The effect of soil type on matric suction and stability of unsaturated slope under uniform rainfall. *KSCE Journal of Civil Engineering*, 20(4), pp.1294–1299. 10.1007/s12205-015-0796-z.

Mahmood, K., Ryu, J.H., Kim, J.M., 2013. Effect of anisotropic conductivity on suction and reliability index of unsaturated slope exposed to uniform antecedent rainfall. *Landslides*, 10, pp.15–22.

Malik, M.K., Karim, I.R., 2020. Seepage and slope stability analysis of Haditha Dam using Geo-Studio Software. In: *IOP conference series: materials science and engineering*. IOP Publishing, p. 022074.

Malla, B., Dahal, B.K., 2021. Effect of Rainfall on Stability of Soil Slope.

Martin, A., Tosunoglu, S., 2000. Image processing techniques for machine vision. *Miami, Florida*, pp.1–9.

Matsui, T., San, K.-C., 1992. Finite element slope stability analysis by shear strength reduction technique. *Soils and foundations*, 32(1), pp.59–70.

Matsushi, Y., Hattanji, T., Matsukura, Y., 2006. Mechanisms of shallow landslides on soil-mantled hillslopes with permeable and impermeable bedrocks in the Boso Peninsula, Japan. *Geomorphology*, 76(1–2), pp.92–108.

Matziaris, V., 2019. *Centrifuge modelling of rainfall-induced landslides in unsaturated soil slopes*.

McKay, S.E., 2006. *Geotechnical analysis of horizontal drains as a landslide mitigation method in western Washington*. University of Nevada, Reno.

McVicar, T.R. et al., 2010. Parsimoniously modelling perennial vegetation suitability and identifying priority areas to support China's re-vegetation program in the Loess Plateau: Matching model complexity to data availability. *Forest Ecology and Management*, 259(7), pp.1277–1290.

Melling, A., 1997. Tracer particles and seeding for particle image velocimetry. *Measurement science and technology*, 8(12), p.1406.

Meng, Q. et al., 2020. Numerical analysis of slope stability under reservoir water level fluctuations using a FEM-LEM-combined method. *Geofluids*, 2020.

Merat, S., Djerbal, L., Bahar, R., 2017. Numerical analysis of climate effect on slope stability. In: *PanAm Unsaturated Soils 2017.* , 2017, pp. 308–318.

Meselhe, E.A., Peeva, ; T, Muste, M., Large Scale Particle Image Velocimetry for Low Velocity and Shallow Water Flows. 10.1061/ASCE0733-94292004130:9937.

Mickovski, S.B. et al., 2009. Mechanical reinforcement of soil by willow roots: impacts of root properties and root failure mechanism. *Soil Science Society of America Journal*, 73(4), pp.1276–1285.

Mirzababaei, M., Mohamed, M., Miraftab, M., 2016. Analysis of Strip Footings on Fiber-Reinforced Slopes with the Aid of Particle Image Velocimetry. 10.1061/(ASCE)MT.1943-5533.

Moayedi, H. et al., 2019. The feasibility of three prediction techniques of the artificial neural network, adaptive neuro-fuzzy inference system, and hybrid particle swarm optimization for assessing the safety factor of cohesive slopes. *ISPRS International Journal of Geo-Information*, 8(9), p.391.

Morgenstern, N.R. u, Price, V.E., 1965. The analysis of the stability of general slip surfaces. *Geotechnique*, 15(1), pp.79–93.

Muntohar, A.S., Ikhsan, J., Liao, H.J., 2013. Influence of rainfall patterns on the instability of slopes. *Civil Engineering Dimension*, 15(2), pp.120–128.

Namdar, A., 2010. Analysis of slope stability using limit equilibrium. *Buletinul Institutului Politehnic din lasi. Sectia Constructii, Arhitectura*, 56(2), p.75.

Naseer, S. et al., 2019. Laboratory and numerical based analysis of floating sand columns in clayey soil [online]. *International Journal of Geo-Engineering*, 10(1), p.10. Available at: https://doi.org/10.1186/s40703-019-0106-6.

Nasiri, M., Hajiazizi, M., 2021. An experimental and numerical investigation of reinforced slope using geotextile encased stone column. *International Journal of Geotechnical Engineering*, 15(5), pp.543–552.

Ng, C.W.W. et al., 2003. Performance of an unsaturated expansive soil slope subjected to artificial rainfall infiltration. *Geotechnique*, 53(2), pp.143–157.

Ng, C.W.W., Zhang, L.M., Ho, K.K.S., 2001. Influence of laterally loaded sleeved piles and pile groups on slope stability. *Canadian Geotechnical Journal*, 38(3), pp.553–566.

Norris, J.E. et al., 2008. *Slope stability and erosion control: ecotechnological solutions*. Springer Science & Business Media.

Oh, S., Lu, N., 2015a. Slope stability analysis under unsaturated conditions: Case studies of rainfall-induced failure of cut slopes. *Engineering Geology*, 184, pp.96–103.

Oh, S., Lu, N., 2015b. Slope stability analysis under unsaturated conditions: Case studies of rainfall-induced failure of cut slopes. *Engineering Geology*, 184, pp.96–103.

Olivares, L., Picarelli, L., 2003. Shallow flowslides triggered by intense rainfalls on natural slopes covered by loose unsaturated pyroclastic soils. *Géotechnique*, 53(2), pp.283–287.

Operstein, V., Frydman, S., 2000. The influence of vegetation on soil strength. *Proceedings of the Institution of Civil Engineers-Ground Improvement*, 4(2), pp.81–89.

Palmerton, J.B., 1984. *Stabilization of Moving Land Masses by Cast-in-Place Piles.* ARMY ENGINEER WATERWAYS EXPERIMENT STATION VICKSBURG MS GEOTECHNICAL LAB.

Pan, B. et al., 2009. Two-dimensional digital image correlation for in-plane displacement and strain measurement: a review. *Measurement science and technology*, 20(6), p.062001.

Patel, S. et al., 2018. *Lecture Notes in Civil Engineering* [online]. Available at: http://www.springer.com/series/15087.

Pearlman, S.L., Wolosick, J.R., 1992. Pin piles for bridge foundations. In: *Proceedings of the 9th Annual International Bridge Conference*. pp. 247–254.

Peng, M., Zhang, L.M., 2012. Breaching parameters of landslide dams. *Landslides*, 9, pp.13–31.

Petley, D.N., Dunning, S.A., Rosser, N.J., 2005. The analysis of global landslide risk through the creation of a database of worldwide landslide fatalities. In: *Landslide risk management*. CRC Press, 2005, pp. 377–384.

Phear, A. et al., 2005. *Soil nailing-best practice guidance*.

Philip, J.R., 1991. Hillslope infiltration: planar slopes. *Water Resources Research*, 27(1), pp.109–117.

Pinyol, N.M., Alonso, E.E., 2012. Design of micropiles for tunnel face reinforcement: undrained upper bound solution. *Journal of geotechnical and geoenvironmental engineering*, 138(1), pp.89–99.

Pizer, S.M. et al., 1987. Adaptive histogram equalization and its variations. *Computer vision, graphics, and image processing*, 39(3), pp.355–368.

PLAXIS, 2021. CONNECT Edition V21.01 - Material Models Manual. , pp.1–274.

Plumelle, C., 1984. Improvement of the bearing capacity of soil by inserts of group and reticulated micro piles. In: *International Symposium on In-situ Reinforcement of Soils and Rocks, Paris, ENPC Presses*. pp. 83–89.

Pohll, G.M. et al., 2013. *Design guidelines for horizontal drains used for slope stabilization.* Washington (State). Dept. of Transportation. Office of Research and Library ….

Popescu, M.E., Schaefer, V.R., 2008. Landslide stabilizing piles: a design based on the results of slope failure back analysis. In: *Proceedings of the Tenth International Symposium on Landslides and Engineered Slopes (Volume 2)*.

Pradel, D., Raad, G., 1993. Effect of permeability on surficial stability of homogeneous slopes. *Journal of geotechnical engineering*, 119(2), pp.315–332.

Qi, S., Vanapalli, S.K., 2015. Hydro-mechanical coupling effect on surficial layer stability of unsaturated expansive soil slopes. *Computers and Geotechnics*, 70, pp.68–82.

Rafek, A.G. et al., 2016. Systematic approach to sustainable rock slope stability evaluation. *Procedia Chemistry*, 19, pp.981–985.

Raffel, M. et al., 2007a. Particle Image Velocimetry. 2 edn Springer.

Raffel, M. et al., 2007b. Particle Image Velocimetry. 2 edn Springer.

Rahardjo, H. et al., 2003. Effectiveness of horizontal drains for slope stability. *Engineering Geology*, 69(3–4), pp.295–308.

Rahardjo, H. et al., 2010. Effects of groundwater table position and soil properties on stability of slope during rainfall. *Journal of geotechnical and geoenvironmental engineering*, 136(11), pp.1555–1564.

Rahardjo, H. et al., 2005. Response of a residual soil slope to rainfall. *Canadian Geotechnical Journal*, 42(2), pp.340–351.

Rahardjo, H., Fredlund, D.G., 1993. *Soil Mechanics for Unsaturated Soils*. New York; Toronto: Wiley.

Rahimi, A., Rahardjo, H., Leong, E.-C., 2011. Effect of antecedent rainfall patterns on rainfall-induced slope failure. *Journal of Geotechnical and Geoenvironmental Engineering*, 137(5), pp.483–491.

Rahimi, A., Rahardjo, H., Leong, E.-C., 2010. Effect of hydraulic properties of soil on rainfall-induced slope failure. *Engineering Geology*, 114(3–4), pp.135–143.

Reese, L.C., 1992. Use of drilled shafts in stabilizing a slope. In: *Proc. Specialty Conference on Stability and Performance of Slopes and Embankments*.

Reuss, D.L., Adrian, R.J., Landreth, C.C., 1986. Two-dimensional velocity measurements in a laminar flame using particle image velocimetry. *Combustion science and technology*, 67(4–6), pp.73–83.

Rodríguez-Iturbe, I., Porporato, A., 2007. *Ecohydrology of water-controlled ecosystems: soil moisture and plant dynamics*. Cambridge University Press.

Rogers Ã, C.D.F., Glendinning, S., Holt, C.C., *Slope stabilization using lime pilesÐa case study*.

Rogers, C.D.F., Glendinning, S., 1997a. Improvement of clay soils in situ using lime piles in the UK. *Engineering geology*, 47(3), pp.243–257.

Rogers, C.D.F., Glendinning, S., 1997b. Improvement of clay soils in situ using lime piles in the UK. *Engineering geology*, 47(3), pp.243–257.

Rogers, C.D.F., Glendinning, S., 1997c. *Improvement of clay soils in situ using lime piles in the UK*.

Rogers, C.D.F., Glendinning, S., 1993. Stabilisation of embankment clay fills using lime piles. In: *ENGINEERED FILLS. PROCEEDINGS OF THE CONFERENCE'ENGINEERED FILLS'93', HELD ON 15-17 SEPTEMBER 1993 IN NEWCASTLE UPON TYNE*.

Rogers, C.D.F., Glendinning, S., 1997d. Stabilization of shallow slope failures with lime piles. *Transportation research record*, 1589(1), pp.83–91.

Rogers, C.D.F., Glendinning, S., 1996. The role of lime migration in lime pile stabilization of slopes. *Quarterly Journal of Engineering Geology and Hydrogeology*, 29(4), pp.273–284.

Romero, V.P. et al., 2016. Modelling the soundscape quality of urban waterfronts by artificial neural networks. *Applied Acoustics*, 111, pp.121–128.

Rashma, R.S. V, B. R, J., Shivashankar R, 2024. Limit equilibrium slope stability analysis of column-supported embankment on weak ground. *World Journal of Engineering*, 21(4), pp.654–664.

Sadzevicius, R., Radzevicius, A., Gjunsburgs, B., 2019. Modelling the Stability of the Aleksotas Hill Slope in Kaunas. In: *IOP Conference Series: Earth and Environmental Science*. Institute of Physics Publishing. 10.1088/1755-1315/222/1/012026.

Sari, M., Ghasemi, E., Ataei, M., 2014. Stochastic modeling approach for the evaluation of backbreak due to blasting operations in open pit mines. *Rock mechanics and rock engineering*, 47, pp.771–783.

Sarma, S.K., 1973. Stability analysis of embankments and slopes. *Geotechnique*, 23(3), pp.423–433.

Sassa, K. et al., 2007. Landslides induced by a combined effect of earthquake and rainfall. In: *Progress in landslide science*. Springer, 2007, pp. 193–207.

Sazzad, M.M., Rahman, F.I., Mamun, A.A., 2016. Effects of water level variation on the stability of slope by LEM and FEM. In: *Proc. of the*.

Scanlan, C.A., Hinz, C., 2010. Insights into the processes and effects of root-induced changes to soil hydraulic properties. In: *2010 19th World Congress of Soil Science, Soil Solutions for a Changing World*. pp. 1–6.

Scholl, P. et al., 2014. Root induced changes of effective 1D hydraulic properties in a soil column. *Plant and soil*, 381(1), pp.193–213.

SCHUSTER, R., 1995. Keynote paper: recent advances in slope stabilization. In: *International Symposium on Landslides*. pp. 1715–1745.

Scott, R.C., 1981. *The geomorphic significance of debris avalanching in the Appalachian Blue Ridge Mountains*. University Microfilms.

Shafique, M., van der Meijde, M., Khan, M.A., 2016. A review of the 2005 Kashmir earthquake-induced landslides; from a remote sensing prospective. *Journal of Asian Earth Sciences*, 118, pp.68–80.

Shavit, U., Lowe, R.J., Steinbuck, J. V, 2007a. Intensity capping: a simple method to improve cross-correlation PIV results. *Experiments in Fluids*, 42(2), pp.225–240.

Shavit, U., Lowe, R.J., Steinbuck, J. V, 2007b. Intensity capping: a simple method to improve cross-correlation PIV results. *Experiments in Fluids*, 42(2), pp.225–240.

Shaw-Shong, L., 2004. Slope failures in tropical residual soil. *Tropical Residual Soil Engineering*, pp.71–102.

Shiferaw, H.M., 2021a. Study on the influence of slope height and angle on the factor of safety and shape of failure of slopes based on strength reduction method of analysis [online]. *Beni-Suef University Journal of Basic and Applied Sciences*, 10(1), p.31. Available at: https://doi.org/10.1186/s43088-021-00115-w.

Shiferaw, H.M., 2021b. Study on the influence of slope height and angle on the factor of safety and shape of failure of slopes based on strength reduction method of analysis. *Beni-Suef University Journal of Basic and Applied Sciences*, 10(1). 10.1186/s43088-021-00115-w.

Shiferaw, H.M., 2021c. Study on the influence of slope height and angle on the factor of safety and shape of failure of slopes based on strength reduction method of analysis. *Beni-Suef University Journal of Basic and Applied Sciences*, 10(1), p.31.

Shin, H., Kim, Y.T., Park, D.K., 2013. Development of rainfall hazard envelope for unsaturated infinite slope. *KSCE Journal of Civil Engineering*, 17, pp.351–356.

Simon, A., Collison, A.J.C., 2002. Quantifying the mechanical and hydrologic effects of riparian vegetation on streambank stability. *Earth surface processes and landforms*, 27(5), pp.527–546.

Slominski, C., Niedostatkiewicz, M., Tejchman, J., 2007. Application of particle image velocimetry (PIV) for deformation measurement during granular silo flow. *Powder Technology*, 173(1), pp.1–18. 10.1016/j.powtec.2006.11.018.

Soga, K. et al., 2016. Trends in large-deformation analysis of landslide mass movements with particular emphasis on the material point method. *Géotechnique*, 66(3), pp.248–273.

Spencer, E., 1967. A method of analysis of the stability of embankments assuming parallel inter-slice forces. *Geotechnique*, 17(1), pp.11–26.

Stamhuis, E., Videler, J., 1995. Quantitative flow analysis around aquatic animals using laser sheet particle image velocimetry. *The Journal of experimental biology*, 198(2), pp.283–294.

Stoffel, M., Huggel, C., 2012. Effects of climate change on mass movements in mountain environments. *Progress in physical geography*, 36(3), pp.421–439.

Stoffel, M., Tiranti, D., Huggel, C., 2014. Climate change impacts on mass movements—case studies from the European Alps. *Science of the Total Environment*, 493, pp.1255–1266.

Stokes, A. et al., 2014. Ecological mitigation of hillslope instability: ten key issues facing researchers and practitioners. *Plant and Soil*, 377(1), pp.1–23.

Su, L., Xu, X., et al., 2017. An integrated geophysical approach for investigating hydro-geological characteristics of a debris landslide in the Wenchuan earthquake area. *Engineering Geology*, 219, pp.52–63.

Su, L., Hu, K., et al., 2017. Characteristics and triggering mechanism of Xinmo landslide on 24 June 2017 in Sichuan, China. *Journal of Mountain Science*, 14(9), pp.1689–1700.

Suemitsu, K., Endo, S., Sato, S., 2024. Classification of Rainfall Intensity and Cloud Type from Dash Cam Images Using Feature Removal by Masking. *Climate*, 12(5). 10.3390/cli12050070.

Sujatha, E.R., Sudarsan, J.S., Nithiyanantham, S., 2023. 10.1007/s13762-023-04832-w.

Sun, H. et al., 2019a. An improved siphon drainage method for slope stabilization. *Journal of Mountain Science*, 16(3), pp.701–713.

Sun, H. et al., 2019b. An improved siphon drainage method for slope stabilization. *Journal of Mountain Science*, 16(3), pp.701–713.

Sun, H.-Y. et al., 2019. A case study of a rainfall-induced landslide involving weak interlayer and its treatment using the siphon drainage method. *Bulletin of Engineering Geology and the Environment*, 78, pp.4063–4074.

Sun, S.W. et al., 2009a. Model tests on anti-sliding mechanism of micropile groups and anti-sliding piles. *Chinese Journal of Geotechnical Engineering*, 31(10), pp.1564–1570.

Sun, S.W. et al., 2009b. Model tests on anti-sliding mechanism of micropile groups and anti-sliding piles. *Chinese Journal of Geotechnical Engineering*, 31(10), pp.1564–1570.

Suradi, M., 2015. *RAINFALL-INDUCED FAILURES OF NATURAL SLOPES IN TROPICAL REGIONS School of Civil, Environmental and Mining Engineering*.

Swanston, D.N., 1974. *Slope stability problems associated with timber harvesting in mountainous regions of the western United States*. Pacific Northwest Research Station, US Department of Agriculture, Forest Service.

Take, W.A., 2015. Thirty-Sixth Canadian Geotechnical Colloquium: Advances in visualization of geotechnical processes through digital image correlation. *Canadian Geotechnical Journal*, 52(9), pp.1199–1220.

Tengfei, P.A.N., Shouzeng, Z.H.U., Zhi, L.I., 2012. Factors Triggering the Frequent Occurrence of Landslides in Enshi Tujia Miao Autonomous Prefecture. *Soil Engineering and Foundation*, 26(6), p.73.

Thielicke, W., Stamhuis, E., 2014. PIVlab–towards user-friendly, affordable and accurate digital particle image velocimetry in MATLAB. *Journal of open research software*, 2(1).

Thielicke, W., Stamhuis, E.J., 2014. PIVlab-time-resolved digital particle image velocimetry tool for MATLAB. *Published under the BSD license, programmed with MATLAB*, 7(0.246), p.R14.

Thomas, H.R., He, Y., 1998. Modelling the behaviour of unsaturated soil using an elastoplastic constitutive model. *Géotechnique*, 48(5), pp.589–603.

Thorne, C.R., 1990. Effects of vegetation on riverbank erosion and stability. *Vegetation and erosion*.

Tien Bui, D. et al., 2019. Predicting slope stability failure through machine learning paradigms. *ISPRS International Journal of Geo-Information*, 8(9), p.395.

Tohari, A. et al., 2021. Effectiveness of siphon drainage method for landslide stabilization in a tropical volcanic hillslope: a case study of Cibitung Landslide, West Java, Indonesia. *Bulletin of Engineering Geology and the Environment*, 80, pp.2101–2116.

Travis, Q.B. et al., 2010. Unsaturated infinite slope stability considering surface flux conditions. *Journal of geotechnical and geoenvironmental engineering*, 136(7), pp.963–974.

Tsaparas, I. et al., 2003. Infiltration characteristics of two instrumented residual soil slopes. *Canadian Geotechnical Journal*, 40(5), pp.1012–1032.

Tsukada, Y. et al., 2006. Mechanism of bearing capacity of spread footings reinforced with micropiles. *Soils and foundations*, 46(3), pp.367–376.

Tsytovich, N.A., Abelev, M.Y., Takhirov, I.G., 1971. Compacting saturated loess by means of lime piles. In: *4th International Conference on Soil Mechanics and Foundation Engineering, Budapest*. pp. 837–842.

Ugai, K., Leshchinsky, D.O. V, 1995. Three-dimensional limit equilibrium and finite element analyses: a comparison of results. *Soils and foundations*, 35(4), pp.1–7.

Vardon, P.J., 2015. Climatic influence on geotechnical infrastructure: a review. *Environmental Geotechnics*, 2(3), pp.166–174.

Varnes, D.J., 1978. Slope movement types and processes. *Special report*, 176, pp.11–33.

Vergani, C., Graf, F., 2016. Soil permeability, aggregate stability and root growth: a pot experiment from a soil bioengineering perspective. *Ecohydrology*, 9(5), pp.830–842.

Vivoda Prodan, M. et al., 2023. Physical Modelling of Rainfall-Induced Sandy and Clay-Like Slope Failures. *Advances in Materials Science and Engineering*, 2023. 10.1155/2023/3234542.

Wadia, D.N., 1928. The geology of Poonch State (Kashmir) and adjacent portions of the Punjab. *Mem. Geol. Surv. India*, 51, pp.185–370.

Wang, D. et al., 2022. Large deformation slope failure—A perspective from multiscale modelling. *Computers and Geotechnics*, 150, p.104886.

Wang, W.T., 1989. Experimentation of improving soft clay with lime column. In: *Engineering problems of regional soils. International conference.* pp. 477–480.

Wang, X. et al., 2024. Contribution of soil matric suction on slope stability under different vegetation types. *Journal of Soils and Sediments*, 24(2), pp.575–588. 10.1007/s11368-023-03653-1.

Wang, X., Zhao, M., Li, S., 2013. An improved cross-correlation algorithm based on wavelet transform and energy feature extraction for pipeline leak detection. In: *ICPTT 2012: Better Pipeline Infrastructure for a Better Life.* , 2013, pp. 577–591.

Waseem, M. et al., 2021. Slope Stability Analysis of the Qalandarabad Landslide. *Technical Journal*, 26(02), pp.1–17.

Weeks, M., Bayoumi, M., 2003. Discrete wavelet transform: architectures, design and performance issues. *Journal of VLSI signal processing systems for signal, image and video technology*, 35, pp.155–178.

Wheeler, S.J., Sivakumar, V., 1995. An elasto-plastic critical state framework for unsaturated soil. *Géotechnique*, 45(1), pp.35–53.

Willert, C., 1996. The fully digital evaluation of photographic PIV recordings. *Applied Scientific Research*, 56(2), pp.79–102.

Willert, C.E., Gharib, M., 1991. Digital particle image velocimetry. *Experiments in fluids*, 10(4), pp.181–193.

Williams, G.P., Guy, H.P., 1973. *Erosional and depositional aspects of Hurricane Camille in Virginia, 1969*. US Government Printing Office.

Won, J. et al., 2005a. Coupled effects in stability analysis of pile–slope systems. *Computers and Geotechnics*, 32(4), pp.304–315.

Won, J. et al., 2005b. Coupled effects in stability analysis of pile–slope systems. *Computers and Geotechnics*, 32(4), pp.304–315.

Wu, K.J., Austin, D.N., 1992. Three-dimensional polyethylene geocells for erosion control and channel linings. In: *Geosynthetics in Filtration, Drainage and Erosion Control*. Elsevier, 1992, pp. 275–284.

Wu, L.Z. et al., 2017. Laboratory characterization of rainfall-induced loess slope failure. *Catena*, 150, pp.1–8.

Wu, T.H., McKinnell III, W.P., Swanston, D.N., 1979. Strength of tree roots and landslides on Prince of Wales Island, Alaska. *Canadian Geotechnical Journal*, 16(1), pp.19–33.

Wu, Y. et al., 2016. Application of analytic hierarchy process model for landslide susceptibility mapping in the Gangu County, Gansu Province, China. *Environmental Earth Sciences*, 75(5), pp.1–11. 10.1007/s12665-015-5194-9.

Xanthakos, P.P., Abramson, L.W., Bruce, D.A., 1994. *Ground control and improvement*. John Wiley & Sons.

Xu, X. et al., 2017. Analysis on shear wave velocity structure of a gravel landslide based on dual-source surface wave method. *Landslides*, 14, pp.1127–1137.

Yamin, M., Liang, R.Y., 2010a. Limiting equilibrium method for slope/drilled shaft system. *International Journal for Numerical and Analytical Methods in Geomechanics*, 34(10), pp.1063–1075.

Yamin, M., Liang, R.Y., 2010b. Limiting equilibrium method for slope/drilled shaft system. *International Journal for Numerical and Analytical Methods in Geomechanics*, 34(10), pp.1063–1075.

Yan, S.W., Chu, J., 2010. Construction of an offshore dike using slurry filled geotextile mats. *Geotextiles and Geomembranes*, 28(5), pp.422–433.

Yang, L.-T. et al., 2012. Drained Behavior of Granular Soil During Rotational Shear. In: *ARMA US Rock Mechanics/Geomechanics Symposium*. ARMA, p. ARMA-2012.

Yang, S.R., Huang, L.J., 2023. Infiltration and Failure Behavior of an Unsaturated Soil Slope under Artificial Rainfall Model Experiments. *Water (Switzerland)*, 15(8). 10.3390/w15081599.

Yu, Y. et al., 2021. A siphon drainage method for stabilizing bank slopes under water drawdown condition. *Natural Hazards*, 105, pp.2263–2282.

Yu, Y. et al., 2019. Robust design of siphon drainage method for stabilizing rainfall-induced landslides. *Engineering Geology*, 249, pp.186–197.

Yuan, B. et al., 2017. Investigation of Deflection of a Laterally Loaded Pile and Soil Deformation Using the PIV Technique. *International Journal of Geomechanics*, 17(6). 10.1061/(asce)gm.1943-5622.0000842.

Yuequan, S. et al., 2015. Siphon drainage method for landslide prevention. 工程地质学报, 23(4), pp.706–711.

Zaki, M.H. et al., 2020. Effect of extreme rainfall intensity on matric suction and ground movement. In: *E3S Web of Conferences*. EDP Sciences. 10.1051/e3sconf/202019501022.

Zhang, L. et al., 2018a. Probabilistic calibration of a coupled hydro-mechanical slope stability model with integration of multiple observations. *Georisk: Assessment and Management of Risk for Engineered Systems and Geohazards*, 12(3), pp.169–182.

Zhang, L. et al., 2018b. Probabilistic calibration of a coupled hydro-mechanical slope stability model with integration of multiple observations. *Georisk: Assessment and Management of Risk for Engineered Systems and Geohazards*, 12(3), pp.169–182.

Zhang, L. et al., *Rainfall-Induced Soil Slope Failure*.

Zheng, G. et al., 2020. Stability analysis of stone column-supported and geosynthetic-reinforced embankments on soft ground. *Geotextiles and Geomembranes*, 48(3), pp.349–356.

Zheng, H., Sun, G., Liu, D., 2009. A practical procedure for searching critical slip surfaces of slopes based on the strength reduction technique. *Computers and Geotechnics*, 36(1–2), pp.1–5.

Zheng, H., Tham, L.G., Liu, D., 2006. On two definitions of the factor of safety commonly used in the finite element slope stability analysis. *Computers and Geotechnics*, 33(3), pp.188–195.

Zheng, J. et al., 2021. A siphon drainage system with variable diameters for landslides: Concept, calculation, and validation. *Journal of Hydrology*, 597, p.126305.

Zienkiewicz, O.C., Humpheson, C., Lewis, R.W., 1975. Associated and non-associated visco-plasticity and plasticity in soil mechanics. *Geotechnique*, 25(4), pp.671–689.